



MONASH University

Nanocomposite Materials for Electrocatalytic Oxidation of Glucose

Mahamarakkalage Chrishani Dilusha Cooray
BSc. (Honours)

A thesis submitted for the degree of Doctor of Philosophy at
Monash University in 2017
Faculty of Science, School of Chemistry

Copyright notice

© The author 2017.

I certify that I have made all reasonable efforts to secure copyright permissions for third-party content included in this thesis and have not knowingly added copyright content to my work without the owner's permission.

Abstract

The design and development of new nanocomposites for electrocatalysis are in high demand, as they make the electrode reactions energy and time efficient. Catalysts involved in these reactions at the electrodes could be either chemical catalysts or biocatalysts. Chemical catalysts can be metals, metal oxides or alloys. Enzymes are the main biocatalysts. In this study, our main focus was to design, develop and fabricate electrocatalytic electrodes for glucose oxidation. Glucose is an inexpensive and abundant substrate, but with high electrochemical stability. It is important to develop novel nanocomposites for electrocatalytic oxidation of glucose.

Electrocatalytic glucose oxidation can lead to two major applications; sensors and fuel cells development, which are both equally important electrochemical devices in the field. Fuel cell applications, require highly efficient oxidation reactions to achieve a sufficiently large power density. Glucose fuel cells have caught the interest as it is simple, more efficient and the fuels used are abundant. Glucose sensing field is growing day by day due to the high demand from the increasing number of people who suffer from diabetes, which have continuous demand on the synthesis of novel materials for fabrication of efficient and reliable sensors.

This thesis discusses four successfully synthesised novel nanocomposites that were used in the fabrication of electrocatalytic electrodes for glucose oxidation. The first two experimental chapters are on second generation enzymatic nanocomposites modified electrodes using ferrocene propionic acid as the mediator. The active site of the enzymes buried under a thick protein layer. Therefore, in enzymatic electrodes fabrication, enzyme immobilisation plays a critical role and also in the performance. In this study, well known hydrogel was employed, branched polyethylenimine (bPEI), the primary amines create the platform to covalently attach components such as mediators and enzymes. This hydrogel with its hydrophilic nature increases the mobility of mediator for effective electron transfer between enzyme and the electrode. Carbon materials were non-covalently functionalised by the π - π interaction with the pyrene which was tethered to

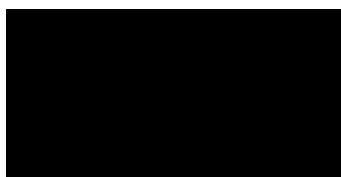
redox relay of ferrocene functionalised branched PEI. Glucose oxidase (GOx) enzyme was crosslinked to nanocomposite using glutaraldehyde (GA) prior to electrode fabrication. Another enzymatic nanocomposite was designed where, gold nanoparticles were synthesised using bPEI as the stabilizer, and further conjugated with ferrocene propionic acid via the 1-ethyl-3-(3-dimethylaminopropyl)carbodiimide (EDC) coupling reaction. EDC activates the carboxyl group for the coupling with primary amines to form amide bonds. After separation and purification, the resulting material was used for covalent attachment of enzyme GOx using GA as linkers. This composite material was then used for the fabrication of glucose oxidase electrodes. Above discussed enzymatic electrodes showed excellent electrocatalysis towards glucose oxidation in neutral pH.

The non-enzymatic electrodes were fabricated using poly(hydroxyl-1,4-naphthoquinone) stabilised gold nanoparticles (AuNQ NPs) was synthesised by one step chemical reduction of AuCl_4^- using 5-hydroxyl-1,4-naphthoquinone, and stabilised by the simultaneously formed poly(hydroxyl-1,4-naphthoquinone). Cobalt selenide flakes decorated reduced graphene oxide (CoSe-rGO) is another non-enzymatic catalyst that was synthesised using a simple hydrothermal method. The electrochemical properties of the AuNQ NPs and CoSe-rGO and their electrocatalytic activities towards glucose oxidation in alkaline media were investigated using a range of techniques, including DC cyclic, rotating disk electrode and Fourier transformed large amplitude AC voltammetry techniques. The results demonstrate that these non-enzymatic catalysts modified electrodes have excellent catalytic activity toward glucose oxidation.

Declaration

This thesis contains no material which has been accepted for the award of any other degree or diploma at any university or equivalent institution and that, to the best of my knowledge and belief, this thesis contains no material previously published or written by another person, except where due reference is made in the text of the thesis.

Signature:



Print Name: Mahamarakkalage Chrishani Dilusha Cooray

Date: 29/ 03/ 2017

Publications during enrolment

- 1) M. C. D. Cooray, Saman Sadanayake, Fengwang Li, Steven J. Langford, Alan M. Bond and Jie Zhang, *Efficient Enzymatic Oxidation of Glucose Mediated by Ferrocene Covalently Attached to Polyethylenimine Stabilized Gold Nanoparticles*, *Electroanalysis*, 2016, Vol.28(11), p.2728-2736.
- 2) M.C.D. Cooray, Yuping Liu, Steven J. Langford, Alan M. Bond and Jie Zhang, *One pot synthesis of poly(5-hydroxyl-1,4-naphthoquinone) stabilized gold nanoparticles using the monomer as the reducing agent for nonenzymatic electrochemical detection of glucose*. *Anal. Chim. Acta*, 2015. **856**: p. 27-34.

Thesis including published works declaration

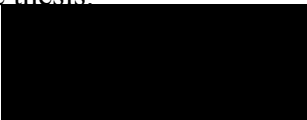
I hereby declare that this thesis contains no material which has been accepted for the award of any other degree or diploma at any university or equivalent institution and that, to the best of my knowledge and belief, this thesis contains no material previously published or written by another person, except where due reference is made in the text of the thesis.

This thesis includes two original papers published in peer reviewed journals and no submitted publications. The core theme of the thesis is Electrocatalysis. The ideas, development and writing up of all the papers in the thesis were the principal responsibility of myself, the student, working within the School of Chemistry under the supervision of Dr. Jie Zhang, Prof. Steven J. Langford and Prof. Alan M. Bond.

The inclusion of co-authors reflects the fact that the work came from active collaboration between researchers and acknowledges input into team-based research. In the case of Chapter 2 to 5 my contribution to the work involved the following:

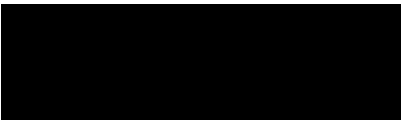
Thesis Chapter	Publication Title	Status (<i>published, in press, accepted or returned for revision, submitted</i>)	Nature and % of student contribution	Co-author name(s) Nature and % of Co-author's contribution*	Co-author(s), Monash student Y/N*
2	Use of Glucose oxidase/Pyrene/ Redox polymer integrated carbon materials for electrocatalytic glucose oxidation	Not submitted	75%. Concept and collecting data and writing first draft	1) Dr. Jie Zhang, Prof. Steven Langford and Prof. Alan Bond; 25% into manuscript by proof reading	Yes
3	Efficient Enzymatic Oxidation of Glucose Mediated by Ferrocene Covalently Attached to Polyethylenimine Stabilized Gold Nanoparticles	Published	70%. Concept and collecting data and writing first draft	1) Yu Ping Liu; 5% by carrying out SEM characterisation 2) Dr. Jie Zhang, Prof. Steven Langford and Prof. Alan Bond; 25% into manuscript by proof reading	Yes
4	One pot synthesis of poly(5-hydroxyl-1,4-naphthoquinone) stabilized gold nanoparticles using the monomer as the reducing agent for nonenzymatic electrochemical detection of glucose	Published	65%. Concept and collecting data and writing first draft	1) Saman Sandanayake; 5% into manuscript by giving ideas to improve the manuscript 2) Fenwang Li; 5% into manuscript by carrying out TEM characterisation 3) Dr. Jie Zhang, Prof. Steven Langford and Prof. Alan Bond; 25% into manuscript by proof reading	Yes
5	Cobalt selenide nanoflakes decorated reduce graphene oxide nanocomposite for efficient glucose electro-oxidation in alkaline medium	Not submitted	60%. Collecting data and writing first draft	1) Xiaolong Zhang; 15% into the manuscript by synthesising the material and carrying out XRD analysis 2) Dr. Jie Zhang, Prof. Steven Langford and Prof. Alan Bond; 25% into manuscript by proof reading	Yes

I have renumbered sections of submitted or published papers in order to generate a consistent presentation within the thesis.

Student signature: 

Date: 29/ 03/ 2017

The undersigned hereby certify that the above declaration correctly reflects the nature and extent of the student's and co-authors' contributions to this work. In instances where I am not the responsible author I have consulted with the responsible author to agree on the respective contributions of the authors.

Main Supervisor signature: 

Date: 29/ 03/ 2017

Acknowledgements

It is my great privilege to acknowledge the individuals who were with me supporting me throughout my candidature as a doctoral candidate.

Firstly, I would like to thank Dr. Jie Zhang and Professor Alan Bond for giving me the opportunity to pursue my Doctoral study with the electrochemistry group of Monash University and for their guidance, encouragement, patience and expertise shared with me to develop my knowledge and skills in electrochemistry.

I would like to thank Professor Steven Langford for allowing me to use the synthesis lab and for his support, patience and knowledge shared with me to develop my knowledge and skills in organic synthesis. Also for the support given to me during scholarship application process.

I take the opportunity to thank my panel members Dr. Kei Saito and Dr. Xinyi Zhang for their valuable comments and suggestions given to me during meetings to shape my thesis study. I would like to extend my thanks to Ms Anna Severin, Dr. Kellie Tuck, Ms Sarah Williams and Ms Flordeliza Verdan for their assistance during my candidature under School of Chemistry. The assistance and cooperation given by technical officers at School of Chemistry was much appreciated.

I would like to express my thanks to Dr. Saman Sandanayake and Dr. Sixuan Guo for the great assistance given throughout the candidature. In addition, I would like to thank my colleagues for making my lab experience a great one. Also the support given by the co-authors of my published work were greatly appreciated.

A very special thanks to my Husband, Mr Dilshan Gunasinghe, who always motivated me to achieve my goals and giving me moral support and keeping me sane. I am most grateful for my parents, Mr. and Mrs Susith Cooray for understanding me and keeping the faith in me. Also for the encouragement and support given to me all the time.

Dilusha Cooray

Symbols

Symbol	Description	Usual units
E_F^0	Formal redox potential	V
E_{ox}^P	Oxidation peak potential	V
E_{red}^P	Reduction peak potential	V
ΔE_p	Separation of the peak potentials	V
E_m	Mid potential	V
I	Current	μA
I_p	Peak current	μA
I_{ox}^P	Oxidation peak current	μA
I_{red}^P	Reduction peak current	μA
I_{ss}	Steady state limiting current	μA
j_{ss}	Steady state current density	$\mu\text{A cm}^{-2}$
j_{max}	Maximum current density	$\mu\text{A cm}^{-2}$
n	Number of electrons	
F	Faraday's constant	96,485 C mol ⁻¹
A	Electrode area	cm ²
C	Concentration	mol cm ⁻³ / mol dm ⁻³
ν	Scan rate	V s ⁻¹
D	Diffusion coefficient	cm ² s ⁻¹
R	Universal gas constant	8.314 J mol ⁻¹ K ⁻¹
T	Absolute temperature	K
t	Time	s
ω	Rotational speed	rad s ⁻¹
Q	Charge	C
Γ	Surface coverage	mol cm ⁻²
K_m'	Apparent Michaelis Menten constant	mmol dm ⁻³
IR_u	Uncompensated resistant	Ω

List of figures

Figure 1: Different types of glucose sensors. Artwork created by Emilia Witkowska-Nery, Martin Jönsson-Niedziółka, and Małgorzata Stani [27].....	5
Figure 2: Schematic diagrams which illustrate the effect of enzyme orientation in (a) a 2D electrode and (b) a 3D electrode.....	17
Figure 3: Schematic diagrams showing two key mechanisms for electron transfer between the enzyme and the electrode, (a) mediated electron transfer and (b) direct electron transfer.....	18
Figure 4: A schematic diagram showing the wave form employed in dc cyclic voltammetry [198].....	26
Figure 5: A cyclic voltammogram for a simple one electron oxidation process. The symbols used in the diagram are as follows; t = time, E = potential versus a reference electrode such as Ag/AgCl, Red = reduced form, Ox = oxidised form, E_{ox}^P = oxidation peak potential, E_{red}^P = reduction peak potential, I_{ox}^P = oxidation peak current, I_{red}^P = reduction peak current [198].....	27
Figure 6: A conventional rotating disc electrode set up.....	28
Figure 7: Sigmoidal curve obtained with a steady state limiting current (I_{ss}) under hydrodynamic conditions at a RDE.....	29
Figure 8: Schematic representation of H-shaped bulk electrolysis setup.....	30
Figure 9: A plot of current vs time in bulk electrolysis.....	31
Figure 10: Schematic representation of the waveform used in ac voltammetry [198].....	32
Figure 11: A schematic representation of data analysis used in FTACV [198].....	33

Table of Contents

Abstract	iii
Declaration	v
Publications during enrolment	vi
Thesis including published works declaration	vi
Acknowledgements	ix
Symbols	x
List of figures	xi
Chapter 1: Introduction	1
1.1. Electrocatalysis	2
1.2. Applications of electrocatalysis	3
1.3. Why we need efficient electrocatalysts for glucose oxidation?	3
1.3.1. Glucose sensing for Diabetes	4
1.3.2. Alternative energy source/ glucose fuel cells	6
1.4. Materials and methods used in fabrication of electrocatalytic electrodes	7
1.4.1. Polymers	8
1.4.2. Carbon materials	8
1.4.3. Porous materials	9
1.5. Types of Electrodes used in electrocatalytic glucose oxidation	9
1.5.1. Non enzymatic electrodes	9
1.5.2. Enzymatic electrodes	14
1.6. Advantages and disadvantages of enzymatic and nonenzymatic electrodes	24
1.7. Electrochemical techniques used in this research study	25
1.7.1. Cyclic Voltammetry	25
1.7.2. Rotating Disc Electrode	28
1.7.3. Bulk electrolysis	30
1.7.4. Fourier Transformed AC Voltammetry	32
1.8. Research Objective	34
1.9. References	35

Chapter 2: Use of glucose oxidase/pyrene/ redox polymer integrated carbon materials for electrocatalytic glucose oxidation	59
Chapter 3: Efficient enzymatic oxidation of glucose mediated by ferrocene covalently attached to polyethylenimine stabilized gold nanoparticles	83
Chapter 4: One pot synthesis of poly(5-hydroxyl-1,4-naphthoquinone) stabilized gold nanoparticles using the monomer as the reducing agent for nonenzymatic electrochemical detection of glucose	99
Chapter 5: Cobalt Selenide nanoflake decorated reduced graphene oxide nanocomposite for efficient glucose electro-oxidation in alkaline medium	115
Chapter 6: Future Perspectives	146
6.1. Use of Conducting Polymer Nanocomposite for Three Dimensional Enzyme Electrode	147
6.2. Future perspective	166
Chapter 7: Conclusion	174

Chapter 1

Introduction

1.1. Electrocatalysis

Electrocatalysis can be defined as ‘the acceleration of a particular redox reaction by the appropriate choice of electrode material’ [1, 2]. The requirement for electrocatalytic materials is obvious, as it makes various processes more economically favoured using electrons to undertake chemical transformation [3]. The function of a catalyst is to lower the free energy that is required to reach the transition state, however, the total difference of free energy of reactants and products does not change [4]. Electrocatalysts will minimise the overpotential required to drive a particular process. In addition, achieves higher current densities than other approaches [5].

The discovery and development of new electrocatalysts is prevalent with the number of new scientific literature related to this topic being more than 800 papers (web of science search, term “electrocatalysis”) per annum. Catalysts can be either chemical catalysts or biocatalysts. Chemical catalysts are mainly metal, metal oxides, and alloys while enzymes represent the largest class of biocatalysts. Scientists work towards improving the electrocatalytic activity of chemical catalysts and biocatalysts for specific reactions. According to the catalytic materials used in electrode fabrication, the modified electrodes can be classified into two types; enzymatic and non-enzymatic based electrodes. An electrode which is modified for an electrocatalytic purpose should have properties such as high stability, resistance to poisoning of the electrode, nor oxidation or reduction [2]. Many different electrochemical techniques with many different catalysts have been used in electrocatalysis such as amperometry, electrochemical impedance spectroscopy and voltammetry[6].

1.2. Applications of electrocatalysis

Catalyst modified electrodes have been used in the application of sensors, energy conversions such as fuel cells and other electrocatalytic reaction processes [7]. Examples for electrocatalytic reaction processes are specific C-H bond transformation, activation and reduction of CO₂ to other useful products and inter-conversion of O₂ and H₂O [7]. The cost targets for catalysts highly depend on the application. As there can be high cost when precious metals and some rare enzymes are used. In this thesis, the focus is on electrocatalytic oxidation of glucose and its use as a model to design and develop new electrocatalytic electrodes.

1.3. Why we need efficient electrocatalysts for glucose oxidation?

Glucose is a simple sugar which is widely available and inexpensive [8]. In plants, glucose is synthesised by photosynthesis via chlorophyll [9]. In humans, glucose is a product of carbohydrate metabolism [10] and acts as a source of energy [11]. The excess is stored as fat [12] and an inability to metabolise glucose will give rise to diabetes [13, 14]. Glucose oxidation can be used in two major applications in sensors to determine glucose concentration and in fuel cells. The electrochemical techniques, such as amperometry, potentiometry[15] are widely adopted due to its relative simplicity [16], low cost instrumentation and miniaturisation[15] compared to surface plasmon resonance[17] and other optical[18] techniques. Development of effective and cheap glucose sensors is required for the food industry and in clinical applications related to diabetes where patients need to continuously monitor their glucose levels to prevent acute clinical conditions. Development of efficient glucose fuel cells is important to produce clean energy and provides an alternative energy source using abundant materials.

1.3.1. Glucose sensing for Diabetes

The glucose sensing field is growing day by day due to the high demand from people who suffer from Diabetes mellitus. Diabetes mellitus is a chronic clinical condition which results in high or low deviations in glucose levels in blood that lie outside the normal range of 80-120 mg/dL (4.4-6.6 mM) [19]. This can be characterised as a metabolic disease [20]. The symptoms are increased thirst and urine volume, recurrent infection and weight loss [21]. There are three main types of diabetes as Type 1, Type 2 and gestational. In all three types, the basic physiological inadequacy is relative or absolute deficiency of insulin [22]. Type 1 diabetes results from a deficiency of insulin secretion from the pancreas. Type 2 diabetes is caused by resistance to insulin action or inadequate response to insulin secretion [12]. Gestational diabetes arise during pregnancy and can be seen only in women [23].

Abnormal levels of glucose cause many long term serious health issues, such as blindness, tissue damage, heart disease and kidney failure [24]. Therefore, it is necessary for diabetic patients to regularly monitor their glucose levels with high accuracy. Since the first discovery of an enzyme electrode in 1962 by Clark and Lyons [25], amperometric glucose sensors have improved dramatically over the last five decades [26, 27]. Many sensors for glucose monitoring have been reported [28-30]. Glucose sensors are medically important devices for the aid of diabetes patients who constitute more than 10% of the world population [31]. Sensors allow biological or chemical changes to be translated into a quantifiable measurement as a signal for determining the quantity of the target analyte devoid of interference [32]. Blood and urine are used as biological fluids to monitor glucose in humans [33]. With the advancement of technology, sweat [34] and tears [35-37] are now been used as samples to monitor glucose levels. A very recent advance in the glucose sensor field is the discovery of “smart tattoos” [34, 38-40]. These smart

tattoos are implantable fluorescent microparticle sensors that can be injected into the skin and are exposed to the interstitial fluid. They monitor fluctuations of glucose concentration that correlates with blood glucose levels [41]. Contact lenses provide another approach, where tears are exploited as the biological fluid. The normal glucose level in tears is between 0.1–0.6 mM [42]. Yao et al. reported contact lenses embedded with single [43] and dual [42] glucose sensors. These contact lenses operate as wireless devices with telecommunication circuits.



Figure 1: Different types of glucose sensors. Artwork created by Emilia Witkowska-Nery, Martin Jönsson-Niedziółka, and Małgorzata Stani [27].

1.3.2. Alternative energy source/ glucose fuel cells

Far the industrialisation of the world, society started consuming for more energy to meet their aspirations [44]. Fossil fuels were the main energy source in their context. Combustion of fossil fuels generates energy, but is a non-renewable source. Alternative renewable energy sources are now needed that produce clean energy and have a low impact on the environment due to minimum secondary waste [45]. The use of renewable energy sources can provide a solution for global warming resulting from use of fossil fuels[44]. Renewable energy sources are solar [46], wind [47], hydroelectric [48], geothermal [49] and fuel cells [50].

Fuel cell technology is dramatically improving via fundamental research and is used in real applications [51]. Fuel cells have attracted interest as they are simple, efficient and the fuels used are abundant [44]. Fuel cells convert chemical energy into electrical energy (via electric current) [52] and thus act as galvanic cells [44]. A fuel cell consists of an anode, a cathode and electrolyte containing substrate (fuel). The anodes and cathodes are fabricated with catalysts that oxidise or reduce the fuel and produce electrons and positively charged hydrogen ions [52]. At the anode, the fuel is oxidised and release protons that flow through the electrolyte towards the cathode. The released electrons flow from the external circuit to the cathode under an electrical potential [53]. There are several types of bio-based fuel cells, such as enzymatic biofuel cells [54], microbial biofuel cells [55].

This thesis focuses on fabricating electrocatalytic electrodes for fuel cells that utilise glucose. Enzymes and metals are employed as catalysts. For glucose enzymatic biofuel cells, glucose oxidase [56], bilirubin oxidase [57], peroxidase [58] and laccase [59] were employed. The short life of enzymes causes a gradual decrease in power output of the

fuel cells. To minimise this problem, precious metals have been used in conjugation with enzymes, although, the use of metal catalysts alone has attracted much interest due to the work done by Stetten et al. [60] since 2010. Glucose is a well known fuel in fuel cell application [61]. The complete oxidation of glucose gives 24 electrons, hydrogen ions and CO₂ [62].



However, a more common reaction for glucose a fuel cells is:



where glucose is oxidised to gluconolactone giving 2 electrons [60]. Finding an efficient catalyst to convert glucose completely to CO₂ is challenging. With the advantage of their small size and high biocompatibility, glucose enzymatic fuel cells have been used in *in vivo* applications [63]. These fuel cells are very useful in providing energy to medical implants, because glucose and O₂ can be found in biological fluids [61]. Miniature biofuel cells that generate electricity at high pressure created through body fluids and powered implanted devices have been proposed [64, 65]

1.4. Materials and methods used in the fabrication of electrocatalytic electrodes

There are two main types of electrodes that have been utilised for electrocatalytic oxidation of glucose. They are categorised according to the catalyst used and known as non-enzymatic or enzymatic electrodes. However, there are many methods to fabricate these electrodes with catalysts such as, layer by layer deposition [66, 67], electrodeposition [68], drop cast [69], spin coating [70], screen printing [71, 72] hot embossing [73] or a combination of the methods listed above [74]. Materials that are used as the host matrix in the fabrication process play the role of anchoring the catalysts and

enhance the performance of the electrode. Mostly polymers, porous architectures and carbon materials are employed.

1.4.1. Polymers

Polymers are widely used materials designed by linking a large number of monomer units together [75]. Polymers can be used as the sensitive component or as the matrix for immobilisation of specific substrates such as enzymes or nanoparticles. Polymers can be categorised according to their properties, such as conductivity, to give conducting [76, 77] and non-conducting [78] polymers. The range of conducting polymer nanocomposites for electrochemical applications is rapidly expanding [79]. Non-conducting polymers have been exploited when mixed with conducting matrixes, for example, carbon nanotubes, inorganic nanoparticles, graphene, and special dopants. These have been used with non-conducting polymers to overcome the low conductivity, in designing composites for electrochemical applications. Metallic nanoparticles stabilised with different polymers offer a great opportunity for enhancing the performance of modified electrodes [80]. The polymer may have a significant influence on the properties of resulting nanomaterials by utilising various forms of functional groups [81].

1.4.2. Carbon materials

Carbon is a fascinating element that has several allotropes [82] such as diamond, graphite and fullerene. However, of all the allotropes, graphite and its derivatives have been most widely used in electrochemical application [83]. Graphite consist of layers of carbon arranged as a honeycomb and stacked planes on top of each layer [84]. Graphene is a single layer of graphite. Graphite has been the source of many interesting carbon based materials such as graphene and graphene oxide [84] that are used in many applications [85, 86]. Their sp^2 hybridised carbons allow non covalent interactions mainly via π - π

stacking [83, 87]. The functional groups on graphene oxide add an additional advantage that allows covalent attachment to other pendant groups or biomolecules [88]. Similarly, in 1991 the discovery of carbon nanotubes (CNT) by Iijima [89] has attracted the attention of material scientists. Sensors [90, 91] and fuel cells [58, 92] now incorporate CNTs as the host matrix. Even though used as a host matrix CNTs have improved the loading of catalysts due to the high surface area and high electron transfer rate derived from the high conductivity [93].

1.4.3. Porous materials

Porous materials can be classified according to the size of the cavity into three classes: *macro* ($x > 50$ nm), *meso* ($2 < x < 50$ nm) and *micro* ($x < 2$ nm) porous [94]. The use of mesoporous materials is now prominent in electrocatalytic applications. Catalysts are embedded in the cavities or if the porous structures are made out of metals they will act as a catalyst with a high surface area for the substrate to oxidise or reduce. If enzymes are used with these porous structures, the cavity should be 4 to 5 times larger than the mean molecular diameter of the enzyme to allow successful immobilisation [95]. There are many methods for creating porous materials, with silicon [96] and carbon [97] porous materials being very popular.

1.5. Types of electrodes used in electrocatalytic glucose oxidation

1.5.1. Non-enzymatic electrodes

In non-enzymatic electrodes, synthetic materials, such as metallic nanoparticles (NPs) [28, 98], conducting polymers [99, 100], polymer films and sol-gel materials [98], have been exploited to synthesis nanocomposites for the detection of glucose. Non-enzymatic electrodes are reported to provide an efficient approach to detect glucose with high sensitivity, reliability, fast response, good selectivity and a low detection limit [101].

However, these electrodes suffer from slow kinetics and surface poisoning due to adsorption of intermediates [102]. Transition metals, such as gold (Au), platinum (Pt), silver (Ag), copper (Cu), nickel (Ni), cobalt (Co), metal oxides and alloys also have been reported to give high catalytic activities in glucose sensor applications [103]. Almost all the non-enzymatic electrodes contain transition metal component as the catalyst.

There are two accepted theories used to obtain non-enzymatic glucose electro-oxidation by transition metal centres [104]:

1. An activated chemisorption model – where glucose molecules adsorb on the surface of the metal centres of transition metal containing electrocatalysts followed by the elimination of hydrogen atom attached to hemiacetal carbon. The elimination of the hydrogen atom acts as the rate limiting step in this mechanism [28].
2. ‘Incipient Hydrous Oxide Adatom Mediator’ (IHOAM) model – where the active metal surface undergo premonolayer oxidation step that creates an incipient hydrous oxide layer of OHads which mediates the glucose oxidation [105]. The glucose becomes oxidised at a low potential and the metal surface is regenerates.

There are thousands of reports of non-enzymatic glucose electrodes based on transition metals catalysts. Interestingly, both macro and nano forms of gold are active towards glucose oxidation [106]. Gold and platinum have the ability to work over a wide range of pH which allows their use within medical implants in humans [28, 107], whereas most other metal nanoparticles are active in alkaline pH. Poyraz *et al.* prepared poly(o-toluidine) (POT) nanofiber/metal nanoparticle composites modified graphite working electrode which gave rapid responses with a sensitivity of $37 \mu\text{A cm}^{-2} \text{mM}^{-1}$ and a limit of detection (LOD) for glucose of $\sim 0.027 \mu\text{M}$ in alkaline medium [108]. Sebez *et al.*

reported the use of polyethyleneimine modified gold nanoparticles on carbon fibers coated with aligned carbon nanotubes in non-enzymatic glucose oxidation at physiological pH of 7.4[109]. It was reported that coating the electrodeposited Au nanoparticles with polymers with intrinsic microporosity provided resistance to poisoning during glucose oxidation at pH 7[110]. Au NPs electrodeposited on amine functionalised mesoporous silica, has been reported to give a sensitivity of $75 \mu\text{A cm}^{-2} \text{mM}^{-1}$ and LOD of $100 \mu\text{M}$ for glucose detection in alkaline medium [111]. Au NPs decorated on multi-walled carbon nanotube functionalised with congo red composites was reported to give a low detection limit of $0.5 \mu\text{M}$ glucose in a basic medium [112]. Feng *et al.* synthesised Au NPs modified with chitosan which was exploited in the application of a glucose sensor with a LOD of 0.37mM [113]. Kurniawan *et al.* [114] fabricated an electrode using layer-by-layer deposition of AuNPs on a gold electrode (AuE) and obtained a sensitivity of $160 \mu\text{A mM}^{-1} \text{cm}^{-2}$, a detection limit of 0.5mM and linear range up to 8mM in alkaline medium. Similarly, Jena and Raj [115] achieved glucose detection at a low potential of 0.16V in phosphate buffer solution (PBS pH 9.2) with high sensitivity of $179 \mu\text{A mM}^{-1} \text{cm}^{-2}$ and low detection limit of 50nM . Yi *et al.*[116] designed an electrode with Ni nanoflakes supported by titanium and obtained a sensitivity of $7320 \mu\text{A mM}^{-1} \text{cm}^{-2}$ and low detection limit of $1.2 \mu\text{M}$ in alkaline medium. Huang *et al.*[117] reported the use of Cu nanobelts in non-enzymatic glucose sensing and obtained a high sensitivity of $4433 \mu\text{A mM}^{-1} \text{cm}^{-2}$ and linear range of $0.01\text{-}1.13 \text{mM}$. These studies provide examples of the many different approaches to fabricating non-enzymatic glucose electrodes [118]. The performances of selected materials are summarised in Table 1.

Table 1: Non-enzymatic glucose sensor performance of nanostructured transition metals.

Electrode Material	Sensitivity / ($\mu\text{A mM}^{-1}$ cm^{-2})	Linear range/ (mM)	LOD/ μM	Operational potential/ V	Medium	Ref.
Au nanofilm	57.5	Up to 57.5	0.72	+0.3 vs SCE	PBS pH7.4	[119]
Au nanocorals	22.6	0.05-30	10	+0.2 vs Ag/AgCl	PBS pH 7.4	[120]
Layer-by-layer AuNPs/Au E	160	Up to 8	500	-	0.1 M NaOH	[114]
Au NPs/ Au E	179	0-8	0.05	+0.16 vs Ag/AgCl	PBS pH 9.2	[115]
Au NPs/ ITO	183.5	0.004- 0.5	-	+0.2 vs SCE	0.01 M NaOH	[121]
AuNPs/SrPdO ₃ / graphite	7157	0.1-6	10	0.4 vs Ag/AgCl	0.1 M NaOH	[122]
AuRu NPs	38.3	0-15	269	-0.65 vs Ag/AgCl	0.1M NaOH	[123]
PtPb nanoporous networks	10.8	1-16.9	-	-0.08 vs Ag/AgCl	PBS pH7.4	[124]
PtPb NPs/ MWCNT	18	Up to 5	7	-0.15 vs Ag/AgCl	PBS pH 7.4	[125]
PtRu/ MWCNTs/IL	10.7	0.2-15	50	-0.1 vs SCE	PBS pH7.4	[126]

PtNi/graphene	20.42	Up to 35	10	-0.35 vs Ag/AgCl	PBS pH 7.4	[127]
Pt ₃ PdNP/rGO/GCE	79.57	0-0.3	0.002	0.06 vs. SCE	0.05 M PBS pH 7.4	[128]
PtAu/ MWCNT	10.71	Up to 24.44	10	+0.3 vs Ag/AgCl	PBS pH7.4	[129]
PtRu NPs/ MWCNTs	28.26	1-15	0.25	+0.55 vs Ag/AgCl	0.1 M NaOH	[130]
PtNi nanowires	920	0.002-2	1.5	+0.45 vs SCE	0.1M NaOH	[131]
Ni nanowire arrays	1043	0.0005-7	0.1	+0.55 vs SCE	0.1 M NaOH	[102]
NiS/ ITO	7430	0.005– 0.045	0.32	+0.5 vs Ag/AgCl	0.1 M NaOH	[132]
Ni nanoflakes/ Ti	7320	0.05-0.6	1.2	+0.5 vs SCE	0.5 M NaOH	[116]
Cu nanobelts	4433	0.01- 1.13	10	+0.6 vs Ag/AgCl	0.05 M NaOH	[117]
Cu NPs/Graphene	157	0-4.5	0.5	+0.5 vs SCE	0.1 M NaOH	[133]
Cu NPs/ SWCNT	3657	Up to 0.5	0.25	+0.65 vs Ag/AgCl	0.02 M NaOH	[134]
Cu–Ag/NF	7745.7	0.005– 3.5	0.08	0.55 V vs Hg/HgO	0.5 M NaOH	[135]
Co ₃ O ₄ NFs- Nafion/GCE	36.25	0-2.04	0.97	+0.59 vs Ag/AgCl	0.1 M NaOH	[136]

3D graphene/ Co ₃ O ₄ nanowire composite	3390	0- 0.080	0.025	+0.58 vs Ag/AgCl	0.1 M NaOH	[137]
Cu-Co NSs/RGO- CHIT/GCE	1921	0.015– 6.95	10	0.45 vs SCE	0.1 M NaOH	[138]
MnO ₂ /Au Composite	95	0.1 - 20		0.271 vs SCE	0.1 M NaOH	[139]
MnO ₂ /MWCNT	396	0 - 28	-	+0.3 vs Ag/AgCl	0.1M NaOH	[140]
PtAu– MnO ₂ / Graphene Paper	58.54	0.1 - 30.0	0.02	0 vs. Ag/AgCl.	0.5M H ₂ SO ₄	[141]
Fe ₂ O ₃ nanowire arrays	726	0.015-8	6	+0.52 vs SCE	PBS pH 7.5	[142]

Abbreviations: NF- nickle foam; ITO – indium tin oxide; NP – nanoparticle; NS – nano sheets; MWCNT – multi wall carbon nanotube; RGO – reduce graphene oxide;

1.5.2. Enzymatic electrodes

The fabrication of enzymatic electrodes is much more complicated than the non-enzymatic ones as there are many factors that influence the electron transfer process between the electrode and the enzyme [29]. Glucose oxidase (GOx) and glucose dehydrogenase (GDH) are the major enzymes that have been exploited in glucose enzymatic sensors. Enzymes are biocatalysts that have significant advantages over chemical catalysts [143]. The advantages are, the ability to work in standard conditions (no extra energy needed), high specificity and catalysis of only a specific reaction using a very narrow range of reactants [144]. However, employing enzymes in electrochemical devices, introduces complications that result from sluggish and inefficient electron transfer between large enzymes and the electrode. Since efficient electron transfer is critical to achieve an ideal functioning of the electrode, many studies have focused on

understanding the factors that influence the electron transfer process and to improve its activity. An ideal enzymatic electrode should have the following properties: high chemical stability, anti-biofouling effect, high sensitivity, strong adherence of the film to the electrode, high immobilisation ratio of enzymes [145].

According to the mechanism involved, glucose biosensors can be categorised into three generations:

1st Generation: In the first generation of biosensors, the enzyme, glucose oxidase utilised O₂ to oxidise glucose. The amount of used O₂ was used in the measurement of glucose concentration [29].



Further developments include the introduction of an oxygen working electrode to correct oxygen background and use of measurement based H₂O₂ detection [146]. Dependence on ambient O₂ concentration, the high overpotentials for the reduction of O₂ or oxidation of H₂O₂ are drawbacks in 1st generation glucose biosensors [28].

2nd Generation: Mediators were introduced to overcome the drawbacks in 1st generation glucose biosensors. These mediators are relatively low molecular weight moieties that have reversible process at low potentials [147]. Ferrocene derivatives [148], osmium complexes[149], ruthenium complexes[150] are examples of mediators. These mediators make the communication more efficient by shuttling the electrons between electrode and enzyme active site. The mechanism is as below [28] is:



In this approach the measurement become independent of oxygen and can be used at lower potentials which minimises interfering reactions [29] and improves selectivity. Medisense commercialised the first personal glucose biosensor in 1987 [29]. The possible leakage of the potentially toxic mediators prevented their use as *in vivo* glucose biosensors [28].

3rd Generation: This generation of biosensors eliminates the use of mediators, and employ direct electron transfer. The enzymatic electrodes of this generation can be operated at low potentials of ~ 0.44 V vs SHE, which is close to the physiological enzyme redox potential[29]. Interfering responses from electroactive species are minimised due to the low potentials. The mechanism [151] is:



The 3rd generation biosensors suffer from a relatively small linear dynamic range compared to 1st and 2nd generation sensors. Therefore, research is needed to increase the performance of these sensors [28].

1.5.2.1. Enzyme immobilisation methods

Enzyme immobilisation plays a critical role in the fabrication of enzymatic electrodes [152] because the active site of the enzymes are buried under a thick protein layer [153]. The orientation and the position that the enzyme docks on the electrode will impact on the efficiency of electron transfer process [154]. This problem arises in a two dimensional (2D) electrode and to overcome this issue it is necessary to fabricate three dimensional (3D) enzymatic electrodes, where orientation and position will no longer be a limiting factor as the polymer wrapped around the enzyme acts as an electrical wire to shuttle

electrons to the electrode [155]. Figure 2 depicts the orientation and position of enzymes in 2D and 3D enzymatic electrodes.

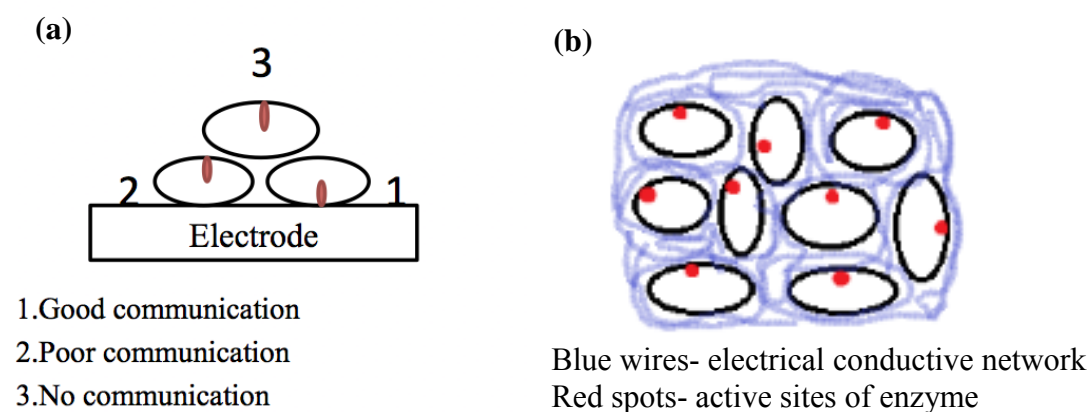


Figure 2: Schematic diagrams which illustrate the effect of enzyme orientation in (a) a 2D electrode and (b) a 3D electrode.

Immobilisation of enzymes can be achieved in three ways:

1. Adsorption- adhesion of enzymes onto the conducting matrix. This can be achieved by electrostatic interactions
2. Entrapment in a polymer matrix
3. Cross-linking

After the enzyme immobilisation on the electrode, it is necessary to achieve efficient electron transfer between the enzyme active site and the electrode. Many studies have focused on understanding the factors that influence the electron transfer process [156, 157]. Mediated electron transfer can be achieved by incorporating reversible electron transfer mediators, which were reported to be useful. The combination of nanomaterials and nanotechnology assist in overcoming the challenging bioanalytical barriers such as specificity, stability and sensitivity [158]. Utilisation of conducting polymers and electron

relays have been used to enhance the contact/ communication between the buried redox centre of the protein and the electrode [159].

1.5.2.2. Electron transfer mechanisms

Enzyme immobilization is a key requirement, as the electron transfer between the electrode and enzyme is an essential factor which enables the biosensor to function with high performance. Theoretically, this can be achieved by either direct electron transfer from the enzyme to the electrode through an electrically conductive pathway or through mediated electron transfer process with the aid of molecular species having well defined electrochemistry (Figure 3). Studies exploring electron transfer between large enzymes and electrode surfaces are highly important in understanding enzyme behaviour and exploiting their specific properties for biosensor applications [160].

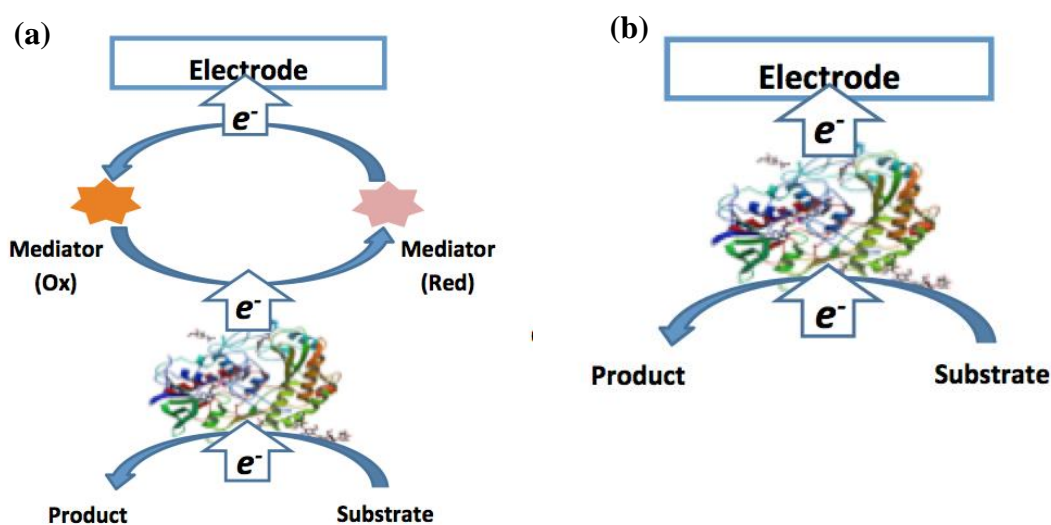


Figure 3: Schematic diagrams showing two key mechanisms for electron transfer between the enzyme and the electrode, (a) mediated electron transfer and (b) direct electron transfer.

One of the main challenges for biosensor is to establish efficient electron transfer pathways between the enzymes and electrode. The mediated electron transfer process, limits the energy loss. Since enzymes are large and hence the distance between the electrode and redox-active site is substantial. This approach is the principle on which most commercial disposable glucose biosensors for *in vitro* glucose monitoring are developed[161] and can be envisaged as a hopping mechanism when the mediators are immobilised on the electrode[162].

Four pathways that have the potential to allow electronic communication between an enzyme and an electrode surface:

i. Direct electron transfer – This method could lead to device inactivity as a result of the interaction of the enzyme with a bare electrode surface, when the potential was applied, the developed current on the electrode can denature the enzyme and will no longer be active. This will cause the inability of the enzyme to strongly communicate with the electrode resulting device inactivity [163]. The enzyme working life can be extended when the electrode is modified with a monolayer of the enzyme nanocomposite material to weaken the interaction between the enzyme and the electrode [164]. This direct method only works efficiently for small or medium size enzyme where the active centres are sufficiently close to the electrode surface, eg $\ll 2$ nm [165].

ii. Freely diffusing redox species through a mediated mechanism- This method may not lead to a robust system as needed for *in vivo* applications [166, 167].

iii. Electron hopping through a redox mediator within a polymer - This leads to a mediated approach with potential for biosensor and biofuel cell application [168-170].

iv. Electron transfer via a conducting polymer chain [163]- This could potentially lead to a direct electron transfer pathway under suitable conditions. Much of the current research

on enzyme electrodes is focusing on the development of stable enzyme electrodes (in particular GOx electrodes) based on the principle of direct electron transfer. The potential for these applications is relatively unexplored, but promising, particularly if a number of important challenges can be addressed. These include solving several aspects of communication between electrodes and metalloenzyme active sites [171], and overcoming the problem of partial denaturing or shape deformation through electrode contact.

Lee *et al.* [172] reported a glucose biosensor based on prussian blue (PB) modified graphite. The glucose oxidase (GOx) was immobilised on PB-G string electrode with biocompatible chitosan overlayer to obtain Chi/GOx/PB-G string electrode which gave a high sensitivity of $641.3 \mu\text{A mM}^{-1} \text{cm}^{-2}$ and a linear range of 0.03 to 1.0 mM for glucose at physiological pH (PBS pH 7.4). It is now becoming more common to use multi enzyme systems in the biosensor field and Wang *et al.*[173] reported graphene nano-sheet bonded polydopamine/metal-organic frameworks (MOF) microcapsules with immobilized glucose oxidase as a mimetic multi-enzyme system for glucose sensing. The MOF mimics the horseradish peroxidase properties and further oxidise H_2O_2 that was produced by glucose oxidation by GOx. Ambarsari *et al.* reported the immobilisation of glucose oxidase onto polyaniline nanofiber modified carbon paste electrodes (GOx/PAniNF/MCPE) as bioanodes in fuel cell having a sensitivity of $57.79 \mu\text{A mM}^{-1} \text{cm}^{-2}$ [174]. Merchant *et al.*[175] used ferrocene (Fc) conjugated linear polyethylenimine (PEI) for glucose oxidase electrode fabrication for glucose determination obtained a sensitivity of $10 \mu\text{A mM}^{-1} \text{cm}^{-2}$ and a short linear range of 0.005-0.1 mM. Ferrocenylhexyl- and ferrocenylpropyl-modified linear PEI (Fc-C6-LPEI) were used with periodate-modified glucose oxidase (p-GOX) in the layer-by-layer assembly of enzymatic electrodes by Godman *et al.*[66] with a high current density of $1417 \pm 63 \mu\text{A}$

cm⁻². A novel glucose biosensor based on a gold nanoparticle/ bovine serum albumin/ Fe₃O₄ (AuNPs/BSA/Fe₃O₄) composite was reported by He *et al.*[176] for immobilising GOx. This enzymatic electrode has a high sensitivity of 115.3 $\mu\text{A mM}^{-1} \text{cm}^{-2}$ and a wide linear range of 0.25 - 7.0 mM with a LOD of 3.54 μM at pH 7.4. Chitosan supported silver nanowires (AgNWs) based enzyme electrodes were fabricated by Kumar-Krishnan *et al.*[177] with a sensitivity of 16.72 $\mu\text{A mM}^{-1} \text{cm}^{-2}$ with a wide linear range of 1–15 mM. Wang *et al.* [178], who integrated the conducting polymer poly(3,4-ethylenedioxythiophene) with a Fc conjugated bPEI, obtained a sensitivity of 66 $\mu\text{A mM}^{-1} \text{cm}^{-2}$ and a linear range of 0.5-4.5 mM in pH 5.5 solution. Cheng *et al.*[179] reported an enzymatic glucose sensor modified with palladium/ reduced graphene oxide and GOx with a high sensitivity of 201 $\mu\text{A mM}^{-1} \text{cm}^{-2}$, a narrow linear range 0- 4 mM and a low detection limit of 0.34 μM . Zhong *et al.*[180] designed multi-wall carbon nanotube/conductive polyaniline nanocomposite with a sensitivity of 128 $\mu\text{A mM}^{-1} \text{cm}^{-2}$, the linear range of 0.003-8.2 mM and a low detection limit of 1 μM . Singh *et al.*[181] prepared a sulfonated poly(ether-ether-ketone) functionalised ternary graphene/AuNPs/chitosan nanocomposite for efficient glucose biosensor and obtained a sensitivity of 6.51 $\mu\text{A mM}^{-1} \text{cm}^{-2}$ with a wide linear range of 0.5-22.2 mM and a low detection limit of 0.13 μM . All these enzymatic sensors are designed to work at physiological pH in order to ensure enzyme stability. A survey of literature relating to enzymatic glucose sensor performance is provided in Table 2.

Table 2: Enzymatic glucose sensor performance.

Electrode Material	Sensitivity ($\mu\text{A mM}^{-1}\text{ cm}^{-2}$)	Linear range (mM)	LOD/ μM	Operational potential/ V	Medium	Ref.
GCE/BCNTs/POAP-GOx	2.43	Up to 8	3.6	+0.60 vs SCE	PBS pH 7.0	[182]
GOx/PAniNF/MCPE	57.79	-	-	+1.0 vs Ag/AgCl	AB pH 4.5	[174]
CS/AgNWs/GOx/GCE	16.72	1–15	-	-0.70 vs SCE	PBS pH 7.4	[177]
Chi/GOx/PB-G string electrode	641.3	0.03 - 1	10	-0.05 vs Ag/AgCl	PBS pH 7.4	[172]
GOx/AuNPs/BSA/Fe ₃ O ₄	115.3	0.25 - 7.0	3.54	+0.4 vs Ag/AgCl	PBS pH 7.4	[176]
GNS-PEI-AuNPs/GOx/GCE	93	0.001- 0.1	0.32	-0.35 vs Ag/AgCl	PBS pH 7.0	[183]
HMMP SiO ₂ -Au bilayer/GOx/ GCE	18	0.1 - 10	50	+0.35 vs Ag/AgCl	PBS pH 6.86	[184]
GOx/NiO/TiO ₂ -Gr/GCE	4.129	1.0– 12.0	1.2	-0.4 vs SCE	PBS pH 7.0	[185]
GOx/PtNP/PAni/Pt	96.1	0.01- 8	0.7	+0.56 vs SCE	PBS pH 5.6	[79]
GOx/AuNPs/PAni/GC	73.25	0.001- 0.8	0.5	+0.6 vs SCE	PBS pH 6.9	[186]
GOx/Pt/MWNT-PAni/GCE	128	0.003- 8.2	1	+0.55 vs SCE	PBS pH 7.0	[180]

GOx/(Pt/C)/GCE	125	0-45	<300	+0.7 vs Ag/AgCl	PBS pH 7.4	[187]
GOx/MWCNT/Pt	52.7	0-28	30	+0.4 vs SCE	PBS pH 7.4	[188]
GNPs/CD-Fc/GOx	18.2	0.08- 11.5	15	+0.25 vs SCE	PBS pH 7.0	[189]
Fc-C ₆ -LPEI/ SWCNT	74	0 – 10	-	0.35 vs SCE	PBS pH 7	[190]
MWCNT-Fc/ chitosan- GOx	25	0 – 3.8	0.003	0.35 vs Ag/AgCl	0.1M PBS pH7	[191]
Fc-PAH-MWCNT/GOx	30.8	0 - 10	-	0.5 vs Ag/AgCl	0.01M PBS pH7	[192]
GOx/Pd/RGO/GCE	201	0-4	0.34	+0.5 vs Ag/AgCl	PBS pH 6.85	[179]
MnO ₂ /GOx/Screen- Printed Carbon Ink	7.6	0.011 - 13	0.0005	+0.48 vs. Ag/AgCl.	0.1 M PBS pH 7.5	[193]
GOx/SPG-AuNPs- CH/ITO	6.51	0.5- 22.2	0.13	+0.3 vs Ag/AgCl	PBS pH 7.0	[181]

Abbreviations: GCE- glassy carbon electrode; BCNT- boron doped carbon nanotubes; POAP - poly(*o*-aminophenol); GOx – glucose oxidase; AB – acetate buffer; CS- chitosan; Chi – chitosan; PB - prussian blue; BSA - bovine serum albumin; GNS - graphene; Gr- graphene; RGO – reduce graphene oxide; HMMP - hierarchical meso-macroporous; PAH - Poly(allylamine hydrochloride); SPG – screen printed graphene; PANi – Polyaniline.

1.6. Advantages and disadvantages of enzymatic and non-enzymatic electrodes

The two electrode approaches have advantages and disadvantages. Consequently, it is necessary to overcome these drawbacks in the fabrication of both electrocatalytic electrodes for glucose sensing and in glucose fuel cell applications. Thus, biocompatibility studies along with stability and lifetime testing are required in achieving high performance. The advantages and disadvantages [103, 194] are listed in Table 3.

Table 3: Advantages and disadvantages of enzymatic and non-enzymatic electrodes

	<i>Advantages</i>	<i>Disadvantages</i>
<i>Enzymatic</i>	<ul style="list-style-type: none"> • Low detection limits • High selectivity and less interference • Active in physiological pHs 	<ul style="list-style-type: none"> • Low stability • Complicated enzyme immobilisation procedures • Sensitive to external conditions, eg – temperature
<i>Non-enzymatic</i>	<ul style="list-style-type: none"> • High sensitivity • Low cost • Good stability • Wide dynamic range 	<ul style="list-style-type: none"> • Prone to surface poisoning • Most catalysts are active in alkaline pH

1.7. Electrochemical techniques used in this study

1.7.1. Cyclic voltammetry

Cyclic voltammetry is a simple, widely used electroanalytical technique [195], which uses a three electrode cell system with an electrolyte. The three electrodes are the working electrode, the reference electrode and an auxiliary electrode. In this technique, the potential applied to the working electrode is varied between the initial value and an upper or lower limit. The initial potential could be the upper or lower values, or the open circuit potential. The potential of the working electrode is controlled relative to the reference electrode. The output current which is the response signal, gives rise to a cyclic voltammogram [195]. Cyclic voltammetry is mostly used to probe the nature of a redox process that taken place at an electrode/electrolyte interface. A simple cyclic voltammogram can provide information on the formal redox potential (E_F^o), oxidation current, reduction current, peak separation/ reversibility, kinetics etc. [196]. The formal redox potential for a reversible process is the average of oxidation peak potential (E_{ox}^P) and reduction peak potential (E_{red}^P) and can be calculated as in equation (1.9);

$$E_F^o = \frac{E_{ox}^P + E_{red}^P}{2} \quad (1.9)$$

The separation of the peak potentials (ΔE_p) gives information regarding the number of electrons (n) transferred in the electrode reaction and it can be evaluated from equation (1.10);

$$\Delta E_p = E_{ox}^P - E_{red}^P \cong \frac{0.057}{n} \quad \text{at } 25^\circ \text{ C} \quad (1.10)$$

The peak current of a reversible process can be evaluated by using the Randles- Sevcik equation [197] given in equation (1.11);

$$I_p = 0.4463nFAC\left(\frac{nFvD}{RT}\right)^{1/2} \quad (1.11)$$

where I_p is the peak current, n is the number of electrons for the redox couple, F = Faraday's constant ($96,485 \text{ C mol}^{-1}$), A = electrode area (cm^2), C = concentration of the analyte (mol cm^{-3}), v = rate at which the potential is swept (V s^{-1}), D = analyte diffusion coefficient ($\text{cm}^2 \text{ s}^{-1}$), R = universal gas constant ($8.314 \text{ J mol}^{-1} \text{ K}^{-1}$), and T = absolute temperature (K).

In electrocatalysis, these parameters and equations provided above are used to assess the performance of the catalyst. Cyclic voltammetry uses a linear potential scan with a triangular waveform as shown in Figure 4 [198]. A typical cyclic voltammogram for a one electron transfer is illustrated in Figure 5. Thus, a voltammogram is a display of current versus potential [195].

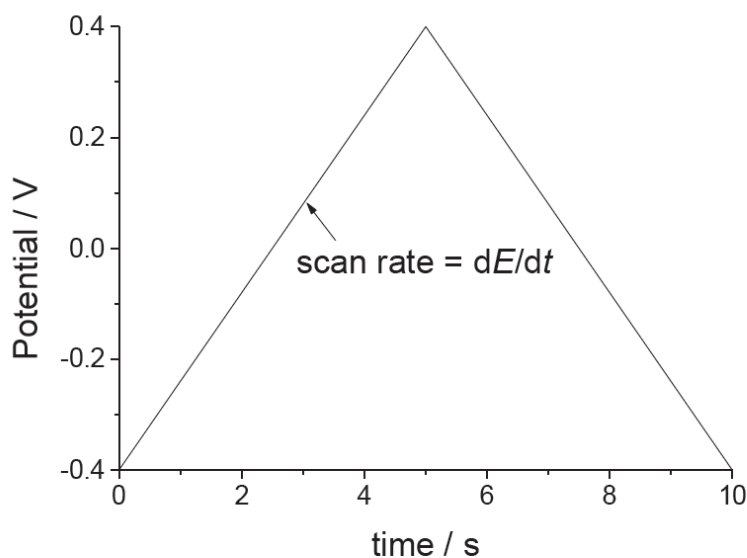


Figure 4: A schematic diagram showing the wave form employed in dc cyclic voltammetry (taken from ref [198]).

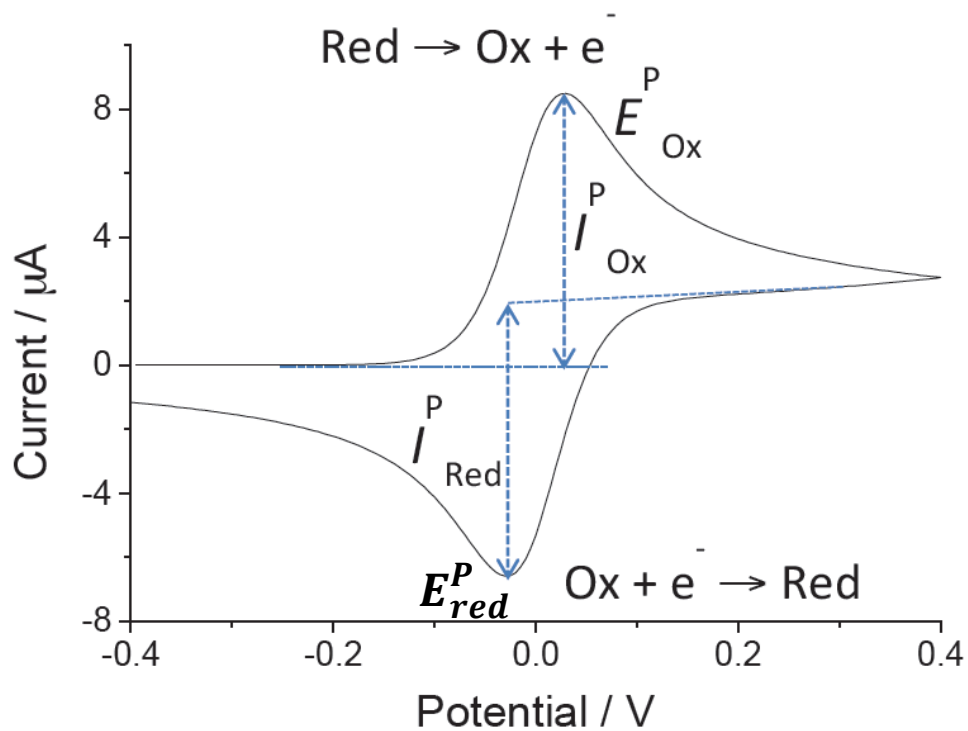


Figure 5: A cyclic voltammogram for a simple one electron oxidation process. The symbols used in the diagram are as follows; t = time, E = potential versus a reference electrode such as Ag/AgCl, Red = reduced form, Ox = oxidised form, E_{Ox}^P = oxidation peak potential, E_{red}^P = reduction peak potential, I_{Ox}^P = oxidation peak current, I_{red}^P = reduction peak current (taken from ref [198]).

1.7.2. Rotating disc electrode

The rotating disc electrode (RDE) technique represents an extended version of voltammetry, in where a stationary electrode was replaced by a rotating disc as the working electrode (typically glassy carbon, platinum or gold) in a conventional three electrode cell. A simple RDE setup is illustrated in Figure 6.

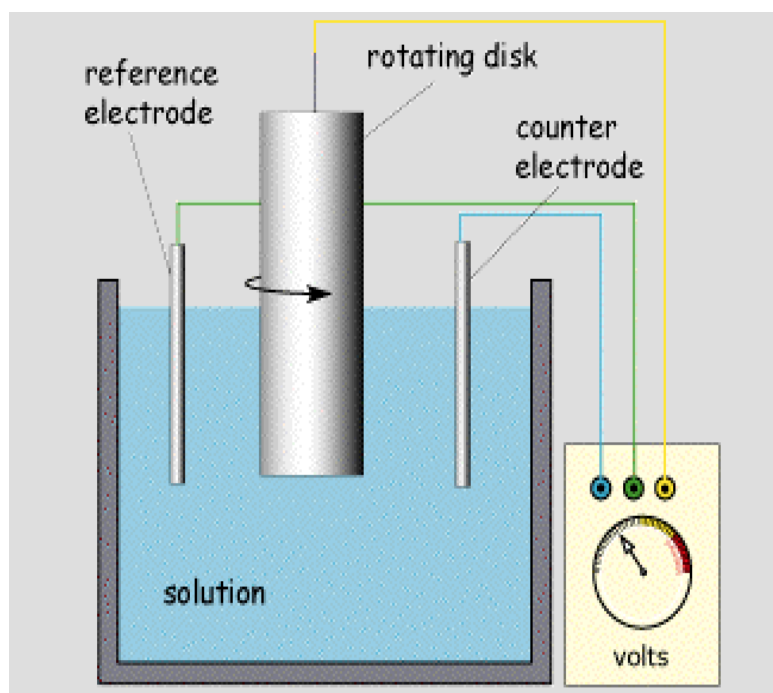


Figure 6: A conventional rotating disc electrode set up

The RDE allows studying kinetics under the hydrodynamic condition [199] and can be used to find out whether a process is kinetically or mass transport controlled. The theory behind RDE was described by Levich in 1942[200] and the variation of the mass transport limiting current as a function of rotation speed can be analysed. The Levich equation (1.12) is:

$$I_{lim} = 0.62nFAD^{2/3}\nu^{-1/6}\omega^{1/2}C \quad (1.12)$$

where I_{lim} = limiting current, n = total number of electrons transferred, F = Faraday constant ($96485.34 \text{ C mol}^{-1}$), A = area of the electrode (cm^2), D = diffusion coefficient ($\text{cm}^2 \text{ s}^{-1}$), ν = kinematic viscosity of the electrolyte ($\text{cm}^2 \text{ s}^{-1}$), ω = rotational speed (rad s^{-1}), C = concentration of the analyte (mol cm^{-3}). Sigmoidal curves (Figure 7) rather than peak shaped one, are obtained with a steady state limiting current (I_{ss}) under hydrodynamic conditions with RDE.

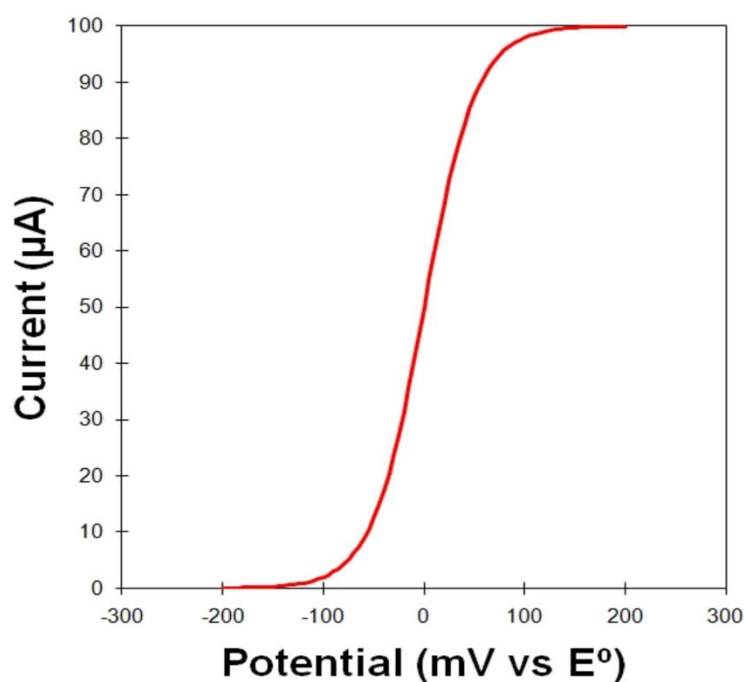


Figure 7: Sigmoidal curve obtained with a steady state limiting current (I_{ss}) under hydrodynamic conditions at a RDE.

1.7.3. Bulk electrolysis

Potentiostatic coulometry or controlled potential coulometry are other names for bulk electrolysis[201, 202]. This method is also carried out in a three electrode system in a one, two or three compartment cell with the working electrode being larger than those used in voltammetry. Continuous stirring[203] (enhances convection) is essential to enhance analyte to contact with working electrode. Figure 8 illustrates H-shaped bulk electrolysis cell setup.

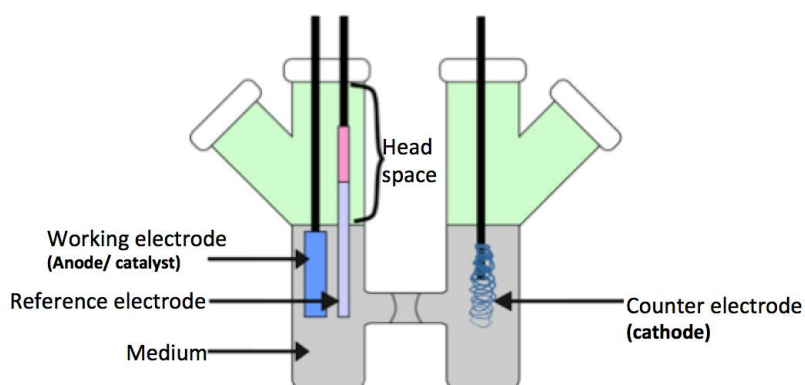


Figure 8: Schematic representation of H-shaped bulk electrolysis setup.

During the experiment, the potential of the working electrode is held constant and the current monitored as a function of time[204]. Upon injection the data are displayed as coulombs (C) versus time (s)[205]. Faraday's law of electrolysis given in equation (1.13) expresses the relationship between charge (Q), current (I) and the electrolysis time (t) [206]:

$$Q = \int_0^t I dt \quad (1.13)$$

During bulk electrolysis the current decreases as the analyte is consumed with time and reaches zero when the substrate conversion is complete [204] as shown in Figure 9. The

mass transfer of the analyte in the solution to the electrode surface determines the rate of electrolysis [204].

Bulk electrolysis is often used in industry for electrometallurgy, cleaning and plating of metals, production of H₂ as fuels, production of chemicals and rust removal etc. [207]. In this study bulk electrolysis is used to evaluate final products of electrolysis and establish the efficiency of new catalysis.

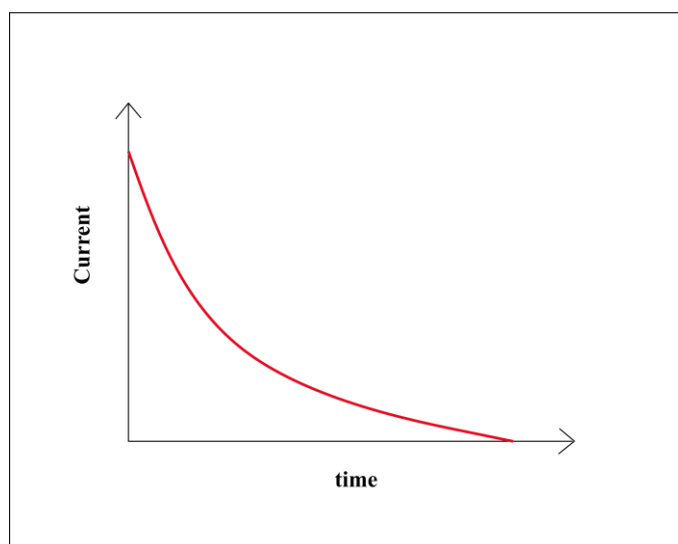


Figure 9: A plot of current vs time in bulk electrolysis.

1.7.4. Fourier transformed AC voltammetry

Fourier transformed AC voltammetry (FTACV) is a very sensitive technique that enables some electrode processes to be studied more efficiently compared to DC voltammetry. In DC voltammetry, the faradaic signal generated from a surface confined redox species is often very small and neglected by background catalysis current [208]. However, the higher mode harmonics in FTACV technique have a very low background. In FTACV as used in this thesis, a large amplitude ac perturbation is superimposed onto the dc ramp. Fourier transformation (FT) and inverse FT are used to resolve dc and ac harmonic components. The higher order harmonics are devoid of background charging current [209] and highly sensitive to the kinetics of heterogeneous electron transfer process [210]. The harmonics are used to evaluate the kinetics of electron transfer processes. Surface heterogeneity also can be more readily identified using the FTACV technique [211]. Figure 10 presents a schematic representation of the waveform used in FTACV and Figure 11 illustrates how data analysis is undertaken.

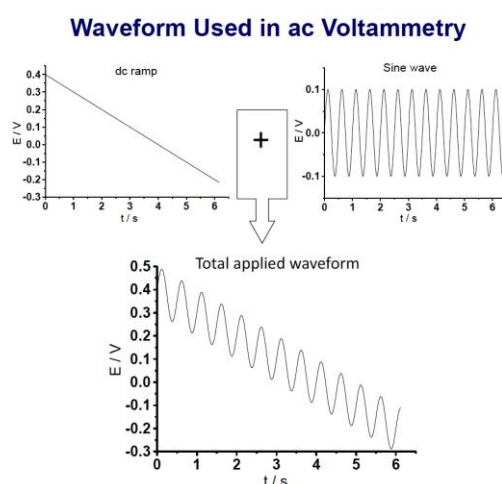


Figure 10: Schematic representation of the waveform used in ac voltammetry, taken from ref [198]

Data Analysis

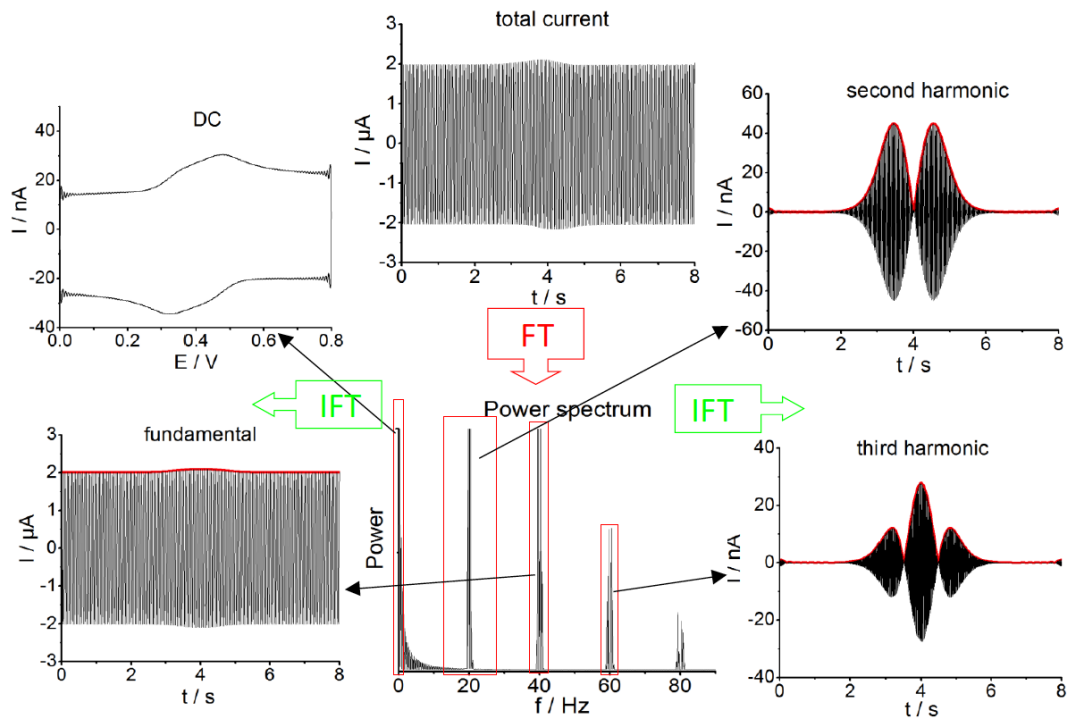


Figure 11: A schematic representation of data analysis used in FTACV, taken from ref [198]

1.8. Research objectives

This thesis study is aimed at developing the science and engineering required for generation of low-cost and recyclable electrodes for electrocatalytic oxidation of glucose. The study seek new pathways to avoid surface poisoning from intermediates and aims to improve the selectivity towards glucose electrocatalytic processes which can be used in glucose sensors and fuel cell applications. To achieve the challenges provided, the following essential aspects need to be addressed:

1. Improve the electron transfer process between the electrode and the catalyst
2. Investigate novel catalysts and polymer nanocomposites to obtain high sensitivity and selectivity for the analytical application of glucose sensors and fuel cells.
3. Design and synthesise of nanocomposites that can immobilise and stabilise Glucose oxidase enzymes.

1.9. References

- [1] J. Lipkowsi, P.N. Ross, *Electrocatalysis*, John Wiley & Sons 1998.
- [2] D. Pletcher, *Electrocatalysis: present and future*, *J. Appl. Electrochem.*, 14 (1984) 403-415.
- [3] G.r. Li, F. Wang, Q.w. Jiang, X.p. Gao, P.w. Shen, *Carbon Nanotubes with Titanium Nitride as a Low-Cost Counter-Electrode Material for Dye-Sensitized Solar Cells*, *Angew. Chem. Int. Ed.*, 49 (2010) 3653-3656.
- [4] M.V. Twigg, M. Twigg, *Catalyst handbook*, CSIRO 1989.
- [5] X. Lu, C. Zhao, *Electrodeposition of hierarchically structured three-dimensional nickel–iron electrodes for efficient oxygen evolution at high current densities*, *Nat. Commun.*, 6 (2015).
- [6] E. Bakker, M. Telting-Diaz, *Electrochemical sensors*, *Anal. Chem.*, 74 (2002) 2781-2800.
- [7] F.A. Armstrong, J. Hirst, *Reversibility and efficiency in electrocatalytic energy conversion and lessons from enzymes*, *Proc. Natl. Acad. Sci.*, 108 (2011) 14049-14054.
- [8] P.C. Hallenbeck, D. Ghosh, M.T. Skonieczny, V. Yargeau, *Microbiological and engineering aspects of biohydrogen production*, *Indian J. Microbiol.*, 49 (2009) 48-59.
- [9] S.I. Beale, *Enzymes of chlorophyll biosynthesis*, *Photosynth. Res.*, 60 (1999) 43-73.
- [10] W.T. Cefalu, J. Ye, Z.Q. Wang, *Efficacy of dietary supplementation with botanicals on carbohydrate metabolism in humans*, *Endocr. Metab. Immune Disord. Drug Targets*, 8 (2008) 78-81.
- [11] D.L. Ladd, A. Altshuler, *The Medical Library Association guide to finding out about diabetes: the best print and electronic resources*, American Library Association 2013.
- [12] G. Boden, M. Laakso, *Lipids and Glucose in Type 2 Diabetes What is the cause and effect?*, *Diabetes care*, 27 (2004) 2253-2259.

- [13] B. Houssay, A. Biasotti, The hypophysis, carbohydrate metabolism and diabetes, *Endocrinology*, 15 (1931) 511-523.
- [14] A.A. Young, C. Bogardus, K. Stone, D.M. Mott, Insulin response of components of whole-body and muscle carbohydrate metabolism in humans, *Am. J. Physiol. Endocrinol. Metab.*, 254 (1988) E231-E236.
- [15] D.G. Rackus, M.H. Shamsi, A.R. Wheeler, Electrochemistry, biosensors and microfluidics: a convergence of fields, *Chem. Soc. Rev.*, 44 (2015) 5320-5340.
- [16] R. Gifford, Continuous Glucose Monitoring: 40 Years, What We've Learned and What's Next, *ChemPhysChem*, 14 (2013) 2032-2044.
- [17] C. Boozer, G. Kim, S. Cong, H. Guan, T. Londergan, Looking towards label-free biomolecular interaction analysis in a high-throughput format: a review of new surface plasmon resonance technologies, *Curr. Opin. Biotechnol.*, 17 (2006) 400-405.
- [18] S. Hosseini, F. Ibrahim, I. Djordjevic, L.H. Koole, Recent advances in surface functionalization techniques on polymethacrylate materials for optical biosensor applications, *Analyst*, 139 (2014) 2933-2943.
- [19] X. Guo, B. Liang, J. Jian, Y. Zhang, X. Ye, Glucose biosensor based on a platinum electrode modified with rhodium nanoparticles and with glucose oxidase immobilized on gold nanoparticles, *Microchimica Acta*, 181 (2014) 519-525.
- [20] A.D. Association, Diagnosis and classification of diabetes mellitus, *Diabetes care*, 29 (2006) 43.
- [21] J. Assal, L. Groop, Definition, diagnosis and classification of diabetes mellitus and its complications, World Health Organization, (1999) 1-65.
- [22] E. Wilkins, Towards implantable glucose sensors: a review, *J. Biomed. Eng.*, 11 (1989) 354-361.

- [23] N.D.D. Group, Classification and diagnosis of diabetes mellitus and other categories of glucose intolerance, *Diabetes*, 28 (1979) 1039-1057.
- [24] H.C. Gerstein, Intensive blood glucose control reduced type 2 diabetes mellitus-related end points, *ACP J. Club*, 130 (1999) 2-2.
- [25] L.C. Clark, C. Lyons, Electrode systems for continuous monitoring in cardiovascular surgery, *Ann. N. Y. Acad. Sci.*, 102 (1962) 29-45.
- [26] S. Park, H. Boo, T.D. Chung, Electrochemical non-enzymatic glucose sensors, *Anal. Chim. Acta.*, 556 (2006) 46-57.
- [27] E. Witkowska Nery, M. Kundys, P.S. Jelen, M. Jonsson-Niedziolka, Electrochemical Glucose Sensing: Is There Still Room for Improvement?, *Anal. Chem.*, 88 (2016) 11271-11282.
- [28] P. Si, Y. Huang, T. Wang, J. Ma, Nanomaterials for electrochemical non-enzymatic glucose biosensors, *Rsc Adv.*, 3 (2013) 3487-3502.
- [29] J. Wang, Electrochemical Glucose Biosensors, *Chem. Rev.*, 108 (2008) 814-825.
- [30] A.P. Turner, Biosensors: sense and sensibility, *Chem. Soc. Rev.*, 42 (2013) 3184-3196.
- [31] S. Poyraz, Z. Liu, Y. Liu, N. Lu, M.J. Kim, X. Zhang, One-step synthesis and characterization of poly (o-toluidine) nanofiber/metal nanoparticle composite networks as non-enzymatic glucose sensors, *Sens. Actuators B Chem.*, 201 (2014) 65-74.
- [32] S. Prakash, T. Chakrabarty, A.K. Singh, V.K. Shahi, Polymer thin films embedded with metal nanoparticles for electrochemical biosensors applications, *Biosens. Bioelectron.*, 41 (2013) 43-53.
- [33] L. Salomon, J.E. Johnson, Enzymatic microdetermination of glucose in blood and urine, *Anal. Chem.*, 31 (1959) 453-456.

- [34] A.J. Bandodkar, W. Jia, C. Yardımcı, X. Wang, J. Ramirez, J. Wang, Tattoo-based noninvasive glucose monitoring: a proof-of-concept study, *Anal. Chem.*, 87 (2014) 394-398.
- [35] R. Badugu, J.R. Lakowicz, C.D. Geddes, A glucose sensing contact lens: a non-invasive technique for continuous physiological glucose monitoring, *J. Fluoresc.*, 13 (2003) 371-374.
- [36] A. Kagie, D.K. Bishop, J. Burdick, J.T. La Belle, R. Dymond, R. Felder, J. Wang, Flexible Rolled Thick-Film Miniaturized Flow-Cell for Minimally Invasive Amperometric Sensing, *Electroanalysis*, 20 (2008) 1610-1614.
- [37] H. Kudo, T. Sawada, E. Kazawa, H. Yoshida, Y. Iwasaki, K. Mitsubayashi, A flexible and wearable glucose sensor based on functional polymers with Soft-MEMS techniques, *Biosens. Bioelectron.*, 22 (2006) 558-562.
- [38] J.Q. Brown, M.J. McShane, Modeling of spherical fluorescent glucose microsensor systems: design of enzymatic smart tattoos, *Biosens. Bioelectron.*, 21 (2006) 1760-1769.
- [39] Y.J. Heo, S. Takeuchi, Towards smart tattoos: implantable biosensors for continuous glucose monitoring, *Adv. Healthc. Mater.*, 2 (2013) 43-56.
- [40] A.J. Bandodkar, W. Jia, J. Wang, Tattoo-Based Wearable Electrochemical Devices: A Review, *Electroanalysis*, 27 (2015) 562-572.
- [41] R. Srivastava, R.D. Jayant, A. Chaudhary, M.J. McShane, "Smart tattoo" glucose biosensors and effect of coencapsulated anti-inflammatory agents, *J. Diabetes Sci. Technol.*, 5 (2011) 76-85.
- [42] H. Yao, Y. Liao, A. Lingley, A. Afanasiev, I. Lähdesmäki, B. Otis, B. Parviz, A contact lens with integrated telecommunication circuit and sensors for wireless and continuous tear glucose monitoring, *J. Micromech. Microeng.*, 22 (2012) 075007.

- [43] H. Yao, A.J. Shum, M. Cowan, I. Lähdesmäki, B.A. Parviz, A contact lens with embedded sensor for monitoring tear glucose level, *Biosens. Bioelectron.*, 26 (2011) 3290-3296.
- [44] L. Carrette, K. Friedrich, U. Stimming, Fuel cells—fundamentals and applications, *Fuel cells*, 1 (2001) 5-39.
- [45] N. Panwar, S. Kaushik, S. Kothari, Role of renewable energy sources in environmental protection: a review, *Renew. Sustainable Energy Rev.*, 15 (2011) 1513-1524.
- [46] D. Bahnemann, Photocatalytic water treatment: solar energy applications, *Solar energy*, 77 (2004) 445-459.
- [47] A. Cherubini, R. Vertechy, M. Fontana, Simplified model of offshore Airborne Wind Energy Converters, *Renew. Energy*, 88 (2016) 465-473.
- [48] D. Vieira, L. Guedes, A. Lisboa, R. Saldanha, Formulations for hydroelectric energy production with optimality conditions, *Energy Convers. Manage.*, 89 (2015) 781-788.
- [49] M.I. Alhamid, Y. Daud, A. Surachman, A. Sugiyono, H. Aditya, T. Mahlia, Potential of geothermal energy for electricity generation in Indonesia: A review, *Renew. Sust. Energ. Rev.*, 53 (2016) 733-740.
- [50] H. Wang, J.-D. Park, Z.J. Ren, Practical energy harvesting for microbial fuel cells: a review, *Environ. Sci. Technol.*, 49 (2015) 3267-3277.
- [51] A. Rabis, P. Rodriguez, T.J. Schmidt, Electrocatalysis for polymer electrolyte fuel cells: recent achievements and future challenges, *Acs Catal.*, 2 (2012) 864-890.
- [52] S.D. Minteer, B.Y. Liaw, M.J. Cooney, Enzyme-based biofuel cells, *Curr. Opin. Biotechnol.*, 18 (2007) 228-234.

- [53] Q. Xu, F. Zhang, L. Xu, P. Leung, C. Yang, H. Li, The applications and prospect of fuel cells in medical field: A review, *Renew. Sustainable Energy Rev.*, 67 (2017) 574-580.
- [54] P. Atanassov, C. Apblett, S. Banta, S. Brozik, S.C. Barton, M. Cooney, B.Y. Liaw, S. Mukerjee, S.D. Minteer, Enzymatic biofuel cells, *Electrochem. Soc. Interface.*, 16 (2007) 28-31.
- [55] K. Rabaey, N. Boon, S.D. Siciliano, M. Verhaege, W. Verstraete, Biofuel cells select for microbial consortia that self-mediate electron transfer, *Appl. Environ. Microbiol.*, 70 (2004) 5373-5382.
- [56] P. Ó Conghaile, M. Falk, D. MacAodha, M.E. Yakovleva, C. Gonaus, C.K. Peterbauer, L. Gorton, S. Shleev, D. Leech, Fully Enzymatic Membraneless Glucose|Oxygen Fuel Cell That Provides 0.275 mA cm⁻² in 5 mM Glucose, Operates in Human Physiological Solutions, and Powers Transmission of Sensing Data, *Anal. Chem.*, 88 (2016) 2156-2163.
- [57] A. Habrioux, K. Servat, S. Tingry, K. Kokoh, Enhancement of the performances of a single concentric glucose/O₂ biofuel cell by combination of bilirubin oxidase/Nafion cathode and Au–Pt anode, *Electrochem. Commun.*, 11 (2009) 111-113.
- [58] G. Göbel, M.L. Beltran, J. Mundhenk, T. Heinlein, J. Schneider, F. Lisdat, Operation of a carbon nanotube-based glucose/oxygen biofuel cell in human body liquids—Performance factors and characteristics, *Electrochim. Acta.*, 218 (2016) 278-284.
- [59] M. Christwardana, K.J. Kim, Y. Kwon, Fabrication of Mediatorless/Membraneless Glucose/Oxygen Based Biofuel Cell using Biocatalysts Including Glucose Oxidase and Laccase Enzymes, *Sci. Rep.*, 6 (2016).
- [60] F.v. Stetten, S. Kerzenmacher, A. Lorenz, V. Chokkalingam, N. Miyakawa, R. Zengerle, J. Duce, A one-compartment, direct glucose fuel cell for powering long-term

medical implants, 19th IEEE international conference on micro electro mechanical systems, IEEE, 2006, pp. 934-937.

[61] S. Kerzenmacher, J. Ducreé, R. Zengerle, F. Von Stetten, Energy harvesting by implantable abiotically catalyzed glucose fuel cells, *J. Power Sources*, 182 (2008) 1-17.

[62] S.K. Chaudhuri, D.R. Lovley, Electricity generation by direct oxidation of glucose in mediatorless microbial fuel cells, *Nat. Biotechnol.*, 21 (2003) 1229-1232.

[63] F. Kang, Y. Wu, T. Li, Research progress in biofuel cell, *Chin. J. Power Sources*, (2003) 723-727.

[64] N. Mano, F. Mao, A. Heller, A miniature biofuel cell operating in a physiological buffer, *J. Am. Chem. Soc.*, 124 (2002) 12962-12963.

[65] N. Mano, F. Mao, W. Shin, T. Chen, A. Heller, A miniature biofuel cell operating at 0.78 V, *Chem. Commun.*, (2003) 518-519.

[66] N.P. Godman, J.L. DeLuca, S.R. McCollum, D.W. Schmidtke, D.T. Glatzhofer, Electrochemical Characterization of Layer-By-Layer Assembled Ferrocene-Modified Linear Poly (ethylenimine)/Enzyme Bioanodes for Glucose Sensor and Biofuel Cell Applications, *Langmuir*, 32 (2016) 3541-3551.

[67] Y. Wang, S. Zhang, W. Bai, J. Zheng, Layer-by-layer assembly of copper nanoparticles and manganese dioxide-multiwalled carbon nanotubes film: A new nonenzymatic electrochemical sensor for glucose, *Talanta*, 149 (2016) 211-216.

[68] X. Cao, K. Wang, G. Du, A.M. Asiri, Y. Ma, Q. Lu, X. Sun, One-step electrodeposition of a nickel cobalt sulfide nanosheet film as a highly sensitive nonenzymatic glucose sensor, *J. Mater. Chem. B*, 4 (2016) 7540-7544.

[69] G. Suganthi, T. Arockiadoss, T. Uma, ZnS nanoparticles decorated graphene nanoplatelets as immobilisation matrix for glucose biosensor, *Nanosystems: Phys. Chem. Math.*, 7 (2016) 637.

- [70] M. Chowdhury, F. Cummings, M. Kebede, V. Fester, Binderless Solution Processed Zn Doped Co₃O₄ Film on FTO for Rapid and Selective Non-enzymatic Glucose Detection, *Electroanalysis*, (2016).
- [71] X.-W. Liu, P. Pan, Z.-M. Zhang, F. Guo, Z.-C. Yang, J. Wei, Z. Wei, Ordered self-assembly of screen-printed flower-like CuO and CuO/MWCNTs modified graphite electrodes and applications in non-enzymatic glucose sensor, *J. Electroanal. Chem.*, 763 (2016) 37-44.
- [72] O. Amor-Gutiérrez, E.C. Rama, A. Costa-García, M. Fernández-Abedul, Paper-based maskless enzymatic sensor for glucose determination combining ink and wire electrodes, *Biosens. Bioelectron.*, (2016).
- [73] S.A. Soper, M. Hashimoto, C. Situma, M.C. Murphy, R.L. McCarley, Y.-W. Cheng, F. Barany, Fabrication of DNA microarrays onto polymer substrates using UV modification protocols with integration into microfluidic platforms for the sensing of low-abundant DNA point mutations, *Methods*, 37 (2005) 103-113.
- [74] S.-S. Lee, J.-D. Hong, C.H. Kim, K. Kim, J.P. Koo, K.-B. Lee, Layer-by-layer deposited multilayer assemblies of ionene-type polyelectrolytes based on the spin-coating method, *Macromolecules*, 34 (2001) 5358-5360.
- [75] M. Ates, A review study of (bio) sensor systems based on conducting polymers, *Materials Science and Engineering: C*, 33 (2013) 1853-1859.
- [76] T.F. Otero, J.M. Sansieña, Soft and wet conducting polymers for artificial muscles, *Adv. Mater.*, 10 (1998) 491-494.
- [77] T.A. Skotheim, J. Reynolds, *Handbook of Conducting Polymers*, 2 Volume Set, CRC press 2007.

- [78] M. Yuqing, C. Jianrong, W. Xiaohua, Using electropolymerized non-conducting polymers to develop enzyme amperometric biosensors, *TRENDS in Biotechnol.*, 22 (2004) 227-231.
- [79] D. Zhai, B. Liu, Y. Shi, L. Pan, Y. Wang, W. Li, R. Zhang, G. Yu, Highly Sensitive Glucose Sensor Based on Pt Nanoparticle/Polyaniline Hydrogel Heterostructures, *ACS Nano*, 7 (2013) 3540-3546.
- [80] M.C.D. Cooray, Y. Liu, S.J. Langford, A.M. Bond, J. Zhang, One pot synthesis of poly(5-hydroxyl-1,4-naphthoquinone) stabilized gold nanoparticles using the monomer as the reducing agent for nonenzymatic electrochemical detection of glucose, *Anal. Chim. Acta*, 856 (2015) 27-34.
- [81] D. Cooray, S. Sandanayake, F. Li, S.J. Langford, A.M. Bond, J. Zhang, Efficient Enzymatic Oxidation of Glucose Mediated by Ferrocene Covalently Attached to Polyethylenimine Stabilized Gold Nanoparticles, *Electroanalysis*, 28 (2016) 2728-2736.
- [82] A.A. Balandin, Thermal properties of graphene and nanostructured carbon materials, *Nat. Mater.*, 10 (2011) 569-581.
- [83] V. Georgakilas, J.N. Tiwari, K.C. Kemp, J.A. Perman, A.B. Bourlinos, K.S. Kim, R. Zboril, Noncovalent Functionalization of Graphene and Graphene Oxide for Energy Materials, Biosensing, Catalytic, and Biomedical Applications, *Chem. Rev.*, 116 (2016) 5464-5519.
- [84] M.S. Dresselhaus, G. Dresselhaus, P.C. Eklund, *Science of fullerenes and carbon nanotubes: their properties and applications*, Academic press 1996.
- [85] K.S. Novoselov, A.K. Geim, S.V. Morozov, D. Jiang, Y. Zhang, S.V. Dubonos, I.V. Grigorieva, A.A. Firsov, Electric field effect in atomically thin carbon films, *science*, 306 (2004) 666-669.

- [86] A.A. Balandin, S. Ghosh, W. Bao, I. Calizo, D. Teweldebrhan, F. Miao, C.N. Lau, Superior thermal conductivity of single-layer graphene, *Nano Lett.*, 8 (2008) 902-907.
- [87] J. Lee, J. Kim, S. Kim, D.-H. Min, Biosensors based on graphene oxide and its biomedical application, *Adv. Drug Deliv. Rev.*, (2016).
- [88] S.-G. Hong, J.H. Kim, R.E. Kim, S.-J. Kwon, D.W. Kim, H.-T. Jung, J.S. Dordick, J. Kim, Immobilization of glucose oxidase on graphene oxide for highly sensitive biosensors, *Biotechnol. Bioprocess Eng* . 21 (2016) 573-579.
- [89] S. Iijima, Helical microtubules of graphitic carbon, *Nature*, 354 (1991) 56-58.
- [90] J. Wang, M. Musameh, Carbon-nanotubes doped polypyrrole glucose biosensor, *Anal. Chim. Acta*, 539 (2005) 209-213.
- [91] F.A. Gutierrez, M.D. Rubianes, G.A. Rivas, Electrochemical sensor for amino acids and glucose based on glassy carbon electrodes modified with multi-walled carbon nanotubes and copper microparticles dispersed in polyethylenimine, *J. Electroanal. Chem.*, 765 (2016) 16-21.
- [92] K. Elouarzaki, M. Holzinger, A. Le Goff, J. Thery, R. Marks, S. Cosnier, Glucose fuel cell based on carbon nanotube-supported pyrene–metalloporphyrin catalysts, *J. Mater. Chem. A*, 4 (2016) 10635-10640.
- [93] J. Wang, Carbon-nanotube based electrochemical biosensors: A review, *Electroanalysis*, 17 (2005) 7-14.
- [94] M.E. Davis, Ordered porous materials for emerging applications, *Nature*, 417 (2002) 813-821.
- [95] Y. Hamano, S. Tsujimura, O. Shirai, K. Kano, Control of the pore size distribution of carbon cryogels by pH adjustment of catalyst solutions, *Mater. Lett.*, 128 (2014) 191-194.

- [96] A.S. Arico, P. Bruce, B. Scrosati, J.-M. Tarascon, W. Van Schalkwijk, Nanostructured materials for advanced energy conversion and storage devices, *Nat. Mater.*, 4 (2005) 366-377.
- [97] J. Chmiola, G. Yushin, Y. Gogotsi, C. Portet, P. Simon, P.-L. Taberna, Anomalous increase in carbon capacitance at pore sizes less than 1 nanometer, *Science*, 313 (2006) 1760-1763.
- [98] M. Moyo, J.O. Okonkwo, N.M. Agyei, Recent advances in polymeric materials used as electron mediators and immobilizing matrices in developing enzyme electrodes, *Sensors (Basel)*, 12 (2012) 923-953.
- [99] M. Gerard, A. Chaubey, B.D. Malhotra, Application of conducting polymers to biosensors, *Biosens. Bioelectron.*, 17 (2002) 345-359.
- [100] J.-C. Vidal, E. Garcia-Ruiz, J.-R. Castillo, Recent Advances in Electropolymerized Conducting Polymers in Amperometric Biosensors, *Microchim. Acta*, 143 (2003) 93-111.
- [101] J. Wang, H. Gao, F. Sun, C. Xu, Nanoporous PtAu alloy as an electrochemical sensor for glucose and hydrogen peroxide, *Sens. Actuator B Chem.*, 191 (2014) 612-618.
- [102] L.-M. Lu, L. Zhang, F.-L. Qu, H.-X. Lu, X.-B. Zhang, Z.-S. Wu, S.-Y. Huan, Q.-A. Wang, G.-L. Shen, R.-Q. Yu, A nano-Ni based ultrasensitive nonenzymatic electrochemical sensor for glucose: Enhancing sensitivity through a nanowire array strategy, *Biosens. Bioelectron.*, 25 (2009) 218-223.
- [103] X. Niu, X. Li, J. Pan, Y. He, F. Qiu, Y. Yan, Recent advances in non-enzymatic electrochemical glucose sensors based on non-precious transition metal materials: opportunities and challenges, *RSC Adv.*, 6 (2016) 84893-84905.
- [104] C. Chen, Q. Xie, D. Yang, H. Xiao, Y. Fu, Y. Tan, S. Yao, Recent advances in electrochemical glucose biosensors: a review, *Rsc Adv.*, 3 (2013) 4473-4491.

- [105] L. Burke, Premonolayer oxidation and its role in electrocatalysis, *Electrochim. Acta.*, 39 (1994) 1841-1848.
- [106] H. Zhang, N. Toshima, Glucose oxidation using Au-containing bimetallic and trimetallic nanoparticles, *Catal. Sci. Tech.*, 3 (2013) 268.
- [107] M. Comotti, C. Della Pina, M. Rossi, Mono- and bimetallic catalysts for glucose oxidation, *J. Mol. Catal. A: Chem.*, 251 (2006) 89-92.
- [108] S. Poyraz, Z. Liu, Y. Liu, N. Lu, M.J. Kim, X. Zhang, One-step synthesis and characterization of poly(o-toluidine) nanofiber/metal nanoparticle composite networks as non-enzymatic glucose sensors, *Sensors and Actuators B*, 201 (2014) 65-74.
- [109] B. Sebez, L. Su, B. Ogorevc, Y. Tong, X. Zhang, Aligned carbon nanotube modified carbon fibre coated with gold nanoparticles embedded in a polymer film: Voltammetric microprobe for enzymeless glucose sensing, *Electrochem. Commun.*, 25 (2012) 94-97.
- [110] Y. Rong, R. Malpass-Evans, M. Carta, N.B. McKeown, G.A. Attard, F. Marken, Intrinsically Porous Polymer Protects Catalytic Gold Particles for Enzymeless Glucose Oxidation, *Electroanal.*, 26 (2014) 904-909.
- [111] J.-J. Yu, S. Lu, J.-W. Li, F.-Q. Zhao, B.-Z. Zeng, Characterization of gold nanoparticles electrochemically deposited on amine-functionalized mesoporous silica films and electrocatalytic oxidation of glucose, *J. Solid State Electrochem.*, 11 (2007) 1211-1219.
- [112] L. Zhou, T. Gan, D. Zheng, J. Yan, C. Hu, S. Hu, High-density gold nanoparticles on multi-walled carbon nanotube films: a sensitive electrochemical nonenzymatic platform of glucose, *J. Exp. Nanosci.*, 7 (2012) 263-273.

- [113] D. Feng, F. Wang, Z. Chen, Electrochemical glucose sensor based on one-step construction of gold nanoparticle–chitosan composite film, *Sensors and Actuators B*, 138 (2009) 539-544.
- [114] F. Kurniawan, V. Tsakova, V.M. Mirsky, Gold Nanoparticles in Nonenzymatic Electrochemical Detection of Sugars, *Electroanal.*, 18 (2006) 1937-1942.
- [115] B.K. Jena, C.R. Raj, Enzyme-Free Amperometric Sensing of Glucose by Using Gold Nanoparticles, *Chem. Eur. J.*, 12 (2006) 2702-2708.
- [116] Q. Yi, W. Huang, W. Yu, L. Li, X. Liu, Hydrothermal synthesis of titanium-supported nickel nanoflakes for electrochemical oxidation of glucose, *Electroanal.*, 20 (2008) 2016-2022.
- [117] T.-K. Huang, K.-W. Lin, S.-P. Tung, T.-M. Cheng, I.C. Chang, Y.-Z. Hsieh, C.-Y. Lee, H.-T. Chiu, Glucose sensing by electrochemically grown copper nanobelt electrode, *J. Electroanal. Chem.*, 636 (2009) 123-127.
- [118] I. Taurino, G. Sanzò, R. Antiochia, C. Tortolini, F. Mazzei, G. Favero, G. De Micheli, S. Carrara, Recent advances in Third Generation Biosensors based on Au and Pt Nanostructured Electrodes, *Trends Anal. Chem.*, 79 (2016) 151-159.
- [119] W. Zhao, J.-J. Xu, C.-G. Shi, H.-Y. Chen, Fabrication, characterization and application of gold nano-structured film, *Electrochem. Commun.*, 8 (2006) 773-778.
- [120] T.-M. Cheng, T.-K. Huang, H.-K. Lin, S.-P. Tung, Y.-L. Chen, C.-Y. Lee, H.-T. Chiu, (110)-Exposed Gold Nanocoral Electrode as Low Onset Potential Selective Glucose Sensor, *ACS Appl. Mater. Interfaces*, 2 (2010) 2773-2780.
- [121] Y. Ma, J. Di, X. Yan, M. Zhao, Z. Lu, Y. Tu, Direct electrodeposition of gold nanoparticles on indium tin oxide surface and its application, *Biosens. Bioelectron.*, 24 (2009) 1480-1483.

- [122] H. Ekram, A. Galal, N.F. Atta, Electrochemistry of glucose at gold nanoparticles modified graphite/srpd 3 electrode—towards a novel non-enzymatic glucose sensor, *J. Electroanal. Chem.*, 749 (2015) 42-52.
- [123] Q. Yi, W. Yu, F. Niu, Novel Nanoporous Binary Au[bond]Ru Electrocatalysts for Glucose Oxidation, *Electroanal.*, 22 (2010) 556-563.
- [124] J. Wang, D.F. Thomas, A. Chen, Nonenzymatic Electrochemical Glucose Sensor Based on Nanoporous PtPb Networks, *Anal. Chem. (Washington, DC, U. S.)*, 80 (2008) 997-1004.
- [125] H.-F. Cui, J.-S. Ye, W.-D. Zhang, C.-M. Li, J.H.T. Luong, F.-S. Sheu, Selective and sensitive electrochemical detection of glucose in neutral solution using platinum-lead alloy nanoparticle/carbon nanotube nanocomposites, *Anal. Chim. Acta*, 594 (2007) 175-183.
- [126] F. Xiao, F. Zhao, D. Mei, Z. Mo, B. Zeng, Nonenzymatic glucose sensor based on ultrasonic-electrodeposition of bimetallic PtM (M=Ru, Pd and Au) nanoparticles on carbon nanotubes-ionic liquid composite film, *Biosens. Bioelectron.*, 24 (2009) 3481-3486.
- [127] H. Gao, F. Xiao, C.B. Ching, H. Duan, One-Step Electrochemical Synthesis of PtNi Nanoparticle-Graphene Nanocomposites for Nonenzymatic Amperometric Glucose Detection, *ACS Appl. Mater. Interfaces*, 3 (2011) 3049-3057.
- [128] L. Zhao, G. Wu, Z. Cai, T. Zhao, Q. Yao, X. Chen, Ultrasensitive non-enzymatic glucose sensing at near-neutral pH values via anodic stripping voltammetry using a glassy carbon electrode modified with Pt3Pd nanoparticles and reduced graphene oxide, *Microchim. Acta*, 182 (2015) 2055-2060.

- [129] J. Ryu, K. Kim, H.-S. Kim, H.T. Hahn, D. Lashmore, Intense pulsed light induced platinum-gold alloy formation on carbon nanotubes for non-enzymatic glucose detection, *Biosens. Bioelectron.*, 26 (2010) 602-607.
- [130] L.-H. Li, W.-D. Zhang, J.-S. Ye, Electrocatalytic oxidation of glucose at carbon nanotubes supported PtRu nanoparticles and its detection, *Electroanal.*, 20 (2008) 2212-2216.
- [131] S.S. Mahshid, S. Mahshid, A. Dolati, M. Ghorbani, L. Yang, S. Luo, Q. Cai, Template-based electrodeposition of Pt/Ni nanowires and its catalytic activity towards glucose oxidation, *Electrochim. Acta*, 58 (2011) 551-555.
- [132] P.K. Kannan, C.S. Rout, High Performance Non-enzymatic Glucose Sensor Based on One-Step Electrodeposited Nickel Sulfide, *Chem. Eur. J.*, 21 (2015) 9355-9359.
- [133] J. Luo, S. Jiang, H. Zhang, J. Jiang, X. Liu, A novel non-enzymatic glucose sensor based on Cu nanoparticle modified graphene sheets electrode, *Anal. Chim. Acta.*, 709 (2012) 47-53.
- [134] K.B. Male, S. Hrapovic, Y. Liu, D. Wang, J.H.T. Luong, Electrochemical detection of carbohydrates using copper nanoparticles and carbon nanotubes, *Anal. Chim. Acta*, 516 (2004) 35-41.
- [135] H. Li, C.-Y. Guo, C.-L. Xu, A highly sensitive non-enzymatic glucose sensor based on bimetallic Cu–Ag superstructures, *Biosens. Bioelectron.*, 63 (2015) 339-346.
- [136] Y. Ding, Y. Wang, L. Su, M. Bellagamba, H. Zhang, Y. Lei, Electrospun Co₃O₄ nanofibers for sensitive and selective glucose detection, *Biosens. Bioelectron.*, 26 (2010) 542-548.
- [137] X.-C. Dong, H. Xu, X.-W. Wang, Y.-X. Huang, M.B. Chan-Park, H. Zhang, L.-H. Wang, W. Huang, P. Chen, 3D graphene–cobalt oxide electrode for high-performance supercapacitor and enzymeless glucose detection, *ACS nano*, 6 (2012) 3206-3213.

- [138] L. Wang, Y. Zheng, X. Lu, Z. Li, L. Sun, Y. Song, Dendritic copper-cobalt nanostructures/reduced graphene oxide-chitosan modified glassy carbon electrode for glucose sensing, *Sens. Actuator B Chem.*, 195 (2014) 1-7.
- [139] Y.J. Yang, S. Hu, Electrodeposited MnO₂/Au composite film with improved electrocatalytic activity for oxidation of glucose and hydrogen peroxide, *Electrochim. Acta.*, 55 (2010) 3471-3476.
- [140] J. Chen, W.-D. Zhang, J.-S. Ye, Nonenzymatic electrochemical glucose sensor based on MnO₂/MWNTs nanocomposite, *Electrochem. Commun.*, 10 (2008) 1268-1271.
- [141] F. Xiao, Y. Li, H. Gao, S. Ge, H. Duan, Growth of coral-like PtAu–MnO₂ binary nanocomposites on free-standing graphene paper for flexible nonenzymatic glucose sensors, *Biosens. Bioelectron.*, 41 (2013) 417-423.
- [142] X. Cao, N. Wang, A novel non-enzymatic glucose sensor modified with Fe₂O₃ nanowire arrays, *Analyst (Cambridge, U. K.)*, 136 (2011) 4241-4246.
- [143] E.M. Ekanayake, D.M. Preethichandra, K. Kaneto, Polypyrrole nanotube array sensor for enhanced adsorption of glucose oxidase in glucose biosensors, *Biosens. Bioelectron.*, 23 (2007) 107-113.
- [144] S. Rodriguez-Mozaz, M.-P. Marco, M. De Alda, D. Barceló, Biosensors for environmental applications: Future development trends, *Pure Appl. Chem.*, 76 (2004) 723-752.
- [145] C. Janaky, C. Visy, Conducting polymer-based hybrid assemblies for electrochemical sensing: a material science perspective, *Anal. Bioanal. Chem.*, 405 (2013) 3489-3511.
- [146] S. Updike, G. Hicks, The enzyme electrode, *Nature*, 214 (1967) 986-988.

- [147] L. Fernández, H. Carrero, Electrochemical evaluation of ferrocene carboxylic acids confined on surfactant–clay modified glassy carbon electrodes: oxidation of ascorbic acid and uric acid, *Electrochim. Acta.*, 50 (2005) 1233-1240.
- [148] F. Qu, Y. Zhang, A. Rasooly, M. Yang, Electrochemical biosensing platform using hydrogel prepared from ferrocene modified amino acid as highly efficient immobilization matrix, *Anal. Chem.*, 86 (2014) 973-976.
- [149] P.Ó. Conghaile, S. Kamireddy, D. MacAodha, P. Kavanagh, D. Leech, Mediated glucose enzyme electrodes by cross-linking films of osmium redox complexes and glucose oxidase on electrodes, *Anal. Bioanal. Chem.*, 405 (2013) 3807-3812.
- [150] P.A. Raymundo-Pereira, A.C. Mascarenhas, M.F. Teixeira, Evaluation of the Oxobridged Dinuclear Ruthenium Ammine Complex as Redox Mediator in an Electrochemical Biosensor, *Electroanalysis*, (2015).
- [151] Y. Xiao, F. Patolsky, E. Katz, J.F. Hainfeld, I. Willner, " Plugging into enzymes": Nanowiring of redox enzymes by a gold nanoparticle, *Science*, 299 (2003) 1877-1881.
- [152] A. Trifonov, K. Herkendell, R. Tel-Vered, O. Yehezkeli, M. Woerner, I. Willner, Enzyme-capped relay-functionalized mesoporous carbon nanoparticles: effective bioelectrocatalytic matrices for sensing and biofuel cell applications, *ACS nano*, 7 (2013) 11358-11368.
- [153] B.A. Gregg, A. Heller, Redox polymer films containing enzymes. 2. Glucose oxidase containing enzyme electrodes, *J. Phys. Chem.* , 95 (1991) 5976-5980.
- [154] I. Matanovic, S. Babanova, M.S. Chavez, P. Atanassov, Protein–Support Interactions for Rationally Designed Bilirubin Oxidase Based Cathode: A Computational Study, *J. Phys. Chem. B*, 120 (2016) 3634-3641.
- [155] M. Vreeke, R. Maidan, A. Heller, Hydrogen peroxide and beta.-nicotinamide adenine dinucleotide sensing amperometric electrodes based on electrical connection of

horseradish peroxidase redox centers to electrodes through a three-dimensional electron relaying polymer network, *Anal. Chem.*, 64 (1992) 3084-3090.

[156] M.H. Osman, A.A. Shah, F.C. Walsh, Recent progress and continuing challenges in bio-fuel cells. Part I: Enzymatic cells, *Biosens. Bioelectron.*, 26 (2011) 3087-3102.

[157] P.V. Bernhardt, Enzyme Electrochemistry - Biocatalysis on an Electrode, *Aust. J. Chem.*, 59 (2006) 233-256.

[158] N. German, A. Ramanaviciene, J. Voronovic, A. Ramanavicius, Glucose biosensor based on graphite electrodes modified with glucose oxidase and colloidal gold nanoparticles, *Microchim. Acta*, 168 (2010) 221-229.

[159] G. Arai, K. Shoji, I. Yasumori, Electrochemical characteristics of glucose oxidase immobilized in poly(quinone) redox polymers, *J. Electroanal. Chem.*, 591 (2006) 1-6.

[160] M. Osman, A. Shah, F. Walsh, Recent progress and continuing challenges in bio-fuel cells. Part I: Enzymatic cells, *Biosens. Bioelectron.*, 26 (2011) 3087-3102.

[161] A.E. Cass, G. Davis, G.D. Francis, H.A.O. Hill, W.J. Aston, I.J. Higgins, E.V. Plotkin, L.D. Scott, A.P. Turner, Ferrocene-mediated enzyme electrode for amperometric determination of glucose, *Anal. Chem.*, 56 (1984) 667-671.

[162] J.-M. Savéant, Elements of molecular and biomolecular electrochemistry: an electrochemical approach to electron transfer chemistry, John Wiley & Sons 2006.

[163] K. Habermüller, M. Mosbach, W. Schuhmann, Electron-transfer mechanisms in amperometric biosensors, *Fresenius J. Anal. Chem.*, 366 (2000) 560-568.

[164] G. Gupta, V. Rajendran, P. Atanassov, Laccase biosensor on monolayer-modified gold electrode, *Electroanalysis*, 15 (2003) 1577-1583.

[165] R.A. Marcus, N. Sutin, Electron transfers in chemistry and biology, *BBA-Rev. Bioenergetics*, 811 (1985) 265-322.

- [166] P.N. Bartlett, P. Tebbutt, R.G. Whitaker, Kinetic aspects of the use of modified electrodes and mediators in bioelectrochemistry, *Prog. React. Kinet.* , 16 (1991) 55-155.
- [167] P. Janda, J. Weber, Quinone-mediated glucose oxidase electrode with the enzyme immobilized in polypyrrole, *J. Electroanal. Chem. Interfacial Electrochem.*, 300 (1991) 119-127.
- [168] W. Schuhmann, Electron-transfer pathways in amperometric biosensors. Ferrocene-modified enzymes entrapped in conducting-polymer layers, *Biosens. Bioelectron.*, 10 (1995) 181-193.
- [169] S. Cosnier, Biosensors based on immobilization of biomolecules by electrogenerated polymer films, *Appl. Biochem. Biotechnol.*, 89 (2000) 127-138.
- [170] B. Willner, E. Katz, I. Willner, Electrical contacting of redox proteins by nanotechnological means, *Curr. Opin. Biotech.* , 17 (2006) 589-596.
- [171] B.L. Vallee, R. Williams, Metalloenzymes: the entatic nature of their active sites, *Proc. Natl. Acad. Sci.*, 59 (1968) 498-505.
- [172] S.H. Lee, J.-H. Chung, H.-K. Park, G.-J. Lee, A Simple and Facile Glucose Biosensor Based on Prussian Blue Modified Graphite String, *J. Sens.*, 2016 (2016).
- [173] Y. Wang, C. Hou, Y. Zhang, F. He, M. Liu, X. Li, Preparation of graphene nano-sheet bonded PDA/MOF microcapsules with immobilized glucose oxidase as a mimetic multi-enzyme system for electrochemical sensing of glucose, *J. Mater. Chem. B*, 4 (2016) 3695-3702.
- [174] L. Ambarsari, I. Setyawati, R. Kurniasih, P.A. Kurniatin, A. Maddu, Immobilization of Glucose Oxidase on Modified-Carbon-Paste-Electrodes for Microfuel Cell, *Indones. J. Chem.*, 16 (2016) 92-97.

- [175] S.A. Merchant, T.O. Tran, M.T. Meredith, T.C. Cline, D.T. Glatzhofer, D.W. Schmidtke, High-Sensitivity Amperometric Biosensors Based on Ferrocene-Modified Linear Poly(ethylenimine), *Langmuir*, 25 (2009) 7736-7742.
- [176] C. He, M. Xie, F. Hong, X. Chai, H. Mi, X. Zhou, L. Fan, Q. Zhang, T. Ngai, J. Liu, A Highly Sensitive Glucose Biosensor Based on Gold Nanoparticles/Bovine Serum Albumin/Fe₃O₄ Biocomposite Nanoparticles, *Electrochim. Acta.*, 222 (2016) 1709-1715.
- [177] S. Kumar-Krishnan, S. Chakaravathy, A. Hernandez-Rangel, E. Prokhorov, G. Luna-Bárceñas, R. Esparza, M. Meyyappan, Chitosan supported silver nanowires as a platform for direct electrochemistry and highly sensitive electrochemical glucose biosensing, *RSC Adv.*, 6 (2016) 20102-20108.
- [178] J.-Y. Wang, L.-C. Chen, K.-C. Ho, Synthesis of Redox Polymer Nanobeads and Nanocomposites for Glucose Biosensors, *ACS Appl. Mater. Interfaces*, 5 (2013) 7852-7861.
- [179] N. Cheng, H. Wang, X. Li, X. Yang, L. Zhu, Amperometric glucose biosensor based on integration of glucose oxidase with palladium nanoparticles/reduced graphene oxide nanocomposite, *Am. J. Anal. Chem.*, 3 (2012) 312-319.
- [180] H. Zhong, R. Yuan, Y. Chai, W. Li, X. Zhong, Y. Zhang, In situ chemo-synthesized multi-wall carbon nanotube-conductive polyaniline nanocomposites: Characterization and application for a glucose amperometric biosensor, *Talanta*, 85 (2011) 104-111.
- [181] J. Singh, P. Khanra, T. Kuila, M. Srivastava, A.K. Das, N.H. Kim, B.J. Jung, D.Y. Kim, S.H. Lee, D.W. Lee, D.-G. Kim, J.H. Lee, Preparation of sulfonated poly(ether-ether-ketone) functionalized ternary graphene/AuNPs/chitosan nanocomposite for efficient glucose biosensor, *Process Biochem. (Oxford, U. K.)*, 48 (2013) 1724-1735.

- [182] X. Chen, J. Chen, C. Deng, C. Xiao, Y. Yang, Z. Nie, S. Yao, Amperometric glucose biosensor based on boron-doped carbon nanotubes modified electrode, *Talanta*, 76 (2008) 763-767.
- [183] P. Rafeighi, M. Tavahodi, B. Haghighi, Fabrication of a third-generation glucose biosensor using graphene-polyethyleneimine-gold nanoparticles hybrid, *Sens. Actuators B Chem.*, 232 (2016) 454-461.
- [184] M. Tang, X. Lin, M. Li, J. Li, L. Ni, S. Yin, Construction of amperometric glucose biosensor based on in-situ fabricated hierarchical meso-macroporous SiO₂ modified Au film electrodes, *J. Wuhan Uni. of Technol. Mat. Sci. Ed.*, 31 (2016) 736-742.
- [185] C.-X. Xu, K.-J. Huang, X.-M. Chen, X.-Q. Xiong, Direct electrochemistry of glucose oxidase immobilized on TiO₂-graphene/nickel oxide nanocomposite film and its application, *J. Solid State Electrochem.*, 16 (2012) 3747-3752.
- [186] Y. Xian, Y. Hu, F. Liu, Y. Xian, H. Wang, L. Jin, Glucose biosensor based on Au nanoparticles-conductive polyaniline nanocomposite, *Biosens. Bioelectron.*, 21 (2006) 1996-2000.
- [187] M. Ammam, E.B. Easton, High-performance glucose sensor based on glucose oxidase encapsulated in new synthesized platinum nanoparticles supported on carbon Vulcan/Nafion composite deposited on glassy carbon, *Sens. Actuators, B*, 155 (2011) 340-346.
- [188] J. Xie, S. Wang, L. Aryasomayajula, V.K. Varadan, Platinum decorated carbon nanotubes for highly sensitive amperometric glucose sensing, *Nanotechnology*, 18 (2007) 065503/065501-065503/065509.
- [189] M. Chen, G. Diao, Electrochemical study of mono-6-thio- β -cyclodextrin/ferrocene capped on gold nanoparticles: Characterization and application to the design of glucose amperometric biosensor, *Talanta*, 80 (2009) 815-820.

- [190] T.O. Tran, E.G. Lammert, J. Chen, S.A. Merchant, D.B. Brunski, J.C. Keay, M.B. Johnson, D.T. Glatzhofer, D.W. Schmidtke, Incorporation of single-walled carbon nanotubes into ferrocene-modified linear polyethylenimine redox polymer films, *Langmuir*, 27 (2011) 6201-6210.
- [191] J.-D. Qiu, W.-M. Zhou, J. Guo, R. Wang, R.-P. Liang, Amperometric sensor based on ferrocene-modified multiwalled carbon nanotube nanocomposites as electron mediator for the determination of glucose, *Anal. Biochem.*, 385 (2009) 264-269.
- [192] L. Deng, Y. Liu, G. Yang, L. Shang, D. Wen, F. Wang, Z. Xu, S. Dong, Molecular "Wiring" Glucose Oxidase in Supramolecular Architecture, *Biomacromolecules*, 8 (2007) 2063-2071.
- [193] E. Turkus̃ íc, K. Kalcher, K. Schachl, A. Komersova, M. Bartos, H. Moderegger, I. Svancara, K. Vytras, Amperometric determination of glucose with an MnO₂ and glucose oxidase bulk-modified screen-printed carbon ink biosensor, *Anal. Lett.*, 34 (2001) 2633-2647.
- [194] N.G. Tsierkezos, U. Ritter, N. Wetzold, A.C. Hübler, Non-enzymatic analysis of glucose on printed films based on multi-walled carbon nanotubes, *Microchim. Acta*, 179 (2012) 157-161.
- [195] P.T. Kissinger, W.R. Heineman, Cyclic voltammetry, *J. Chem. Educ.*, 60 (1983) 702.
- [196] R.S. Nicholson, Theory and Application of Cyclic Voltammetry for Measurement of Electrode Reaction Kinetics, *Anal. Chem.*, 37 (1965) 1351-1355.
- [197] V. Gau, S.-C. Ma, H. Wang, J. Tsukuda, J. Kibler, D.A. Haake, Electrochemical molecular analysis without nucleic acid amplification, *Methods*, 37 (2005) 73-83.

- [198] G. Si-Xuan, B. Alan M, Z. Jie, Fourier Transformed Large Amplitude Alternating Current Voltammetry: Principles and Applications, *Review of Polarography*, 61 (2015) 21-32.
- [199] F. Shu, G. Wilson, Rotating ring-disk enzyme electrode for surface catalysis studies, *Anal. Chem.*, 48 (1976) 1679-1686.
- [200] F. Opekar, P. Beran, Rotating disk electrodes, *J. Electroanal. Chem. Interfacial Electrochem.*, 69 (1976) 1-105.
- [201] A.J. Bard, L.R. Faulkner, J. Leddy, C.G. Zoski, *Electrochemical methods: fundamentals and applications*, Wiley New York 1980.
- [202] D.A. Skoog, D.M. West, F.J. Holler, S.R. Crouch, *Fundamentals of analytical chemistry*, Nelson Education 2013.
- [203] K. Kato, K. Kano, T. Ikeda, Electrochemical Characterization of Carbon Felt Electrodes for Bulk Electrolysis and for Biocatalyst-Assisted Electrolysis, *J. Electrochem. Soc.*, 147 (2000) 1449-1453.
- [204] F. Fan, J. Fernandez, B. Liu, J. Mauzeroll, C. Zoski, C. Zoski, *Handbook of Electrochemistry*, Handbook of Electrochemistry, (2007).
- [205] P. Kissinger, W.R. Heineman, *Laboratory Techniques in Electroanalytical Chemistry*, revised and expanded, CRC press 1996.
- [206] F.C. Strong, Faraday's laws in one equation, *J. Chem. Educ.*, 38 (1961) 98.
- [207] W. Crookes, J.H. Gardiner, G. Druce, H.B. Ryan, *The Chemical News and Journal of Industrial Science: With which is Incorporated the " Chemical Gazette". A Journal of Practical Chemistry in All Its Applications to Pharmacy, Arts and Manufactures*, Chemical news office 1871.

- [208] B.D. Fleming, J. Zhang, D. Elton, A.M. Bond, Detailed analysis of the electron-transfer properties of azurin adsorbed on graphite electrodes using dc and large-amplitude Fourier transformed ac voltammetry, *Anal. Chem.*, 79 (2007) 6515-6526.
- [209] S.X. Guo, J. Zhang, D.M. Elton, A.M. Bond, Fourier transform large-amplitude alternating current cyclic voltammetry of surface-bound azurin, *Anal. Chem.*, 76 (2004) 166-177.
- [210] J. Zhang, S.X. Guo, A.M. Bond, F. Marken, Large-amplitude Fourier transformed high-harmonic alternating current cyclic voltammetry: kinetic discrimination of interfering Faradaic processes at glassy carbon and at boron-doped diamond electrodes, *Anal. Chem.*, 76 (2004) 3619-3629.
- [211] C.-Y. Lee, B.D. Fleming, J. Zhang, S.-X. Guo, D.M. Elton, A.M. Bond, Systematic evaluation of electrode kinetics and impact of surface heterogeneity for surface-confined proteins using analysis of harmonic components available in sinusoidal large-amplitude Fourier transformed ac voltammetry, *Anal. Chim. Acta.*, 652 (2009) 205-214.

Chapter 2

Use of Glucose oxidase/Pyrene/ Redox polymer Integrated Carbon Materials for Electrocatalytic Glucose Oxidation

1. Introduction

Enzymes are complex proteins produced by living cells that catalyse a specific biochemical reaction. Enzymatic co-factors assist the enzymes to achieve efficient electron transfer in its natural environment. The glucose oxidase (GOx) enzyme is widely used in glucose oxidation [1], due to its simplicity in use in systems/nanocomposites for different electrochemical applications, such as biosensors [2] and biofuel cells [3]. In GOx, the active redox center lies deep in the apoenzyme which makes the electron transfer kinetics slow [4]. However, this could be achieved via mediated electron transfer while the enzyme was immobilised onto the surface of the electrode [5]. Use of mediators would overcome the sluggish electron transfer between the enzyme and the electrode. The key process of activation of the bioelectrocatalytic function of the enzyme relies on the effectiveness of the electrical contacting of the redox center of the enzyme with electrode supports [6].

Glucose biosensors and biofuel cells can be considered as important electronic devices, which are mainly used in clinical/medical applications. According to the global report on diabetes 2016 published by the World Health Organisation, the number of diabetic patients has increased to 422 million from the world population [7]. The development of accurate and reliable biosensors are required to assist diabetes patients to continuously monitor glucose level in human blood. The requirement of development of efficient biofuel cells is now in high demand as it has attracted the attention of scientist as it can be used to power medical implants in human body which has a continuous supply of glucose and oxygen via blood[8]. Biofuel cells consist of bioanodes and biocathodes which are designed by employing enzymes or microorganisms as the catalyst to convert target analyte into electrical power output[9]. Considering all plausible enzyme pathways which could be used in biofuel cell application, glucose oxidase (GOx) was reported to be the best enzyme as it is stable, inexpensive, high

catalytic activity and use glucose as a fuel which is wide spread[4]. Key structural components of an enzyme electrode are enzyme, immobilisation matrix and mediator.

A wide range of polymers have been used to provides the basic platform for the covalent attachment of biomolecules [5]. Among them the linear and branched forms of polyethylenimine (PEI), is a popular choice. It is a polyamine with high solubility in water [10] which is widely used for the attachment of biomolecules such as enzymes and DNA [11]. Since branched PEI (bPEI) is nonconductive, it cannot be directly used for enzyme electrode fabrication. In order to improve the electrical conductivity, integration with other conductive substrates is essential. Carbon materials, such as carbon nanotube (CNT) and graphene derivatives, are known as emerging supporting substrates for functional nanomaterials due to their remarkable properties [12]. CNT are non-metallic graphene nanowires with different constituent, length, diameter and chirality. These exhibit high specific surface area, biocompatibility, antifouling properties and most importantly high conductivity [5, 13]. Since the discovery of carbon nanotubes (CNT) by Iijima in 1991 [14] it has attracted material scientists with its properties compared to metals. A whole lot of work has been done in biosensor and biofuel cell field incorporating CNTs as the host matrix. Even though it was used as a host matrix it has improved the loading of enzymes due to high surface area, high electron transfer rate due to high conductivity etc. These remarkable properties have been synchronised by J. Liu *et al.* [15] in synthesising CNTs immobilised ferrocenecarboxaldehyde with GOx immobilised silk films for the fabrication of an enzymatic electrode for the glucose biofuel cells. They have obtained a high current density of 0.5 mA cm^{-2} . Qiu *et al.* [12] reported a ferrocene modified MWCNT with chitosan modified GOx for glucose biosensor application. Analytical performance of this biosensor showed a sensitivity of $25 \mu\text{A mM}^{-1} \text{ cm}^{-2}$, a detection limit of $3.0 \mu\text{M}$ and a current density of $57 \mu\text{A cm}^{-2}$. A comparison study between polyethylenimine (PEI) and poly(acrylic acid) (PAA) has been conducted by Yan *et*

al. [16] using CNTs coated with PEI or PAA then carried out covalent binding of Fc derivative and GOx accordingly to develop an enzymatic electrode for glucose oxidation. The CNT/PEI-Fc-GOx electrode showed excellent performance over CNT/PAA-Fc-GOx electrode having a current density of 0.3 mA cm^{-2} . Tran *et al.* [17] has reported single wall carbon nanotubes incorporated with Fc modified linear PEI redox polymer hydrogels with GOx in glucose oxidation and has obtained a remarkably high current density of 3 mA cm^{-2} . Similarly, reduced graphene oxide carries these above mentioned properties [18]. Qiu and co-workers [19] reported a chitosan-ferrocene/graphene oxide/glucose oxidase (CS-Fc/GO/GOx) nanocomposite film for the fabrication of glucose biosensor which showed a linear response to glucose in the concentration range from 0.02 to 6.78 mM with a detection limit of 7.6 M and exhibited a sensitivity of $10 \text{ A mM}^{-1} \text{ cm}^{-2}$.

In the present study, carbon materials were non-covalently functionalised by the π - π interaction with the pyrene which was tethered to redox relay of ferrocene functionalised branched PEI (bPEI). This was employed for the development of enzymatic electrodes. We compare the activity of Fc-Py-bPEI-MWCNT/GOx fabricated electrodes with Fc-Py-bPEI-rGO/GOx fabricated electrodes towards glucose oxidation. The results revealed that MWCNT nanocomposite fabricated electrode has a maximum current density of 1.4 mA cm^{-2} over the rGO nanocomposite fabricated electrode, which has a maximum current density 0.98 mA cm^{-2} , which shows that there is no significant difference in the activity of these two carbon materials proving the concept published in the review by Wenrong *et al.*[20].

2. Experimental

2.1. Chemicals

The chemicals branched polyethylenimine (bPEI, 97%), 1-pyrenebutyric acid (Py, 97%), *N*-hydroxysuccinimide (NHS, 98%), 1-ethyl-3-(3-dimethylaminopropyl) carbodiimide hydrochloride (EDC, commercial grade), glutaraldehyde solution in H₂O (GA, 50% (w/v)) and D-glucose (99%) were purchased from Sigma Aldrich. Multiwall carbon nanotubes (MWCNT, 20-30nm diameter, 0.5-2 μm length, 95%) was purchased from Nanostructured & Amorphous Nanomaterials Inc. (USA) Sodium dihydroxyphosphate (99%) and disodium hydrogen phosphate (99%) from Merck were used for the preparation of buffer solutions. Glucose oxidase (GOx, 211 U mg⁻¹) was purchased from Fluka. Acetonitrile (MeCN, reagent grade) from LiChrosolv Merck. All of the above mentioned chemicals were used as received. Deionised water was utilised for preparation of solutions.

Ferrocene propionic acid (Fc) was synthesised according to a literature reported procedure and analysis was in agreement with literature[21].

2.2. Coupling of Fc and Py with bPEI (Fc-bPEI-Py)

The carboxylic acid functional group on Fc and Py was coupled with the amine functional groups on bPEI using the EDC coupling method forming amide bonds. A 2.5 mg of bPEI was weighed and dissolved in deionised water. Ferrocene propionic acid (2 mg) and pyrenebutaric acid (0.25 mg) were dissolved in MeCN. This mixture was mixed with bPEI under stirring. Then, EDC and NHS (1.5 molar equivalent with respect to Fc) were added to the solution. The solution was stirred overnight. Fc-Py-bPEI formed were isolated by centrifugation at a rotation rate of 13000 rpm (Eppendorf, mini spin plus) and then washed with MeCN to remove any unreacted Fc or Py. This material was then redissolved in 500 μL

deionised water and stored in a refrigerator until used with carbon materials which acts as host matrixes.

2.3. Preparation of Fc-Py-bPEI stabilised MWCNT (Fc-Py-bPEI-MWCNT) and Fc-Py-bPEI stabilised rGO (Fc-Py-bPEI-rGO)

For the preparation of Fc-Py-bPEI stabilised MWCNT, an aliquot of 100 μL of the above Fc-Py-bPEI mixture was mixed with 100 μL of MWCNT solution (0.1, 0.2, 0.5 mg in 100 μL deionised water). This mixture was then sonicated for 4 min to obtain a homogeneous mixture. Similarly, rGO stabilised Fc-Py-bPEI was prepared by mixing of 100 μL of Fc-Py-bPEI with 0.20 mg rGO solution (in 100 μL deionised water) which will give rise to 200 μL of total volume. Graphene oxide was synthesised by modified Hummer's method[22] and rGO was achieved by a chemical method using tri-sodium citrate[23]. Furthermore, the mixture was sonicated for 4 minutes to obtain a homogeneous mixture. Both mixtures were stored in the fridge until further use in experiments.

2.4. Crosslinking of GOx to Fc-Py-bPEI-MWCNT and fabrication of the Fc-Py-bPEI-MWCNT and Fc-Py-bPEI-MWCNT /GOx modified electrodes

To obtain more stability and to prevent possible leakage of GOx from the enzyme electrodes to the electrolyte media during electrochemical analysis, $-\text{NH}_2$ sites of the enzyme and the bPEI were crosslinked via amide bonds using GA as the cross-linking agent to form Fc-Py-bPEI-MWCNT /GOx. In this procedure, Fc-Py-bPEI-MWCNT solution (3 μL) was mixed with 6 μg of GOx (0.6 μL of 1 mg/ mL GOx solution) to obtain a homogeneous solution. Mixing with GA was then undertaken to crosslink the primary amines on GOx and bPEI. The amount of added GA was varied by using 1.0 μL aliquot of a 0.03, 0.01, 0.015, and 0.003% (w/v) solutions.

A glassy carbon electrode (GCE, 3mm diameter, CH Instruments, Texas, USA), was used to prepare the modified electrodes used in voltammetric studies. Initially, the electrode was

polished with an aqueous 0.3 μm alumina slurry followed by rinsing with water, sonication and rinsing again with water before drying under a nitrogen atmosphere. Then 4.0 μL of Fc-Py-bPEI-MWCNT or Fc-Py-bPEI-rGO /GOx solution was drop-casted on the electrode surface and left to dry in air, before use in an electrochemical measurement. The GC rotating disk electrode (GC-RDE, 3 mm, BAS, Tokyo, Japan) was modified in a similar manner.

2.5. Electrochemical measurements

Voltammetric measurements were carried out at 20 ± 2 $^{\circ}\text{C}$ using a CH Instrument 760E electrochemical workstation with a conventional three-electrode cell. Phosphate buffer saline (PBS, 0.1 M, pH 7) was used as the electrolyte. The modified GCE or GC-RDE, Ag|AgCl(1 M KCl) and platinum wire were employed as working, reference and auxiliary electrodes respectively. Appropriate aliquots of a 1.00 M glucose stock solution were added to the PBS pH 7 solution in the cell to obtain the required concentration of glucose. To remove oxygen, all solutions were degassed with high purity nitrogen for at least 10 min prior to commencing the electrochemical measurements. A scan rate of 0.01 V s^{-1} was used, unless otherwise stated. The catalytic current was obtained by subtracting the background current for ferrocene from the electrocatalytic current obtained by glucose oxidation at 0.45 V vs Ag|AgCl(1 M KCl).

3. Results and Discussion

3.1. Electrochemical characterisation of redox active Fc-Py-bPEI-MWCNT/GOx modified electrodes

The electrochemical behaviour of the redox active Fc-Py-bPEI/MWCNT modified GC electrode was investigated using cyclic voltammetry. A cyclic voltammogram obtained at a scan rate of 0.01 V s^{-1} in phosphate buffer pH 7 medium showed a well-defined redox potential at 0.22 V with a peak to peak separation of 50 mV (Figure 1a). The effect of scan rate on the modified electrode was evaluated over the scan rate range of $0.01 - 0.25 \text{ Vs}^{-1}$. The oxidation peak currents increased linearly with scan rate, (Figure 1b) which implies that the

Fc-Py-bPEI/MWCNT material is surface confined. To obtain the surface coverage of Fc, a cyclic voltammogram obtained with the slow scan rate of 0.01 V s^{-1} was used to ensure the complete oxidation of Fc to Fc^+ . The peak area of the oxidation process was integrated to obtain the total charge which then allows the calculation of the surface coverage. This allows the surface coverage to be estimated via use of equation (1):

$$\Gamma_{total} = Q/nFA \quad (1)$$

where, Γ_{total} is total surface coverage, Q is the total charge, n is the number of electrons transferred, F is the Faraday constant and A is the geometrical surface area of the GC electrode (0.07 cm^2). With respect to the CV obtained the surface coverage of Fc was calculated according to equation (1) and obtained a value of 12 nmol cm^{-2} .

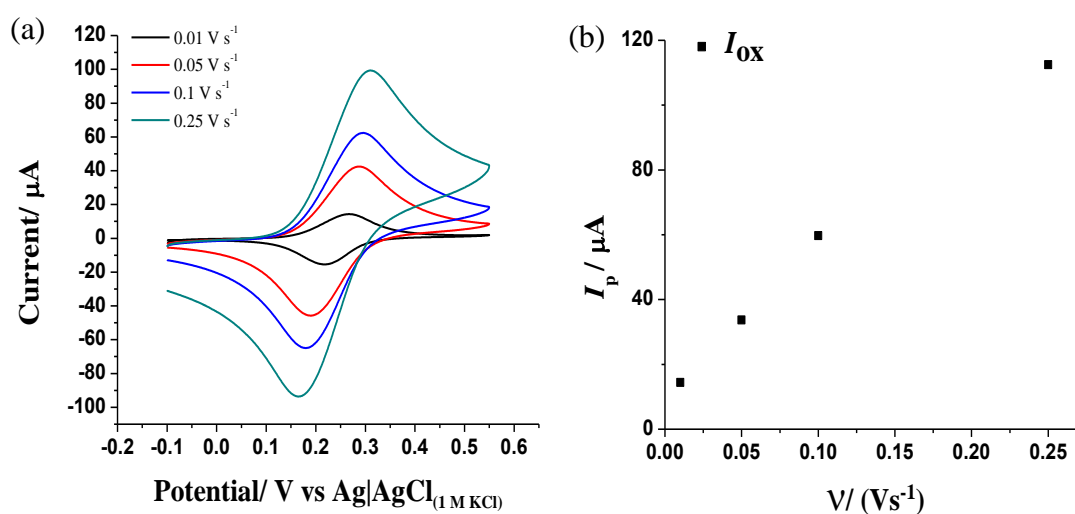


Figure 1: (a) Cyclic voltammograms obtained using Fc-Py-bPEI-MWCNT modified GCE in 0.1 M PBS pH 7 as a function of scan rate and (b) the relationship between the peak current and scan rate.

3.2. Optimisation of compositions of different components of Fc-Py-bPEI-MWCNT/GOx for the electrocatalytic glucose response

To achieve optimal performance from the Fc-Py-bPEI-MWCNT/GOx modified electrode the influence of the concentrations of individual components, GOx loading, crosslinking concentration, pH and loading mass of the nanocomposite was investigated. The synthesis of Fc-bPEI-MWCNT was undertaken in the absence of Py previously[16]. However, it was revealed in this study that Py has an important role to play in increasing the stability. The key to achieve the highly stable formation is that Py allows mediator coupled bPEI to bind strongly to the MWCNTs by creating π - π interactions between the aromatic rings of sp^2 hybridized carbon [24] on both the pyrene and carbon material (MWCNT/ rGO). Without Py incorporation in the Fc-bPEI-MWCNT/GOx nanocomposite, the catalytic current of the enzymatic electrode was found to be very low in the presence of 10 mM glucose (Figure 2) compared to the enzymatic electrode fabricated with Fc-Py-bPEI-MWCNT/GOx nanocomposite (Figure 4). The sigmoidal shape of the cyclic voltammogram of Fc-bPEI-MWCNT/GOx modified electrode conveys kinetically controlled behaviour while Fc-Py-bPEI-MWCNT/GOx modified electrode express mass transport controlled behaviour in the presence of 10.0 mM glucose. The results with the Fc-bPEI-MWCNT nanocomposite modified GOx electrode are comparable with the literature data reported with Fc-bPEI-MWCNT[16] and similar materials. This could be due to low interaction of the redox polymer with MWCNT. Thus, Py was incorporated into the synthesis of the Fc-Py-bPEI-MWCNT nanocomposite. The optimisation of individual components were carried out using electrocatalytic glucose oxidation current as an indicator using Fc-Py-bPEI-MWCNT/GOx modified electrodes. The catalytic current was obtained by subtracting the background current for ferrocene from the electrocatalytic current obtained by glucose oxidation at 0.45 V vs Ag|AgCl_(1 M KCl).

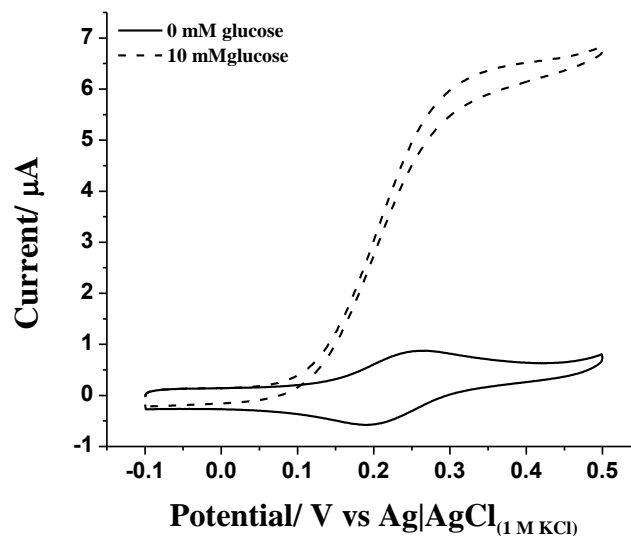


Figure 2: Cyclic voltammograms obtained at a scan rate of 0.01 V s^{-1} in $0.1 \text{ M PBS pH } 7$ in the presence and absence of 10.0 mM glucose with Fc-bPEI-MWCNT/ GOx (the film contains $73 \mu\text{g}$ Fc-bPEI-MWCNT, $6 \mu\text{g}$ GOx and $0.173 \mu\text{g}$ GA)

During the synthesis of Fc-Py-bPEI-MWCNT, the bPEI weight was kept constant at 2.5 mg/mL while optimising the composition of Py, Fc and MWCNT. The electrochemical experiments carried out revealed that the optimum weight of Py is 0.25 mg/ mL which gave a PEI: Py weight ratio of 10:1. A higher Py loading diminished the electrocatalytic current. This could be a result of less $-\text{NH}_2$ sites being available for other components to attach to the polymer. The optimum Fc loading was found to be 2.0 mg/ mL and 1 mg/ mL of MWCNT gave the optimum nanocomposite. A weight of $74 \mu\text{g}$ of the Fc-Py-bPEI-MWCNT polymer nanocomposite was kept constant and the weight of GOx was varied in order to investigate the optimum weight of GOx with the polymer nanocomposite. Enzymatic electrodes with different GOx weight compositions ($3, 6, 12, 18 \mu\text{g}$) were then used in cyclic voltammetry at a scan rate of 0.01 V s^{-1} in the presence and absence of 10 mM glucose in $\text{PBS pH } 7$ buffer.

The resultant electrocatalytic current obtained at a potential of 0.45 V vs Ag|AgCl(1 M KCl), after subtracting the background current measured in the absence of glucose. These experimental results revealed that 6 μg is the optimum weight of GOx that the enzymatic electrode could accommodate with the polymer nanocomposite. An increase in GOx weight leads to overcrowding of the nanocomposite and gives a lower catalytic current since every GOx unit cannot communicate efficiently with the Fc centers on the nanocomposite [11].

Crosslinking of the enzyme onto a Fc-Py-bPEI-MWCNT nanocomposite provided high stability and efficient communication between the enzyme and the electrode. Thus, crosslinking of the enzyme using GA was carried out before fabrication of Fc-Py-bPEI-MWCNT/GOx on the GC electrode. Use of smaller amounts of GA will achieve crosslinking of GOx. However, will promote leakage of the unbound enzymes and create instability in the electrode. On the other hand, a high amount of GA will screen the activity of the enzyme[25]. Therefore it is required to use an optimum amount of crosslinker. The optimum GA weight was determined to be 0.173 μg . In summary, the optimised weight % of the film components are: Fc-Py-bPEI-MWCNT 92%, GOx 7% and GA 1%. After optimising the composition of the Fc-Py-bPEI-MWCNT/GOx modified enzyme electrode, MWCNT was replaced by rGO to fabricate Fc-Py-bPEI-rGO/GOx modified electrodes for comparison of activity.

3.3. Investigation of the effect of pH and composite loading of Fc-Py-bPEI-MWCNT/GOx on the electrocatalytic glucose oxidation response

The optimum loading of the Fc-Py-bPEI-MWCNT/GOx was carried out in the presence of 5.0 mM glucose. A plot of electrocatalytic current as a function of loading was plotted and it was found that 80.2 μg of the Fc-Py-bPEI-MWCNT/GOx loading gave the optimum electrocatalytic current (Figure 3a) as the amount of mediator communicating between the enzyme and the electrode had become saturated. Further increase of the loading does not increase the electrocatalytic current.

As enzymes activity is dependent on pH. Consequently, experiments were carried out to find the optimum pH for the Fc-Py-bPEI-MWCNT/ GOx enzyme electrode in the pH range of 6.5 to 8.0 The enzyme electrode showed a maximum response at pH 7 (Figure 3b), which was consistent with other studies[12, 26]. Thus, the performance of the Fc-Py-bPEI-MWCNT/ GOx enzyme electrode was evaluated at pH 7.0 (PBS 0.1 M) throughout the study.

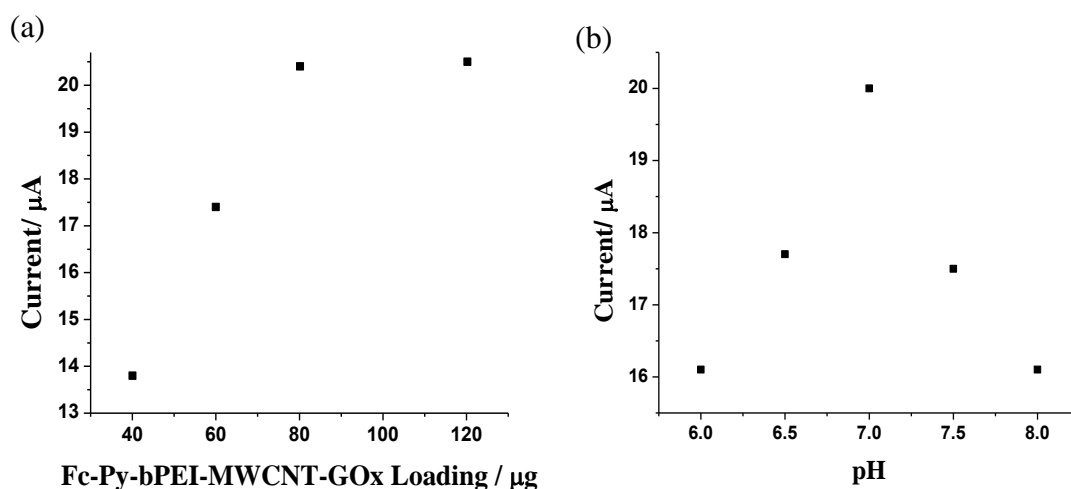


Figure 3 : Catalytic current obtained with Fc-Py-bPEI-MWCNT/GOx modified GCEs in the presence of 5.0 mM glucose as a function of (a) Fc-Py-bPEI-MWCNT/GOx loading and (b) pH (the film contains 74 μg Fc-Py-bPEI- MWCNT, 6 μg GOx and 0.173 μg GA).

3.4. Glucose oxidation by Fc-Py-bPEI- MWCNT/GOx

The MWCNT provides a high surface area for coverage[12] by Fc-Py-PEI, which also allows high amount of the enzyme to immobilise. The target substrate for GOx enzyme is glucose[27]. Therefore, the electrocatalytic oxidation of glucose using crosslinked Fc-Py-bPEI-MWCNT/GOx modified electrode was investigated in the PBS pH 7 buffer medium in the presence and absence of 10 mM glucose concentration at a scan rate of 0.01 Vs^{-1} . The voltammograms obtained are illustrated in Figure 4. A current output of 21 μA was obtained for glucose oxidation after background correction at 0.45 V vs $\text{Ag}|\text{AgCl}_{(1 \text{ M KCl})}$.

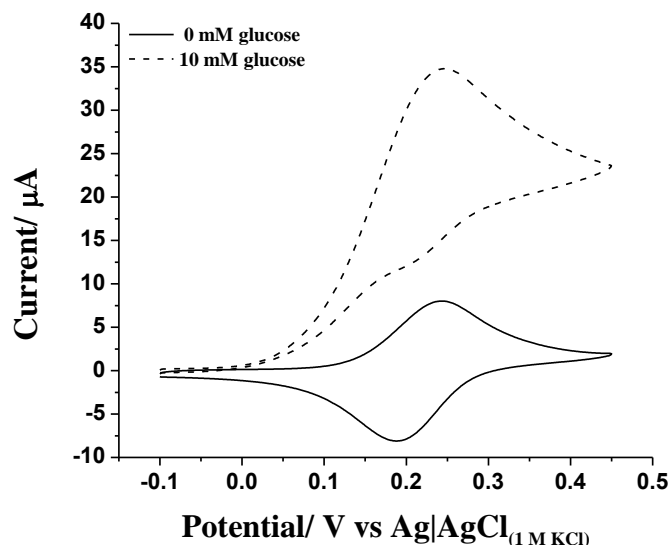


Figure 4: Cyclic voltammograms obtained at a scan rate of 0.01 V s^{-1} in $0.1 \text{ M PBS pH } 7$ in the presence and absence of 10.0 mM glucose with Fc-Py-bPEI-MWCNT/GOx (the film contains $74 \text{ }\mu\text{g}$ Fc-Py-bPEI-MWCNT, $6 \text{ }\mu\text{g}$ GOx and $0.173 \text{ }\mu\text{g}$ GA) modified GCEs.

3.5. Fc-Py-bPEI-rGO/GOx

As reported with use of MWCNT, the Fc-Py-bPEI-rGO nanocomposite was fabricated with a similar composition i. e. 2.5 mg/mL of bPEI, 0.25 mg/mL of Py and 2.0 mg/mL of Fc. This optimised Fc-Py-bPEI material was combined with 1 mg/mL rGO instead of MWCNT to create Fc-Py-bPEI-rGO. To form Fc-Py-bPEI-rGO/ GOx, $74 \text{ }\mu\text{g}$ of the Fc-Py-bPEI-rGO was crosslinked to $6 \text{ }\mu\text{g}$ of GOx using $0.173 \text{ }\mu\text{g}$ GA as the crosslinker via amide bonds.

3.5.1. Electrochemical characterisation of redox active Fc-Py-bPEI- rGO/GOx modified electrodes

The electrochemical behaviour of the redox active Fc-Py-bPEI-rGO modified GC electrode also was investigated by cyclic voltammetry. At a scan rate of 0.01 V s^{-1} in $\text{PBS pH } 7$ medium a well defined process with a potential of 0.262 V with a peak to peak separation of 60 mV for Fc/Fc^+ redox process in Fc-Py-bPEI-rGO modified GCE (Figure 5a). Over the scan rate

range 0.01 – 0.25 Vs^{-1} , the oxidation peak currents increased linearly with scan rate which implies that Fc-Py-bPEI-rGO material is surface confined (Figure 5b). Using equation (1) the surface coverage of Fc was evaluated and found to be 5 nmol cm^{-2} . Thus, the Fc coverage in Fc-Py-bPEI-rGO is lower than in Fc-Py-bPEI/MWCNT. This could be due to aggregation of Fc-Py-bPEI-rGO material.

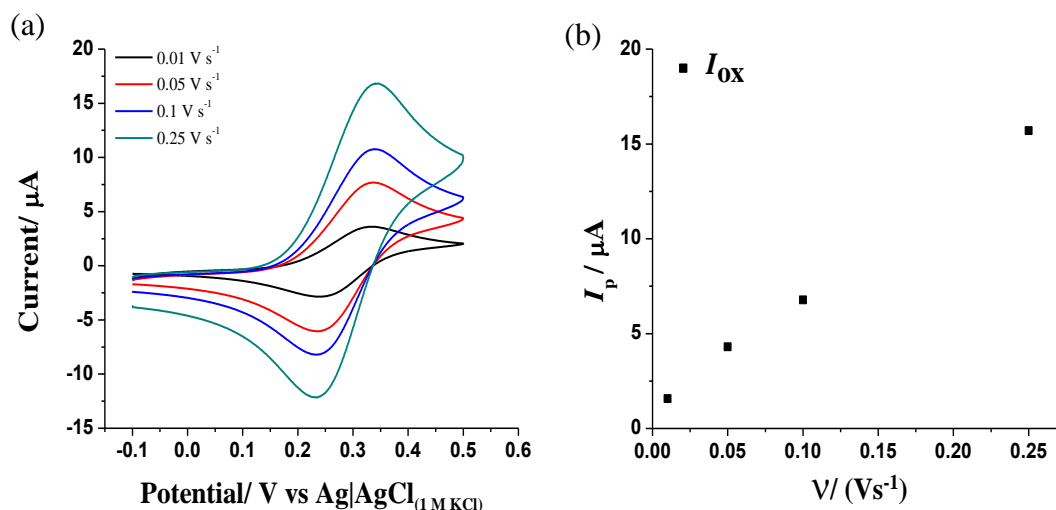


Figure 5: (a) Cyclic voltammograms obtained at Fc-Py-bPEI-rGO modified GC in 0.1 M PBS pH 7 as a function of scan rate and (b) the relationship between the peak current and scan rate.

3.5.2 Glucose oxidation by Fc-Py-bPEI-rGO/GOx

The electron transfer activity towards glucose oxidation via GOx of the two carbon materials compared with a similar composition and conditions. The electrocatalytic oxidation of glucose was investigated in the PBS pH 7 buffer medium in the presence and absence of 10 mM glucose concentration at a scan rate of 0.01 Vs^{-1} using a Fc-Py-bPEI-rGO/ GOx modified GCE. However, this modified electrode gave a significantly lower current output of $15 \mu\text{A}$ (Figure 6) compared to the value of $21 \mu\text{A}$ which was obtained from Py-bPEI-MWCNT/GOx modified GCE.

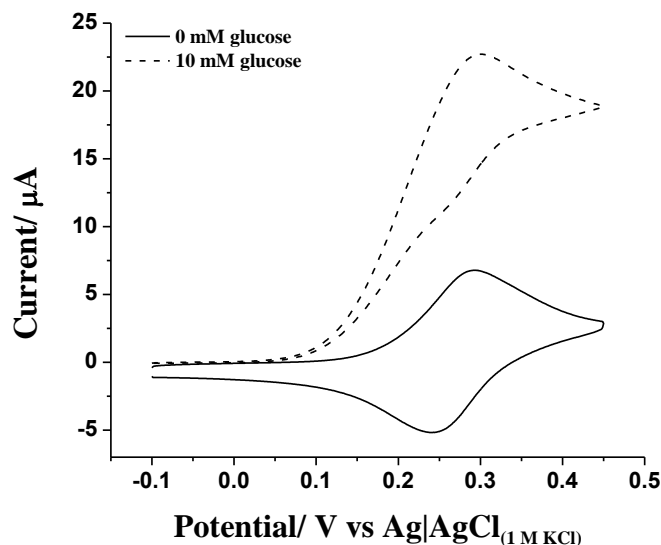


Figure 6: Cyclic voltammograms obtained at a scan rate of 0.01 V s^{-1} in $0.1 \text{ M PBS pH } 7$ in the presence and absence of 5.0 mM glucose with Fc-Py-bPEI-rGO/GOx (the film contains $74 \mu\text{g}$ Fc-Py-bPEI-rGO, $6 \mu\text{g}$ GOx and $0.173 \mu\text{g}$ GA) modified GCEs.

3.6. Enzyme kinetics of the optimised crosslinked Fc-Py-bPEI-MWCNT/GOx and Fc-Py-bPEI-rGO/GOx modified enzyme Electrode

After the enzymes have been immobilised onto the Fc-Py-bPEI-MWCNT matrix, glucose oxidation can be monitored electrochemically. However, immobilisation of the enzyme in a matrix will change its behaviour/ activity compared to a free enzyme[28]. Kinetics studies are therefore essential to evaluate enzyme activity in the redox polymer. Rotating disk electrode voltammetry allows to study the kinetics under hydrodynamic conditions as the stationary enzyme electrode limits for a range of reasons[29]. Experiments carried out under hydrodynamic conditions with a Fc-Py-bPEI-MWCNT/GOx modified GC RDE (scan rate = 0.01 V s^{-1}) in the presence of 10.0 mM glucose, provided a steady state limiting current (I_{ss}) that was independent of rotation rate (the angular frequency (ω) is proportional to rotation rate) in the electrode rotation rate range of $500 - 2000 \text{ rpm}$ (Figure 7a). Similar results were

obtained from a Fc-Py-bPEI-rGO/GOx modified GC RDE (Figure 7b). This result implies that the process is kinetically rather than mass transport controlled under these conditions. Both enzyme electrodes showed high stability and excellent mechanical strength since they were capable of surviving under high rotation rates without any loss of activity[29].

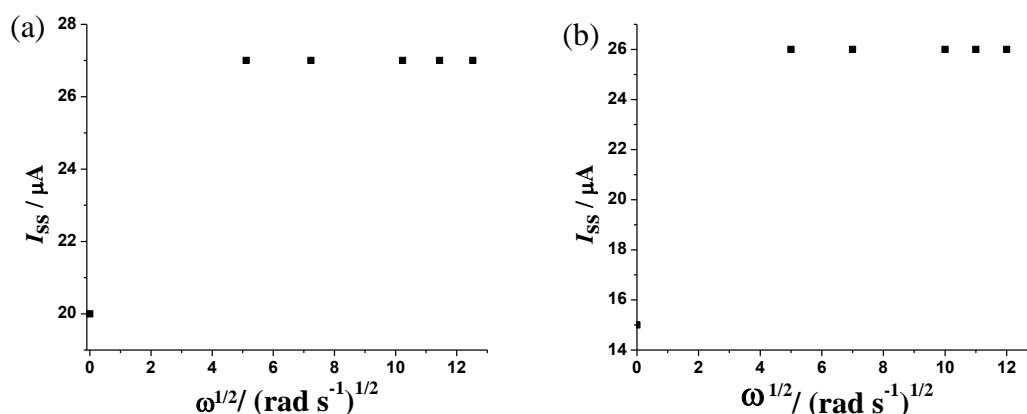


Figure 7: The relationship between $\omega^{1/2}$ and background corrected steady-state mass transport limiting current measured at 0.45 V obtained from (a) Fc-Py-bPEI-MWCNT/GOx and (b) Fc-Py-bPEI-rGO/GOx modified GCE in a 10 mM Glucose (0.1 M PBS pH7) solution at a scan rate of 0.01 V s⁻¹ at different rotation rates.

The apparent Michaelis constant (K_m') represents the enzymatic electrode[30]. This is required for the enzyme affinity to be evaluated towards the substrate inside the redox polymer because the enzyme is immobilised via covalent bond will not have the same affinity as in its native configuration[31]. The experiment required was carried out over a wide glucose concentration range under hydrodynamic conditions with Fc-Py-bPEI-MWCNT/GOx and Fc-Py-bPEI-rGO/GOx modified GC RDEs separately using a rotation rate of 2000 rpm and a scan rate of 0.01 V s⁻¹. This relatively high rotation rates was used to avoid concentration polarization at low glucose concentrations[30]. The Eadie Hofstee form of the

Michaelis Menten equation was used to obtain K_m' as the enzymatic reaction is rate controlling[32], given from equation (2) below:

$$j_{ss} = j_{max} - K_m' (j_{ss} / C^*) \quad (2)$$

where j_{ss} is the steady state current density, j_{max} is the maximum current density, K_m' is the apparent Michaelis Menten constant and C^* is the bulk solution concentration of glucose[30].

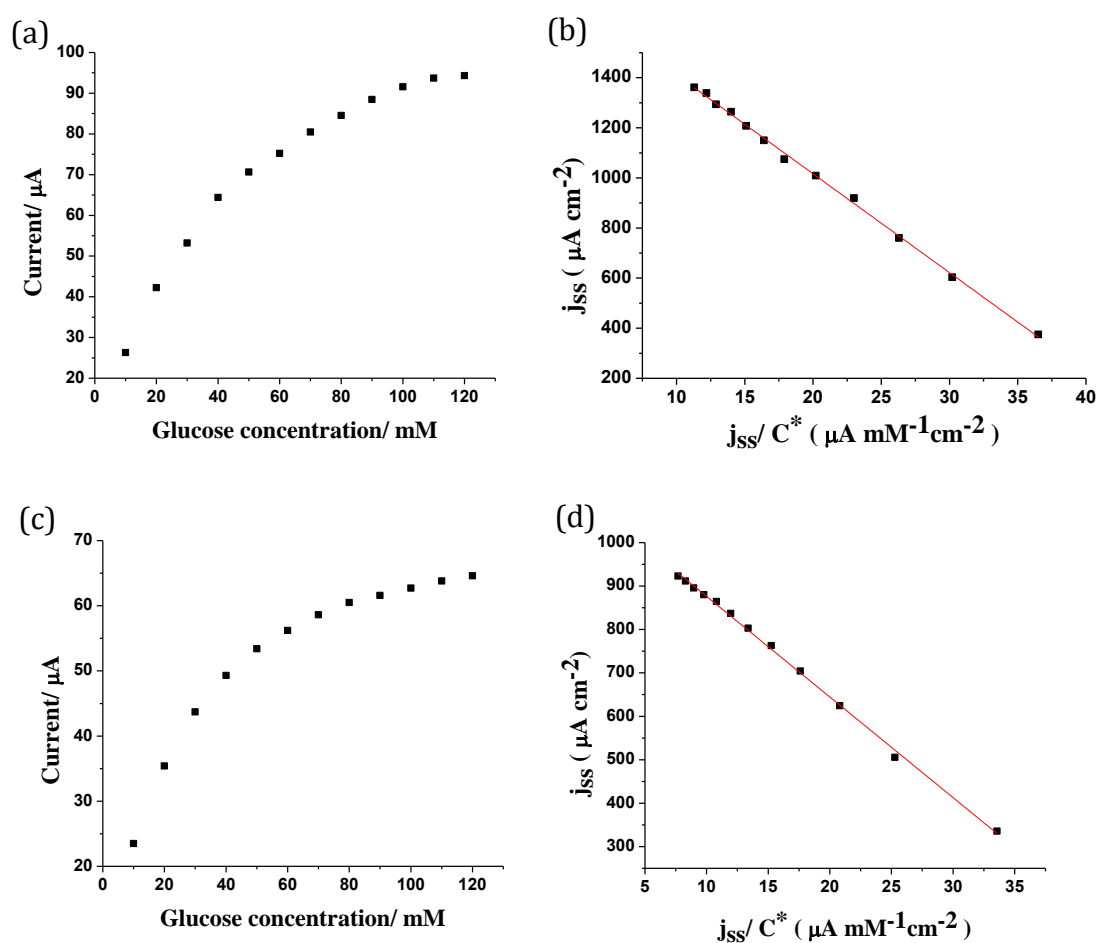


Figure 8: I_{ss} current obtained at a glassy carbon RDE modified with (a) Fc-Py-bPEI-MWCNT/GOx and (c) Fc-Py-bPEI-rGO/GOx as a function of glucose concentration (0.1 M PBS pH 7) (scan rate = 0.01 V s⁻¹; rotation rate = 2000 rpm). The Eadie- Hofstee plot (b) is obtained from the data shown in (a) and (d) using data from (c).

The Fc-Py-bPEI-MWCNT/GOx modified GC RDE exhibited a K_m' value of 39.5 mM (Figure 8a and 8b) from the gradient of Eadie Hofstee plot. The Fc-Py-bPEI-rGO/GOx modified GC RDE gave a lower K_m' value of 23 mM (Figure 8c and 8d) compared to Fc-Py-bPEI-MWCNT/GOx. Lower the K_m' value, higher the enzyme affinity towards substrate. The results revealed that the GOx enzyme affinity towards glucose was high in Fc-Py-bPEI-rGO/GOx than in Fc-Py-bPEI-MWCNT/GOx.

3.7. Analytical performance

The Fc-Py-bPEI-MWCNT/GOx modified electrode shows excellent catalytic activity towards glucose oxidation in a PBS pH 7 buffer medium. The analytical performance of the modified enzymatic electrode for glucose sensing was assessed by cyclic voltammetry under stationary electrode conditions. A plot of catalytic current (measured at 0.45 V vs Ag|AgCl(1 M KCl) after background subtraction) versus glucose concentration is shown in (Figure 9a). A linear response ($R^2 = 0.992$) with a slope of $27 \mu\text{A mM}^{-1} \text{cm}^{-2}$ was obtained over the concentration range of 5.0 to 40.0 mM. Deviation from linearity was observed above 50.0 mM and a plateau was reached at 90.0 mM glucose concentration. The limit of detection (LOD) of 0.3 mM was estimated from the standard deviation of ten measurements in an aqueous 0.1 M PBS pH 7 solution containing 0.50 mM glucose according to a well-documented protocol[33]. The modified enzyme electrode showed a maximum current density of $1.4 \pm 0.005 \text{ mA cm}^{-2}$. This is again attributed to the high efficiency of glucose oxidation achieved with redox hydrogel based glucose oxidase electrodes. Electrode-to-electrode reproducibility with five electrodes gave a RSD of 2.1 % confirming the suitability of this modified electrode for glucose detection. Fc-Py-bPEI-MWCNT/GOx electrode also provides the high current density needed for glucose fuel cell applications.

The performance of Fc-Py-bPEI-rGO/GOx modified electrode was evaluated in a similar manner. Compared to the Fc-Py-bPEI-MWCNT/GOx modified electrode it showed

interesting performance with a current density of $0.98 \pm 0.007 \text{ mA cm}^{-2}$. A plot of catalytic current (measured at 0.45 V vs Ag|AgCl(1 M KCl) after background subtraction) versus glucose concentration is shown in Figure 9b. A linear response ($R^2 = 0.988$) with a slope of $20 \mu\text{A mM}^{-1} \text{ cm}^{-2}$ is obtained over the concentration range of 5.0 to 30.0 mM. For this electrode, deviation from linearity was observed above 40.0 mM, a plateau current was reached at 90.0 mM glucose concentration, the limit of detection was calculated to be 0.4 mM and the electrode-to-electrode reproducibility with five electrodes gave a RSD value of 3.9 %.

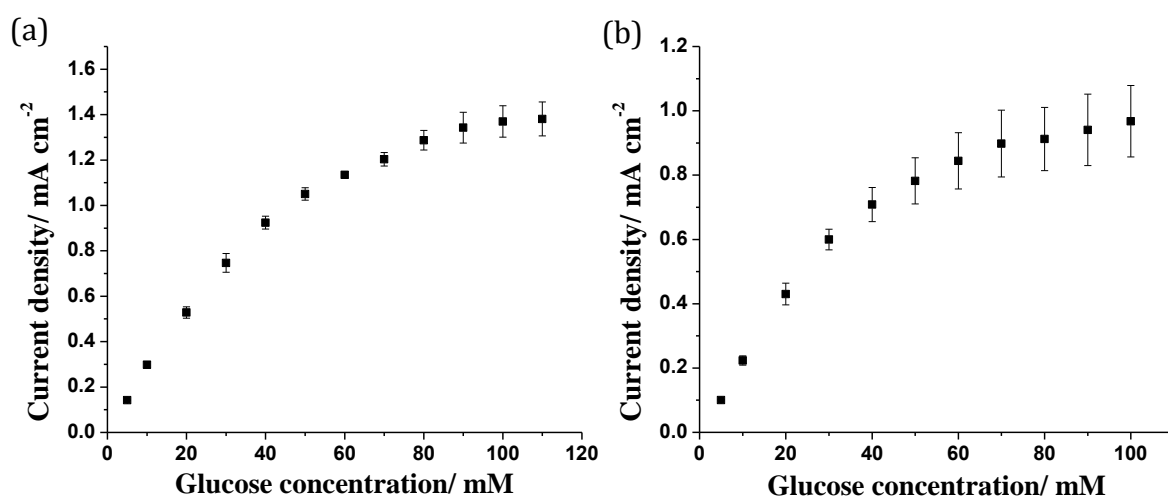


Figure 9: Calibration curve for the determination of glucose in 0.1 M PBS pH 7. The data produced represent the average of results obtained from three crosslinked (a) Fc-Py-bPEI-MWCNT /GOx and (b) Fc-Py-bPEI-rGO /GOx modified GCEs.

Table 1: Comparison of literature data reported for enzyme electrodes using carbon material decorated redox polymer performance and Fc is the mediator

Electrode	Electrolyte medium	Working electrode potential/ V	Max. current density/ mA cm ⁻²	Ref.
CNTs-Fc/SF-GOx	0.1M PBS pH7	0.5 vs SCE	0.51	[15]
MWCNT-Fc/chitosan-GOx	0.1M PBS pH7	0.35 vs Ag/AgCl	0.057	[12]
SWCNT/PEI-Fc-GOx	0.1M PBS pH7	0.35 vs Ag/AgCl	0.3	[16]
SWCNT/PAA-Fc-GOx	0.1M PBS pH7	0.4 vs Ag/AgCl	0.05	[16]
Fc-PAH-MWCNT/GOx	0.01M PBS pH7	0.5 vs Ag/AgCl	0.38	[34]
CS-Fc/GO/GOx	0.1 M PBS pH 6.98	0.3 vs Ag/AgCl	0.071	[19]
Fc-C ₆ -LPEI/SWCNT	0.05 M PBS pH7	0.35 vs SCE	3.0	[17]
Fc-Py-bPEI-MWCNT/GOx	0.1M PBS pH7	0.45 vs Ag/AgCl	1.4	This work
Fc-Py-bPEI-rGO/GOx	0.1M PBS pH7	0.45 vs Ag/AgCl	0.98	This work

Abbreviations: SF– silk film, PAA- poly(acrylic acid), CS- chitosan, PAH- poly(allylamine)

4. Conclusion

Carbon materials, such as multi wall carbon nanotubes and reduced graphene oxide have been non-covalently functionalised by π - π interaction with pyrene tethered to the redox relay of ferrocene functionalised branched PEI (bPEI). These materials can be employed for the development of enzymatic electrodes for the applications of electrocatalytic glucose oxidation. A comparison of the activity of Fc-Py-bPEI-MWCNT/GOx and Fc-Py-bPEI-rGO/GOx fabricated electrodes towards glucose oxidation revealed that Fc-Py-bPEI-MWCNT/GOx fabricated electrode has a maximum current density of 1.4 mA cm⁻² versus 0.98 mA cm⁻² for the Fc-Py-bPEI-rGO/ GOx fabricated electrode. The modified Fc-Py-bPEI-MWCNT/GOx showed a linear dynamic range of 5- 40 mM with a sensitivity of 27 μ A mM⁻¹

cm⁻² and a limit of detection of 0.3 mM. The results obtained under hydrodynamic conditions revealed a K_m' value of 39.5 mM. The Fc-Py-bPEI-rGO/GOx modified GCE showed a linear dynamic range of 5- 30 mM with a sensitivity of 20 $\mu\text{A mM}^{-1} \text{cm}^{-2}$ and a limit of detection of 0.4 mM. The results obtained under hydrodynamic conditions gave a K_m' value of 23 mM.

References

- [1] R. Wilson, A. Turner, Glucose oxidase: an ideal enzyme, *Biosens. Bioelectron.*, 7 (1992) 165-185.
- [2] Y. Shao, J. Wang, H. Wu, J. Liu, I.A. Aksay, Y. Lin, Graphene based electrochemical sensors and biosensors: a review, *Electroanalysis*, 22 (2010) 1027-1036.
- [3] I. Willner, Y.M. Yan, B. Willner, R. Tel-Vered, Integrated Enzyme-Based Biofuel Cells—A Review, *Fuel Cells*, 9 (2009) 7-24.
- [4] D. Ivnitski, B. Branch, P. Atanassov, C. Apblett, Glucose oxidase anode for biofuel cell based on direct electron transfer, *Electrochem. Commun.*, 8 (2006) 1204-1210.
- [5] M. Holzinger, A. Le Goff, S. Cosnier, Carbon nanotube/enzyme biofuel cells, *Electrochim. Acta*, 82 (2012) 179-190.
- [6] A. Trifonov, K. Herkendell, R. Tel-Vered, O. Yehezkeli, M. Woerner, I. Willner, Enzyme-capped relay-functionalized mesoporous carbon nanoparticles: effective bioelectrocatalytic matrices for sensing and biofuel cell applications, *ACS nano*, 7 (2013) 11358-11368.
- [7] W.H. Organization, Global report on diabetes, (2016).
- [8] S. Kerzenmacher, J. Ducr e, R. Zengerle, F. Von Stetten, Energy harvesting by implantable abiotically catalyzed glucose fuel cells, *J. Power Sources*, 182 (2008) 1-17.
- [9] M. Zhou, J. Wang, Biofuel Cells for Self-Powered Electrochemical Biosensing and Logic Biosensing: A Review, *Electroanalysis*, 24 (2012) 197-209.

- [10] H.J. Kong, D.J. Mooney, The effects of poly (ethyleneimine)(PEI) molecular weight on reinforcement of alginate hydrogels, *Cell transplant.*, 12 (2003) 779-785.
- [11] D. Cooray, S. Sandanayake, F. Li, S.J. Langford, A.M. Bond, J. Zhang, Efficient Enzymatic Oxidation of Glucose Mediated by Ferrocene Covalently Attached to Polyethylenimine Stabilized Gold Nanoparticles, *Electroanalysis*, 28 (2016) 2728-2736.
- [12] J.-D. Qiu, W.-M. Zhou, J. Guo, R. Wang, R.-P. Liang, Amperometric sensor based on ferrocene-modified multiwalled carbon nanotube nanocomposites as electron mediator for the determination of glucose, *Anal. Biochem.*, 385 (2009) 264-269.
- [13] X. Jia, S. Dong, E. Wang, Engineering the bioelectrochemical interface using functional nanomaterials and microchip technique toward sensitive and portable electrochemical biosensors, *Biosens. Bioelectron.*, 76 (2016) 80-90.
- [14] S. Iijima, Helical microtubules of graphitic carbon, *Nature*, 354 (1991) 56-58.
- [15] J. Liu, X. Zhang, H. Pang, B. Liu, Q. Zou, J. Chen, High-performance bioanode based on the composite of CNTs-immobilized mediator and silk film-immobilized glucose oxidase for glucose/O₂ biofuel cells, *Biosens. Bioelectron.*, 31 (2012) 170-175.
- [16] Y.-M. Yan, I. Baravik, O. Yehezkeli, I. Willner, Integrated electrically contacted glucose oxidase/carbon nanotube electrodes for the bioelectrocatalyzed detection of glucose, *J. Phys. Chem. C*, 112 (2008) 17883-17888.
- [17] T.O. Tran, E.G. Lammert, J. Chen, S.A. Merchant, D.B. Brunski, J.C. Keay, M.B. Johnson, D.T. Glatzhofer, D.W. Schmidtke, Incorporation of single-walled carbon nanotubes into ferrocene-modified linear polyethylenimine redox polymer films, *Langmuir*, 27 (2011) 6201-6210.
- [18] A.K. Geim, K.S. Novoselov, The rise of graphene, *Nat. Mater.*, 6 (2007) 183-191.
- [19] J.-D. Qiu, J. Huang, R.-P. Liang, Nanocomposite film based on graphene oxide for high performance flexible glucose biosensor, *Sens. Actuators B: Chem.*, 160 (2011) 287-294.

- [20] W. Yang, K.R. Ratinac, S.P. Ringer, P. Thordarson, J.J. Gooding, F. Braet, Carbon nanomaterials in biosensors: should you use nanotubes or graphene?, *Angew. Chem. Int. Ed.*, 49 (2010) 2114-2138.
- [21] E. Métay, M.C. Duclos, S. Pellet-Rostaing, M. Lemaire, J. Schulz, R. Kannappan, C. Bucher, E. Saint-Aman, C. Chaix, Conformational analysis and anion-binding properties of ferrocenyl-calixarene receptors, *Supramol. Chem.*, 21 (2009) 68-80.
- [22] W.S. Hummers Jr, R.E. Offeman, Preparation of graphitic oxide, *J. Am. Chem. Soc.*, 80 (1958) 1339-1339.
- [23] Z. Zhang, H. Chen, C. Xing, M. Guo, F. Xu, X. Wang, H.J. Gruber, B. Zhang, J. Tang, Sodium citrate: a universal reducing agent for reduction/decoration of graphene oxide with Au nanoparticles, *Nano Res.*, 4 (2011) 599-611.
- [24] J. Liu, N. Kong, A. Li, X. Luo, L. Cui, R. Wang, S. Feng, Graphene bridged enzyme electrodes for glucose biosensing application, *Analyst*, 138 (2013) 2567-2575.
- [25] N. Conrath, B. Gründig, K. Cammann, A novel enzyme sensor for the determination of inorganic phosphate, *Anal. Chim. Acta*, 309 (1995) 47-52.
- [26] V.B. Kandimalla, V.S. Tripathi, H. Ju, A conductive ormosil encapsulated with ferrocene conjugate and multiwall carbon nanotubes for biosensing application, *Biomaterials*, 27 (2006) 1167-1174.
- [27] J. Wang, Glucose biosensors: 40 years of advances and challenges, *Electroanalysis*, 13 (2001) 983.
- [28] J. Parker, C. Schwartz, Modeling the kinetics of immobilized glucose oxidase, *Biotechnol. Bioeng.*, 30 (1987) 724-735.
- [29] F. Shu, G. Wilson, Rotating ring-disk enzyme electrode for surface catalysis studies, *Anal. Chem.*, 48 (1976) 1679-1686.

- [30] B.A. Gregg, A. Heller, Cross-linked redox gels containing glucose oxidase for amperometric biosensor applications, *Anal. Chem.*, 62 (1990) 258-263.
- [31] A. Heller, Electrical connection of enzyme redox centers to electrodes, *J. Phys. Chem.* , 96 (1992) 3579-3587.
- [32] J.F. Castner, L.B. Wingard Jr, Mass transport and reaction kinetic parameters determined electrochemically for immobilized glucose oxidase, *Biochemistry*, 23 (1984) 2203-2210.
- [33] D. MacDougall, W.B. Crummett, Guidelines for data acquisition and data quality evaluation in environmental chemistry, *Anal. Chem.*, 52 (1980) 2242-2249.
- [34] L. Deng, Y. Liu, G. Yang, L. Shang, D. Wen, F. Wang, Z. Xu, S. Dong, Molecular “wiring” glucose oxidase in supramolecular architecture, *Biomacromolecules*, 8 (2007) 2063-2071.

Chapter 3

Efficient Enzymatic Oxidation of Glucose

Mediated by

Ferrocene Covalently Attached to Polyethylenimine

Stabilized Gold Nanoparticles

Efficient Enzymatic Oxidation of Glucose Mediated by Ferrocene Covalently Attached to Polyethylenimine Stabilized Gold Nanoparticles

M. C. Dilusha Cooray,^[a] Saman Sandanayake,^[a] Fengwang Li,^[a] Steven J. Langford,^[a] Alan M. Bond,^[a] and Jie Zhang^{*[a]}

Abstract: Bioanodes for fuel cell applications require highly efficient oxidation reactions to achieve a sufficiently large current density. In this study, gold nanoparticles have been synthesized using branched polyethylenimine (bPEI), a well-known polymer that forms a hydrogel in water, as the stabilizer. Primary amine groups available in bPEI provide active sites for further conjugation with ferrocene propionic acid via the 1-Ethyl-3-(3-dimethylaminopropyl)carbodiimide coupling reaction, with the enzyme glucose oxidase, using glutaraldehyde as linkers. This composite material was then used for the fabrication of glucose oxidase electrodes by drop casting of aqueous solutions onto glassy carbon electrodes. The three-dimensional structure offered by the new hydrogel facilitates

communication between the enzyme and the electrode through the redox mediator ferrocene. This allows the glucose oxidase electrode to exhibit excellent activity towards electrocatalytic oxidation of glucose in phosphate buffer solutions at pH 7 with a maximum current density of approximately $800 \mu\text{A cm}^{-2}$, one of the highest values reported so far for redox hydrogel based glucose oxidase electrodes. Over a wide glucose concentration range, the enzyme response follows that predicted by the Michaelis-Menten equation with a Michaelis constant of 8.4 mM. In the sensing context, this electrode also exhibits a wide linear dynamic glucose concentration range of 0.5–10 mM with a limit of detection of 0.04 mM.

Keywords: Enzymes • Glucose oxidase • Hydrogel • Nanoparticles • Ferrocene

1 Introduction

Enzyme electrodes, which utilize immobilized oxidoreductase as the catalysts for electrochemical oxidation/reduction of a substrate, are very important for sensing and energy applications [1–7]. In the field of sensing, electrochemical glucose sensors, which utilize immobilized glucose oxidase/dehydrogenase as catalysts for electrochemical oxidation of glucose, provide a facile, cost-effective, precise and simple method for the determination of glucose for diabetic patients to prevent the occurrence of blindness, kidney failure and heart disease [8] which are more pronounced in humans having abnormal blood glucose concentrations outside of the region of 4.4 mM–6.6 mM [9]. Reliable and commercially successful electrochemical biosensors are now available [6,7]. However, the development of enzyme electrodes is not confined to sensing requirements as they are also of interest in bioanodes for fuel cell applications, where high current density and long term stability are the key requirements [1–5]. The primary objective of the work described in this paper is with respect to achieving high current density in a glucose modified electrode as needed in fuel cells and other high current density applications.

A glucose oxidase electrode often consists of three key components: 1) an enzyme, 2) an enzyme immobilising matrix and 3) an electron shuttle between the isolated

enzyme active centres and electrode. Designing a single material, which accommodates all properties required for electrochemical oxidation of glucose with high energy efficiency and long term stability is challenging [1–5]. Therefore, the concept of using composite materials for electrode fabrication has been introduced and a wide variety of materials have been tested for electrochemical glucose sensing and biofuel applications [6, 9–16]. Redox hydrogels are among the most promising materials investigated so far [14,15].

Redox hydrogels represent a class of polymer which enable enzyme active sites to communicate efficiently with the electrode via covalently attached mediators [17–20]. Iron (ferrocene) [21], osmium [22,23] and ruthenium [24] derivatives have been used as mediators so far. Heller and co-workers have introduced a series of redox hydrogels for the fabrication of electrochemical glucose biosensors and achieved commercial success [6,25,26].

[a] M. C. Dilusha Cooray, S. Sandanayake, F. Li, S. J. Langford, A. M. Bond, J. Zhang
School of Chemistry, Monash University, Clayton, Victoria
3800, Australia
*e-mail: jie.zhang@monash.edu

Supporting information for this article is available on the WWW under <http://dx.doi.org/10.1002/elan.201600201>.

The development of redox hydrogels is still in a growth stage with respect to meeting requirements for new high current density applications highlighted above [1–7]. However, suitable technology also is emerging from the glucose sensing areas. For example, branched polyethylenimine (bPEI) is a well-known highly water soluble polymer that has excellent biocompatibility for bioengineering applications [27,28] and as a consequence has been used to synthesize redox hydrogels for enzyme electrode sensing applications. Thus, Merchant *et al.* [29] used ferrocene (Fc) conjugated linear PEI for glucose oxidase electrode fabrication for glucose determinations. Glucose sensing capability was also achieved by Chuang *et al.* [30] where bPEI was used instead of the linear one and by Wang *et al.* [31] who integrated the conducting polymer poly(3,4-ethylenedioxythiophene) with a Fc conjugated bPEI.

It is now also widely acknowledged that nanostructured materials can significantly enhance the performance of electrochemical biosensors [32–35]. In particular, metallic nanoparticles can serve as an efficient relay to facilitate electron transfer over a long distance [36–38]. PEI can be used as a stabilizer for the formation of nanoparticles [39,40], which provides a facile route for their integration into PEI based materials in the generation of a new class of nanocomposite materials. To assess the usefulness of these materials for high current density enzyme electrode development, in this study gold nanoparticles were synthesized using bPEI as the stabilizer, and then further conjugated with ferrocene propionic acid via the 1-ethyl-3-(3-dimethylaminopropyl)carbodiimide (EDC) coupling reaction. EDC activates the carboxyl group for the coupling of primary amines to form amide bonds. After separation and purification, the resulting material was used for covalent attachment of enzyme glucose oxidase using glutaraldehyde (GA) as linkers. This composite material was then used for the fabrication of glucose oxidase electrodes. The catalytic activities of the enzyme electrodes and current density were assessed in aqueous buffered media. While not the main goal of this study, assessment of performance as an electrochemical sensor was also undertaken.

2 Experimental

2.1 Chemicals

The chemicals branched polyethylenimine (bPEI, 97%), gold(III) chloride trihydrate ($\text{HAuCl}_4 \cdot 3\text{H}_2\text{O}$, 99.9%), N-hydroxysuccinimide (NHS, 98%), 1-ethyl-3-(3-dimethylaminopropyl)carbodiimide hydrochloride (EDC, commercial grade), glutaraldehyde solution in H_2O (GA, 50% (w/v)), triethyl phosphonoacetate (98%), ammonium chloride (99%), sodium hydride (60% dispersion in mineral oil), ferrocene carboxaldehyde (98%), and D-glucose (99%) were purchased from Sigma Aldrich. Sodium dihydroxyphosphate (99%) and disodium hydrogen phosphate (99%) from Merck were used for the preparation of

buffer solutions. Glucose oxidase (GOx, 211 U mg^{-1}) was purchased from Fluka. Acetonitrile (MeCN, reagent grade) was obtained from LiChrosolv Merck. All of the above mentioned chemicals were used as received. Deionised water was utilized for preparation of solutions.

2.2 Preparation of bPEI Stabilized Au Nanoparticles (bPEI-AuNPs)

The synthesis of AuNPs was carried out at $20 \pm 2^\circ\text{C}$. Firstly, bPEI (2 mg) was dissolved in 1 mL of deionised water. The solution was magnetically stirred continuously. A 25.0 μL solution of 0.2 M $\text{HAuCl}_4 \cdot 3\text{H}_2\text{O}$ (5 mM) was added to the bPEI solution. Upon addition of NaBH_4 (0.73 mg mL^{-1}) the solution turned wine red indicating the formation of AuNPs due to the reduction of AuCl_4^- to metallic AuNPs that are stabilised by a coating layer of bPEI. This dispersion was stirred for 15 min allowing the reaction to go to completion. The AuNPs formed were then separated by centrifugation at a rotation rate of 21000 rpm (Beckman Coulter, Allegra 64R centrifuge); re-dispersed in a solution containing 0.5 mL water and 1 mL of MeCN and isolated again using centrifugation. Finally, the purified bPEI-AuNPs were dispersed in 250 μL water and stored in a refrigerator until coupled with the mediator ferrocene propionic acid. The bPEI-AuNPs dispersion was stable for a long period without any noticeable aggregation of the particles. A similar procedure was employed in the synthesis of bPEI-AuNPs with different PEI concentrations.

2.3 Coupling of Fc with bPEI-AuNPs

The EDC coupling method was employed to couple ferrocene propionic acid with bPEI-AuNPs according to a well-documented protocol [41]. Ferrocene propionic acid was synthesised according to a literature procedure [42]. An (100 μL) aliquot of the b-PEI-AuNPs was mixed with 200 μL ferrocene propionic acid (4 mg mL^{-1}) MeCN solution. Then, NHS and EDC (1.5 molar equivalent with respect to ferrocene propionic acid) were added to the solution. The solution was stirred for 2.5 hrs. Fc-bPEI-AuNPs formed were isolated by centrifugation at a rotation rate of 14500 rpm (Eppendorf, mini spin plus) and then washed with MeCN to remove unreacted ferrocene propionic acid. Finally, the modified nanoparticles were re-dissolved in 200 μL of water and stored in a refrigerator until used in subsequent studies.

2.4 Microscopic and Spectroscopic Characterization of Fc-bPEI-AuNPs

High resolution images were obtained with a FEI Tecnai G2 T20 TWIN LaB6 Transmission Electron Microscope (TEM) to determine the morphology and size of Fc-bPEI-AuNPs. Energy Dispersive X-ray spectroscopy analysis was conducted at 10 keV to confirm the composition of Fc-bPEI-AuNPs. UV-Visible spectra were recorded

Full Paper

ELECTROANALYSIS

with a UV-Vis-NIR spectrometer (Carry 500). Direct Light Scattering (DLS) measurements were obtained from a Zetasizer Nano instrument (Malvern Instruments).

2.5 Crosslinking of GOx to Fc-bPEI-AuNPs and Fabrication of the Fc-bPEI-AuNPs and Fc-bPEI-AuNPs/GOx Modified Electrodes

To prevent leakage of GOx from the enzyme electrodes to the electrolyte media during sample analysis, the $-NH_2$ sites of the enzyme and the bPEI were crosslinked using GA as the cross-linking agent to form Fc-bPEI-AuNPs/GOx. In this procedure, Fc-bPEI-AuNPs solution (30 μ L) was mixed with GOx (dissolved in 10 μ L H_2O) to obtain a homogeneous solution. Mixing with GA was then undertaken to crosslink the primary amines on GOx and bPEI. The amount of added GA was varied by using 0.5, 1.0, 1.5 μ L etc. aliquots of a 3% (w/v) solution.

A glassy carbon electrode (GCE, 3mm diameter, CH Instruments, Texas, USA), was used to prepare the modified electrodes used in voltammetric studies. Initially, the electrode was polished with an aqueous 0.3 μ m alumina slurry followed by rinsing with water, sonication and rinsing again with water before drying under a nitrogen atmosphere. Then 4.0 μ L of Fc-bPEI-AuNPs or Fc-bPEI-AuNPs/GOx solution was drop-casted on the electrode surface and left to dry in air, before use in an electrochemical measurement. The GC rotating disk electrode (GC-RDE, 3 mm, BAS, Tokyo, Japan) was modified in a similar manner.

2.6 Electrochemical Measurements

Voltammetric measurements were carried out at $20 \pm 2^\circ C$ using a CH Instrument 760D electrochemical workstation with a conventional three-electrode cell. Phosphate Buffer Saline (PBS) (0.1 M, pH 7) was used as the electrolyte. The modified GCE or GC-RDE, $Ag|AgCl_{(1M KCl)}$ and platinum wire were employed as working, reference and auxiliary electrodes respectively. Appropriate aliquots of a 1.00 M glucose stock solution were added to the PBS pH 7 solution in the cell to obtain the required concentration of glucose. To remove oxygen, all solutions were degassed with high purity nitrogen for at least 10 min prior to commencing the electrochemical measurements. A scan rate of 0.01 $V s^{-1}$ was used, unless otherwise stated. The catalytic current was obtained by subtracting the diffusion current for ferrocene from the electrocatalytic current obtained from glucose oxidation at 0.4 V vs. $Ag|AgCl_{(1M KCl)}$.

3 Results and Discussion

3.1 Characterisation of Fc-bPEI-AuNPs

To obtain the size distribution of the synthesised nanoparticles, TEM and DLS measurements were undertaken.

The calculated average diameter using TEM was 3.6 ± 0.8 nm (Figure 1a). The average diameter is 8.2 nm according to the DLS data (Figure 1b), which is considerably larger than the value obtained with TEM. In DLS analysis, the size of the particle includes the polymer cap, while the TEM gives the size of the metallic core of the polymer stabilised AuNPs. Thus, DLS reveals a larger particle diameter. The EDX spectrum (Figure 1c) shows the characteristic signals of N and C from PEI, Fe and O from ferrocene propionic acid and Au from the AuNPs. Fc-bPEI-AuNPs was also characterized by UV-visible spectroscopy. The UV-visible spectrum shown in Figure 1d exhibits a characteristic surface plasma absorption band for AuNPs around 503 nm, which is characteristic of AuNPs having diameters between 2.5 and 10 nm [43].

3.2 Characterisation of Redox Active Fc-bPEI-AuNPs Modified Electrodes

PEI is a well-known very hydrophilic polymer that forms a hydrogel in water [44]. A high percentage of bPEI in the nanocomposite is expected to destabilize the modified electrode during analytical applications due to dissolution. Therefore, the bPEI content should be optimized. In the synthesis of Fc-bPEI-AuNPs, different quantities of bPEI were used while keeping the $AuCl_4^-$ concentration constant in order to establish the optimum bPEI concentration. From these experiments with variable bPEI concentration, it was found that use of high concentration of bPEI lowered the stability of the modified electrodes during analytical measurements in aqueous media. Thus, with 20 $mg mL^{-1}$ bPEI, cycling the potential led to a drastic decrease in both background capacitance and faradaic currents, implying that dissolution of Fc-bPEI-AuNPs has occurred from the electrode surface (Figure 2). bPEI is highly water soluble. Conjugation with Fc and the presence of AuNPs lowers the solubility of Fc-bPEI-AuNPs. However, use of very low PEI concentrations (or high AuNPs content), although enhancing the stability of the modified electrode, also is not ideal as the resulting Fc-bPEI-AuNPs material is over rigid. Consequently, the covalently attached Fc mediators have low mobility in the modified electrode and hence communicate poorly with the enzyme and electrode. Ultimately, it was discovered that use of 4 $mg mL^{-1}$ bPEI concentration was ideal to achieve the best balance of stability and hydrophilicity of Fc-bPEI-AuNPs films.

The Fc derivative used in this application acts as a mediator to shuttle electrons between isolated enzyme active sites and the electrode. Fc is covalently attached to bPEI to minimise leakage [45,46]. Gold nanoparticles with different PEI:Fc weight ratios were synthesised using a range concentrations of ferrocene propionic acid in the EDC coupling reaction. Cyclic voltammetric characterization of electrodes modified with these nanocomposite materials was undertaken in 0.1 M PBS pH 7 to determine the optimum Fc loading (scan rate of 0.01 $V s^{-1}$ used over the potential range of -0.05 – 0.4 V). A well-defined oxi-

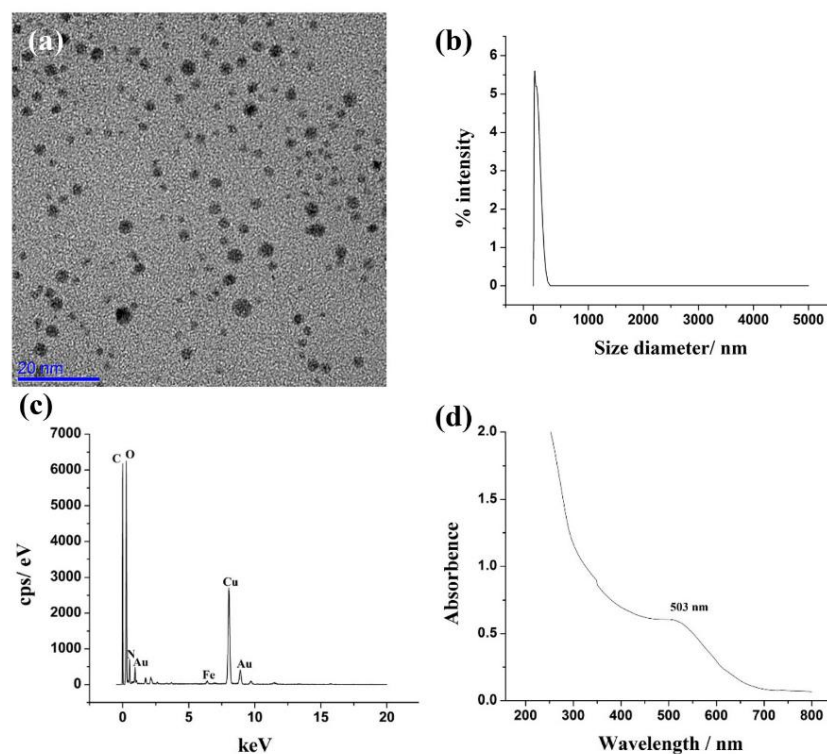


Fig. 1. Electron microscopic and spectroscopic characterization of Fc-bPEI-AuNPs: (a) TEM image, (b) DLS spectrum, (c) EDX spectrum and (d) UV-vis spectrum.

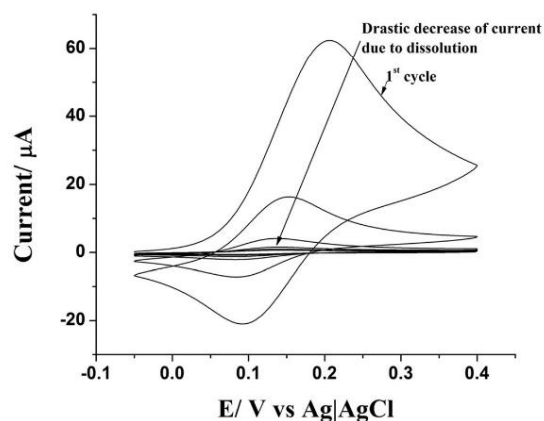


Fig. 2. Cyclic voltammogram obtained in 0.1 M PBS pH 7 at a scan rate of 0.01 V s^{-1} when Fc-bPEI-AuNPs with a high bPEI content were used for GCE modification.

dation process associated with Fc was observed under all conditions (Figure 3). When Fc-bPEI-AuNPs were synthesized using 2 mg mL^{-1} ferrocene propionic acid, the reversible potential (taken as the average of the oxidation and reduction peak potentials as an approximation) for the ferrocene process is $0.237 \text{ V vs. Ag|AgCl}_{(1 \text{ M KCl})}$. However, the peak-to-peak separation of 39 mV differs from the theoretically predicted value of 0 V for an ideal reversible surface-confined process because of incomplete depletion of Fc on the voltammetric timescale under the thick film conditions used. When the loading of ferrocene propionic acid was increased, the peak current associated with the Fc/Fc^+ process increased almost proportionally while the reversible potential remained similar. These results suggest that the film hydrophilicity remains essentially unaltered. However, a further increase of the loading ferrocene propionic acid decreases the hydrophilicity of the film, resulting in decrease of peak current and a shift in reversible potential to more positive values. As a result of these studies, a 4 mg mL^{-1} ferrocene propionic acid solution was chosen to synthesize Fc-bPEI-AuNPs.

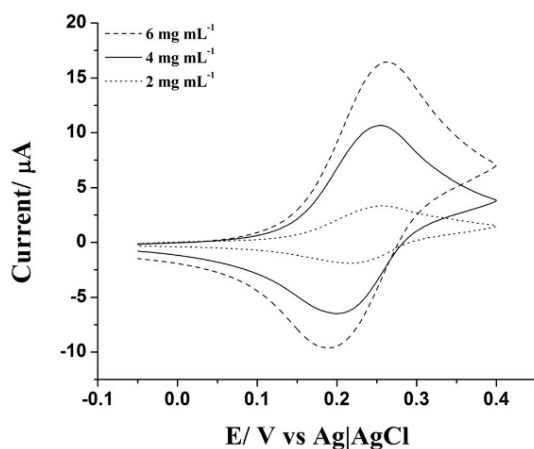


Fig. 3. Cyclic voltammograms obtained in 0.1 M PBS pH 7 at a scan rate of 0.01 V s^{-1} with GCEs modified with Fc-bPEI-AuNPs synthesized using designated concentrations of ferrocene propionic acid.

3.3 Glucose Oxidation by GOx With and Without Crosslinking to Fc-bPEI-AuNPs

The hydrogel bPEI contains $-\text{NH}_2$ sites, which are positively charged at pH 7 due to protonation. This enables immobilisation of negatively charged [47] GOx due to electrostatic interactions. However, this simple mixing of enzyme with redox active polymer could not completely prevent enzyme leakage when the electrode is placed in contact with analyte solutions. Bio-conjugation of enzymes with the redox active polymer will give rise to a 3-dimensional (3D) structure that results in a higher loading of GOx and higher stability of the enzyme electrodes [48,49]. In this arrangement the amines on bPEI and the enzymes will be cross-linked via the aldehyde groups on GA to give an amide bond [50]. Examination of the voltammogram in Figure 4 shows that crosslinking of the

enzyme gives higher electrocatalytic current density (Figure 4b) than found with the non-crosslinked modified electrode (Figure 4a). Crosslinking of the enzyme inhibits possible leakage and increases the stability of Fc-bPEI-AuNPs/GOx film.

It is interesting to note that there is a peak in both forward (oxidative) and reverse (reductive) potential sweep in the presence of 5.0 mM glucose under both crosslinked and non-crosslinked conditions (Figure 4). The average of the oxidation and reduction peak potentials coincides with the reversible potential for the $\text{Fc}^{0/+}$ process. This voltammetric characteristic, which is not evident at high glucose concentration (not shown), is attributed to the depletion of glucose due to the presence of relatively high concentrations of Fc and GOx. Consequently, the excessive amount of electrogenerated Fc^+ is reduced in the reverse potential sweep.

3.4 Optimisation of Enzyme Weight Percentage and Fc-bPEI-AuNPs Loading

Since the loading of GOx will also affect the performance of the enzyme electrodes, optimisation of the percentage in the film was undertaken. Electrodes modified with films containing $28 \mu\text{g}$ Fc-bPEI-AuNPs, $1.73 \mu\text{g}$ GA and various amount of GOx were used for voltammetric experiments in 0.1 M PBS (pH 7) in the presence and absence of 5.0 mM glucose. Catalytic glucose oxidation currents were obtained at 0.4 V after subtracting the background current measured in the absence of glucose and plotted as a function of GOx weight (Figure 5a). Since GOx is the catalyst for glucose oxidation, an increase of catalytic current can be expected when the loading of GOx increases. However, when the loading of GOx is too high, the catalytic current may decrease, since not all GOx can communicate effectively with the Fc mediators. The results show that 12 μg of GOx (or 29% weight from the total film) gives the optimal catalytic response towards glucose oxidation.

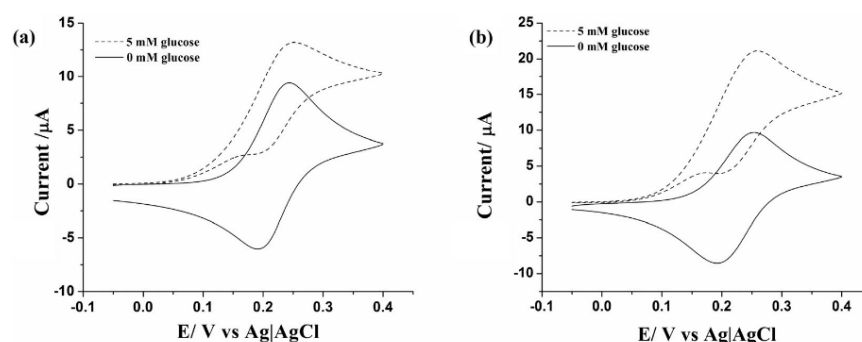


Fig. 4. Cyclic voltammograms obtained at a scan rate of 0.01 V s^{-1} in 0.1 M PBS pH 7 in the presence and absence of 5.0 mM glucose with (a) non-crosslinked (the film contains $12 \mu\text{g}$ GOx and $28 \mu\text{g}$ Fc-bPEI-AuNPs) and (b) crosslinked (the film contains $12 \mu\text{g}$ GOx, $28 \mu\text{g}$ Fc-bPEI-AuNPs and $1.73 \mu\text{g}$ GA) Fc-bPEI-AuNPs/GOx modified GCEs.

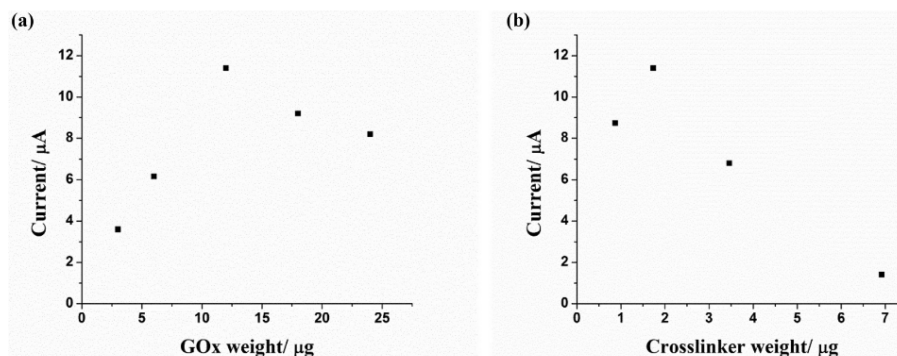


Fig. 5. Catalytic current obtained at Fc-bPEI-AuNPs/GOx modified GCEs in the presence of 5.0 mM glucose (0.1 M PBS pH 7) as a function of the weight of (a) GOx (in addition to GOx, the film also contains 28 µg Fc-bPEI-AuNPs and 1.73 µg GA) and (b) GA (in addition to GA, the film also contains 28 µg Fc-bPEI-AuNPs and 12 µg GOx).

Although crosslinking of GOx with Fc-bPEI-AuNPs improves the stability of the enzyme electrodes, overcrosslinking decreases GOx activity [51]. Experiments were also undertaken to identify the optimal amount of GA. A set of data, with 5.0 mM glucose was collected with constant Fc-bPEI-AuNPs (28 µg) and GOx (12 µg) weights, but the GA amount was varied. The results are displayed in Figure 5b and show that the optimum weight of GA to crosslink 12 µg of GOx is 1.73 µg (4% weight from the total film). In summary, the optimised weight % of the film components are: Fc-bPEI-AuNPs 67%, GOx 29% and GA 4%.

The effect of the film thickness was studied by varying the amount of material that was applied to the surface of the electrode. Figure S1 reveals that the catalytic current from 5.0 mM glucose initially increased with film loading up to 596 µg cm⁻² and then slightly diminished, presumably due to the mass transport limitation associated with glucose. The optimum film loading of 596 µg cm⁻² was employed in subsequent experiments.

3.5 Effect of pH on Glucose Response

The activity of the enzyme is influenced by pH [29,52] as is the electrical communication between the mediator and the enzyme active sites since the hydrogel property of bPEI is also pH dependent. For the Fc-bPEI-AuNPs nanocomposites the highest electrocatalytic current density at 0.4 V vs. Ag|AgCl_(1M KCl) for 5.0 mM glucose was found to be at pH 7 over the pH range of 6 to 8 (Figure S2). Therefore, pH 7 is recommended as it provides a suitable environment for GOx, and in the context of sensing application is conveniently close to the physiological pH of blood [53].

3.6 Kinetics of the Optimised Cross Linked Fc-bPEI-AuNPs/GOx Modified Enzyme Electrode

Experiments undertaken under hydrodynamic conditions with an Fc-bPEI-AuNPs/GOx modified GC RDE (scan

rate = 0.01 V s⁻¹) in the presence of 5.0 mM glucose, provided a steady state limiting current (I_{ss}) that was independent of rotation rate in the range of 500–2000 rpm (Figure S3). The result implies that the process was kinetically rather than mass transport controlled under these conditions. Thus, although the diffusion coefficient of the substrate into the redox hydrogel nanocomposite matrix [54] could not be calculated precisely at the RDE using the Levich equation [55], the kinetics of the reaction can be determined. For this latter purpose, the GC RDE was drop casted with the crosslinked Fc-bPEI-AuNPs/GOx coating solution. Aliquots of 1 M glucose solution were then injected into the cell, which contained 5 mL of 0.1 M PBS pH 7 solution as the electrolyte and finally cyclic voltammograms were obtained at a scan rate of 10 mV s⁻¹ and a rotation rate of 2000 rpm. This high rotation rate was employed to avoid concentration polarisation at low glucose concentrations so that the process is kinetically limited [49,56].

The I_{ss} values obtained from RDE experiments as a function of glucose concentrations are presented in Figure 6a. An excellent linear relationship was observed when the concentration of glucose is low suggesting that oxidation of glucose by GOx is the rate-limiting step. The I_{ss} value approaches a plateau when the concentration of glucose is high since the oxidation of GOx by Fc⁺ now becomes the rate-limiting step. The apparent Michaelis constant, K'_m , which quantifies the activity of the enzyme in the redox polymer film [57], can be obtained based on an Eadie-Hofstee type of Michaelis-Menten equation [58] given below,

$$j_{ss} = j_{max} - K'_m (j_{ss}/C^*) \quad (2)$$

where j_{ss} is the steady state current density, j_{max} is the maximum current density, K'_m is the apparent Michaelis Menten constant and C^* is the bulk solution concentration of glucose [58]. The Eadie-Hofstee plot in Figure 6b shows an excellent linearity ($R^2 = 0.995$) with a gradient

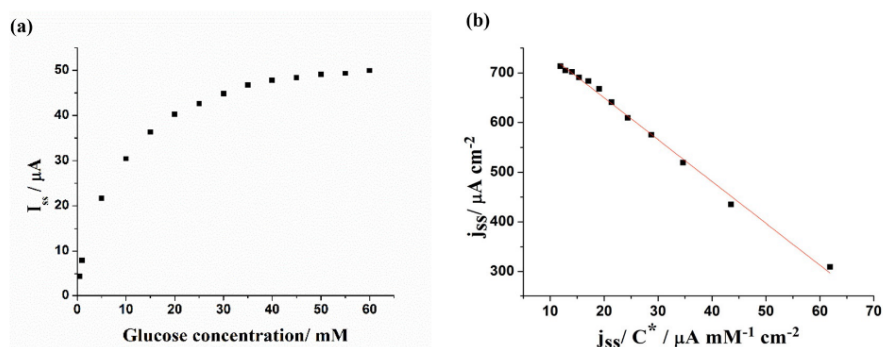


Fig. 6. (a) I_{ss} current obtained at a glassy carbon RDE modified with Fc-bPEI-AuNPs/GOx as a function of glucose concentration (0.1 M PBS pH 7) (scan rate = 0.01 V s^{-1} ; rotation rate = 2000 rpm) (b) Eadie-Hofstee plot of the data shown in (a).

($-K'_m$) of 8.4 mM and an intercept (j_{max}) of $818 \mu\text{A cm}^{-2}$. The j_{max} value provides a measure of current density and is one of the highest values reported so far for redox hydrogel based glucose oxidase electrodes [31,59]. The K'_m value for glucose oxidation of 8.4 mM is comparable to those reported in literature for immobilized [57,60,61] and dissolved [62] GOx.

3.7 Glucose Sensing Performance

The major goal of this work was to achieve high current density via efficient oxidation of glucose. However, of course the strategy to achieve this outcome as in this study also forms a platform for a glucose sensor, which was briefly assessed. Not surprisingly, the method works well in buffered media but suffers from the usual interferences [6,7] that would need to be addressed if practical applications in blood were to become viable. The Fc-bPEI-AuNPs/GOx modified GCE clearly shows excellent catalytic activity towards glucose oxidation under pH 7 PBS (0.1 M) which is the physiological pH. The analytical performance of the modified enzymatic electrode for glucose sensing in the buffer media was assessed by cyclic voltammetry under stationary electrode conditions. A plot of catalytic current (measured at 0.400 V vs. Ag|AgCl_(LMKCl) after background subtraction) versus glucose concentration is shown in Figure 7. A linear response ($R^2 = 0.989$) with a slope of $50 \mu\text{A mM}^{-1} \text{ cm}^{-2}$ is obtained over the concentration range of 0.5 to 10 mM. Deviation from linearity is detected when the concentration is above 10 mM and a plateau is reached at around 40 mM. Since the normal human blood glucose level lies in the range of 4.4 mM to 6.6 mM [9], the linear range lies within the required blood glucose level. The limit of detection (LOD) of 0.04 mM was estimated from the standard deviation of ten measurements in an aqueous 0.1 M PBS pH 7 solution containing 0.5 mM glucose according to a well-documented protocol [63]. The modified enzyme electrode showed a maximum current density of $793 \pm 1.1 \mu\text{A cm}^{-2}$, which is also in good agreement with

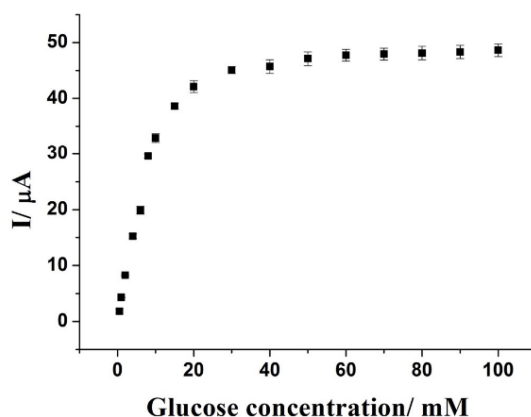


Fig. 7. Calibration curve for the determination of glucose in 0.1 M PBS pH 7. The data produced represent the average of results obtained from three crosslinked Fc-bPEI-AuNPs/GOx modified GCEs.

the j_{max} value of $818 \mu\text{A cm}^{-2}$ obtained from the extrapolation of the Eadie-Hofstee plot. This is again attributed to the high efficiency of glucose oxidation achieved with redox hydrogel based glucose oxidase electrodes. Electrode-to-electrode reproducibility with five electrodes gave a RSD of 0.12% confirming the suitability of this modified electrode for glucose detection. The above data are summarized in Table 1 and compared with the literature values for the ferrocene mediator based polymer nanocomposite glucose oxidase electrodes. Our glucose oxidase electrode provides high sensitivity, and a linear range suitable for glucose determination in blood.

3.8 Interferences

In glucose sensing, ascorbic acid (AA) and uric acid (UA) are the main species interfering with the determination of glucose in biological samples. Trace amounts of

Table 1. Comparison of performance of ferrocene mediator based polymer nanocomposite enzyme electrodes for glucose sensing.

Electrode material ^[a]	Sensitivity ($\mu\text{A mM}^{-1} \text{cm}^{-2}$)	Linear range (mM)	Operational potential/V (Ag- AgCl KCl _{sat})	pH Ref
Fc-LPEI/GOx/GC	10 ^[b]	0.005–0.1	0.456	7.0 [29]
bPEI-Fc/PEDOT:PSS/GOx/SPCE	66	0.5–4.5	0.45	5.5 [31]
PyCO ₂ H/PPy-Fc/GOx/GCE	1.796	1.0–4.0	0.38	7.0 [64]
Fc-polysiloxane/Chi/GOx/GCE	0.86	1–6	0.456	7.0 [65]
Th/Th-COOH/Th-Fc/GOx/GCE	0.04	0.5–3.0	0.35	7.4 [66]
GNPs/CD-Fc/GOD	18.2	0.08–11.5	0.295	7.0 [67]
Fc-bPEI-AuNPs/GOx/GCE	50	0.5–10	0.425	7.0 This work

[a] Abbreviations: PEDOT:PSS – poly(3,4-ethylenedioxythiophene) polystyrene sulfonate; SPCE – screen printed carbon electrode; PyCO₂H – 1-(2-carboxyethyl)pyrrole; PPy-Fc – N-(3-(1H-pyrrol-1-yl) ethyl) ferrocenecarboxate; Chi – chitosan; Th – thiophene; GNP – gold nanoparticles; CD – cyclodextrin. [b] calculated based on the cyclic voltammograms shown in Figure 2 of reference [29].

metabolites of drugs also may be problematic [8]. Therefore, an interference study was undertaken in the presence of physiological amounts of either AA or UA in aqueous 0.1 M PBS pH 7 solution using the Fc-PEI-AuNPs/GOx modified GCE. In the presence of 0.50 mM UA, the voltammetric response from 5.0 mM glucose remains essentially unaffected (Figure S4). However, the presence of 2.5 mM AA does affect the voltammetric response from 5 mM glucose (Figure S5). An additional process around 0.18 V for AA oxidation was observed. The fact that the process associated with the oxidation of Fc is also present suggests that the oxidation of AA is not mediated by Fc, unlike glucose. Interference from the oxidation of AA in principle can be solved by applying a polycarbonate coating that allows glucose only [68]. Furthermore, since oxidation of AA occurs via a totally independent pathway where neither GOx nor Fc is involved and the AA and glucose oxidation processes are well-resolved, in principle the electrochemical response from AA oxidation can be measured separately and subtracted from the measured total current.

4 Conclusions

The crosslinked Fc-bPEI-AuNPs/GOx nanocomposite facilitates electron transport between the enzyme GOx and GC electrode via mediator as evident by the catalytic current detected in the presence of glucose. The synthesis and isolation of the material is straightforward. Crosslinking of the mediator and enzyme prevents possible leakage and provided excellent stability towards the detection of glucose. The presence of AuNPs in this composite material modifies its solubility and consequently enhances the stability of the modified electrodes. Compared to Fc-PEI/GOx [29], the new Fc-bPEI-AuNPs/GOx composite reported in this study demonstrates superior activity for electrochemical oxidation of glucose giving rise to one of highest current densities for the redox hydrogel based glucose oxidase electrodes, presumably by facilitating the electron transfer processes [36–38]. The glucose oxidation by this nanocomposite modified electrode is kinetically controlled and showed a sensitivity of $50 \mu\text{A mM}^{-1} \text{cm}^{-2}$,

a linear dynamic range of 0.5–10 mM, LOD of 0.04 mM with a K'_m value of 8.4 mM which also makes it potentially suitable for biosensor applications, provided the usually encountered matrix and AA interference problems are addressed.

Acknowledgements

JZ thanks the Australian Research Council for funding. The authors thank Ms. Shuang Wang for assistance with the DLS measurements.

References

- [1] S. C. Barton, J. Gallaway, P. Atanassov, *Chem. Rev.* **2004**, *104*, 4867–4886.
- [2] D. Leech, P. Kavanagh, W. Schuhmann, *Electrochim. Acta* **2012**, *84*, 223–234.
- [3] M. J. Moehlenbrock, S. D. Minteer, *Chem. Soc. Rev.* **2008**, *37*, 1188–1196.
- [4] A. Heller, *Phys. Chem. Chem. Phys.* **2004**, *6*, 209–216.
- [5] S. Cosnier, A. Le Goff, M. Holzinger, *Electrochem. Commun.* **2014**, *38*, 19–23.
- [6] A. Heller, B. Feldman, *Chem. Rev.* **2008**, *108*, 2482–2505.
- [7] J. Wang, *Chem. Rev.* **2008**, *108*, 814–825.
- [8] M. C. D. Cooray, Y. Liu, S. J. Langford, A. M. Bond, J. Zhang, *Anal. Chim. Acta* **2015**, *856*, 27–34.
- [9] J. Wang, *Chem. Rev.* **2008**, *108*, 814–825.
- [10] R. A. Bullen, T. C. Arnot, J. B. Lakeman, F. C. Walsh, *Biosens. Bioelectron.* **2006**, *21*, 2015–2045.
- [11] J. Wang, *Electroanalysis* **2005**, *17*, 7–14.
- [12] M. Gerard, A. Chaubey, B. D. Malhotra, *Biosens. Bioelectron.* **2002**, *17*, 345–359.
- [13] D. T. McQuade, A. E. Pullen, T. M. Swager, *Chem. Rev.* **2000**, *100*, 2537–2574.
- [14] M. V. Pishko, A. C. Michael, A. Heller, *Anal. Chem.* **1991**, *63*, 2268–2272.
- [15] A. Heller, *Acc. Chem. Res.* **1990**, *23*, 128–134.
- [16] I. Willner, E. Katz, *Angew. Chem. Int. Ed.* **2000**, *39*, 1180–1218.
- [17] P. Åsberg, O. Inganäs, *Biosens. Bioelectron.* **2003**, *19*, 199–207.
- [18] R. A. Etchenique, E. J. Calvo, *Anal. Chem.* **1997**, *69*, 4833–4841.

- [19] W. E. Hennink, C. F. van Nostrum, *Adv. Drug Delivery Rev.* **2002**, *54*, 13–36.
- [20] S. E. Moulton, G. G. Wallace, *J. Control. Release* **2014**, *193*, 27–34.
- [21] H. Zheng, J. Zhou, J. Zhang, R. Huang, H. Jia, S.-i. Suye, *Microchim. Acta* **2009**, *165*, 109–115.
- [22] P. O'Conghaile, S. Kamireddy, D. MacAodha, P. Kavanagh, D. Leech, *Anal. Bioanal. Chem.* **2013**, *405*, 3807–3812.
- [23] K. Murata, W. Akatsuka, T. Sadakane, A. Matsunaga, S. Tsujimura, *Electrochim. Acta* **2014**, *136*, 537–541.
- [24] E. J. Calvo, R. Etchenique, C. Danilowicz, L. Diaz, *Anal. Chem.* **1996**, *68*, 4186–4193.
- [25] A. Heller, *Acc. Chem. Res.* **1990**, *23*, 128–134.
- [26] A. Heller, *Curr. Opin. Chem. Biol.* **2006**, *10*, 664–672.
- [27] W. Godbey, K. K. Wu, A. G. Mikos, *J. Control. Release* **1999**, *60*, 149–160.
- [28] R. Duncan, *Nat. Rev. Drug Discov.* **2003**, *2*, 347–360.
- [29] S. A. Merchant, T. O. Tran, M. T. Meredith, T. C. Cline, D. T. Glatzhofer, D. W. Schmidtke, *Langmuir* **2009**, *25*, 7736–7742.
- [30] C. L. Chuang, Y. J. Wang, H. L. Lan, *Anal. Chim. Acta* **1997**, *353*, 37–44.
- [31] J.-Y. Wang, L.-C. Chen, K.-C. Ho, *ACS Appl. Mater. Interfaces* **2013**, *5*, 7852–7861.
- [32] X. L. Luo, A. Morrin, A. J. Killard, M. R. Smyth, *Electroanalysis* **2006**, *18*, 319–326.
- [33] G. A. Rivas, M. D. Rubianes, M. C. Rodriguez, N. E. Ferrera, G. L. Luque, M. L. Pedano, S. A. Miscoria, C. Parrado, *Talanta* **2007**, *74*, 291–307.
- [34] E. Katz, I. Willner, *Angew. Chem. Int. Ed.* **2004**, *43*, 6042–6108.
- [35] M. Pumera, A. Ambrosi, A. Bonanni, E. L. K. Chng, H. L. Poh, *Trends Anal. Chem.* **2010**, *29*, 954–965.
- [36] Y. Xiao, F. Patolsky, E. Katz, J. F. Hainfeld, I. Willner, *Science* **2003**, *299*, 1877–1881.
- [37] J.-N. Chazalviel, P. Allongue, *J. Am. Chem. Soc.* **2010**, *133*, 762–764.
- [38] A. Barfidokht, S. Ciampi, E. Luais, N. Darwish, J. J. Gooding, *Anal. Chem.* **2012**, *85*, 1073–1080.
- [39] K. Kim, H. B. Lee, J. W. Lee, H. K. Park, K. S. Shin, *Langmuir* **2008**, *24*, 7178–7183.
- [40] F. Qu, N. B. Li, H. Q. Luo, *Langmuir* **2013**, *29*, 1199–1205.
- [41] S. Sam, L. Touahir, J. Salvador Andres, P. Allongue, J.-N. Chazalviel, A. Gouget-Laemmel, C. H. de Villeneuve, A. Moraillon, F. Ozanam, N. Gabouze, *Langmuir* **2009**, *26*, 809–814.
- [42] E. Metay, M. C. Duclos, S. Pellet-Rostaing, M. Lemaire, J. Schulz, R. Kannappan, C. Bucher, E. Saint-Aman, C. Chaix, *Supramol. Chem.* **2009**, *21*, 68–80.
- [43] W. Haiss, N. T. K. Thanh, J. Aveyard, D. G. Fernig, *Anal. Chem.* **2007**, *79*, 4215–4221.
- [44] H. J. Kong, D. J. Mooney, *Cell transplant.* **2003**, *12*, 779–785.
- [45] T. J. Ohara, R. Rajagopalan, A. Heller, *Anal. Chem.* **1993**, *65*, 3512–3517.
- [46] A. Heller, *J. Phys. Chem.* **1992**, *96*, 3579–3587.
- [47] N. Mano, F. Mao, A. Heller, *J. Am. Chem. Soc.* **2002**, *124*, 12962–12963.
- [48] Y. Miao, L. Chia, N. Goh, S. Tan, *Electroanalysis* **2001**, *13*, 347–349.
- [49] J. F. Rusling, R. J. Forster, *J. Colloid Interface Sci.* **2003**, *262*, 1–15.
- [50] B. Wu, G. Zhang, S. Shuang, M. M. F. Choi, *Talanta* **2004**, *64*, 546–553.
- [51] N. Conrath, B. Gründig, K. Cammann, *Anal. Chim. Acta* **1995**, *309*, 47–52.
- [52] H. J. Bright, M. Appleby, *J. Biol. Chem.* **1969**, *244*, 3625–3634.
- [53] J. A. Kellum, *Crit. Care* **2000**, *4*, 6–14.
- [54] J. F. Castner, L. B. Wingard Jr, *Biochemistry* **1984**, *23*, 2203–2210.
- [55] J.-L. Lee, Y.-S. Shih, *J. Chin. Chem. Soc.* **1990**, *37*, 265–271.
- [56] S. Treimer, A. Tang, D. C. Johnson, *Electroanalysis* **2002**, *14*, 165–171.
- [57] J. F. Castner, L. B. Wingard Jr., *Biochemistry* **1984**, *23*, 2203–2210.
- [58] B. A. Gregg, A. Heller, *Anal. Chem.* **1990**, *62*, 258–263.
- [59] D. Zhai, B. Liu, Y. Shi, L. Pan, Y. Wang, W. Li, R. Zhang, G. Yu, *ACS Nano* **2013**, *7*, 3540–3546.
- [60] F. Iyanauskas, I. Kaunietis, V. Laurinavičius, J. Razumienė, R. Šimkus, *J. math. chem.* **2008**, *43*, 1516–1526.
- [61] R. A. Kamin, G. S. Wilson, *Anal. Chem.* **1980**, *52*, 1198–1205.
- [62] H. H. Weetall, L. S. Hersh, *Biochim. Biophys. Acta* **1970**, *206*, 54–60.
- [63] D. MacDougall, W. B. Crummett, *Anal. Chem.* **1980**, *52*, 2242–2249.
- [64] M. Şenel, *Synt. Met.* **2011**, *161*, 1861–1868.
- [65] R. K. Nagarale, J. M. Lee, W. Shin, *Electrochim. Acta* **2009**, *54*, 6508–6514.
- [66] M. F. Abasiyanik, M. Şenel, *J. Electroanal. Chem.* **2010**, *639*, 21–26.
- [67] M. Chen, G. Diao, *Talanta* **2009**, *80*, 815–820.
- [68] J. D. Newman, A. P. F. Turner, *Biosens. Bioelectron.* **2005**, *20*, 2435–2453.

Received: March 29, 2016

Accepted: May 13, 2016

Published online: July 15, 2016

Supporting information

Efficient Enzymatic Oxidation of Glucose Mediated by Ferrocene Covalently Attached to Polyethylenimine Stabilized Gold Nanoparticles

M. C. Dilusha Cooray, Saman Sadanayake, Fengwang Li, Steven J. Langford, Alan
M. Bond and Jie Zhang*

School of Chemistry, Monash University, Clayton, Victoria 3800, Australia

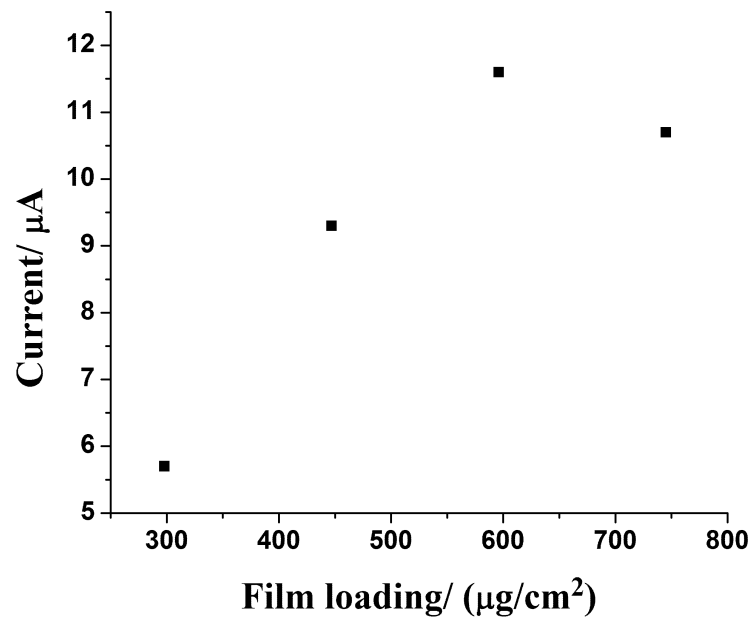


Figure S1: Effect of the film loading on the catalytic current obtained with a Fc-bPEI-AuNPs/GOx modified GCE from a 5.0 mM glucose solution (0.1 M PBS pH 7).

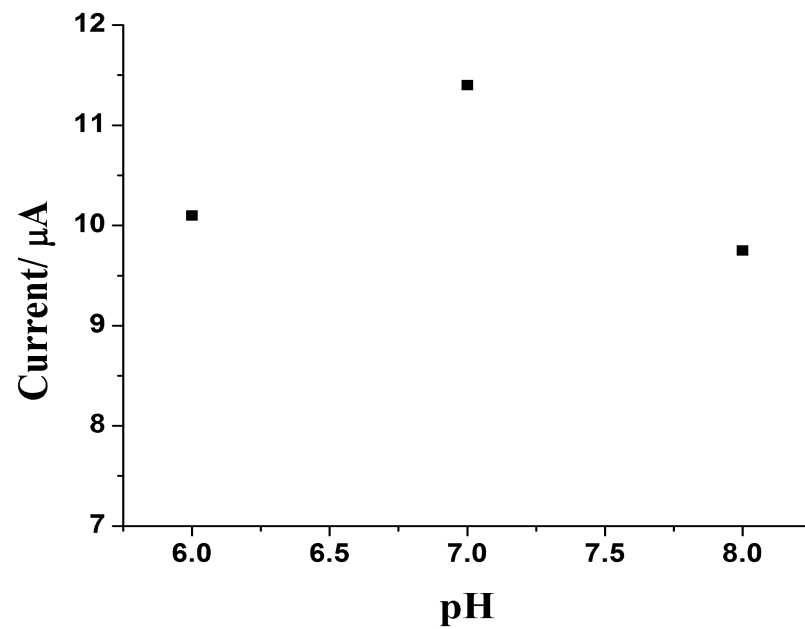


Figure S2: Catalytic current as a function of pH. The Fc-bPEI-AuNPs/GOx modified GCE was placed in contact with 0.1 M PBS containing 5.0 mM glucose. Scan rate = 0.01 V s^{-1} .

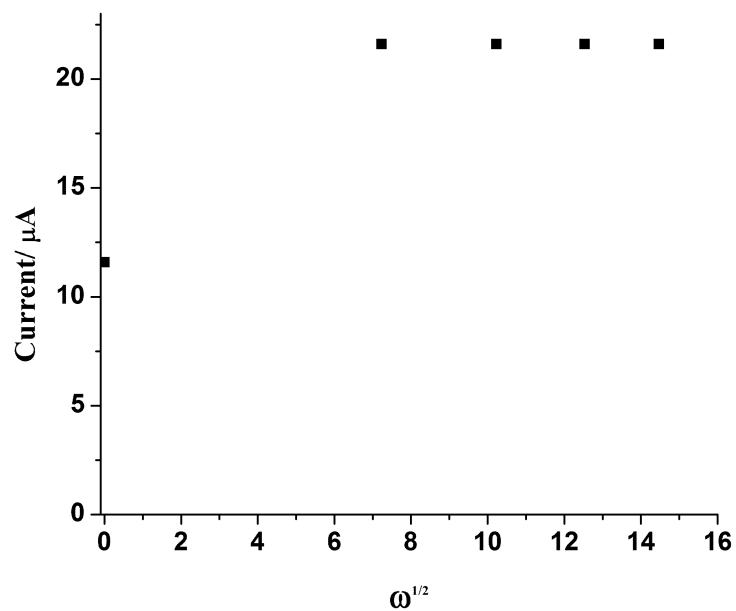


Figure S3: Plot of the catalytic current for glucose oxidation detected at 0.4 V as a function of the square root of the angular frequency of rotation. The Fc-bPEI-AuNPs/GOx modified glassy carbon RDE was placed in contact with 0.1 M PBS containing 5.0 mM glucose.

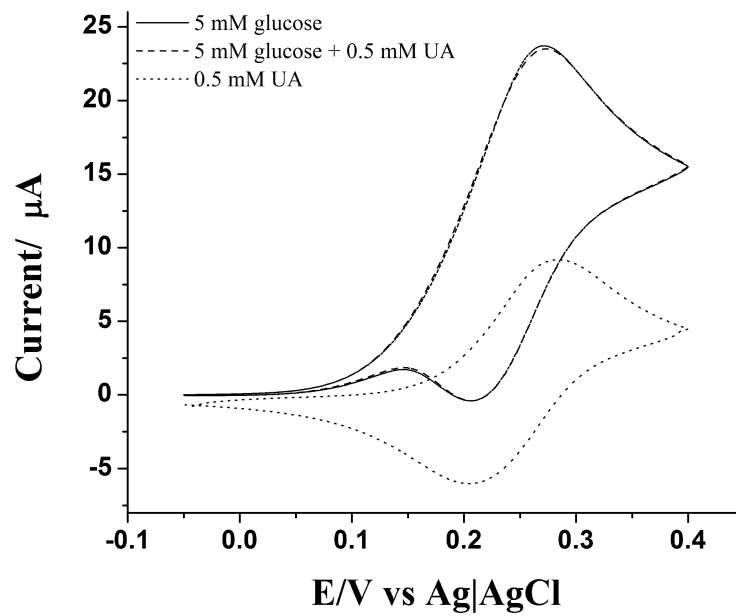


Figure S4: Cyclic voltammograms obtained with 5.0 mM glucose in 0.1 M PBS pH 7 at a scan rate of 0.01 V s^{-1} in the absence (—) and presence (----) of 0.50 mM UA. The response obtained with 0.50 mM UA alone (.....) is also provided for comparison.

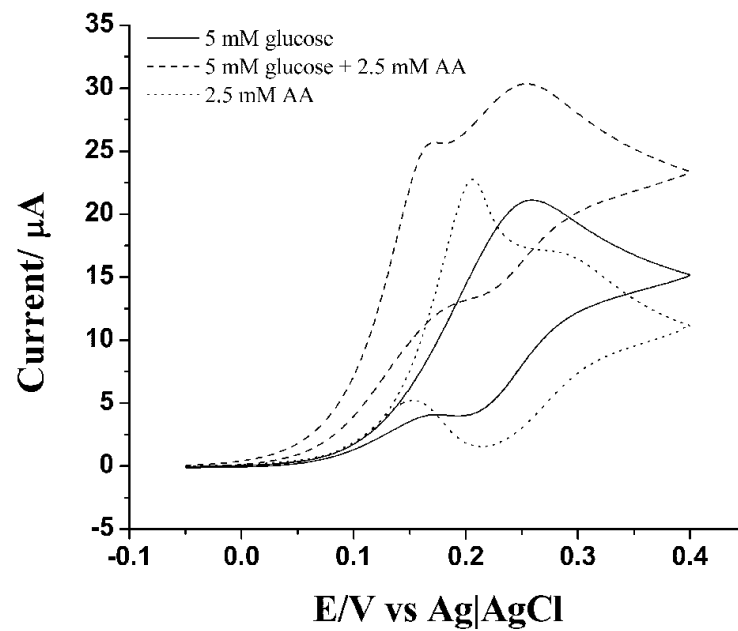


Figure S5: Cyclic voltammograms obtained with 5.0 mM glucose in 0.1 M PBS pH 7 at a scan rate of 0.01 V s^{-1} in the absence (—) and presence (----) of 2.5 mM AA. The response obtained with 2.5 mM AA alone (.....) is also provided for comparison.

Chapter 4

One pot synthesis of poly (5-hydroxyl-1,4-naphthoquinone) stabilized gold nanoparticles using monomer as the reducing agent for nonenzymatic electrochemical detection of glucose



One pot synthesis of poly(5-hydroxyl-1,4-naphthoquinone) stabilized gold nanoparticles using the monomer as the reducing agent for nonenzymatic electrochemical detection of glucose



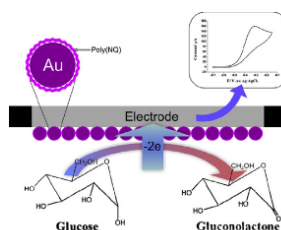
M.C. Dilusha Cooray, Yuping Liu, Steven J. Langford, Alan M. Bond, Jie Zhang*

School of Chemistry, Monash University, Clayton, Victoria 3800, Australia

HIGHLIGHTS

- Polymer stabilized Au nanoparticles were synthesized.
- The monomer was used as the reducing agent.
- The nanoparticle modified electrode is excellent for nonenzymatic detection of glucose.
- Glucose sensing was undertaken under mass transport controlled conditions.
- FTAC voltammetry was employed to obtain mechanistic information.

GRAPHICAL ABSTRACT



ARTICLE INFO

Article history:
Received 18 September 2014
Accepted 26 November 2014
Available online 29 November 2014

Keywords:
Nonenzymatic
Gold nanoparticle
Naphthoquinone
Electrochemical
Glucose
Polymer

ABSTRACT

Monodispersed and highly stable gold nanoparticles with a diameter between 8 and 9 nm were synthesized in a weakly alkaline medium by chemical reduction of AuCl_4^- using 5-hydroxyl-1,4-naphthoquinone, and stabilized by the simultaneously formed poly(hydroxyl-1,4-naphthoquinone). The electrochemical properties of the resultant poly(hydroxyl-1,4-naphthoquinone) stabilized gold nanoparticles (AuNQ NPs) and its electrocatalytic activity for glucose oxidation in alkaline media were then investigated using a range of techniques, including dc cyclic, rotating disk electrode and Fourier transformed large amplitude ac voltammetry. The results demonstrate that these AuNQ NP modified electrodes exhibit excellent catalytic activity toward glucose oxidation in the potential region where the premonolayer oxidation process occurs. The overall catalytic glucose oxidation process was found to be mass transport controlled under the experimental conditions employed, allowing measurements to be conducted with a high reproducibility. The AuNQ NP modified electrodes showed a high sensitivity of $183 \mu\text{A mM}^{-1} \text{cm}^{-2}$ with a wide linear dynamic range of 0.5–50 mM and a detection limit of 61 μM . However, despite its excellent tolerance toward ascorbic acid, significant interference from uric acid was found with this AuNQ NP modified electrode.

© 2014 Elsevier B.V. All rights reserved.

1. Introduction

Diabetes mellitus is a chronic clinical condition which exhibit high or low deviation in glucose level in blood from the normal range of $80\text{--}120 \text{ mg dL}^{-1}$ ($4.4\text{--}6.6 \text{ mM}$) [1]. Abnormal levels of glucose cause many long term serious health issues, such as

* Corresponding author. Tel.: +61 399 056 289.
E-mail address: jie.zhang@monash.edu (J. Zhang).

blindness, tissue damage, heart disease and kidney failure. Therefore, it is crucial for diabetic patients to regularly monitor the glucose levels with high accuracy. So far, many sensors for glucose monitoring have been reported [2,3]. The majority of these sensors were developed based on the principles of electrochemistry due to the simplicity and low cost of electrochemical sensors [4].

Since direct electrooxidation of glucose is kinetically very sluggish, catalysts are normally required to speed up the process and to offer adequate selectivity that is required for glucose detection in blood samples [5,6]. According to the catalyst used, glucose sensors can be categorized as enzymatic glucose sensors and nonenzymatic glucose sensors [7]. The former class exploit the application of glucose oxidase or glucose dehydrogenase as the biocatalysts [8], while the latter mainly utilize metal nanoparticles (NPs) as the catalysts for glucose oxidation [1,2,5,9]. Enzymes such as glucose oxidase and dehydrogenase, while exhibiting excellent activity and selectivity for glucose oxidation, are unstable in acidic or alkaline media [7,10]. The relatively small active site number to volume ratio is also a drawback in the use of enzymes. In contrast, nanoparticle catalysts are superior in these regards. The state of the art nanotechnology has opened up new opportunities for materials scientists and electrochemists to acquire novel materials which could be employed to replace biocatalysts for electrooxidation of glucose. Particles of gold (Au) and platinum (Pt) metals and alloys have proven attractive for their ability to oxidize glucose with excellent activity [9,11–15]. Interestingly, as the size of the particles goes down the hierarchy, macro to nano, the NPs exhibit more advantageous properties due to the increased percentage of the surface atoms and quantum size effects [16,17].

Polymer stabilized nanoparticle composites have attracted the interest of scientists and have been utilized for the oxidation of glucose in nonenzymatic glucose sensors. Au nanoparticles have received attention for this application due to the ease of synthesis using wet chemical methods with excellent size and shape control [17–19] in addition to their aforementioned high catalytic activity for glucose oxidation. Importantly, the polymer stabilized Au NPs are highly stable, and their high activity is retained due to their relatively weak interaction with the polymer. Consequently, the substrate molecules can easily access the surface of the Au NPs during catalysis. Poyraz et al. prepared poly(*o*-toluidine) (POT) nanofiber/metal nanoparticle composite modified graphite working electrodes which gave rapid responses with a sensitivity of $37 \mu\text{A cm}^{-2} \text{mM}^{-1}$ and a limit of detection (LOD) of $\sim 0.027 \mu\text{M}$ in alkaline medium [7]. Sebez et al. reported the use of polyethyleneimine modified gold nanoparticles on carbon fiber coated with aligned carbon nanotubes in nonenzymatic glucose oxidation at physiological pH of 7.4 [18]. Rong et al. showed that electrodeposited Au nanoparticles coated with polymers with intrinsic microporosity are highly resistive to poisoning during glucose oxidation in pH 7 [20]. Au NPs electrodeposited on amine functionalized mesoporous silica, has been reported to give a sensitivity of $75 \mu\text{A cm}^{-2} \text{mM}^{-1}$ and LOD of $100 \mu\text{M}$ for glucose detection in alkaline medium [12]. Au NPs decorated on multi-walled carbon nanotubes functionalized with congo red composites was reported by Zhou et al. to give a low detection limit of $0.5 \mu\text{M}$ glucose in basic medium [21]. Feng et al. synthesized Au NPs modified with chitosan which was exploited in the application of glucose sensor with a LOD of 0.37 mM [22].

In this study, highly stable and monodispersed Au nanoparticles with a diameter between 8 and 9 nm were synthesized conveniently in weak alkaline media using 5-hydroxyl-1,4-naphthoquinone as a reducing agent for AuCl_4^- . The chemical oxidation of 5-hydroxyl-1,4-naphthoquinone by AuCl_4^- leads to the formation of a conducting polymer poly(5-hydroxyl-1,4-naphthoquinone) which in turn stabilizes the Au nanoparticles produced from this

reaction. These poly(5-hydroxyl-1,4-naphthoquinone) stabilized Au nanoparticles (AuNQ NPs) were characterized by a range of electrochemical, spectroscopic and microscopic techniques and their catalytic activity explored for the electrochemical oxidation of glucose in alkaline media.

2. Experimental

2.1. Chemicals

The chemicals 5-hydroxyl-1,4-naphthoquinone (NQ, 97%), gold (III) chloride trihydrate ($\text{HAuCl}_4 \cdot 3\text{H}_2\text{O}$, 99.9%), L-ascorbic acid ($\text{C}_6\text{H}_8\text{O}_6$, 99.9%), uric acid ($\text{C}_5\text{H}_4\text{N}_4\text{O}_3$, 99%), D-(+)-gluconic acid δ -lactone ($\text{C}_6\text{H}_{10}\text{O}_6$, 99.9%) and D-glucose were purchased from Sigma–Aldrich. Sodium hydroxide pellets (NaOH, 99%) were purchased from Merck. The above mentioned chemicals were used as received. Distilled water was utilized for preparation of solutions.

Indium tin oxide (ITO) coated glass slides (surface resistivity: $8\text{--}12 \Omega$ per square, Aldrich) were treated using a literature method, before being used as electrodes [23].

2.2. Preparation of poly(5-hydroxyl-1,4-naphthoquinone) stabilized Au nanoparticles (AuNQ NPs)

To prepare Au NPs, 5-hydroxyl-1,4-naphthoquinone (1.3 mg, $7.5 \mu\text{mol}$) was dissolved in $25.0 \mu\text{L}$ 1 M NaOH ($25 \mu\text{mol}$) aqueous solution and the final volume was made to 5.00 mL with distilled water. The mixture was then stirred using a magnetic stirrer. Upon addition of $50.0 \mu\text{L}$ of 0.1 M $\text{HAuCl}_4 \cdot 3\text{H}_2\text{O}$ ($5.0 \mu\text{mol}$), the solution turned bright purple indicating the formation of Au NPs due to the reduction of AuCl_4^- to metallic Au NPs by 5-hydroxyl-1,4-naphthoquinone and their stabilization by poly(5-hydroxyl-1,4-naphthoquinone) which is simultaneously formed during the reaction via head-to-tail coupling in a manner similar to aniline [24], and presumably provides as a coating layer for the nanoparticles. This solution mixture was stirred for 90 min allowing the reaction to go to completion. AuNQ NPs formed were then isolated using centrifugation at a rotation rate of 8000 rpm (Eppendorf, mini spin plus). Finally the AuNQ NPs were re-dissolved in 1.5 mL distilled water and isolated again using centrifugation to remove impurities. The separated AuNQ NPs were dispersed in 0.5 mL distilled water and stored in a refrigerator for use in subsequent studies. The AuNQ NP dispersion was stable for a long period without any noticeable aggregation of the particles, which implies the excellent stabilizing role of poly(5-hydroxyl-1,4-naphthoquinone).

2.3. Microscopic and spectroscopic characterization of AuNQ NPs

Scanning electron microscopy (SEM) and energy dispersive X-ray spectroscopy (EDX) measurements were undertaken using a FEI Nova NanoSEM 450 FEG SEM Instrument to determine the surface morphology and the size of AuNQ NPs. EDX analysis was conducted at 10 keV. Images with higher resolution were obtained using a FEI Tecnai G2 T20 TWIN LaB6 transmission electron microscope (TEM). Raman spectroscopic measurements were undertaken using a Renishaw inVia Raman Microscope. An Innova Ar⁺ laser (emitting at 514 nm) was used as the light source over the $2000\text{--}400 \text{ cm}^{-1}$ range. UV–vis spectra were recorded with a UV–Vis–NIR spectrometer (Cary 5000).

2.4. Fabrication of the AuNQ NPs modified electrode

A glassy carbon electrode (GCE, 3 mm diameter, CH Instruments Inc., Texas, USA) was used to prepare the modified electrode.

Initially, the electrode was polished with 0.3 μm alumina slurry followed by rinsing with distilled water, sonication and rinsing again with distilled water and finally drying under a nitrogen gas. Then 5.0 μL AuNQ NP solution was drop-casted on the electrode surface and left to dry in air, before use in an electrochemical measurement. The glassy carbon rotating disk electrode (GC-RDE, 3 mm, BAS Inc., Tokyo, Japan) was modified in a similar manner using 5.0 μL of AuNQ NP solution. A gold disc electrode (AuE, 2 mm diameter, CH Instruments Inc., Texas, USA), cleaned electrochemically in 0.5 M aqueous H_2SO_4 by cycling the potential in the region where Au/Au oxide processes are present, was used for comparison with the AuNQ NP modified GCE.

2.5. Electrochemical measurements

Electrochemical measurements were carried out at $21 \pm 2^\circ\text{C}$ using a CH Instrument 760D electrochemical workstation with a conventional three-electrode cell. An alkaline medium (0.1 M NaOH, pH 13) was used for all measurements. The modified GCE, GC-RDE or AuE, Ag/AgCl|KCl_{sat} and a platinum wire were employed as working electrode (WE), reference electrode and auxiliary electrode, respectively. Large amplitude Fourier transformed ac (FTAC) voltammetric measurements were carried out with home-built apparatus [25], using a sine wave perturbation (amplitude 80 mV and frequency 9.02 Hz) superimposed onto the dc ramp (scan rate = 78.23 mV s^{-1}). A power spectrum was then obtained by applying Fourier transformation on the total current resulting from this applied potential waveform. After the frequency band of interest was selected, inverse Fourier transformation was used to generate the desired dc or ac harmonic components. Appropriate

aliquots of 1 M glucose stock solution were added to the NaOH solution in the cell, to obtain the required concentration of glucose. All the solutions were degassed with high purity nitrogen for at least 10 min prior to the electrochemical measurements in order to remove oxygen. In dc voltammetry, the scan rate used was 50 mV s^{-1} , unless otherwise stated.

3. Results and discussion

3.1. Microscopic and spectroscopic characterization of AuNQ NPs

Electron microscopic measurements were undertaken using both SEM and TEM to obtain the size distribution and information on the crystallinity of the AuNQ NPs. A SEM image obtained from AuNQ NPs drop-casted on an indium tin oxide (ITO) glass slide (Fig. 1a) shows the uniformity of both the size and the spherical shape of AuNQ NPs. Excellent crystallinity is evident from the TEM image (Fig. 1b). TEM images also shows that the size of AuNQ NP diameter was between 8 and 9 nm. The EDX spectrum (Fig. 1c) shows the characteristic signals of C from NQ and Au from the gold nanoparticles.

AuNQ NPs were subjected to UV–vis spectroscopic characterization. As shown in Fig. 1d, an absorption band is observed at a wavelength of 523 nm, which is a characteristic surface plasma absorption band for gold nanoparticles with a diameter in the range of 7.5–33 nm [26].

The poly(5-hydroxy-1,4-naphthoquinone) coating layer is not clearly visible in the TEM image, presumably due to its extreme thinness. Therefore, Raman spectroscopy was used to confirm its presence. Raman spectra obtained from AuNQ NPs, as well as from

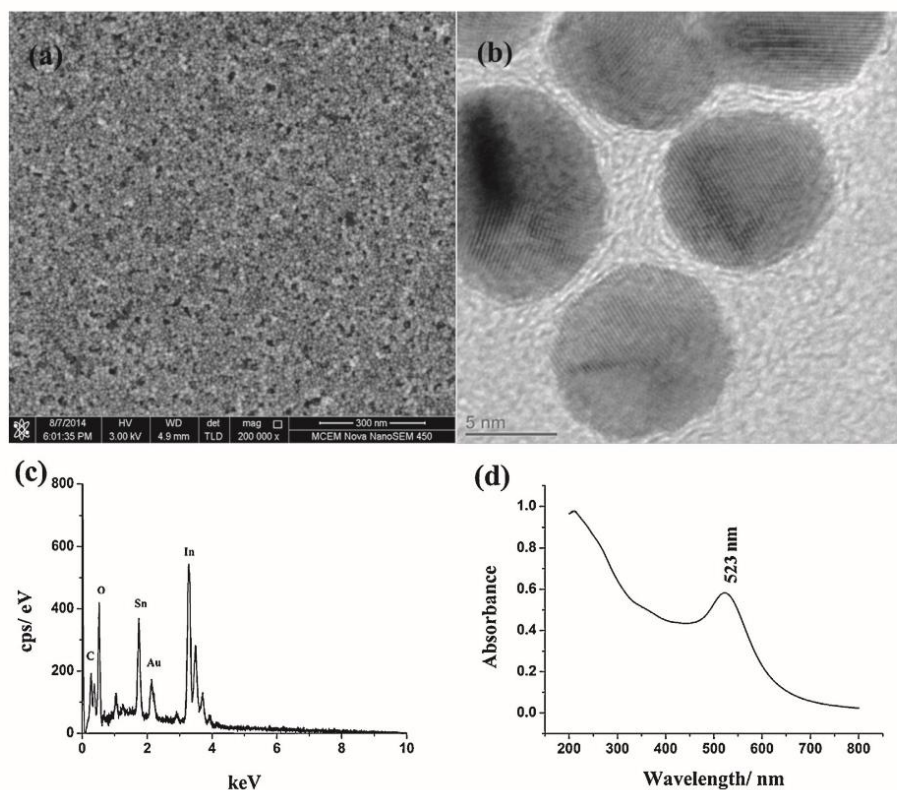


Fig. 1. Electron microscopic and spectroscopic characterization of AuNQ NPs. (a) SEM image, (b) TEM image, (c) EDX spectrum and (d) UV-vis spectrum.

molecular 5-hydroxy-1,4-naphthoquinone are illustrated in Fig. 2. Similar bands were observed in both cases in the range of 1550–1670 cm^{-1} , which are assigned to the C=O group of the quinone moiety [27]. The Raman band at 1301 cm^{-1} in molecular NQ, due to the O–H vibration, is shifted to 1328 cm^{-1} in AuNQ NPs. This shift could be a result of the formation of a C–O–C bond between two NQ molecules occurring during polymer formation. The Raman spectra data indicates the presence of poly NQ on Au NPs, presumably acting as the capping layer to stabilize Au NPs.

3.2. Electrochemical characterization of the AuNQ NP modified electrode

The electrochemical behavior of AuNQ NPs was investigated in 0.1 M NaOH. Dc cyclic voltammograms of AuNQ NPs in this medium contain three processes consisting of a small process I/I' (in the potential region of ~ -0.15 V) and much larger unresolved processes II/II' and III/III' (~ -0.2 V) (Fig. 3a). Based on literature reports [2,28], process I is assigned to premonolayer oxidation of highly active Au adatoms of low coordination numbers to surface-bonded hydrated oxide species, and processes II and III represent the formation of monolayer gold oxide. Similar processes were also observed at an electrochemically cleaned AuE but with lower magnitudes, presumably due to smaller surface area compared to a AuNQ NP modified GCE (Fig. 3b). The latter observation confirms that all three of the above mentioned processes are associated with Au.

In order to obtain qualitative information on the kinetics of electron transfer during the formation of Au oxide layers on the AuNQ NP modified electrode, the more sensitive and sophisticated Fourier transformed ac voltammetric (FTACV) technique [29] was employed. In FTACV, a large amplitude ac perturbation is superimposed onto a dc ramp. Fourier transformation (FT) and inverse FT are used to obtain dc and different ac harmonic components. The higher order harmonics are devoid of background charging current [30] and highly sensitive to the kinetics of heterogeneous electron transfer process [31]. This technique has been utilized to obtain information regarding the surface active sites on a copper electrode in alkaline medium with greatly improved sensitivity compared to conventional dc cyclic voltammetry [32]. With a sinusoid perturbation (frequency = 9.02 Hz and amplitude = 80 mV) superimposed onto a dc ramp (scan rate = 78.23 mV s^{-1}), two well defined processes were observed in dc and ac components up to the 8th harmonic (Fig. S1). The background charging current free 5th harmonic component is shown in Fig. 4a. For comparison, measurements with an electrochemically cleaned AuE were carried out under the same

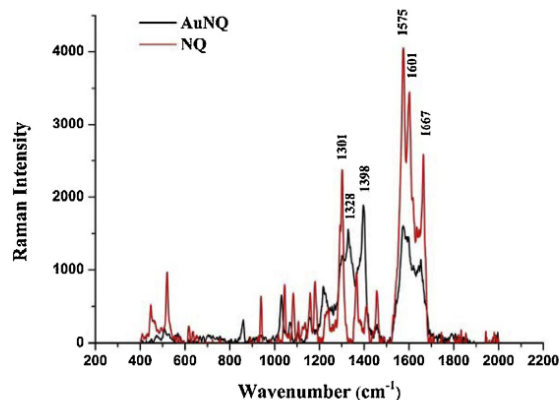


Fig. 2. Raman spectra of molecular NQ (red line, —) and AuNQ NPs (—) obtained using a 514 nm argon laser with a power of 100 mW. (For interpretation of the references to color symbol in this figure legend, the reader is referred to the web version of this article.)

conditions and the results are shown in Fig. S2 and Fig. 4b. Processes II/II' and III/III' which were partially resolved under dc cyclic voltammetric conditions, are completely merged under FTACV conditions. Process I/I', which is much smaller compared to processes II/II' and III/III' under dc conditions (Fig. 3a and b), now becomes dominant and much better defined in comparison with processes II/II' and III/III', especially at the AuNQ NP modified electrode (Fig. 4a and b, Figs. S1 and S2). This observation suggests that the electron transfer kinetics associated with process I/I' is considerably faster than for processes II/II' and III/III' and is reversible or close to reversible under the experimental conditions [33].

3.3. Electrocatalytic oxidation of glucose

Electrocatalytic properties of the AuNQ NP modified electrode for glucose oxidation were also examined in aqueous 0.1 M NaOH containing 10 mM glucose. The results are shown in Fig. 5. Results obtained with an electrochemically cleaned AuE are also shown for comparison. Two processes (1 and 2) were observed at both AuNQ NP modified electrode and AuE in the potential regions where electron transfer processes involving surface gold atoms (I,II and III in Figs. 3 and 4) were detected. In contrast, no oxidation process was detected at a bare GCE confirming that Au is the active component of the catalyst. Based on previous reports, process 1 is

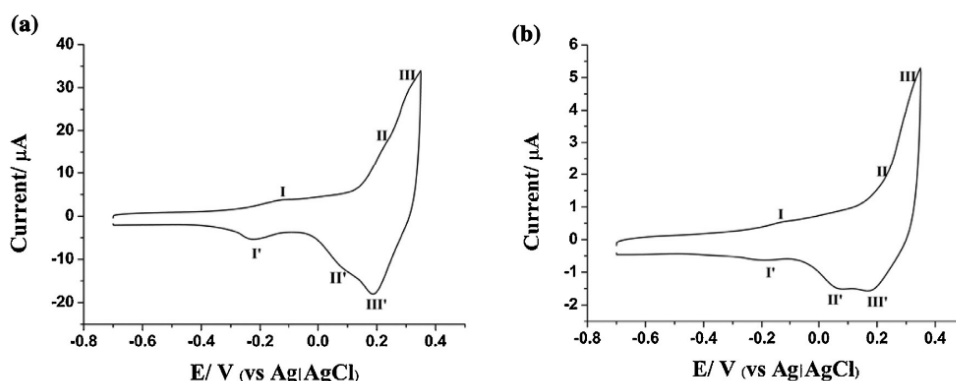


Fig. 3. Cyclic voltammograms obtained in 0.1 M NaOH at a scan rate of 0.05 V s^{-1} with (a) AuNQ NP modified GCE and (b) electrochemically cleaned AuE.

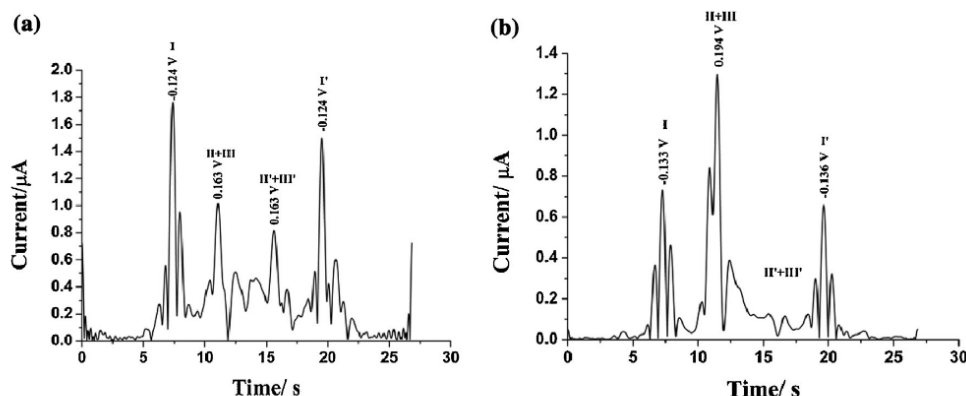


Fig. 4. 5th harmonic component of FTAC voltammogram obtained in 0.1 M NaOH at (a) AuNQ NP modified GCE and (b) electrochemically cleaned Au disc electrode in the potential range between -0.7 and 0.35 V.

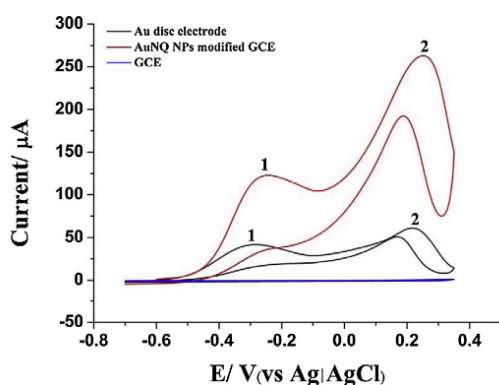


Fig. 5. Cyclic voltammograms obtained with 10 mM glucose solution (0.1 M NaOH) at a scan rate of 0.05 V s^{-1} over the potential range of -0.7 – 0.35 V at an AuNQ NP modified GC (red line, —), electrochemically cleaned gold (—) and GC electrodes (blue line, —). (For interpretation of the references to color symbol in this figure legend, the reader is referred to the web version of this article.)

assigned to the two-electron oxidation of glucose to form gluconolactone [34,35] and process 2 is derived from further oxidation of gluconolactone [12,21,36]. The origin of process 2 was confirmed by cyclic voltammetric measurements with 5 mM

α -(+)-gluconic acid δ -lactone, which gave rise to a similar process at the potential of process 2 (see Fig. S3). Process 2 exhibits the features of a surface confined process. In contrast, process 1 is diffusion controlled as suggested by the approximately linear relationship between the peak current (I_p) and the square root of the scan rate (Fig. 6). A small deviation from linearity especially at higher scan rate may be attributed to slow electrode kinetics or/ and the effect of uncompensated resistance (iR_u effect). Mass transport control is supported by results obtained under hydrodynamic conditions of RDE with an AuNQ NP modified GC RDE electrode (Fig. S6), which show that the steady-state mass transport limiting currents (I_{ss}) is proportional to the square root of the rotation rate. A diffusion coefficient of $4 \times 10^{-6} \text{ cm}^2 \text{ s}^{-1}$ for glucose is estimated based on the Levich equation [37], assuming two electrons are transferred in this oxidation process. This value is in good agreement with a literature value of $5 \times 10^{-6} \text{ cm}^2 \text{ s}^{-1}$ [38].

The results described above are consistent with the ‘Incipient Hydrated Oxide Adatom Mediator’ (IHOAM) model introduced by Burke [2,28]. In this model, the catalytic activity of gold towards glucose is attributed to the highly active Au adatoms of low coordination numbers, which are electrochemically oxidized to catalytic active surface-bonded hydrated oxide species. Similar results were obtained at the electrochemically cleaned AuE. The smaller current magnitude associated with the first catalytic oxidation process at the electrochemically cleaned AuE is due to its smaller geometric area (i.e., 2.25 times smaller). This result again is

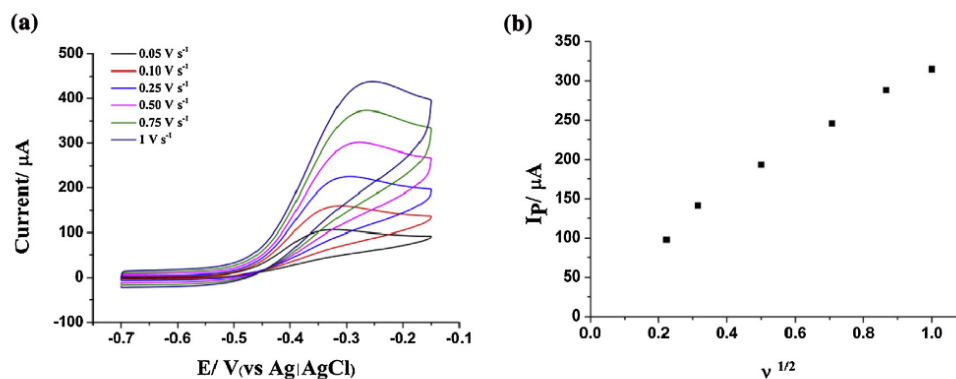


Fig. 6. (a) Cyclic voltammograms obtained at an AuNQ NP modified GC in 10 mM glucose (0.1 M NaOH) as a function of scan rate and (b) the relationship between the peak current and the square root of the scan rate.

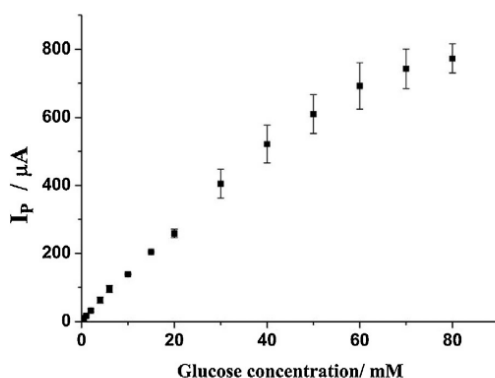


Fig. 7. Calibration curve for the determination of glucose in 0.1 M NaOH based on average results obtained from three AuNQ NP modified GCEs.

consistent with the fact that this catalytic process is mass transport controlled. In addition to the advantage of having a higher tolerance to interference from ascorbic acid (*vide infra*), in comparison with a bulk AuE electrode, equivalent analytical performance is achieved with the AuNQ NP modified electrode, but with a minimal amount of Au.

FTACV measurements also were undertaken under catalytic turnover conditions in an aqueous 0.1 M NaOH solution containing 5 mM glucose (Figs. S4 and S5). According to both theoretical [39,40] and experimental [33,40,41] studies, the higher harmonic components of FTACV are very sensitive to the fast heterogeneous electron transfer process, but very insensitive to the catalytic process. Therefore, the electron transfer process associated with the premonolayer oxidation of gold clearly can be observed from the higher harmonic components even in the presence of catalytic oxidation of glucose. Again well-defined voltammograms (up to 7th harmonic components) associated with the premonolayer oxidation of gold was observed under FTACV conditions, which suggest that the kinetics of the electron transfer process associated with the premonolayer oxidation of gold remains fast under catalytic conditions. Comparison of Figure 4a and S2 with Figs. S4 and S5 suggests that the higher harmonic peak currents decrease in the presence of glucose. This is attributed to the iR_u effect, which is much more pronounced under catalytic glucose oxidation conditions at the higher magnitude of total current [42].

3.4. Analytical performance of an AuNQ NP modified electrode for glucose determination

As demonstrated above, the AuNQ NP modified electrode shows excellent catalytic activity towards glucose oxidation in alkaline media in the potential region of premonolayer oxidation. However, in this case, the overall process is controlled by the mass transport of glucose, in contrast with other electrochemical based nonenzymatic glucose sensors where catalytic glucose oxidation is exclusively a kinetically controlled process [2]. This fundamental difference could lead to improved electrode-to-electrode reproducibility. In order to assess the application of the modified electrode for glucose sensing, cyclic voltammetric measurements were undertaken in aqueous 0.1 M NaOH solutions as a function of concentrations of glucose. Plot of oxidation peak current versus glucose concentration are shown in Fig. 7. Linearity ($R^2 = 0.997$) relationship with a slope of $183 \mu A mM^{-1} cm^{-2}$ is obtained in the low concentration range of 0.5–50 mM. When the concentration is above 50 mM, deviation from linearity is detected, presumably due to iR_u drop or as a result of a change from mass transport controlled to kinetically controlled current at high concentrations. A limit of detection (LOD) of 61 μM was estimated from the standard deviation of ten measurements in an aqueous 0.1 M NaOH solution containing 0.5 mM glucose according to the well documented protocol [43]. The reproducibility of the peak current response in five successive measurements of 10 mM glucose in 0.1 M NaOH at a AuNQ NPs modified GCE yielded a relative standard deviation (RSD) of 1.8%, verifying excellent intra-electrode stability. Electrode-to-electrode reproducibility with four electrodes gave a RSD of 5.3% confirming the advantage of using this modified electrode for glucose detection under mass transport controlled conditions where small variations of the catalyst loading should not affect the sensor response.

The AuNQ NP modified electrode shows excellent catalytic activity toward the oxidation of glucose under mass transport controlled conditions. For analytical applications, good selectivity towards the glucose analyte is also important. Likely interferences from co-existing species in blood were therefore investigated. Blood and urine are the main biological fluids used in the determination of glucose in humans [13,21,44]. These matrices contain not only glucose but also ascorbic acid (AA), uric acid (UA) and metabolites of drugs consumed by humans. The determination of the glucose concentration electrochemically at a relatively low oxidation potential is advantageous in avoiding interference from other physiological components [45,46]. Uric acid and ascorbic acid are two commonly reported interferences for glucose

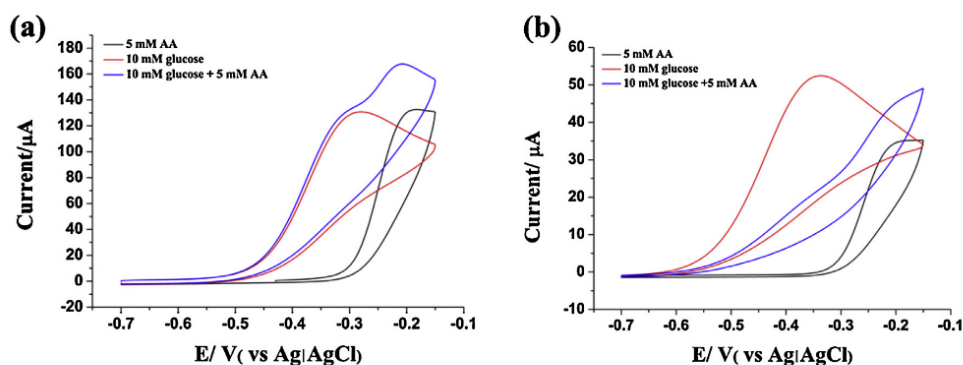


Fig. 8. Comparison of cyclic voltammograms obtained with 10 mM glucose in 0.1 M NaOH in the absence (—) and presence (—) of 5 mM AA, or 5 mM AA (—) at (a) an AuNQ NP modified GCE and (b) an electrochemically cleaned AuE.

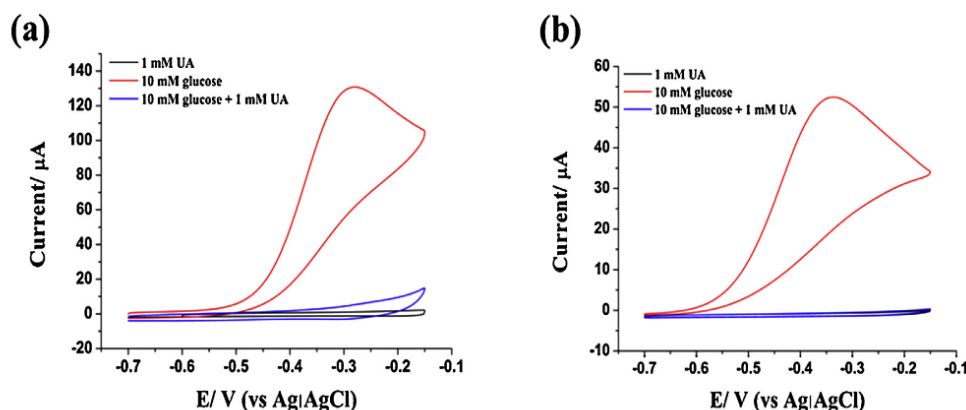


Fig. 9. Comparison of cyclic voltammograms obtained with 10 mM glucose in 0.1 M NaOH in the absence (—) and presence (—) of 1 mM UA, or 1 mM UA (—) at (a) an AuNQ NP modified GCE and (b) an electrochemically cleaned AuE.

determination, therefore their influences on glucose determination using the AuNQ NP modified electrode were examined. For control purposes, experiments were again undertaken using an electrochemically cleaned AuE under the same conditions. In the presence of 5 mM AA in aqueous 0.1 M NaOH solution containing 10 mM glucose, the voltammetric response from glucose remains almost unaffected at the AuNQ NP modified electrode since AA oxidation occurs at far more positive potentials (Fig. 8a). In contrast, glucose oxidation is suppressed at an electrochemically cleaned AuE when AA is present even though the oxidation of glucose and AA occurs at a similar potential at both electrodes (Fig. 8b). The lower level of AA interference with the AuNQ NP modified electrode may be attributed to two factors: (1) the presence of a polymer coating layer on AuNQ NPs which minimize the adsorption of AA; and/or (2) the higher density of the active sites, so that the glucose oxidation process remains mass transport controlled even when some active sites are deactivated. However, in the presence of 1.0 mM UA in aqueous 0.1 M NaOH solution containing 10.0 mM glucose, the voltammetric response from glucose was completely suppressed at both the AuNQ NP modified electrode and the electrochemically cleaned AuE even though the oxidation of UA does not occur in this potential region (Fig. 9), presumably due to the strong interaction of UA with the active sites. Further studies are needed to establish how to avoid interference from UA.

4. Conclusion

A new type of AuNQ NPs with excellent stability was synthesized using a simple one step method and characterized using a range of electrochemical, spectroscopic and microscopic techniques. The application of these AuNQ NPs for electrocatalytic oxidation of glucose in alkaline media was explored. The results demonstrate that these AuNQ NPs exhibit excellent catalytic activity toward glucose oxidation in the potential region where premonolayer oxidation process occurs. The overall catalytic glucose oxidation process was found to be mass transport controlled under the experimental conditions employed allowing the measurements to be conducted with high reproducibility. However, despite its excellent tolerance toward AA interference, this AuNQ NP modified electrode has a low tolerance from interference by UA.

Acknowledgements

The authors would like to acknowledge Dr Karen Wohnrath for her help in analyzing Raman spectra, the Monash Centre for electron microscopy for assistance in obtaining the SEM and TEM images, and Dr Si-Xuan Guo for helpful discussions. JZ would like to thank the Australian Research Council for financial support.

Appendix A. Supplementary data

Supplementary data associated with this article can be found, in the online version, at <http://dx.doi.org/10.1016/j.aca.2014.11.033>.

References

- [1] X. Guo, B. Liang, J. Jian, Y. Zhang, X. Ye, Glucose biosensor based on a platinum electrode modified with rhodium nanoparticles and with glucose oxidase immobilized on gold nanoparticles, *Microchim. Acta* 181 (2014) 519–525.
- [2] P. Si, Y. Huang, T. Wang, J. Ma, Nanomaterials for electrochemical non-enzymatic glucose biosensors, *RSC Adv.* 3 (2013) 3487.
- [3] J. Wang, *Electrochemical glucose biosensors*, *Chem. Rev.* (Washington, DC, U. S.) 108 (2008) 814–825.
- [4] R. Gifford, Continuous glucose monitoring: 40 years, what we've learned and what's next, *ChemPhysChem* 14 (2013) 2032–2044.
- [5] S. Park, H. Boo, T.D. Chung, Electrochemical non-enzymatic glucose sensors, *Anal. Chim. Acta* 556 (2006) 46–57.
- [6] J. Kim, H. Jia, P. Wang, Challenges in biocatalysis for enzyme-based biofuel cells, *Biotechnol. Adv.* 24 (2006) 296–308.
- [7] S. Poyraz, Z. Liu, Y. Liu, N. Lu, M.J. Kim, X. Zhang, One-step synthesis and characterization of poly(o-toluidine) nanofiber/metal nanoparticle composite networks as non-enzymatic glucose sensors, *Sens. Actuators B* 201 (2014) 65–74.
- [8] S. Ferri, K. Kojima, K. Sode, Review of glucose oxidases and glucose dehydrogenases: a bird's eye view of glucose sensing enzymes, *J. Diabetes Sci. Technol.* 5 (2011) 1068–1076.
- [9] Z. Liu, L. Huang, L. Zhang, H. Ma, Y. Ding, Electrocatalytic oxidation of D-glucose at nanoporous Au and Au–Ag alloy electrodes in alkaline aqueous solutions, *Electrochim. Acta* 54 (2009) 7286–7293.
- [10] K.E. Toghiani, R.G. Compton, Electrochemical non-enzymatic glucose sensors: a perspective and an evaluation, *Int. J. Electrochem. Sci.* 5 (2010) 1246–1301.
- [11] H. Zhang, N. Toshima, Glucose oxidation using Au-containing bimetallic and trimetallic nanoparticles, *Catal. Sci. Tech.* 3 (2013) 268.
- [12] J.-J. Yu, S. Lu, J.-W. Li, F.-Q. Zhao, B.-Z. Zeng, Characterization of gold nanoparticles electrochemically deposited on amine-functionalized mesoporous silica films and electrocatalytic oxidation of glucose, *J. Solid State Electrochem.* 11 (2007) 1211–1219.
- [13] F. Kurniawan, V. Tsakova, V.M. Mirsky, Gold nanoparticles in nonenzymatic electrochemical detection of sugars, *Electroanalysis* 18 (2006) 1937–1942.
- [14] J. Dolinska, P. Kannan, V. Sashuk, M. Jonsson-Niedziolka, Z. Kaszkur, W. Lisowski, M. Opallo, Electrocatalytic synergy on nanoparticulate films prepared from oppositely charged Pt and Au nanoparticles, *Chem. Electrochem.* 1 (2014) 1023–1026.

- [15] Y. Fu, F. Liang, H. Tian, J. Hu, Nonenzymatic glucose sensor based on ITO electrode modified with gold nanoparticles by ion implantation, *Electrochim. Acta* 120 (2014) 314–318.
- [16] X. Wu, L. Tan, D. Chen, X. Meng, F. Tang, Icosahedral gold-platinum alloy nanocrystals in hollow silica: a highly active and stable catalyst for Ullmann reactions, *Chem. Commun.* 50 (2014) 539–541.
- [17] S. Hebie, K.B. Kokoh, K. Servat, T.W. Napporn, Shape-dependent electrocatalytic activity of free gold nanoparticles toward glucose oxidation, *Gold Bull. (Berlin, Germany)* 46 (2013) 311–318.
- [18] B. Sebez, L. Su, B. Ogorcev, Y. Tong, X. Zhang, Aligned carbon nanotube modified carbon fibre coated with gold nanoparticles embedded in a polymer film: voltammetric microprobe for enzymeless glucose sensing, *Electrochem. Commun.* 25 (2012) 94–97.
- [19] F. Terzi, B. Zanfognini, C. Zanardi, L. Pigani, R. Seeber, Poly(3,4-ethylenedioxythiophene)/Au-nanoparticles composite as electrode coating suitable for electrocatalytic oxidation, *Electrochim. Acta* 56 (2011) 3575–3579.
- [20] Y. Rong, R. Malpass-Evans, M. Carta, N.B. McKeown, G.A. Attard, F. Marken, Intrinsically porous polymer protects catalytic gold particles for enzymeless glucose oxidation, *Electroanalysis* 26 (2014) 904–909.
- [21] L. Zhou, T. Gan, D. Zheng, J. Yan, C. Hu, S. Hu, High-density gold nanoparticles on multi-walled carbon nanotube films: a sensitive electrochemical nonenzymatic platform of glucose, *J. Exp. Nanosci.* 7 (2012) 263–273.
- [22] D. Feng, F. Wang, Z. Chen, Electrochemical glucose sensor based on one-step construction of gold nanoparticle–chitosan composite film, *Sens. Actuators B* 138 (2009) 539–544.
- [23] J. Zhang, D.P. Burt, A.L. Whitworth, D. Mandler, P.R. Unwin, Polyaniline langmuir-blodgett films: formation and properties, *Phys. Chem. Chem. Phys.* 11 (2009) 3490–3496.
- [24] M.C. Pham, J.E. Dubois, Behavior of electrodes modified with poly (naphthoquinone) films – electrocatalytic effect in the reduction of oxygen, *J. Electroanal. Chem.* 199 (1986) 153–164.
- [25] A.M. Bond, N.W. Duffy, S.-X. Guo, J. Zhang, D. Elton, Changing the look of voltammetry, *Anal. Chem.* 77 (2005) 186A–195A.
- [26] L.M. Liz-Marzan, A.P. Philpse, Stable hydrosols of metallic and bimetallic nanoparticles immobilized on imogolite fibers, *J. Phys. Chem.* 99 (1995) 15120–15128.
- [27] D. Sajan, K.P. Laladhas, I.H. Joe, V.S. Jayakumar, Vibrational spectra and density functional theoretical calculations on the antitumor drug, plumbagin, *J. Raman Spectrosc.* 36 (2005) 1001–1011.
- [28] L.D. Burke, Premonolayer oxidation and its role in electrocatalysis, *Electrochim. Acta* 39 (1994) 1841–1848.
- [29] A.M. Bond, N.W. Duffy, S.X. Guo, J. Zhang, D. Elton, Changing the look of voltammetry, *Anal. Chem.* 77 (2005) 186A–195A.
- [30] S.X. Guo, J. Zhang, D.M. Elton, A.M. Bond, Fourier transform large-amplitude alternating current cyclic voltammetry of surface-bound azurin, *Anal. Chem.* 76 (2004) 166–177.
- [31] J. Zhang, S.X. Guo, A.M. Bond, F. Marken, Large-amplitude Fourier transformed high-harmonic alternating current cyclic voltammetry: kinetic discrimination of interfering Faradaic processes at glassy carbon and at boron-doped diamond electrodes, *Anal. Chem.* 76 (2004) 3619–3629.
- [32] M.J.A. Shiddiky, A.P. O'Mullane, J. Zhang, L.D. Burke, A.M. Bond, Large amplitude Fourier transformed AC voltammetric investigation of the active state electrochemistry of a copper/aqueous base interface and implications for electrocatalysis, *Langmuir* 27 (2011) 10302–10311.
- [33] S.-X. Guo, Y. Liu, A.M. Bond, J. Zhang, P. Esakki Karthik, I. Maheshwaran, S. Senthil Kumar, K.L.N. Phani, Facile electrochemical co-deposition of a graphene-cobalt nanocomposite for highly efficient water oxidation in alkaline media: direct detection of underlying electron transfer reactions under catalytic turnover conditions, *PCCP* 16 (2014) 19035–19045.
- [34] S. Ben Aoun, Electrochemical oxidation of glucose at gold nanoparticle-modified pfc electrodes in an alkaline solution, *J. Mater. Environ. Sci.* 4 (2013) 887–892.
- [35] G. Chang, H. Shu, K. Ji, M. Oyama, X. Liu, Y. He, Gold nanoparticles directly modified glassy carbon electrode for non-enzymatic detection of glucose, *Appl. Surf. Sci.* 288 (2014) 524–529.
- [36] Y. Fu, F. Liang, H. Tian, J. Hu, Nonenzymatic glucose sensor based on ITO electrode modified with gold nanoparticles by ion implantation, *Electrochim. Acta* 120 (2014) 314–318.
- [37] A.J. Bard, L.R. Faulkner, *Electrochemical Methods: Fundamental and Applications*, 2nd ed., Wiley, New York, 2001.
- [38] K. Groebe, S. Erz, W. Mueller-Klieser, Glucose diffusion coefficients determined from concentration profiles in Emt6 tumor spheroids incubated in radioactively labeled α -glucose, in: M. Hogan, O. Mathieu-Costello, D. Poole, P. Wagner (Eds.), *Oxygen Transport to Tissue XVI*, Springer, US, 1994, pp. 619–625.
- [39] J. Zhang, A.M. Bond, Theoretical studies of large amplitude alternating current voltammetry for a reversible surface-confined electron transfer process coupled to a pseudo first-order electrocatalytic process, *J. Electroanal. Chem.* 600 (2007) 23–34.
- [40] B.D. Fleming, J. Zhang, A.M. Bond, S.G. Bell, L.L. Wong, Separation of electron-transfer and coupled chemical reaction components of biocatalytic processes using Fourier transform ac voltammetry, *Anal. Chem.* 77 (2005) 3502–3510.
- [41] Y.P. Liu, S.X. Guo, A.M. Bond, J. Zhang, Y.V. Geletii, C.L. Hill, Voltammetric determination of the reversible potentials for $\{\text{Ru}_3\text{O}_4(\text{OH})_2(\text{H}_2\text{O})_4\}$ ($\gamma\text{-SiW10O36}\}$ (2) (10-) over the pH range of 2–12: electrolyte dependence and implications for water oxidation catalysis, *Inorg. Chem.* 52 (2013) 11986–11996.
- [42] J. Zhang, S.X. Guo, A.M. Bond, Discrimination and evaluation of the effects of uncompensated resistance and slow electrode kinetics from the higher harmonic components of a Fourier transformed large-amplitude alternating current voltammogram, *Anal. Chem.* 79 (2007) 2276–2288.
- [43] D. MacDougall, W.B. Crummett, Guidelines for data acquisition and data quality evaluation in environmental chemistry, *Anal. Chem.* 52 (1980) 2242–2249.
- [44] J. Ping, J. Wu, Y. Wang, Y. Ying, Simultaneous determination of ascorbic acid, dopamine and uric acid using high-performance screen-printed graphene electrode, *Biosens. Bioelectron.* 34 (2012) 70–76.
- [45] Y. Liu, Y. Ding, Y. Zhang, Y. Lei, Pt–Au nanocorals Pt nanofibers and Au microparticles prepared by electrospinning and calcination for nonenzymatic glucose sensing in neutral and alkaline environment, *Sens. Actuators B* 171–172 (2012) 954–961.
- [46] J. Wang, H. Gao, F. Sun, C. Xu, Nanoporous PtAu alloy as an electrochemical sensor for glucose and hydrogen peroxide, *Sens. Actuators B* 191 (2014) 612–618.

Supplementary data

One pot synthesis of poly (5-hydroxyl-1,4-naphthoquinone) stabilized gold nanoparticles using monomer as the reducing agent for nonenzymatic electrochemical detection of glucose

M. C. Dilusha Cooray, Yuping Liu, Steven J. Langford, Alan M. Bond and Jie Zhang*

School of Chemistry, Monash University, Clayton, Victoria 3800, Australia

* Corresponding author: jie.zhang@monash.edu

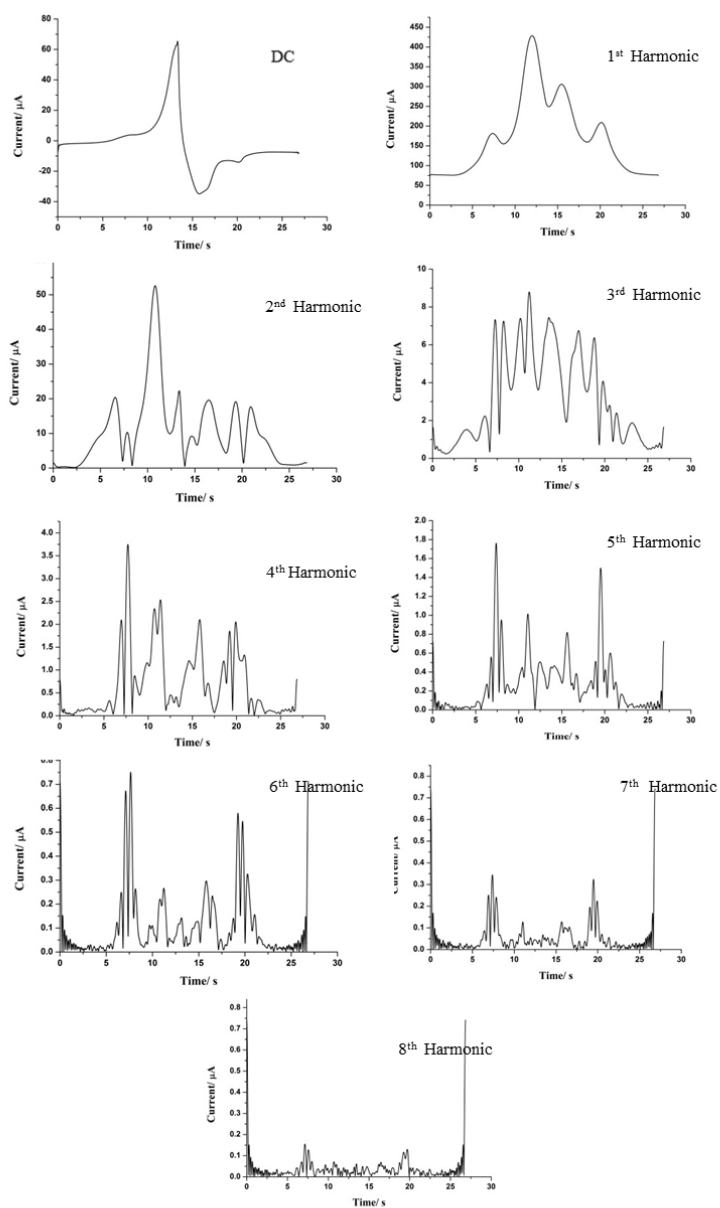


Figure S1: Dc and ac harmonic (1st to 8th) components of FTAC voltammogram obtained at an AuNQ NPs modified GCE in 0.1 M NaOH medium in the potential range between -0.7 to 0.35 V.

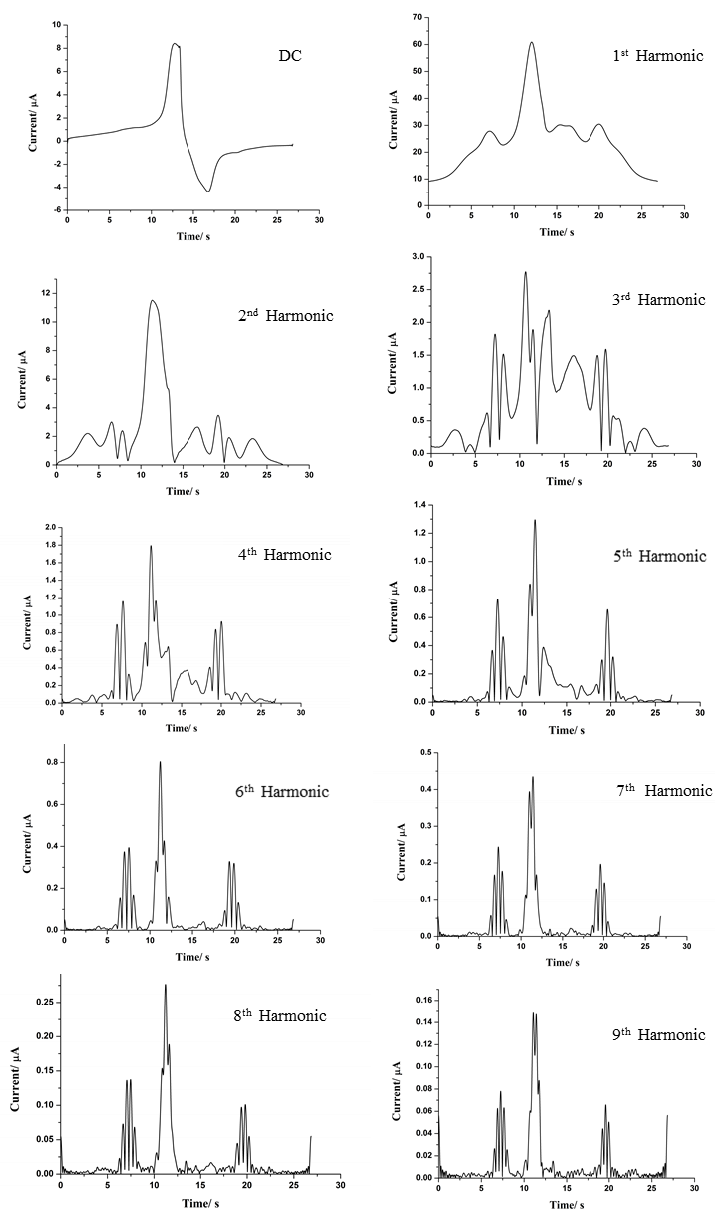


Figure S2: Dc and ac harmonic (1st to 9th) components of FTAC voltammogram obtained at an electrochemically cleaned AuE in 0.1 M NaOH medium in the potential range between -0.7 to 0.35 V.

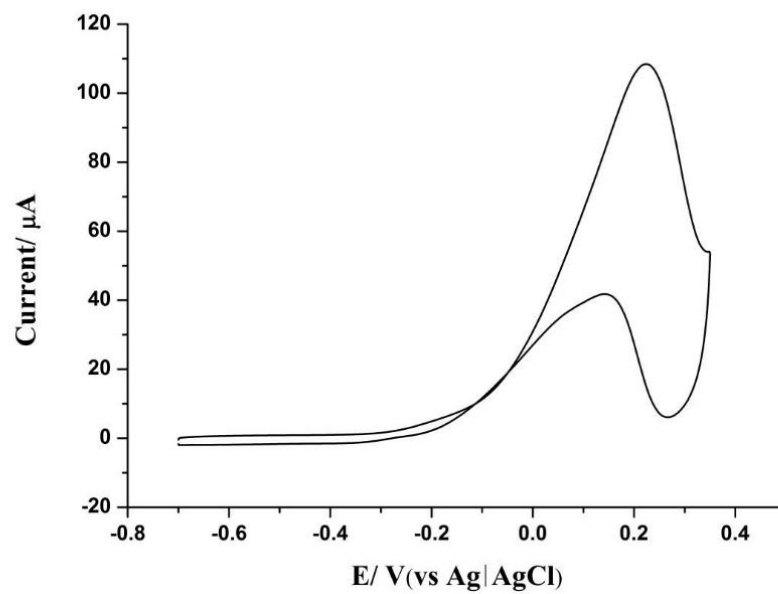


Figure S3: Cyclic voltammogram obtained at an AuNQ NPs modified GCE in a 5 mM of D-(+)-gluconic acid δ -lactone solution (0.1 M NaOH) at a scan rate of 0.05 V s^{-1} .

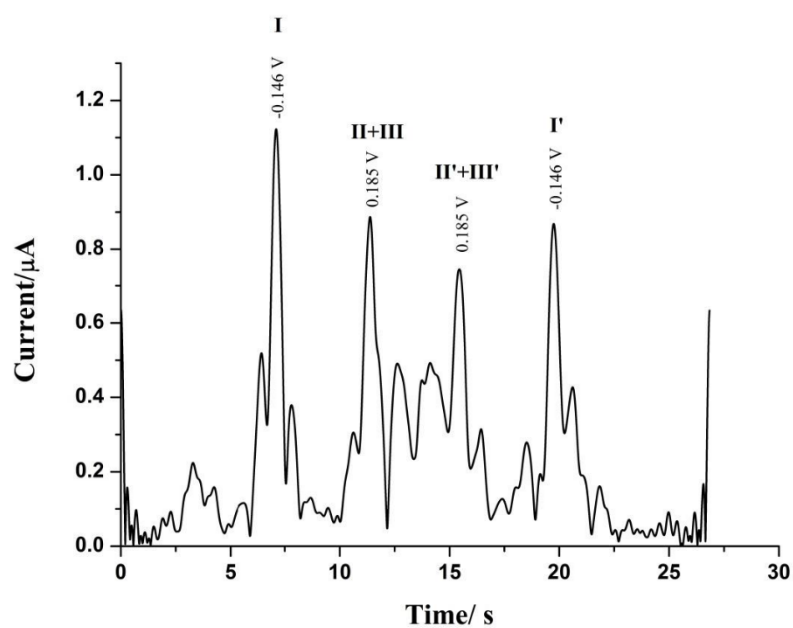


Figure S4: The 5th harmonic component of FTAC voltammogram obtained at an AuNQ NPs modified electrode in a 5 mM glucose (0.1 M NaOH) solution at a scan rate of 78.23 mV s^{-1} in the potential range between -0.7 to 0.35 V .

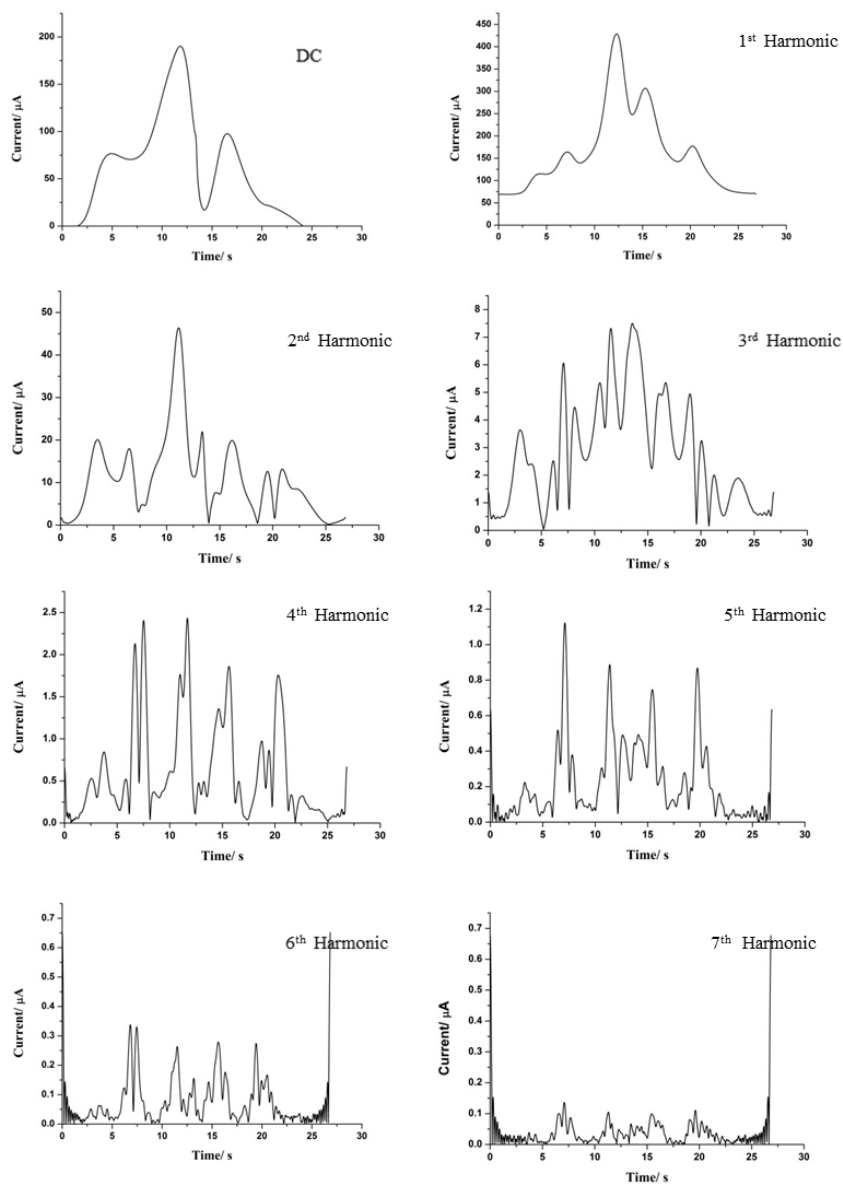


Figure S5: Dc and ac harmonic (1st to 7th) components of FTAC voltammogram obtained at an AuNQ NPs modified GCE in a 5 mM glucose solution (0.1 M NaOH) in the potential range between -0.7 to 0.35 V.

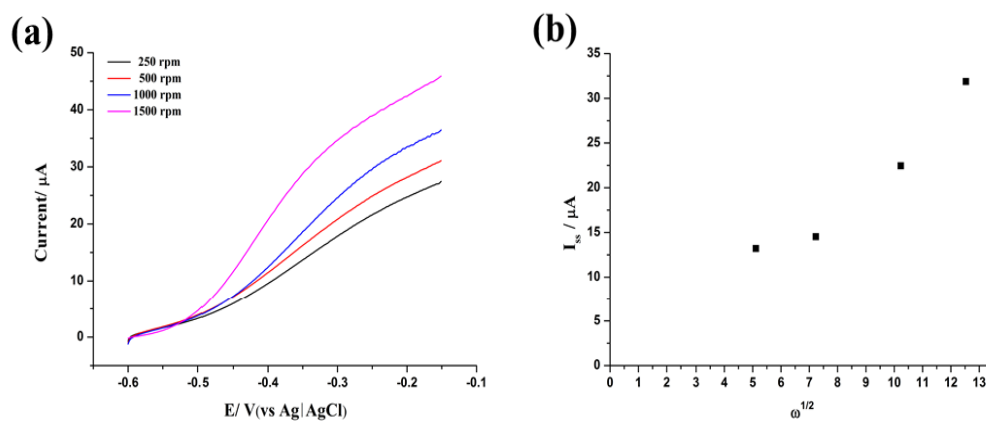


Figure S6: (a) Near steady state RDE voltammograms obtained at a AuNQ NPs modified GC RDE in a 2 mM Glucose (0.1 M NaOH) solution at a scan rate of 0.02 V s⁻¹ at different rotation rates and (b) the relationship between $\omega^{1/2}$ and background corrected steady-state mass transport limiting current measured at -0.2 V.

Chapter 5

Cobalt Selenide Nanoflake Decorated Reduced Graphene Oxide Nanocomposite for Efficient Glucose Electro-Oxidation in Alkaline Medium

1. Introduction

Nanotechnology has opened the doors to innovative pathways providing novel materials for the glucose oxidation [1]. Non-enzymatic electrodes based on catalytic nanocomposites provide efficient, reliable approaches for the detection of glucose concentration[2, 3]. Nanomaterials which are active towards glucose oxidation were being reported with the rising demand in sensor [4] and fuel cell [5] applications.

The application of two dimensional (2D) materials for electrocatalysis has been widely explored since the discovery of graphene due to their intrinsically high activities resulted from unique structural and electronic properties[6, 7]. However, the applications of 2D catalysts for electrochemical oxidation of glucose remains surprisingly scarce despite the commercial significance of this reaction. In this paper, we now introduce 2D cobalt selenide (CoSe) as an electrocatalyst for glucose oxidation. 2D CoSe is an excellent electrocatalyst for water oxidation displaying enhanced catalytic activity compared to cobalt oxides[8-12]. Since the electrochemical oxidation of water and glucose involves adsorption of hydroxyl group (OHads) as an important step, CoSe is expected to be a superior glucose oxidation catalyst[13, 14]. However, the electrical conductivity of semiconductor CoSe is low. To further increase the conductivity of the catalyst layer which is a crucial requirement for electrochemical applications, CoSe should be immobilized on a conductive support, such as reduced graphene oxide (rGO). To test the hypothesis that CoSe-rGO may be a more generally useful catalyst, we now report a one pot synthesis of CoSe decorated reduced graphene oxide using a simple hydrothermal procedure, followed by characterisation and evaluation of the performance with respect to electrocatalytic oxidation of glucose.

In this study, we introduce cobalt selenide (CoSe) as the electrocatalyst for glucose oxidation. Studies have been reported that employ different approaches of fabricating Co metal forms, its oxides and alloys for non-enzymatic glucose electrodes, which are summarised in Table 1. Materials with two or more metals or a combination of metal and non-metal as electrocatalysts can improve the electrocatalysis [15]. On this basis, we report a one pot synthesis of CoSe decorated reduced graphene oxide using a simple hydrothermal procedure, followed by characterisation and evaluation of the analytical performance with respect to electrocatalytic oxidation of glucose.

2. Experimental

2.1. Chemicals

Cobalt(II) nitrate hexahydrate ($\text{Co}(\text{NO}_3)_2 \cdot 6\text{H}_2\text{O}$, 98%), sodium selenite (Na_2SeO_3 , 99%), L-ascorbic acid ($\text{C}_6\text{H}_8\text{O}_6$, 99.9%), uric acid ($\text{C}_5\text{H}_4\text{N}_4\text{O}_3$, 99%), hydrazine (NH_2NH_2 , 98%), D-(+)-gluconic acid δ -lactone ($\text{C}_6\text{H}_{10}\text{O}_6$, 99.9%), formic acid (HCOOH , 98%), chitosan (75%) and D-glucose were purchased from Sigma Aldrich. Sodium hydroxide pellets (NaOH , 99%) was purchased from Merck. All chemicals were used as received. Deionised water was used for preparation of solutions.

Graphene oxide (GO) was synthesised from natural graphite (crystalline, 300 mesh, Alfa Aesar) using the method described by Hummers *et al.* [16].

2.2. Synthesis of CoSe-rGO

CoSe-rGO was synthesised by modifying a reported method [17]. To synthesise the CoSe-rGO composite, 32 mg of graphene oxide (GO) was dispersed in 12 mL of deionised water and stirred for 4 h. Then 73 mg (0.25 mmol) of $\text{Co}(\text{NO}_3)_2 \cdot 6\text{H}_2\text{O}$ and 43 mg (0.25 mmol) of Na_2SeO_3 were added. After vigorous stirring of this mixture for 10 min, 1 mL of hydrazine (98%) was added into the solution. Further stirring for 10 min was carried out before the

solution was transferred into a 20 mL Teflon-lined stainless steel autoclave and maintained at 140 °C for 24 h. After cooling to room temperature, the final product was collected by centrifugation and washed with deionised water and ethanol and oven at 60 °C.

2.3. Microscopic and spectroscopic characterisation

High resolution images were obtained with a FEI Tecnai G2 T20 TWIN LaB6 Transmission Electron Microscope (TEM) to determine the morphology and size of particles in the CoSe-rGO composite drop-casted onto a Cu grate. Energy Dispersive X-ray spectroscopy analysis was conducted at 10 keV. X-ray diffraction (XRD) data were collected with a Bruker D8 ADVANCE X-ray diffractometer (Cu K α radiation) using a scan step of 0.02° and a step time of 0.5 s. ¹H-NMR spectra were recorded with a Bruker DRX400 spectrometer at a frequency of 400 MHz using D₂O as the solvent.

2.4. Gas chromatography

Gas chromatography (GC) was employed to characterize gaseous products after bulk electrolysis using an Agilent (7820 A) GC instrument equipped with a HP-plot molesieve (5Å) column and a thermal conductive detector was used to identify CO₂ at a temperature of 200 °C.

2.5. Fabrication of CoSe-rGO/chit electrodes

A solution of 0.375 mg/mL CoSe-rGO solution containing 0.15 w/v % chitosan was used to stabilise and aid dispersion of the nanocomposite. A 3 μ L aliquot was drop cast on the glassy carbon electrode (GCE, 3mm diameter) and dried prior to undertaking electrochemical measurements. In bulk electrolysis experiments, a glassy carbon plate (37 mm \times 15 mm) was modified with 200 μ L of 0.25 mg/ mL CoSe-rGO solution containing 0.1 % chitosan.

2.6. Electrochemical measurements

Voltammetric measurements were carried out at 20 ± 2 °C using a CH Instrument 760E electrochemical workstation with a conventional three-electrode cell using NaOH (0.3 M) as the supporting electrolyte. A CoSe-rGO/chit modified GCE or a GC-RDE, Hg|HgO(1 M NaOH) and platinum wire were employed as working, reference and auxiliary electrodes respectively.

To obtain the required concentration of glucose, appropriate aliquots of a 1.00 M glucose stock solution were added to the 0.3 M NaOH electrolyte solution. The catalytic current density was obtained by subtracting the background current density arise from Co_3O_4 from the electrocatalytic current density obtained by glucose oxidation at 0.65 V vs Hg|HgO(1 M NaOH).

Bulk electrolysis was carried out using a gas tight 'H-shaped' two compartment cell with a porous glass frit employed to separates the compartments. CH Instrument 760E workstation was used as in voltametric experiments. In this case a glassy carbon plate (37 mm × 15 mm) was used as the working electrode and placed in one compartment. The Hg|HgO(1 M NaOH) reference electrode was located in the same compartment with the working electrode. A Pt mesh wire acts as the auxiliary electrode and located in the other compartment. NaOH (0.3 M) again was used as the supporting electrolyte. Glucose or gluconolactone concentrations were 20 mM and both compartments were filled with 15.0 mL of solution. Controlled potential electrolysis was performed at 0.7 V vs Hg|HgO(1 M NaOH) for about 1 h under continuous stirring.

3. Results and Discussion

3.1. Microscopic and spectroscopic characterisation of CoSe-rGO

A simple one-pot hydrothermal synthesis procedure was carried out to synthesise the CoSe decorated rGO. The Co^{2+} and Se^{2+} were reduced to $\text{Co}(0)$ and $\text{Se}(0)$ respectively by hydrazine. At high temperature (140°C) Co reacts with Se to form $\text{Co}_{0.85}\text{Se}$ [17] (symbolised hereafter as CoSe for simplicity). Simultaneously graphene oxide was reduced by hydrazine to give CoSe decorated rGO. The reactions that took place during the formation of this material are as follows [17]:



TEM images were used to obtain the size distribution of CoSe-rGO and information on the crystallinity. The image in Figure 1(a) reveals the presence of nanoflakes grown on rGO, a uniform distribution of CoSe nanoflakes (darker spots) on rGO sheets (transparent gray portion) is evident. The EDX spectrum (Figure 1(b)) contains the characteristic Co and Se signals detected from CoSe, C mainly from the rGO and Cu signal is due to the grid that was used to fabricate the material for EDX measurement. Therefore, the results reveal that the material is pure.

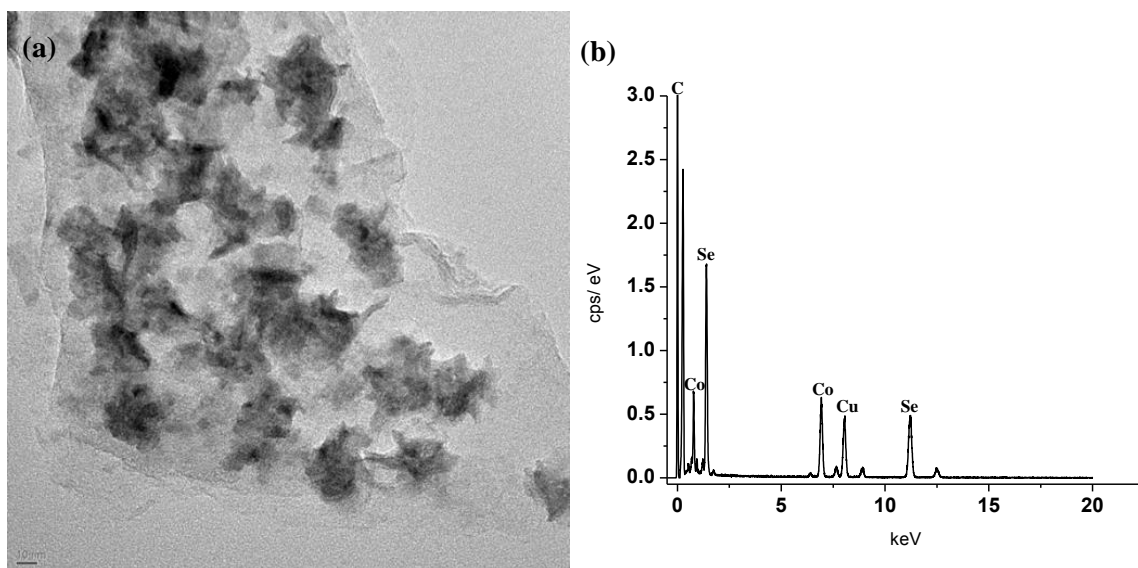


Figure 1: Electron microscopic and elemental characterisation of CoSe-rGO. (a) TEM image (b) EDX spectrum

XRD analysis demonstrated that CoSe is a mixture of Co: Se in ~1:1 stoichiometric ratio. As shown in Figure 2, the CoSe-rGO composite (JCPDS 89-2004) develops a similar diffraction pattern to that of pure CoSe, in agreement with other literature [18]. The broad peak around $2\theta = 25^\circ$ is attributed to the rGO (002) facet in the material [19-22], which is a result of the formation of graphene layers during sample preparation [20]. The spectrum manifest peaks at $2\theta = 33.22^\circ$, 44.78° , 50.47° , 60.09° and 61.77° which can be indexed as (1 0 1), (1 0 2), (1 1 0), (1 0 3) and (2 0 1) facets of the CoSe-rGO composite (JCPDS 89-2004), respectively. The (1 0 1), (1 0 2) and (1 1 0) facets can be attributed to presence of the hexagonal closed packed (hcp) structure of CoSe [17].

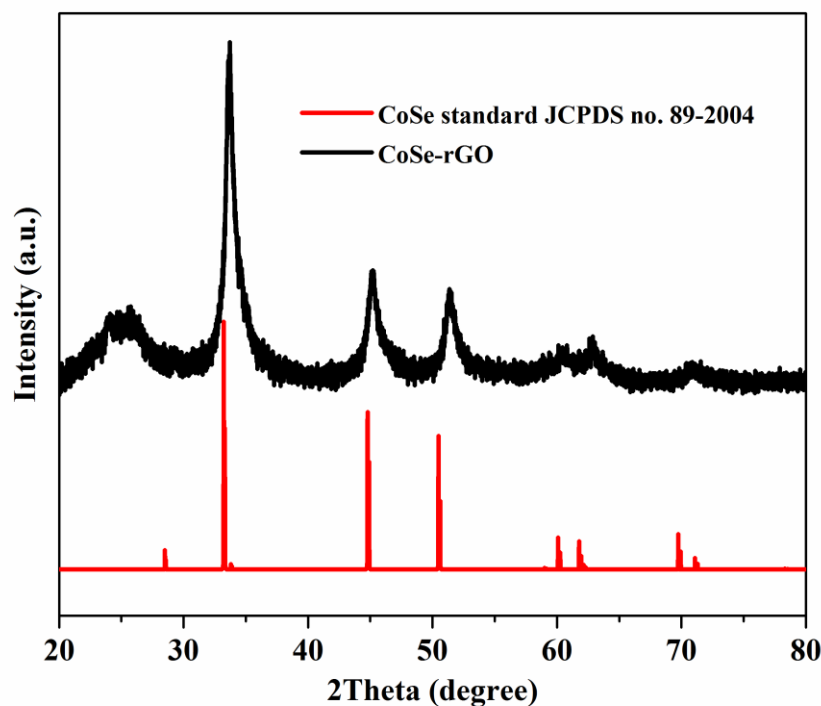


Figure 2: XRD spectrum obtained from CoSe-rGO.

3.2. Electrochemical characterisation of the CoSe-rGO/chit modified electrode

A GCE modified with CoSe-rGO/chit was used for electrochemical assessment. Chitosan acts as the binder and enables the CoSe-rGO nanocomposite to disperse well in water. The electrochemical behaviour of the redox active CoSe-rGO/chit modified GC electrode was investigated in an aqueous 0.3 M NaOH electrolyte medium using cyclic voltammetry by cycling the potential between of 0 V to 0.68 V vs Hg|HgO_(1 M NaOH) at a scan rate of 0.02 V s⁻¹. The cyclic voltammogram illustrated in Figure 3 shows two reversible processes and one irreversible process noted as I/I', II/II' and III accordingly. For the redox couple I/I', a well defined mid-potential (E_m) of 0.188 V with a peak to peak separation of 32 mV was obtained implying that process I/I' in CoSe-rGO/chit modified GCE is close to reversible. The redox couple II/II' with a E_m of about 0.57 V displays much broader peaks but notably smaller

peak-to-peak separation, implying faster kinetics[23]. The process III is associated with electrocatalytic water oxidation [23, 24].

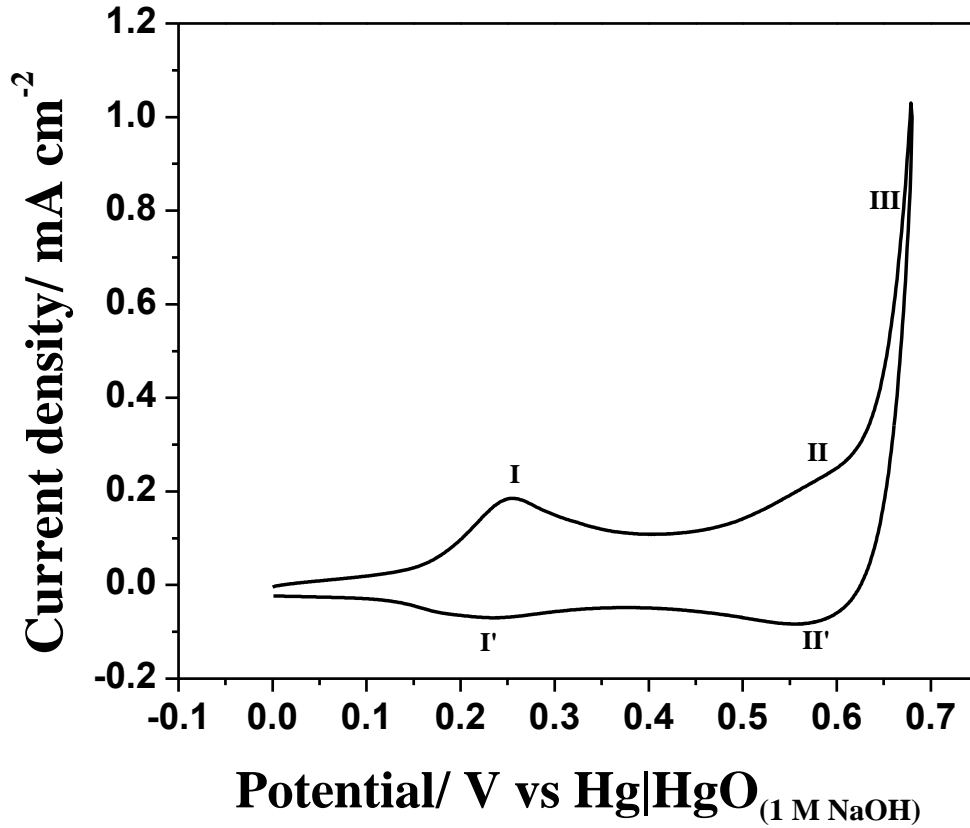
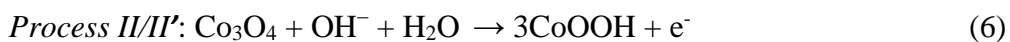


Figure 3: DC Cyclic voltammogram obtained at a scan rate of 0.02 V s^{-1} with CoSe-rGO/chit modified GCE in 0.3 M NaOH .

In the alkaline medium the hydrolysis of CoSe was confirmed by XRD analysis carried out after incubating the CoSe-rGO material in 0.3 M NaOH solution for 3 h at room temperature (Figure 4) revealing that CoSe spontaneously forms Co(OH)_2 which is shown by equation (4). Considering the results obtained from XRD and considering other reported literature [23], the reaction equations can be listed as follows:



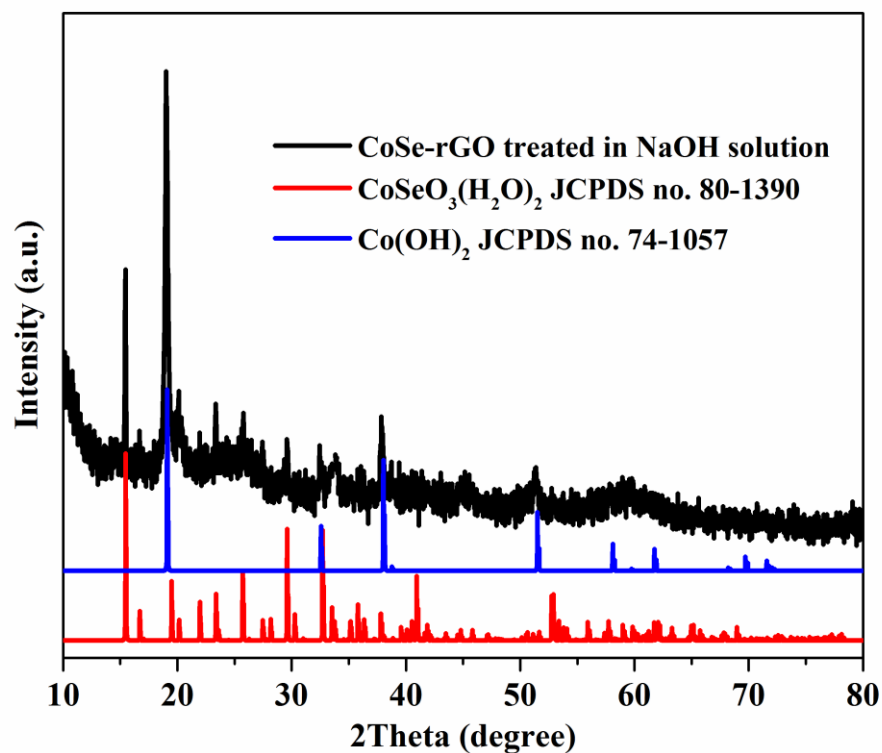


Figure 4: XRD spectra obtained (—) after incubating the CoSe-rGO material in 0.3 M NaOH solution for 3 h at RT with, (—) Co(OH)₂ standard, and (—) Co(SeO₃)(H₂O)₂ standard spectra.

As shown in Figure 5 the oxidation and reduction peak current densities increased linearly with the increased scan rate over the range of 0.02 – 0.75 V s⁻¹ indicating surface confined electron transfer for processes I/I' and II/II'.

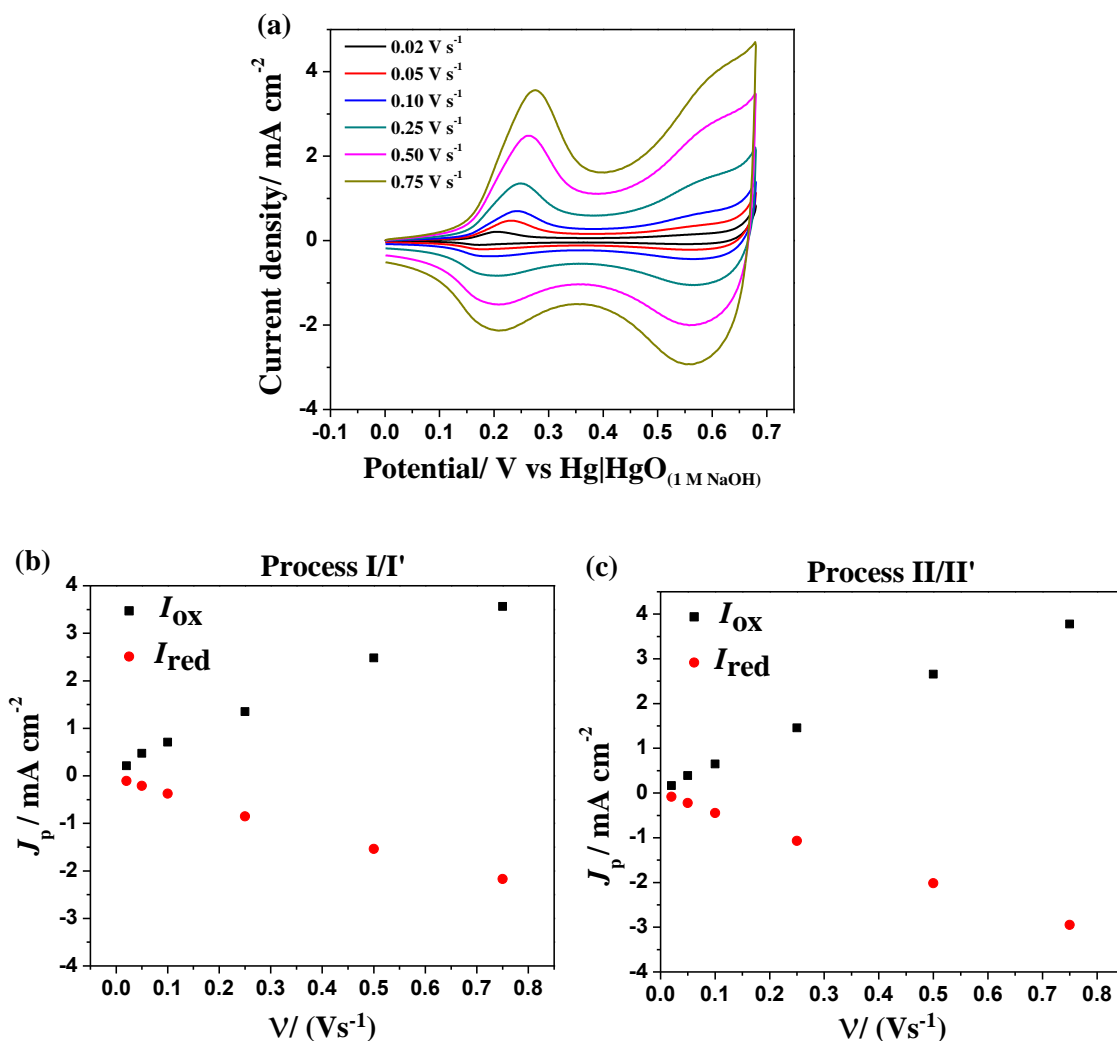


Figure 5 : (a) Cyclic voltammograms obtained with CoSe-rGO/chit modified GCE in 0.3 M NaOH as a function of scan rate and the relationship between the peak current density (J_p) versus scan rate for processes (b) I/I' and (c) II/II'.

3.3. Electrocatalytic oxidation of glucose

The electrocatalytic oxidation of glucose was investigated using the CoSe-rGO/chit modified GCE. Cyclic voltammograms were obtained in the presence and absence of 5.0 mM glucose in 0.3 M NaOH at a scan rate of 0.02 V s⁻¹ between the potential range of 0 – 0.68 V vs Hg|HgO_(1 M NaOH). The results were illustrated in Figure 6. The redox process

occurring around 0.18 V does not have any influence in the presence of glucose, and electrocatalytic oxidation of glucose commence from 0.5 V vs Hg|HgO_(1 M NaOH). Apparently, process II/ II' (equation (6)) is shown to be directly involved in the glucose electrocatalytic oxidation. Therefore, the mechanism responsible for the aforementioned electrocatalytic oxidation of glucose can be summarised by equation (7):

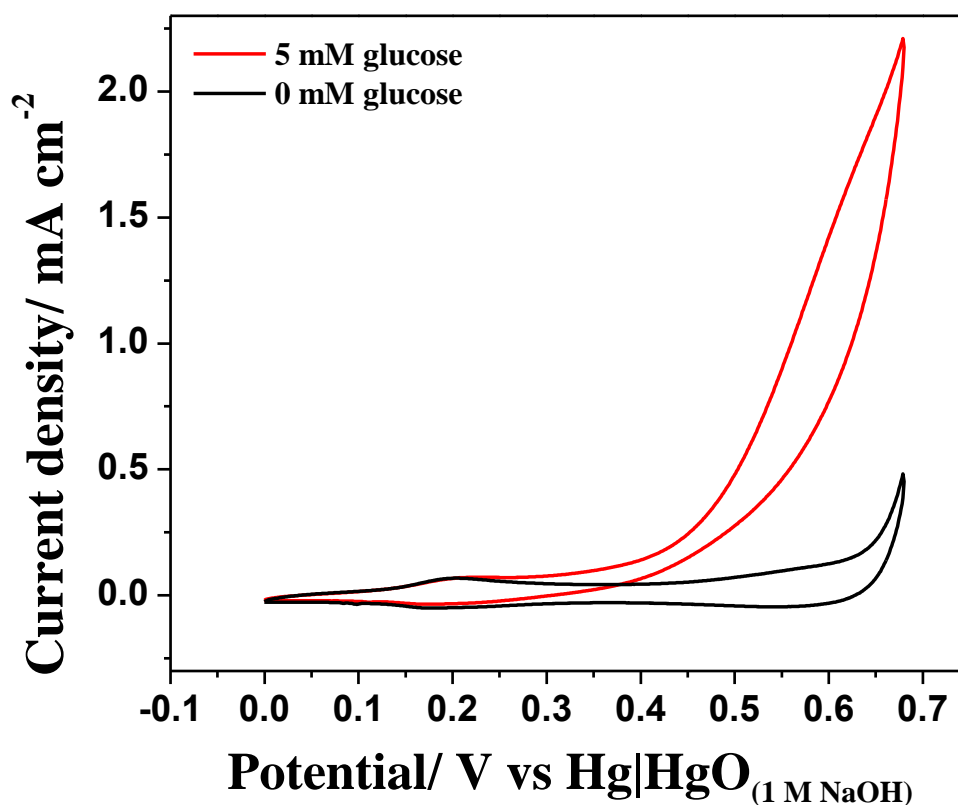
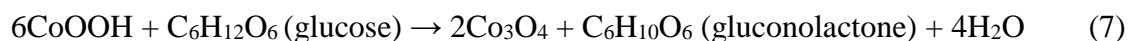


Figure 6: Cyclic voltammograms obtained in 0.3 M NaOH at a scan rate of 0.02 V s⁻¹ over the potential range of 0 to 0.68 V using a CoSe-rGO/chit modified GC electrode in the absence (—) and presence (—) of 5.0 mM glucose.

No oxidation process was detected in this potential range at a bare GC electrode or rGO modified electrode confirming that Co is the active component of the catalyst. Based on

previous reports [25], the oxidation process taking place at around 0.5 V can be assigned to oxidation of glucose by electrogenerated CoOOH to form gluconolactone as one of the products (equation(7)). Similar experiments using a CoSe-rGO/chit modified GCE in the phosphate buffered saline (PBS) pH 7 solution containing 10.0 mM glucose did not yield electrocatalytic oxidation of glucose (results not shown). This revealed the critical role of OH⁻ in the formation of catalytically active cobalt species, as expressed in equations 4- 6.

3.4. Optimisation of conditions

To optimise the performance of the modified electrode the effects of electrolyte concentration was evaluated. Experiments were carried out to investigate the optimum supporting electrolyte concentration over the range of 0.1 – 0.5 M NaOH. The electrocatalytic current density was determined at 0.65 V vs Hg|HgO_(1 M NaOH) after subtracting the background current density obtained in the absence of glucose and plotted as a function of electrolyte concentration. The results revealed 0.3 M NaOH concentration to be the optimum concentration of the electrolyte as shown in Figure 7. Similar cyclic voltammetry experiments were carried out to investigate the effects on the electrocatalytic current density with the loading weight of the catalyst CoSe-rGO. The results revealed the increment of the loading catalyst was directly proportional to the increase of electrocatalytic current density up to 0.75 μg and reached the plateau after 1.25 μg (Figure 8). Therefore, the loading weight of the CoSe-rGO catalyst was kept at 4 μL from the prepared nanocomposite solution, which corresponds to 1.5 μg of loading weight.

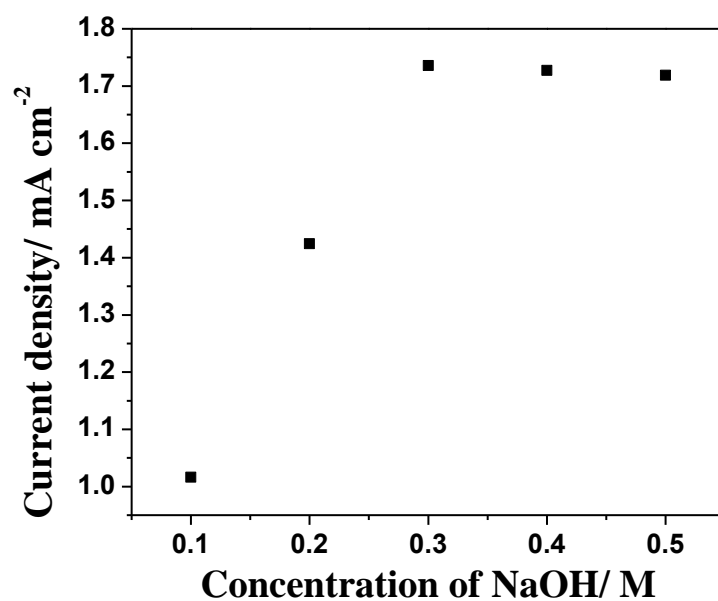


Figure 7: Electrocatalytic current density obtained from CoSe-rGO/chit modified GCE in the presence of 5.0 mM glucose as a function of the NaOH concentration.

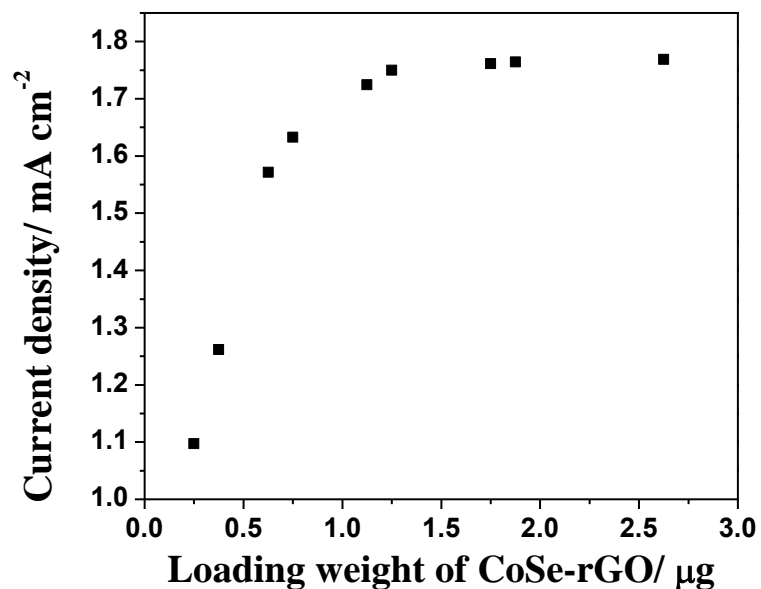


Figure 8: Electrocatalytic current density obtained from CoSe-rGO/chit modified GCE in the presence of 5.0 mM glucose as a function of the CoSe-rGO loading weight.

3.5. Measurements under hydrodynamic conditions using CoSe-rGO/chit modified Rotating disc Electrode

The experiments were carried out under hydrodynamic conditions using CoSe-rGO/chit modified GCE (scan rate 0.02 V s^{-1}) in the presence of 5.0 mM glucose at different rotation rates. According to Figure 9, the results revealed that the electrocatalytic current density was independent of rotation rate in the electrode rotation rate range of $500 - 1500 \text{ rpm}$ suggesting that the process was kinetically controlled.

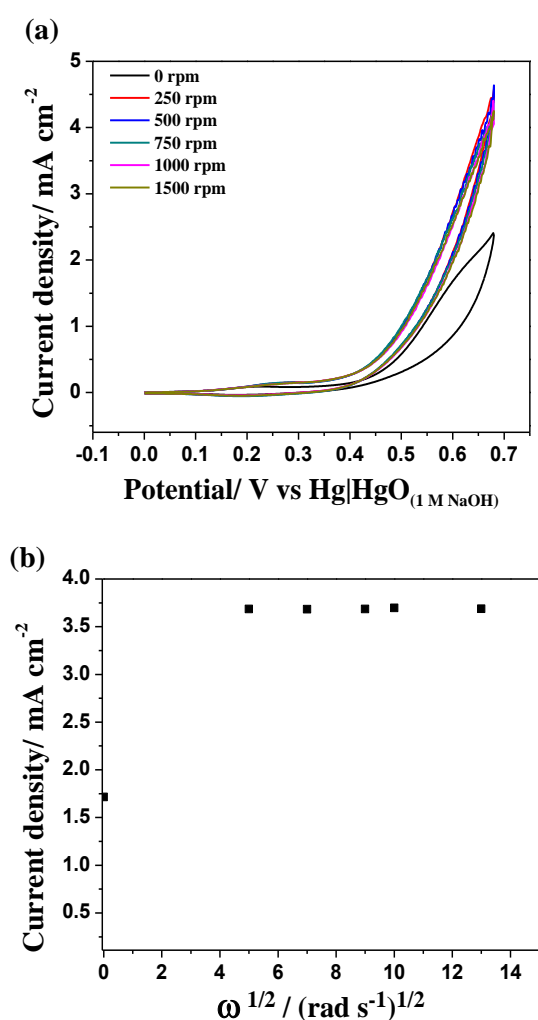


Figure 9: (a) RDE voltammograms obtained at a CoSe-rGO/chit modified GC RDE in a 5.0 mM Glucose (0.3 M NaOH) solution at a scan rate of 0.02 V s^{-1} at different rotation rates and (b) the relationship between $\omega^{1/2}$ and background corrected current density measured at 0.65 V .

3.6. Further oxidation of Gluconolactone by CoSe-rGO/chit modified GC electrode

In literature, for most of the catalysts, the common final product of glucose oxidation is gluconolactone, where glucose is oxidised to gluconolactone giving 2 electrons [26, 27]. CoSe-rGO is a novel catalyst in electrocatalytic glucose oxidation. Therefore, it is essential to investigate the final products of electrocatalytic glucose oxidation for this new catalyst. As a control experiment cyclic voltammetric measurements were carried out with 5.0 mM D-(+)-gluconic acid δ -lactone (gluconolactone) in 0.3 M NaOH. The cyclic voltammogram (Figure 10) showed that CoSe-rGO catalyst has the ability to further oxidise gluconolactone. This suggests that gluconolactone is not the final product of the catalytic glucose oxidation reaction.

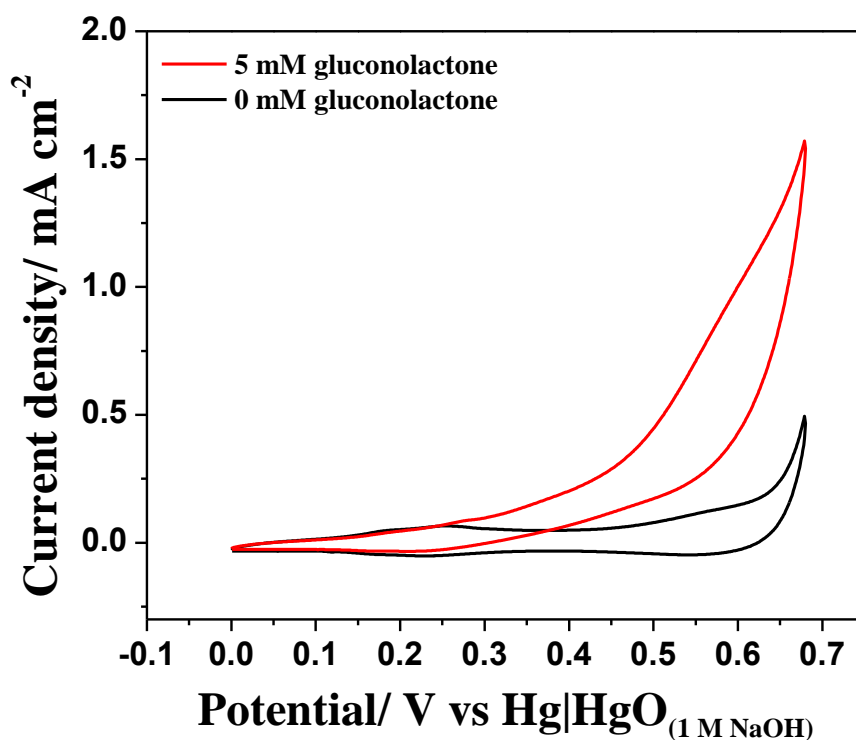


Figure 10: Cyclic voltammograms obtained in 0.3 M NaOH at a scan rate of 0.02 V s⁻¹ over the potential range of 0 to 0.68 V on a CoSe-rGO/chit modified GC electrode in the absence (—) and presence (—) of 5.0 mM gluconolactone.

3.7. Bulk electrolysis and product characterisation

Bulk electrolysis method was employed to investigate all possible products of glucose electrocatalytic oxidation using CoSe-rGO/chit modified GC electrode (37mm x 15 mm) in alkaline medium followed by $^1\text{H-NMR}$ spectra analysis. Bulk electrolysis was carried out using 20.0 mM glucose in 0.3 M NaOH medium with controlled potential at 0.7 V vs Hg|HgO_(1 M NaOH). As a control, this experiment was repeated with the exact conditions to find out possible products of gluconolactone (20.0 mM) electrocatalytic oxidation. The $^1\text{H-NMR}$ spectrum obtained after electrolysis of glucose (Figure 11a) using the electrolysis medium together with D₂O solvent, and similarly $^1\text{H-NMR}$ spectrum obtained after electrolysis of gluconolactone (Figure 11b). The complex spectra between 2.8 – 5.2 ppm were attributed to six-membered carbon derivatives which make it difficult to investigate due to the complexity[28]. The high alkaline concentration of the electrolysis medium restricted further product characterisation by mass spectrometry. The peak observed at 8.2 ppm was observed after the bulk electrolysis experiments of both glucose and gluconolactone which can be attributed to the presence of formate (HCOO^-) in accordance with the previous literature[29]. This was further confirmed by adding an aliquot of standard formic acid to the same NMR tube containing bulk electrocatalysis medium of glucose and the enhanced peak implies that the peak observed at 8.2 ppm reconfirmed the presence of formate. The formation of formate revealed the complete cleavage of the C-C bond during electrolysis[28, 30]. However, the yield of formate was very low since it can be further oxidised to form CO₂ as the final product.

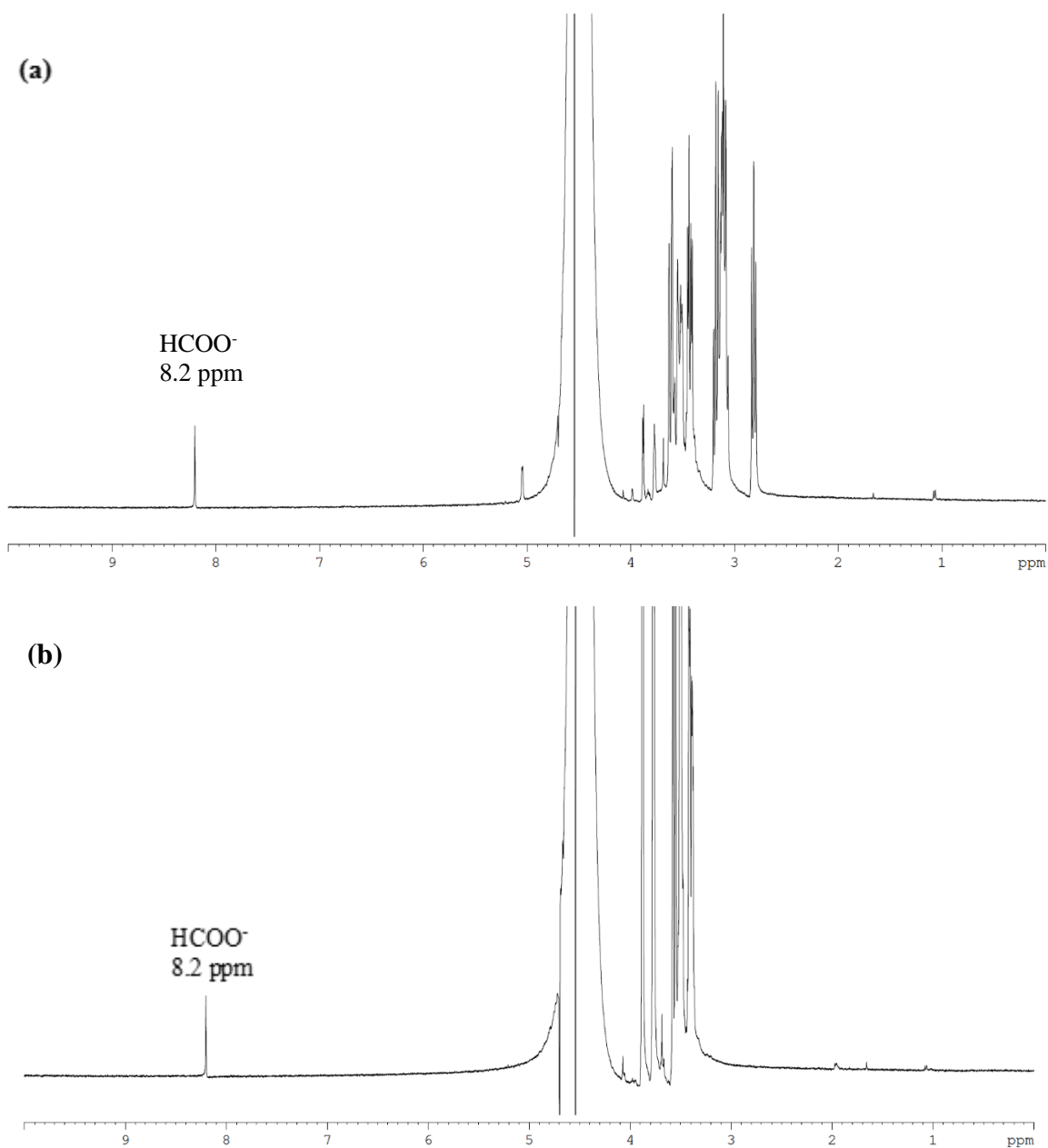


Figure 11: ¹H-NMR spectra were obtained at a frequency of 400 MHz using D₂O as the solvent after bulk electrolysis of (a) glucose and (b) gluconolactone at 300 K.

The results obtained above (Figure 11) suggest that gluconolactone is not the final product. The possibility to produce CO₂ by oxidation of formate was further confirmed by cyclic voltammetry employing CoSe-rGO/chit modified GCE in the absence and presence of 60.0 mM formic acid in 0.3 M NaOH. The results with the increase electrocatalytic current density conveyed (Figure 12) the further oxidation of formate to CO₂ is possible with CoSe-rGO/chit modified GCE. According to previous literature [31, 32], a mechanism can be attributed as follows for the product formation:

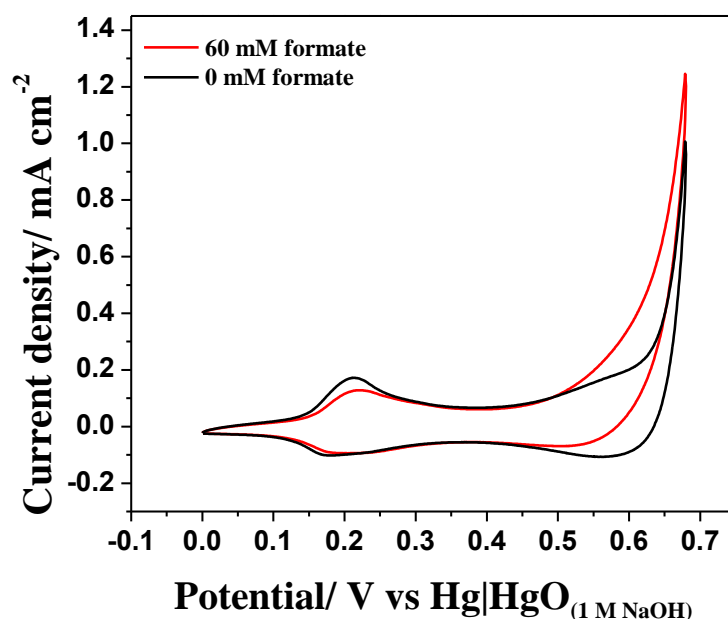
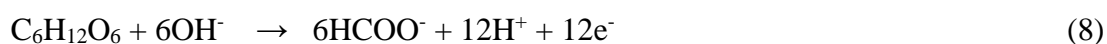


Figure 12: Cyclic voltammograms obtained in 0.3 M NaOH at a scan rate of 0.02 V s⁻¹ over the potential range of 0 to 0.68 V at a CoSe-rGO/chit modified GC electrode in the absence (—) and presence (—) of 60.0 mM formic acid.

The results obtained from formic acid oxidation (Figure 12) suggest the possibility of formation of CO₂ from glucose bulk electrolysis. Therefore, closed cell bulk electrolysis was

carried out to confirm the presence of CO₂ in the head space of the electrolysis cell after bulk electrolysis for 1 h. The gas sample (0.2 mL) collected in the closed cell was subjected to GC analysis at 200 °C. Pure CO₂ (0.2 mL) was used to investigate the retention time in GC. A control experiment using an air sample (0.2 mL) was carried out at 200 °C in GC under same conditions, the resulted chromatogram does not show a peak for CO₂ at 4 min retention time implying that the amount of CO₂ in air is not sensitive for GC analysis. Therefore, the detected CO₂ peak from the sample is due to the electrocatalytic oxidation of glucose. The chromatogram revealed the presence of CO₂ (Figure 13) in the gas sample collected after electrolysis with a similar retention time of ~ 4 min as the pure CO₂. This suggests that CoSe-rGO catalyst has the ability to electrocatalytically oxidise glucose to CO₂. However, the Faraday efficiency of this process is low implying low yield of CO₂. The mechanism can be assigned as in equation (10):

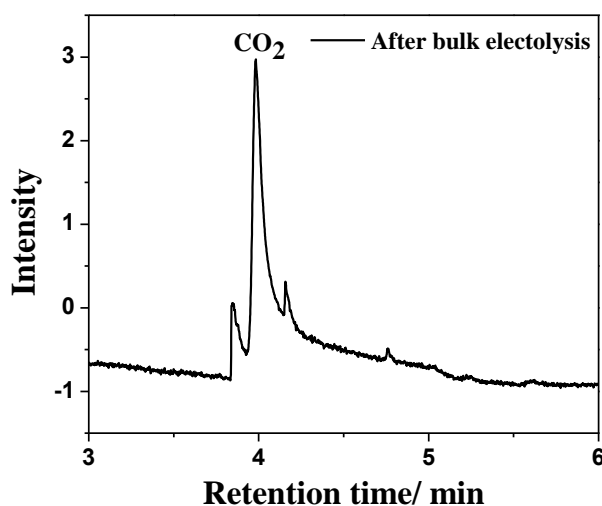


Figure 13: Gas chromatogram obtained at 200 °C from the gas sample collected from the head space of the closed cell after electrolysis.

3.8. Stability of CoSe-rGO/chit modified GC

The stability of the catalyst during bulk electrolysis was investigated through comparison of cyclic voltammograms of CoSe-rGO/chit modified GC electrode (3 mm diameter) before and after holding the potential at 0.7 V for 1 h in 0.3 M NaOH in the presence of 20.0 mM glucose. The results revealed that even after 1 h, catalyst activity remained the same (Figure 14). Furthermore, plot of current vs time (not shown) showed constant current throughout the time frame of the experiment. In conclusion, these results confirm the stability of the CoSe-rGO catalyst during bulk electrolysis.

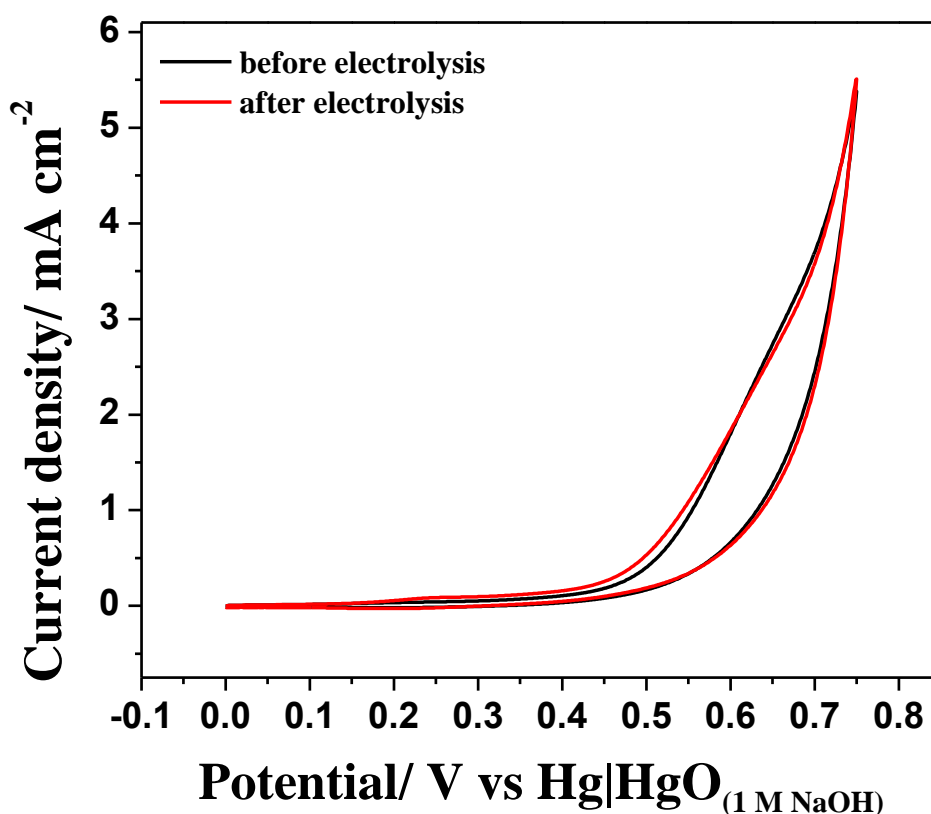


Figure 14: Cyclic voltammograms obtained before and after 1 h of electrolysis of 20 mM glucose in 0.3 M NaOH.

3.9. Analytical performance of a CoSe-rGO/chit modified electrode for glucose determination

The results demonstrated earlier revealed the ability of electrocatalytic oxidation of glucose by the CoSe-rGO/chit modified GC electrodes in alkaline medium. The cyclic voltammograms (Figure 15a) and the plot of electrocatalytic current density versus glucose concentration are shown in Figure 15b and illustrate an excellent linearity ($R^2 = 0.986$) relationship with a slope of $480 \mu\text{A mM}^{-1} \text{cm}^{-2}$ obtained in the concentration range of 0 to 10 mM glucose. Above 10 mM, deviation from linearity is detected due to the kinetic limitation. A limit of detection (LOD) of $2.5 \mu\text{M}$ ($S/N = 3$) was estimated from the standard deviation of ten measurements in an aqueous 0.3 M NaOH solution containing 1 mM glucose according to the well documented protocol [33]. The modified electrode showed a maximum current density of $5.41 \pm 0.03 \text{ mA cm}^{-2}$. This can be attributed to the high efficiency of glucose oxidation achieved at CoSe-rGO/chit modified GC electrodes. The electrode to electrode reproducibility was investigated using five CoSe-rGO/chit modified GC electrodes in the presence of 5.0 mM glucose in 0.3 M NaOH and a RSD of 2.3 % was achieved. In addition, five measurements of 5.0 mM glucose using the same electrode yielded a RSD of 1.1 %. These results revealed excellent intra-electrode and inter-electrode reproducibility.

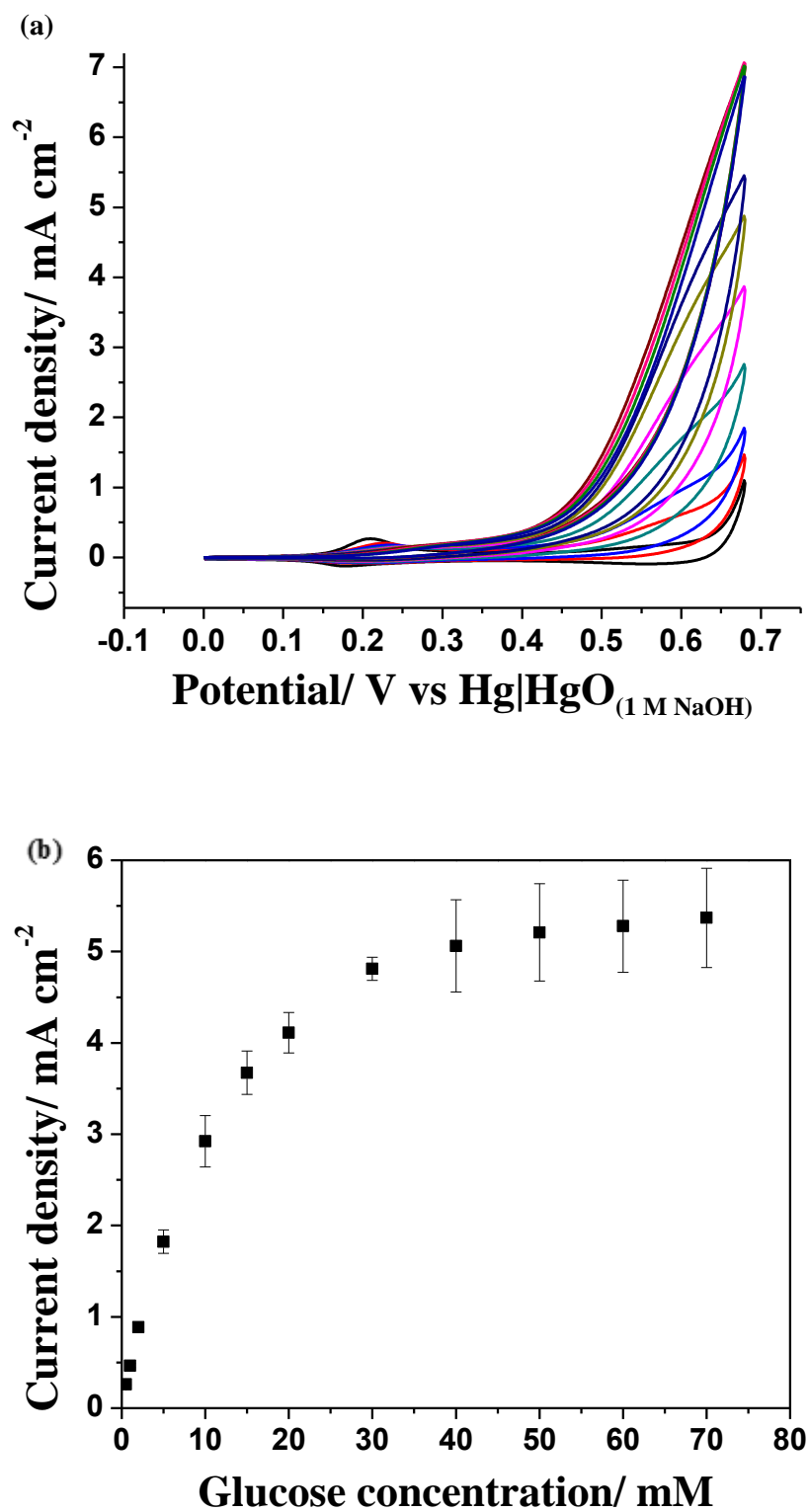


Figure 15: (a) Plot of cyclic voltammograms obtained at different glucose concentration and the (b) calibration curve for the determination of glucose concentration in 0.3 M NaOH based on average results obtained from three CoSe-rGO/chit modified GCEs.

There are many non-enzymatic electrodes fabricated using Co as the active metal catalysts for electrocatalytic glucose oxidation carrying their own advantages and limitations. The performance of these modified electrodes have been summarised in Table 1.

Table 1: Performance of modified electrodes with Co based nanocomposites for glucose electro-oxidation

Electrode	Working potential/ V	Medium	Sensitivity/ $\mu\text{A cm}^{-2}\text{mM}^{-1}$	Max. current density/ $\mu\text{A cm}^{-2}$	LOD/ μM	Linear dynamic range/ mM	Ref.
CoO nanorods/FTO	0.5 vs. Ag/AgCl	1 M NaOH	571.8	2500	0.058	0- 3.5	[34]
Co ₃ O ₄ NFs-Nafion/GCE	0.59 vs. Ag/AgCl	0.1 M NaOH	36.25	-	0.97	0-2.04	[25]
CoOOH nanosheets	0.40 vs. Ag/AgCl	0.1 M NaOH	967	790	10.9	0.03- 0.7	[35]
CoOxNPs/ ERGO/GCE	0.60 vs SCE	0.05 M NaOH	79.3	-	2	0.01– 0.55	[36]
3D graphene/Co ₃ O ₄ nanowire composite	0.58 vs. Ag/AgCl	0.1 M NaOH	3390	600	0.025	0- 0.080	[37]
CoOx·nH ₂ O–MWCNTs	0.55 vs. Ag/AgCl	0.2 M NaOH	162.8	1555	2	0-4.5	[38]
Co ₃ O ₄ UNS-Ni(OH) ₂	0.35 vs. Ag/AgCl	0.1 M NaOH	1089	2000	1.08	0.005– 0.040	[39]
CoSe/rGO/chit/GCE	0.65 vs Hg/HgO	0.3 M NaOH	480	5414	2.5	0- 10	This work

Abbreviations: FTO - Fluorine doped Tin Oxide, NFs - nanoflakes, ERGO - electrochemically reduced graphene oxide, UNS - ultra-nanosheets.

3.10. Interferences

The selectivity of CoSe-rGO/chit modified GCE was investigated which will be an important factor in glucose sensing. In glucose sensing, the main species interfering with the glucose measurement in biological samples are ascorbic acid (AA) and uric acid (UA). However, trace amounts of metabolites of drugs also can act as interferents [27]. The interference study was carried out in the presence of physiological amounts of AA and UA in aqueous 0.3 M NaOH solution using the CoSe-rGO/chit modified GCE [27]. In the presence of 0.50 mM UA, the voltammetric response from 5.0 mM glucose remains unaffected (Figure 16).

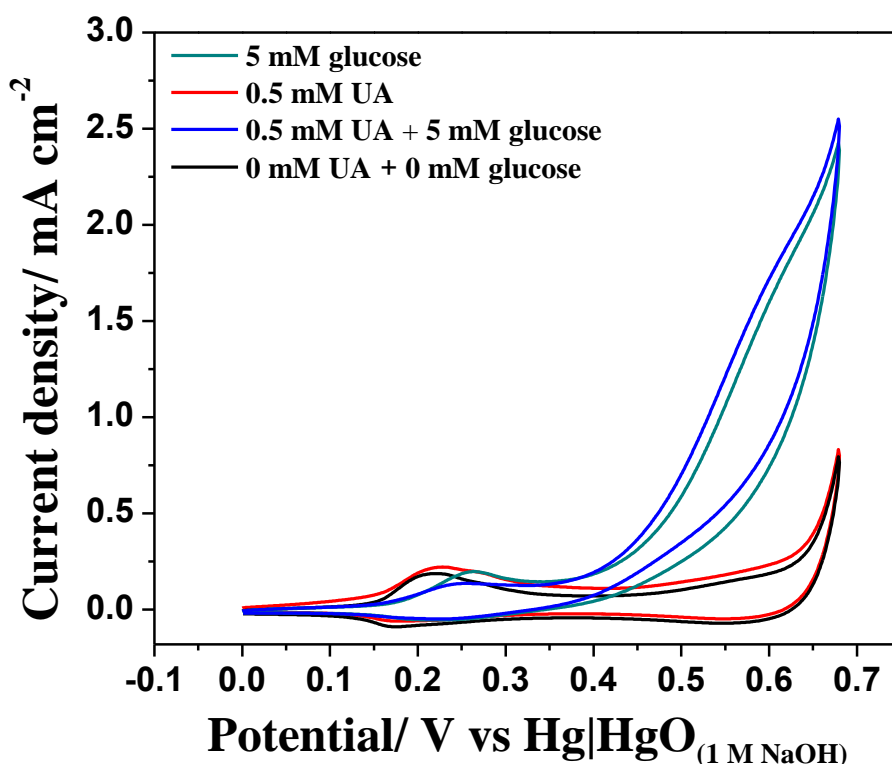


Figure 16: Cyclic voltammograms obtained with 5.0 mM glucose in 0.3 M NaOH at a scan rate of 0.02 V s⁻¹ in the absence and presence of 0.5 mM UA. The response obtained with 0.5 mM UA alone is also provided for comparison.

Similarly, the presence of 2.5 mM AA, the voltammetric response from 5.0 mM glucose (Figure 17) was not affected, even though AA acid can be oxidised by CoSe-rGO/chit modified GCE. This is advantageous in sensor application as many of the non-enzymatic electrodes suffer from UA and AA interference in glucose oxidation.

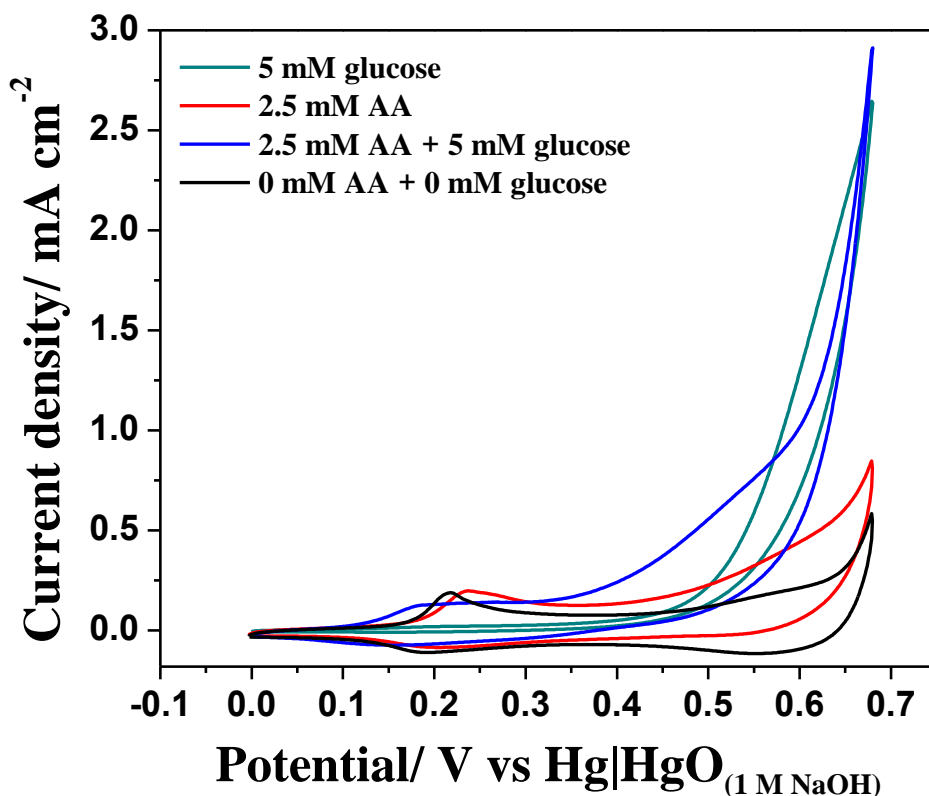


Figure 17: Cyclic voltammograms obtained with 5.0 mM glucose in 0.3 M NaOH at a scan rate of 0.02 V s⁻¹ in the absence and presence of 2.5 mM AA. The response obtained with 2.5 mM AA alone is also provided for comparison.

4. Conclusion

The reduced graphene oxide decorated with CoSe nano flakes were successfully synthesised using a simple hydrothermal procedure. A range of electrochemical, spectroscopic and microscopic techniques were employed to characterise this novel glucose oxidising catalyst. The ability to electro-oxidise glucose in alkaline medium was investigated using CoSe-

rGO/chit modified GCE with excellent performance. A sensitivity of $480 \mu\text{A mM}^{-1} \text{cm}^{-2}$, a linear range of 0 to 10 mM and a LOD of $2.5 \mu\text{M}$ was achieved. A high current density of $5.4 \pm 0.03 \text{ mA cm}^{-2}$ was illustrated with excellent intra-electrode and inter-electrode reproducibility. Bulk electrolysis measurements carried out on CoSe-rGO/chit modified GCE revealed that the oxidation of glucose can proceed beyond the formation of gluconolactone by confirming the formate production from $^1\text{H-NMR}$ and CO_2 by GC, showing the ability for complete oxidation of glucose to CO_2 . Finally, interference caused by AA and UA in biological samples was found to be negligible.

Reference

- [1] S. Park, H. Boo, T.D. Chung, Electrochemical non-enzymatic glucose sensors, *Anal. Chim. Acta.*, 556 (2006) 46-57.
- [2] J. Wang, H. Gao, F. Sun, C. Xu, Nanoporous PtAu alloy as an electrochemical sensor for glucose and hydrogen peroxide, *Sens. Actuator B Chem.*, 191 (2014) 612-618.
- [3] P. Si, Y. Huang, T. Wang, J. Ma, Nanomaterials for electrochemical non-enzymatic glucose biosensors, *Rsc Adv.*, 3 (2013) 3487-3502.
- [4] E. Witkowska Nery, M. Kundys, P.S. Jelen, M. Jonsson-Niedziolka, Electrochemical Glucose Sensing: Is There Still Room for Improvement?, *Anal. Chem.*, 88 (2016) 11271-11282.
- [5] S. Kerzenmacher, J. Ducreé, R. Zengerle, F. Von Stetten, Energy harvesting by implantable abiotically catalyzed glucose fuel cells, *J. Power Sources*, 182 (2008) 1-17.
- [6] D.H. Deng, K.S. Novoselov, Q. Fu, N.F. Zheng, Z.Q. Tian, X.H. Bao, Catalysis with two-dimensional materials and their heterostructures, *Nat. Nanotechnol.*, 11 (2016) 218-230.
- [7] Z.W. Seh, J. Kibsgaard, C.F. Dickens, I. Chorkendorff, J.K. Nørskov, T.F. Jaramillo, Combining theory and experiment in electrocatalysis: Insights into materials design, *Science*, 355 (2017) eaad4998.

- [8] Y.R. Zheng, M.R. Gao, Q. Gao, H.H. Li, J. Xu, Z.Y. Wu, S.H. Yu, An efficient CeO₂/CoSe₂ nanobelt composite for electrochemical water oxidation, *Small*, 11 (2015) 182-188.
- [9] M.-R. Gao, Y.-F. Xu, J. Jiang, Y.-R. Zheng, S.-H. Yu, Water oxidation electrocatalyzed by an efficient Mn₃O₄/CoSe₂ nanocomposite, *J. Am. Chem. Soc.*, 134 (2012) 2930-2933.
- [10] Y. Hou, M.R. Lohe, J. Zhang, S. Liu, X. Zhuang, X. Feng, Vertically oriented cobalt selenide/NiFe layered-double-hydroxide nanosheets supported on exfoliated graphene foil: an efficient 3D electrode for overall water splitting, *Energy Environ. Sci.*, 9 (2016) 478-483.
- [11] T. Liu, Q. Liu, A.M. Asiri, Y. Luo, X. Sun, An amorphous CoSe film behaves as an active and stable full water-splitting electrocatalyst under strongly alkaline conditions, *Chem. Commun.*, 51 (2015) 16683-16686.
- [12] Y. Liu, H. Cheng, M. Lyu, S. Fan, Q. Liu, W. Zhang, Y. Zhi, C. Wang, C. Xiao, S. Wei, Low overpotential in vacancy-rich ultrathin CoSe₂ nanosheets for water oxidation, *J. Am. Chem. Soc.*, 136 (2014) 15670-15675.
- [13] L. Burke, Premonolayer oxidation and its role in electrocatalysis, *Electrochim. Acta.*, 39 (1994) 1841-1848.
- [14] Y. Liu, S.-F. Zhao, S.-X. Guo, A.M. Bond, J. Zhang, G. Zhu, C.L. Hill, Y.V. Geletii, Electrooxidation of Ethanol and Methanol Using the Molecular Catalyst [$\{\text{Ru}_4\text{O}_4(\text{OH})_2(\text{H}_2\text{O})_4\}(\gamma\text{-SiW}_{10}\text{O}_{36})_2\}]^{10-}$, *J. Am. Chem. Soc.*, 138 (2016) 2617-2628.
- [15] V.R. Stamenkovic, B.S. Mun, M. Arenz, K.J. Mayrhofer, C.A. Lucas, G. Wang, P.N. Ross, N.M. Markovic, Trends in electrocatalysis on extended and nanoscale Pt-bimetallic alloy surfaces, *Nat. Mater.*, 6 (2007) 241-247.
- [16] W.S. Hummers Jr, R.E. Offeman, Preparation of graphitic oxide, *J. Am. Chem. Soc.*, 80 (1958) 1339-1339.

- [17] C.-C. Liu, J.-M. Song, J.-F. Zhao, H.-J. Li, H.-S. Qian, H.-L. Niu, C.-J. Mao, S.-Y. Zhang, Y.-H. Shen, Facile synthesis of tremelliform Co_{0.85}Se nanosheets: An efficient catalyst for the decomposition of hydrazine hydrate, *Appl. Catal. B*, 119 (2012) 139-145.
- [18] Z. Zhang, S. Pang, H. Xu, Z. Yang, X. Zhang, Z. Liu, X. Wang, X. Zhou, S. Dong, X. Chen, Electrodeposition of nanostructured cobalt selenide films towards high performance counter electrodes in dye-sensitized solar cells, *RSC Adv.*, 3 (2013) 16528-16533.
- [19] K. Chang, W. Chen, In situ synthesis of MoS₂/graphene nanosheet composites with extraordinarily high electrochemical performance for lithium ion batteries, *Chem. Commun.*, 47 (2011) 4252-4254.
- [20] T. Kavitha, A.I. Gopalan, K.-P. Lee, S.-Y. Park, Glucose sensing, photocatalytic and antibacterial properties of graphene–ZnO nanoparticle hybrids, *Carbon*, 50 (2012) 2994-3000.
- [21] W. He, H. Jiang, Y. Zhou, S. Yang, X. Xue, Z. Zou, X. Zhang, D.L. Akins, H. Yang, An efficient reduction route for the production of Pd–Pt nanoparticles anchored on graphene nanosheets for use as durable oxygen reduction electrocatalysts, *Carbon*, 50 (2012) 265-274.
- [22] J. Li, C.-y. Liu, Y. Liu, Au/graphene hydrogel: synthesis, characterization and its use for catalytic reduction of 4-nitrophenol, *J. Mater. Chem.*, 22 (2012) 8426-8430.
- [23] S.-X. Guo, Y. Liu, A.M. Bond, J. Zhang, P.E. Karthik, I. Maheshwaran, S.S. Kumar, K. Phani, Facile electrochemical co-deposition of a graphene–cobalt nanocomposite for highly efficient water oxidation in alkaline media: direct detection of underlying electron transfer reactions under catalytic turnover conditions, *Phys. Chem. Chem. Phys.*, 16 (2014) 19035-19045.
- [24] L. Wang, Y. Zheng, X. Lu, Z. Li, L. Sun, Y. Song, Dendritic copper-cobalt nanostructures/reduced graphene oxide-chitosan modified glassy carbon electrode for glucose sensing, *Sens. Actuator B Chem.*, 195 (2014) 1-7.

- [25] Y. Ding, Y. Wang, L. Su, M. Bellagamba, H. Zhang, Y. Lei, Electrospun Co₃O₄ nanofibers for sensitive and selective glucose detection, *Biosens. Bioelectron.*, 26 (2010) 542-548.
- [26] F.v. Stetten, S. Kerzenmacher, A. Lorenz, V. Chokkalingam, N. Miyakawa, R. Zengerle, J. Ducle'e, A one-compartment, direct glucose fuel cell for powering long-term medical implants, 19th IEEE international conference on micro electro mechanical systems, IEEE, 2006, pp. 934-937.
- [27] M.C.D. Cooray, Y. Liu, S.J. Langford, A.M. Bond, J. Zhang, One pot synthesis of poly(5-hydroxyl-1,4-naphthoquinone) stabilized gold nanoparticles using the monomer as the reducing agent for nonenzymatic electrochemical detection of glucose, *Anal. Chim. Acta*, 856 (2015) 27-34.
- [28] S.T. Farrell, C.B. Breslin, Oxidation and photo-induced oxidation of glucose at a polyaniline film modified by copper particles, *Electrochim. Acta*, 49 (2004) 4497-4503.
- [29] M.Z. Luo, R.P. Baldwin, Characterization of carbohydrate oxidation at copper electrodes, *J. Electroanal. Chem.*, 387 (1995) 87-94.
- [30] J.M. Marioli, T. Kuwana, Electrochemical characterization of carbohydrate oxidation at copper electrodes, *Electrochim. Acta*, 37 (1992) 1187-1197.
- [31] M. Tominaga, T. Shimazoe, M. Nagashima, H. Kusuda, A. Kubo, Y. Kuwahara, I. Taniguchi, Electrocatalytic oxidation of glucose at gold–silver alloy, silver and gold nanoparticles in an alkaline solution, *J. Electroanal. Chem.*, 590 (2006) 37-46.
- [32] S.K. Chaudhuri, D.R. Lovley, Electricity generation by direct oxidation of glucose in mediatorless microbial fuel cells, *Nat. Biotechnol.*, 21 (2003) 1229-1232.
- [33] D. MacDougall, W.B. Crummett, Guidelines for data acquisition and data quality evaluation in environmental chemistry, *Anal. Chem.*, 52 (1980) 2242-2249.

- [34] C.-W. Kung, C.-Y. Lin, Y.-H. Lai, R. Vittal, K.-C. Ho, Cobalt oxide acicular nanorods with high sensitivity for the non-enzymatic detection of glucose, *Biosens. Bioelectron.*, 27 (2011) 125-131.
- [35] K.K. Lee, P.Y. Loh, C.H. Sow, W.S. Chin, CoOOH nanosheets on cobalt substrate as a non-enzymatic glucose sensor, *Electrochem. Commun.*, 20 (2012) 128-132.
- [36] S.-J. Li, J.-M. Du, J. Chen, N.-N. Mao, M.-J. Zhang, H. Pang, Electrodeposition of cobalt oxide nanoparticles on reduced graphene oxide: a two-dimensional hybrid for enzyme-free glucose sensing, *J. Solid State Electrochem.*, 18 (2014) 1049-1056.
- [37] X.-C. Dong, H. Xu, X.-W. Wang, Y.-X. Huang, M.B. Chan-Park, H. Zhang, L.-H. Wang, W. Huang, P. Chen, 3D graphene-cobalt oxide electrode for high-performance supercapacitor and enzymeless glucose detection, *ACS nano*, 6 (2012) 3206-3213.
- [38] J. Yang, S. Gunasekaran, A low-potential, H₂O₂-assisted electrodeposition of cobalt oxide/hydroxide nanostructures onto vertically-aligned multi-walled carbon nanotube arrays for glucose sensing, *Electrochim. Acta*, 56 (2011) 5538-5544.
- [39] M. Mahmoudian, W. Basirun, P.M. Woi, M. Sookhajian, R. Yousefi, H. Ghadimi, Y. Alias, Synthesis and characterization of Co₃O₄ ultra-nanosheets and Co₃O₄ ultra-nanosheet-Ni(OH)₂ as non-enzymatic electrochemical sensors for glucose detection, *Mater. Sci. Eng. C*, 59 (2016) 500-508.

Chapter 6

Future Perspectives

6.1. Use of Conducting Polymer Nanocomposite for Three Dimensional Enzyme Electrode

6.1.1. Introduction

In the year 2000 Hideki Shirakawa (along with Alan Heeger and Alan MacDiarmid) was honoured with the Nobel Prize for his groundbreaking discovery of the properties of polyacetylene (PA) doped with iodine [1]. This non-metallic material displayed high electrical conductivity and other metallic properties which triggered the discovery, development and application of novel materials in the conducting polymer (CP) field [2, 3]. As a result, various modified CPs were developed to resist oxidative degradation, to provide a distinct advantage over PA. More versatile CPs were developed using polyanilines [4], polypyrroles [5], polythiophenes [6], and poly(p-phenylene vinylenes) [7]. Polyanilines surpass other CPs via their capability of producing high conductivity, cost-effectively in bulk amounts. However, the toxic benzidine products produced upon degradation have limited the applicability of these CPs [6].

Another interesting CP developed at the Bayer AG Research Laboratories is a polythiophene derivative, poly(3,4-ethylenedioxythiophene) abbreviated as PEDT or PEDOT. PEDOT displays properties such as insolubility in water, transparency, oxidised films and very high stability in the oxidised state. Its insolubility was overcome by doping with poly(styrene sulfonic acid) during polymerisation, which resulted in PEDOT/PSS. This hybrid generated good film properties, high conductivity, high visible light transmissivity and excellent stability making it widely recognised as one of the best CPs in the world [6].

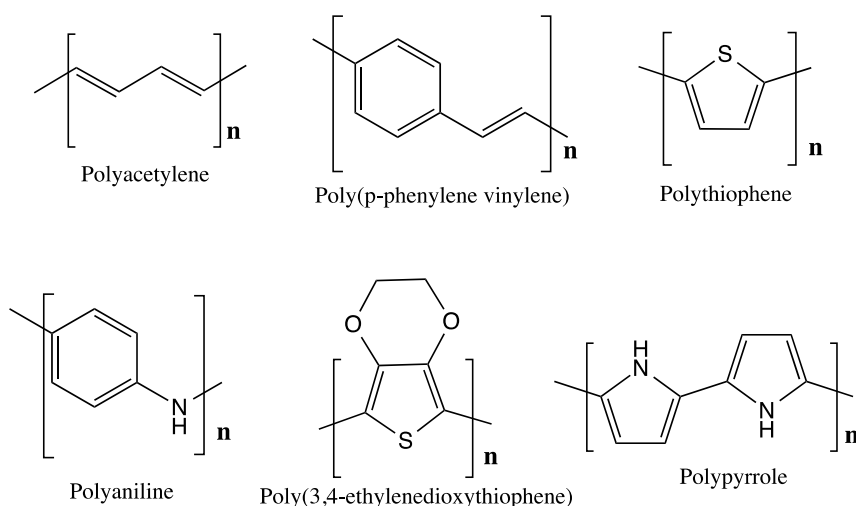


Figure 1: Different types of conducting polymers

PEDOT has also found application in the fabrication of enzymatic electrodes [8-10]. Covalent functionalisation of the conducting polymer to ensure biocompatibility could be achieved by subsequent polymerisation of thiophene functionalised monomers [11]. However, designing a single compound having the functional groups needed to tune the properties of the material, is quite challenging. Consequently, the concept of using composites for electrode fabrication was introduced [12] with the nanostructured architecture allowing the physical properties of electrodes to be altered. This concept has been most widely adopted in the area of glucose sensing [13-15]. Carbon nanotubes, inorganic nanoparticles, graphene, ternary systems and special dopants have been used with conducting polymers to develop composites in amperometric sensing [12]. Metallic nanoparticles stabilised with different polymers offer significant advantages for enhancing the performance of such sensors.

As mentioned above, the polymer may influence the properties of nanomaterials due to the presence of functional groups [16]. Thus, polymer architecture can be tuned to give properties desired by incorporating the functional groups onto one well-organised matrix [17]. In this study, a new thiophene monomer was synthesised to fabricate an enzyme electrode for use in glucose sensing.

6.1.2. Experimental

6.1.2.1. Chemicals

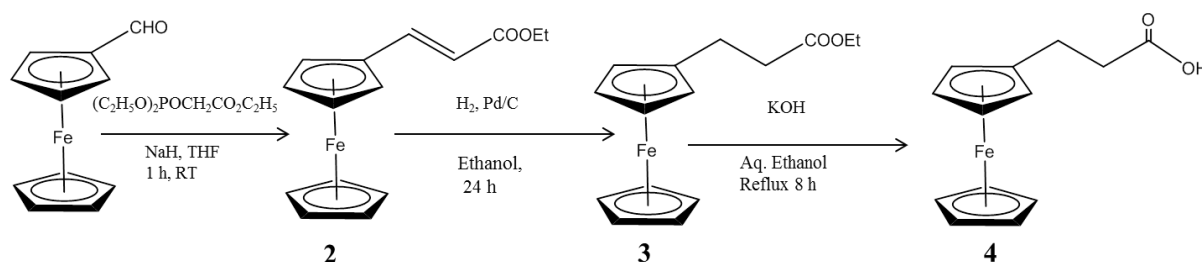
Sodium hydride (NaH, 60 % dispersion in mineral oil), sodium bicarbonate (NaHCO₃, 99.7%), triethyl phosphonoacetate (C₈H₁₇O₅P, 98%), ferrocene carboxaldehyde (C₁₁H₁₀FeO, 98%), ammonium chloride (NH₄Cl, 99.7%), magnesium sulfate (MgSO₄, 99.5%), palladium on charcoal (Pd/C, 10 wt. % loading), potassium hydroxide (KOH, 85%), potassium iodide (KI, 99.5%), sodium hydroxide (NaOH, 98%), boric acid (H₃BO₃, 99.5%), p-toluenesulfonic acid monohydrate (CH₃C₆H₄SO₃H·H₂O, 98%), 2-[2-(2-chloroethoxy)-ethoxy]ethanol [EG, Cl(CH₂CH₂O)₂CH₂CH₂OH, 96%], 3,4-dihydro-2H-pyran (C₅H₈O, 97%), poly(sodium 4-styrenesulfonate) (PSS, (C₈H₇NaO₃S)_n, average M_w ~1,000,000, powder), lithium tetrafluoroborate (LiBF₄, 98%), triethylamine (Et₃N, 99%), *N,N'*-dicyclohexylcarbodiimide (DCC, C₆H₁₁N=C=NC₆H₁₁, 99%), 4-dimethylaminopyridine (C₇H₁₀N₂, 99%), tetrahydrofuran (THF) Celite, hydroxymethyl EDOT (EDOT-OH, C₇H₈O₃S, 95%) were purchased from Sigma Aldrich. Hydrochloric acid (HCl, 36.5%) were purchased from Thermo Fisher Scientific Australia. *n*-Hexane, methanol (MeOH), ethanol (EtOH), *N,N*-dimethylformamide (DMF) were purchased from Merck Pty Ltd. Dichloromethane (DCM), ethyl acetate (EA), diethyl ether ((C₂H₅)₂O) were purchased from Chem Supply Pty Ltd. All materials and solvents were used without further purification.

TLC was performed on Silica gel 60 F254 TLC aluminium sheets. ¹H-NMR and ¹³C-NMR spectra were recorded on a Bruker DRX400 spectrometer at a frequency of 400 MHz for ¹H and 75 MHz for ¹³C. Abbreviations used are: s (singlet), d (doublet), t (triplet), q (quadruplet), m (multiplet) and br (broad). Mass spectra were recorded using high-resolution electrospray

ionisation mass spectrometry by Agilent 6220 Accurate Mass LC-TOF system with Agilent 1200 Series HPLC, usually in the positive ion mode.

6.1.2.2. Synthesis of ferrocene propionic acid

This compound was synthesised according to a literature reported procedure and analysis was in agreement with literature [18].



Scheme 1: Synthesis of ferrocene propionic acid

Ethyl ferrocenylacrylate (2)

Sodium hydride (0.232 g, 9.6 mmol) was dissolved in dry THF (10 mL). The mixture was stirred at 0°C and triethyl phosphonoacetate was added (1.10 mL) to the mixture to give a white foam under N_2 . This mixture was allowed to warm to room temperature for 1 h. Again it was cooled in an ice bath and ferrocene carboxaldehyde **1** (1.1 g, 4.6 mmol) was added as a solution in THF (10 mL). After 20 min, the mixture was allowed to warm to RT and stirred for 1 h. A saturated aqueous ammonium chloride solution (50 mL) was added to the mixture. Diethyl ether was then added and the combined layers were washed with deionised water and dried with $MgSO_4$. The solvent was removed under reduced pressure followed by purification by column chromatography (flash silica, DCM) to yield (**2**) (1.36 g, 4.7 mmol, 94%) as a dark orange solution. 1H NMR (300 MHz, $CDCl_3$) 7.56 (d, 1H, CH), 6.03 (d, 1H, CH), 4.48 (m, 2H, HFc), 4.40 (m, 2H, HFc), 4.22 (q, 2H, CH_2), 4.15 (s, 5H, HFc), 1.32 (t, 3H, CH_3). ESIMS: m/z =284.1011

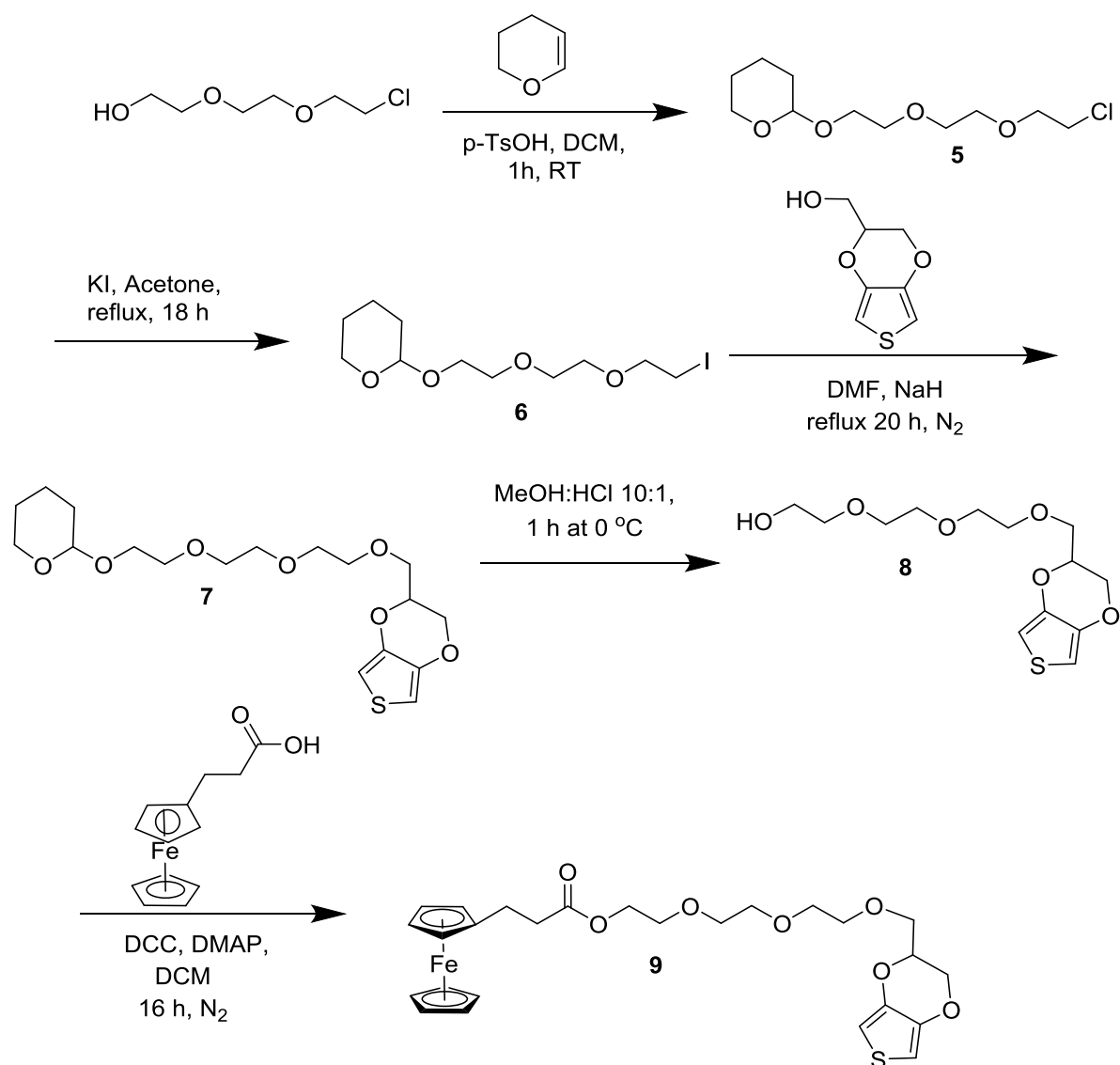
Ferrocenepropionic acid (**4**)

A solution of ethyl ferrocenylacrylate (**2**) (1.36 g, 4.7 mmol) and Pd/C (0.250 g, 2.5 mmol) in ethanol (70 mL) was degassed with N₂. Then the reaction mixture was stirred vigorously under H₂ for 24 hours at room temperature. The reaction mixture was filtered through celite and the solvent removed under reduced pressure. Purification was done using column chromatography (DCM) to afford a yellow syrup corresponding to ethyl 3-ferrocenylpropanoate **3** (1.15 g, 86%).

ESIMS: $m/z = 286.0651$

A solution of potassium hydroxide (1.96 g, 35 mmol) in deionised water (5 mL) was added to a solution of ethyl-3-ferrocenylpropanoate **3** (1.0 g, 3.5 mmol) in ethanol (30 mL) under N₂ while stirring. The solution was then refluxed for 6 h under N₂. The reaction mixture was concentrated under vacuum, diluted with deionised water and washed with diethyl ether. The aqueous phase was acidified with 1 M HCl and extracted with diethyl ether. The diethyl ether layers were combined, dried over MgSO₄ and concentrated under vacuum to obtain ferrocenepropionic acid **4** as yellow crystals (0.44g, 48%). ¹H NMR (400 MHz, D₂-DCM): 11.03 (s br, 1H), 4.18 – 4.11 (m, 9H, HFc), 2.7 – 2.6 (m, 4H, CH₂), ESIMS: $m/z = 258.0335$.

6.1.2.3. Synthesis of 2-(2-(2-((2,3-dihydrothieno[3,4-b][1,4]dioxin-2-yl)methoxy)ethoxy)ethoxy)ethyl-3-ferrocenepropanoate



Scheme 2: Synthesis pathway of monomer (Fc-EG-EDOT)

2-2-(2-Chloroethoxy)ethoxy/tetrahydropyranyl-ethanol (5)

p-Toluenesulfonic acid (50 mg, 0.29 mmol) was added to a stirred ice cold solution of 2-[2-(2-chloroethoxy)-ethoxy]ethanol (2.0 g, 11.86 mmol) and dihydropyran (1.6 mL, 17.79 mmol) in dry DCM (20 mL). The reaction mixture was allowed to warm to room temperature and further stirred for 1 h before being neutralised with Et_3N , concentrated, and the crude product purified

by flash chromatography (n-hexane/EtOAc, 4:1). The title compound was afforded (2.2 g, 75%) as a colorless syrup; $R_f = 0.3$ (4:1 hexane/EtOAc); $^1\text{H NMR}$ (400 MHz, CDCl_3): δ 4.6 (m, 1H, OCHO), 3.87-3.74 (m, 6H, CH_2Cl , 2OCH_2), 3.69-3.62 (m, 6H, 3OCH_2) 3.61-3.60 (m, 2H, ring- OCH_2), 1.71-1.49 (m, 6H, 3CH_2); ESIMS: $m/z = 275.1019$ $[\text{M}+\text{Na}]^+$ observed for $\text{C}_{11}\text{H}_{21}\text{O}_4\text{Cl}$ (252.11). This compound was synthesised according to a literature reported procedure and analysis is in agreement with literature [19].

2-(2-(2-(2-iodoethoxy)ethoxy)ethoxy)tetrahydro-2H-pyran (6)

A suspension of potassium iodide (1.5 g, 9.0 mmol) and 2-[2-(2-chloroethoxy)-ethoxy]tetrahydropyranylethanol (2.2 g, 8.7 mmol) in acetone (25 mL) was refluxed for 18 h. The mixture was allowed to cool down to room temperature. The solid residue was filtered off and filtrate concentrated under reduced pressure. The resultant compound was taken to the next step without any further purification.

2-((2-(2-((tetrahydro-2H-pyran-2-yl)oxy)ethoxy)ethoxy)ethoxy)methyl)-2,3-dihydrothieno[3,4-*b*][1,4]dioxine (7)

A solution of hydroxymethyl EDOT (1 g, 5.8 mmol) and NaH (400 mg, 16.6 mmol) in dry DMF (20 mL) was added to a solution of 2-(2-(2-(2-iodoethoxy)ethoxy)ethoxy)tetrahydro-2H-pyran (2.2 g, 6.39 mmol) in dry DMF (10 mL) under N_2 and was heated to 120 °C overnight. The reaction mixture was neutralised by adding deionised water and then extracted with ethyl acetate, washed thrice with deionised water and dried with MgSO_4 . Finally, the solvent was removed under reduced pressure. Flash chromatography (hexane: ethyl acetate, 1:1) was carried out to separate the compound of interest giving **7** as a colorless syrup (0.5 g, 23%). $^1\text{H NMR}$ (D_6 -DMSO): δ 6.5 (m, 2H, CHS), 4.58 (m, 1H, OCHO), 4.32- 4.24 (m, 3H, OCH), 4.07-3.96 (m, 2H, OCH_2 , EDOT), 3.75-3.3 (m, 16H, OCH_2), 1.49-1.44 (m, 6H, ring- CH_2), $^{13}\text{C NMR}$ (jmod,

D₆-DMSO): 141.3, 99.6, 99.5, 98.0, 72.4, 70.3, 69.8, 69.7, 68.8, 66.0, 65.4, 61.2, 59.7, 30.1, 24.9, 20.7, 19.0, 14.0, ESIMS: $m/z = 411.1449$ [M+Na]⁺ observed for C₁₈H₂₈O₇S (388.47).

2-(2-(2-((2,3-dihydrothieno[3,4-*b*][1,4]dioxin-2-yl)methoxy)ethoxy)ethoxy)ethan-1-ol (8)

Compound **7** (51 mg, 0.14 mmol) in MeOH (0.5 mL) was treated with HCl (10% HCl in MeOH, 0.25 mL) and stirred for 1 hour at 0 °C. Then, a saturated NaHCO₃ solution was used to quench the acid and mixture was concentrated under reduced pressure[19]. Flash chromatography was carried out to purify (1% MeOH in DCM) giving the deprotected product **8** as a colourless syrup (32.7 mg, 0.107 mmol, 77%). ¹H NMR: δ 6.37 (m, 2H, CHS), 5.37 (m, 1H, OH), 4.38-4.27 (m, 1H, CH), 4.11-4.07 (m, 2H, CH₂), 3.79-3.5 (m, 14H, OCH₂), ¹³C NMR (CD₂Cl₂): 142.1, 99.8, 74.0, 73.1, 72.8, 71.9, 71.5, 71.0, 70.8, 70.6, 69.9, 66.5, 62.0, ESIMS= 327.0871 [M+Na]⁺ observed for C₁₃H₂₀O₆S (304.1)

2-(2-(2-((2,3-dihydrothieno[3,4-*b*][1,4]dioxin-2-yl)methoxy)ethoxy)ethoxy)ethyl-3-ferrocenepropanoate (EDOT-EG-Fc)(9)

A mixture of compound **8** (30 mg, 0.1 mmol), compound **4** (26 mg, 0.1 mmol), *N,N'*-dicyclohexylcarbodiimide (DCC) (25 mg, 0.12 mmol) and 4-dimethylaminopyridine (DMAP) (1.2 mg, 0.01 mmol) in dry DCM (20 mL) was stirred at room temperature for 16 h under N₂. The reaction mixture was filtered to remove solid precipitate and the filtrate was collected and evaporated under reduced pressure[20]. The residue was purified using flash chromatography (hexane: ethyl acetate, 3:2) to obtain compound **9** (47 mg, 86%) as a yellow coloured syrup. ¹H NMR: δ 7.28 (s, 9H, HFc), 6.34 (s, 2H, CHS), 4.33-3.68 (m, 12H, OCH₂), 2.5-0.5 (br, analysis is complex) ¹³C NMR (CDCl₃): 173.3, 142.1, 142.0, 99.8, 88.0, 73.1, 71.5, 70.9, 70.8, 69.9, 69.5, 69.0, 68.4, 67.8, 66.5, 63.9, 35.8, 30.0, 25.0, ESIMS: $m/z = 567.1114$ [M+Na]⁺ observed for C₂₆H₃₂O₇SFe (544.12).

6.1.2.4. Synthesis of EDOT-EG-Fc capped gold nanoparticle

Gold nanoparticles (AuNPs) were synthesised using a mixture of monomers of EDOT-EG-Fc (3.1 mg, 5.8 μmol), hydroxymethyl EDOT (EDOT-OH) (1 mg, 5.8 μmol) and poly(sodium 4-styrenesulfonate) (PSS) (1 mg, 4.8 μmol). To prepare Au NPs, 10.0 μl of 0.2 M $\text{HAuCl}_4 \cdot 3\text{H}_2\text{O}$ (2 μmol) was mixed with 1950 μL of deionised water and PSS was dissolved in the gold(III) solution. The mixture was then stirred using a magnetic stirrer. EDOT-EG-Fc and EDOT-OH were dissolved in 50.00 μL acetonitrile to make a homogeneous solution. Upon addition of this organic solution, the gold(III) solution turns bright purple color indicating the formation of the Au NPs. This solution mixture was stirred for 30 min allowing the reaction to complete. Au NPs formed were then isolated using centrifugation at 6000 rpm (Eppendorf, mini spin plus) for 20 min. Finally, NPs were re-dissolved in 1.5 mL deionised water and isolated using centrifugation to remove any impurities. The separated Au NPs were dispersed in 0.1 mL deionised water and was stored in a refrigerator to be used in further studies.

6.1.2.5. Electropolymerisation and electrochemical measurements

Electrochemical polymerisation was carried out with EDOT-EG-Fc/ EDOT-OH at 21 ± 2 °C using a CH Instrument 760E electrochemical workstation with a conventional three-electrode cell in acetonitrile medium, utilising LiBF_4 as the supporting electrolyte. Other voltammetric measurements in aqueous media were carried out in phosphate buffered saline (PBS 0.1 M, pH 7). The glassy carbon electrode (GCE, 3mm diameter, CH Instruments Inc, Texas, USA) and gold disc electrode (AuE, 1.6 mm diameter, CH Instruments Inc, Texas, USA) were employed as working electrodes (WE), platinum wire (in organic medium) and $\text{Ag}|\text{AgCl}(\text{1 M KCl})$ (in aqueous medium) were employed as reference electrode and Pt wire as the auxiliary electrode. Initially, the GC and Au electrodes were polished with 0.3 μm alumina slurry followed by

rinsing with deionised water, sonication and rinsing again with deionised water before finally drying under a nitrogen gas prior to electrochemical measurements.

6.1.2.6. Microscopic characterisation Au-EDOT-FcNPs

Scanning Electron Microscopy (SEM) measurements using a FEI Nova NanoSEM 450 FEG SEM instrument were undertaken to determine the surface morphology and the size of Au-EDOT-FcNPs.

6.1.3. Results and Discussion

6.1.3.1. EDOT-EG-Fc monomer

Three precursors were combined covalently to form the compound EDOT-EG-Fc. EDOT is a well-known thiophene which gives rise to the polymer backbone when polymerised. Due to the conjugated structure of polythiophene, electron transition takes place along the polymer backbone [21]. Ethylene glycol (EG) acts as the spacer between the polymer backbone and the Fc mediator. The length of the spacer plays a critical role in communication between the enzyme and the electrode [22]. Schuhmann *et al.* reported that the spacer length should be long enough (> 10 bonds) for the mediator to approach the enzyme redox centre [23]. Taking this into account, the new monomer contains 15 bond chains. Ferrocene acts as the redox mediator [11] and was covalently attached to the spacer via the EG to prevent leakage. The intention is that the EDOT-EG-Fc polymeric redox system will act as an “electrical wire” facilitating the electron transfer between the enzyme and the electrode [24]. The compound is predicted to be relatively water soluble, as it contains water soluble moieties such as EDOT and EG. However, the final compound showed water solubility of ~ 0.1 mM. However, in organic solutions the solubility was high.

6.1.3.2. Electrochemical co-polymerisation

Cyclic voltammetry was employed to electrochemically induce polymerisation of the EDOT-EG-Fc monomer. This is an *in situ* polymerisation method, which forms a film on the electrode surface while avoiding the difficulties of polymer purification [25]. To optimise the electrochemical polymerisation a variety of conditions were studied. Direct electrochemical polymerisation of EDOT-EG-Fc was not successful. This could be due to steric constraints of the bulky (pendant) mediating group, or complexation of the redox active groups in the polymerisation process. Therefore, EDOT-OH was introduced in order to reduce the steric constraints and to form a co-polymer containing both thiophene units, but lowering the concentration of the Fc mediator. This technique is an efficient approach to obtain polymers having the combined properties of the individual homopolymers [26]. Electrochemical polymerisation of EDOT-EG-Fc monomer (2mM) and EDOT-OH (5mM) was carried out in acetonitrile medium containing 0.1 M LiBF₄ as the electrolyte on a bare GCE by cycling the potential between -0.2 V to +1.2 V vs Pt_(wire). The cyclic voltammogram (CV) associated with electrochemical polymerisation (Figure 2(a)) contains a reversible process at 0.1 V vs Pt_(wire) due to Fc/Fc⁺ redox process followed by irreversible oxidation of the electrochemically polymerised PEDOT. The gradual increase of capacitance implies the successful electrochemical polymerisation of the monomers. Electrochemical characterisation of the electropolymerised polymer film on GCE was carried out in 0.1 M PBS pH 7 medium at a scan rate of 0.1 V s⁻¹. The cyclic voltammogram (Figure 2(b)) illustrates high capacitance and the presence of surface confined Fc/Fc⁺ redox process around 0.32 V vs Ag|AgCl_(1 M KCl).

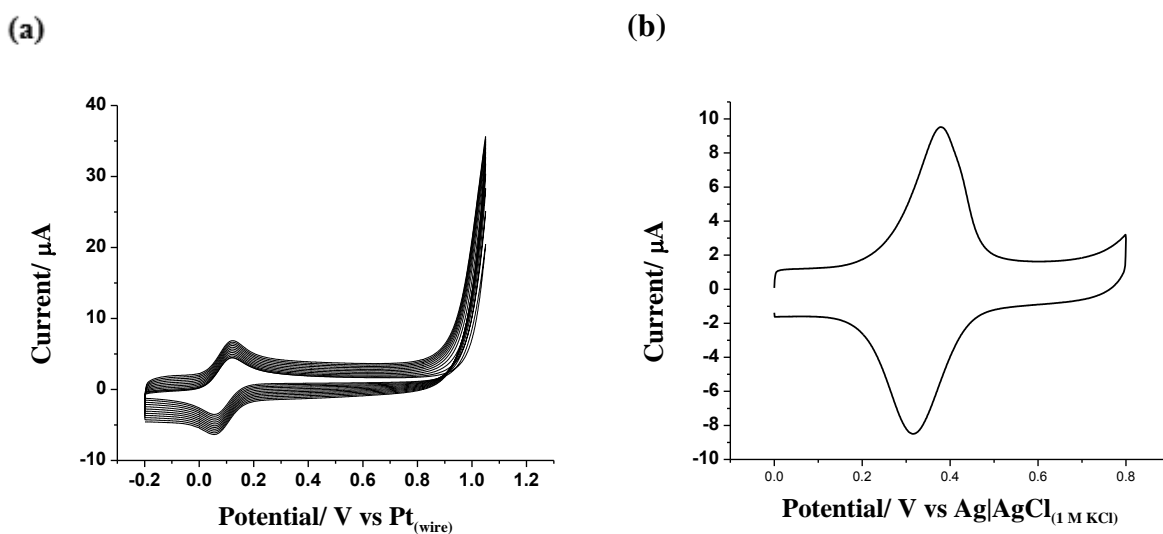


Figure 2: (a) Electrochemical polymerisation of EDOT-EG-Fc (2mM), EDOT-OH (5mM) in MeCN medium at a scan rate of 0.1 V s^{-1} and (b) Electrochemical characterisation of the electropolymerised polymer film on GCE in an aqueous PBS (0.1 M, pH 7) medium at a scan rate of 0.1 V s^{-1}

The film thickness can be controlled by changing the number of cycles (3, 5, 6 cycles) used for electropolymerisation. Experiments were carried out by modifying electrodes with use of a different number of cycles for electropolymerisation followed by enzyme modification through adsorption. Cyclic voltammograms were obtained with these modified electrodes, in the presence and absence of 10 mM glucose at a scan rate on 0.05 V s^{-1} in 0.1 M PBS pH 7. Results revealed no significant increase in electrocatalytic current from glucose oxidation (results not shown). Therefore, number of cycles was selected to be 3 for the remaining experiments, as a higher number of cycles produce a polymer composite that is too rigid. The newly formed electrochemically polymerised electrode was used to immobilise GOx via adsorption using electrostatic interactions of positively charged PEDOT polymer backbone[27] and negatively charged enzyme[28]. Since the isoelectric point of native GOx in water is 4.05[29], the enzyme is negatively charged at neutral pH. Electrostatic adsorption was carried out by dipping the modified GCE in a GOx solution (10 mg/ mL in pH7 PBS)[30] for time durations of 15 min,

30 min, 1 h and overnight prior to electrochemical measurements. The electrode was gently washed using deionised water to remove any unbound enzyme. However, their electrochemical measurements revealed the absence of electrocatalytic oxidation process of glucose in 0.1 M PBS pH 7 via mediated electron transfer instead, showing a decrease in the Fc/Fc⁺ process with increasing glucose concentration as illustrated in Figure 3. This could be a result of surface blocking by glucose as the current can be restored close to its initial value by rinsing the electrode with deionised water and carrying out cyclic voltammetry in PBS pH 7 solution in the absence of glucose.

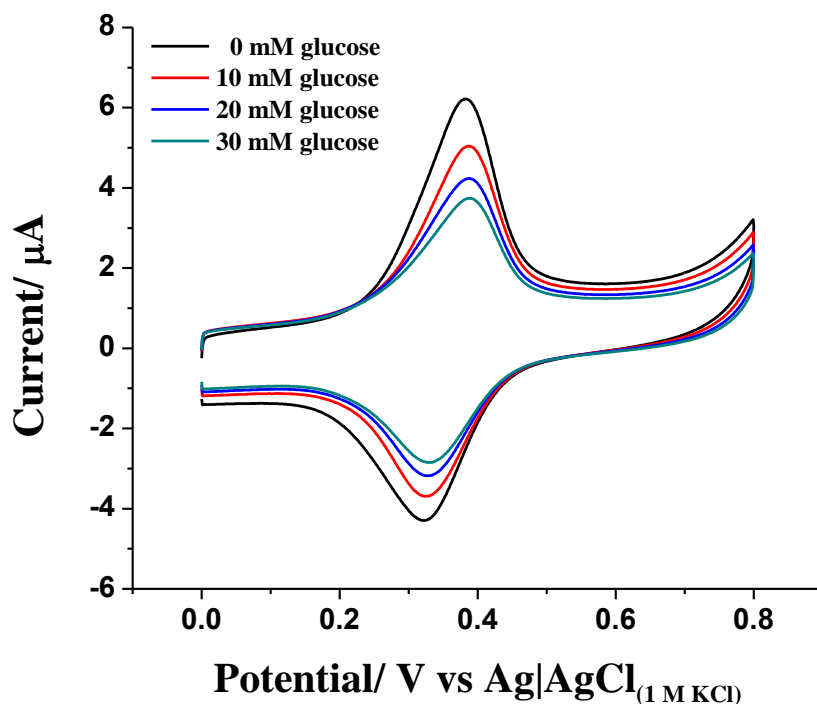


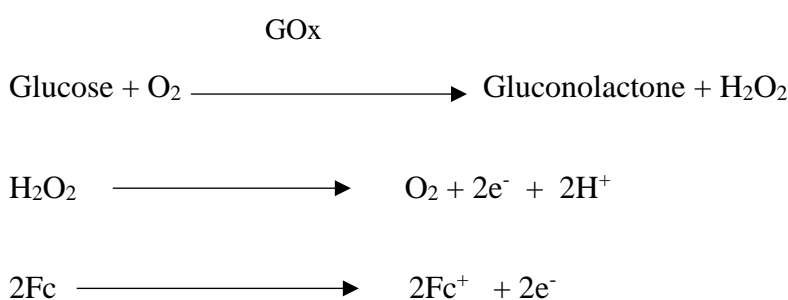
Figure 3: Cyclic voltammograms obtained as a function of glucose concentrations (0.1 M PBS) at a scan rate of 0.05 V s⁻¹ over the potential range of 0 to 0.8 V using an enzyme immobilised electropolymerised EDOT-EG-Fc modified GC electrode.

The feasibility of electrochemical polymerisation in aqueous medium was explored using EDOT-EG-Fc (0.1 mM), EDOT-OH (1 mM) and LiClO₄ (0.1 M) as the supporting electrolyte

at a GCE. The CV revealed successful electrochemical polymerisation by the gradual increase of the capacitance. Immobilisation of GOx was carried out as before and followed with electrochemical characterisation in the absence and presence of glucose. CVs revealed no electrocatalytic oxidation of glucose. This could be due to two reasons

1. Unsuccessful immobilisation of GOx on electrode
2. A lack of communication between the enzyme and mediator (Fc) as it acts as a 2D enzymatic electrode.

In 2D enzymatic electrodes, the orientation and position of the enzyme on the electrode plays a significant role in the electrocatalytic processes. To confirm the influence of hypothesis 1, a control experiment was performed. Fc derivatives have been used as mediators in H₂O₂ detection[31]. Glucose oxidation in the presence of O₂ by GOx produces gluconolactone and H₂O₂. This H₂O₂ will be oxidised to O₂ giving 2 electrons. The Fc/ Fc⁺ will act as the mediator for mediated electron transfer [32].



As a consequence, a modified GCE was used for electrochemical polymerisation (3 cycles) of EDOT-EG-Fc and EDOT-OH to give a similar composition as in previous experiments in MeCN followed by immobilisation of enzyme. The modified electrode was then gently rinsed with water to remove any unbound enzyme followed by electrochemical characterisation in 0.1 M PBS pH 7 in the presence of O₂ and 10 mM glucose. The CV does not show any difference

between the presence and absence of glucose, implying the absence of GOx on the electrode and hence the adsorption of GOx was unsuccessful. Attempts to construct a catalytically active electrode by polymerisation of EDOT-EG-Fc and EDOT-OH in the presence of GOx were also unsuccessful. This lack of success prompted a change in direction of the study to chemical polymerisation.

Before carrying out chemical polymerisation, the feasibility of mediating electron transfer process between the monomer and enzyme during electrocatalysis was verified. A CV was obtained with a scan rate of 0.05 V s^{-1} from a solution which contains EDOT-EG-Fc (0.1 mM) and glucose (50 mM) in 0.1 M PBS pH 7 in the presence and absence of GOx under N_2 . The CVs (Figure 4) contained catalytic current in the presence of 0.05 mg/mL GOx and an increase in GOx resulted in enhanced catalytic current. This implies that mediation of the electron transfer process occurs between the Fc derived EDOT monomer and the enzyme[25].

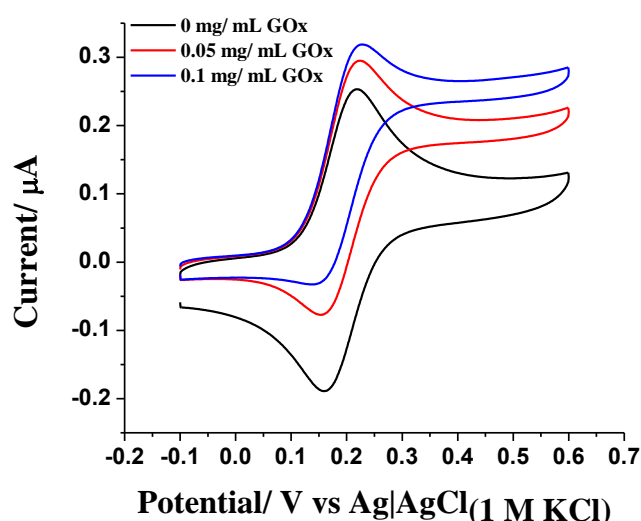


Figure 4: Cyclic voltammograms obtained in 0.1 M PBS pH 7 solution which contains EDOT-EG-Fc (0.1 mM) and glucose (50 mM) at a scan rate of 5 mV s^{-1} in the presence and absence of GOx under N_2 .

6.1.3.3. Characterisation of Au-EDOT-FcNPs

Au-EDOT-FcNPs were synthesised as previously described, which is advantageous as it enables us to employ a large amount of EDOT-EG-Fc in an aqueous medium. Furthermore, other studies have employed Fc containing nanoparticles in biosensor assemblies to improve the electron transfer properties of Fc [33]. Therefore, poly(EDOT-EG-Fc-co-EDOT-OH) was fused with gold (AuCl_4^-) solution to synthesis Au-EDOT-FcNPs for the fabrication of glucose oxidase electrodes. The reduction of AuCl_4^- to metallic AuNPs by EDOT and their stabilisation by copolymer, poly(EDOT-EG-Fc-co-EDOT-OH)/PSS simultaneously formed during the reaction, presumably introducing a coating layer for the nanoparticles.

Scanning electron microscopic (SEM) images were used to obtain the size distribution and uniformity of the Au-EDOT-FcNPs. The SEM image obtained from the Au-EDOT-FcNPs drop-cast on an indium tin oxide (ITO) glass slide (Figure 5) reveals a variety of sizes and shapes of the Au-EDOT-FcNPs. Use of a variety of compositions and conditions in an attempt to obtain uniform nanoparticles were unsuccessful.

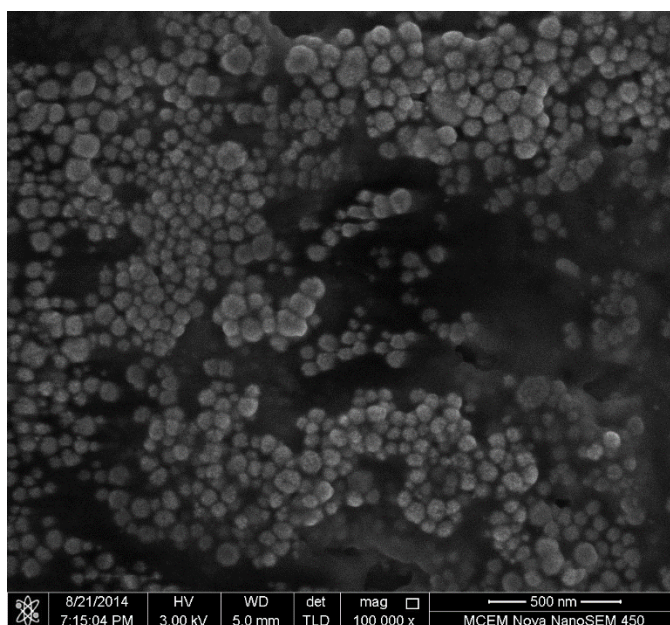


Figure 5: Scanning electron micrograph of Au-EDOT-FcNPs synthesised in this study.

6.1.3.4. Electrochemical characterisation

Synthesised Au-EDOT-FcNPs were drop cast (3 μL) on a polished GCE. This modified electrode was characterised in 0.1 M PBS pH 7 using $\text{Ag}|\text{AgCl}_{(1\text{ M KCl})}$ as the reference electrode and Pt wire as the auxiliary electrode. The CV used for electrochemical characterisation illustrates a reversible process at the potential of 0.29 V associated with oxidation and reduction of the ferrocene moiety (Figure 6), verifying that Fc has not lost its activity during chemical polymerisation. Thus, Au-EDOT-FcNPs were used in experiments on the use of mediator and glucose oxidase base electrocatalytic glucose oxidation.

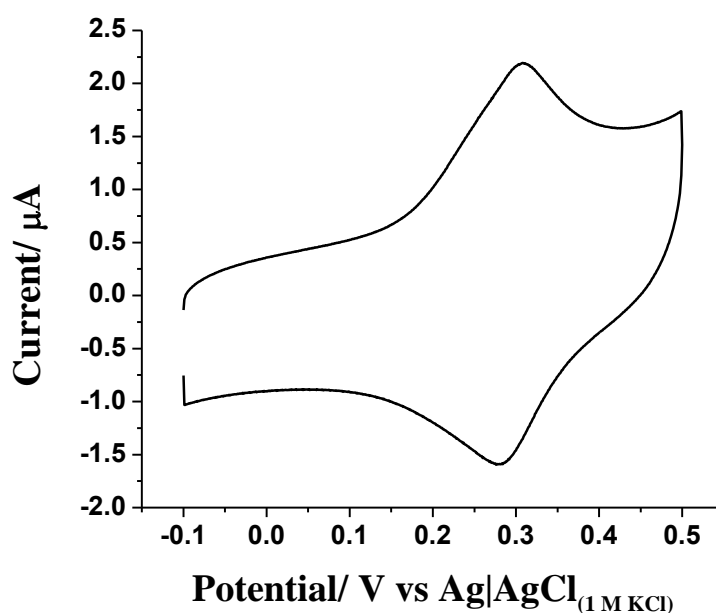


Figure 6: Cyclic voltammogram obtained from chemically synthesised Au-EDOT-FcNPs drop cast on a GCE at 0.1 V s^{-1} in PBS pH 7 buffer medium.

6.1.3.5. Electrocatalytic oxidation of glucose

In this study, GOx was utilised as the enzyme catalyst together with Au-EDOT-FcNPs. Immobilisation of the enzyme was carried out via adsorption (electrostatic interactions). Adsorption alone would not be sufficient to confine the enzyme on the GCE surface, as the

electrostatic interactions are too weak. Therefore, a third component, chitosan was introduced to the system, which will act as a hydrogel. At pH 7, the hydrogel will be positively charged and the enzyme negatively charged. Hence the chitosan will hold enzymes and AuNPs together on the surface to give a 3D enzyme electrode which allows electrons to diffuse freely to the electrode. In this study, 0.1% w/w chitosan was used as the hydrogel. GCEs were fabricated with 3 μL of the mixtures of chitosan: Au-EDOT-FcNPs:GOx. The compositions of each component of the mixture and pH were varied to obtain optimum electrocatalytic current. To investigate the influence of pH, 0.04 M Britton Robinson Buffer [34] (BRB), universal buffer, was employed instead of PBS. Electrochemical measurements were obtained in 0.04 M BRB electrolyte solution at a scan rate of 0.02 V s^{-1} . Appropriate aliquots of 1 M glucose stock solution were added to the BRB solution in the cell, to obtain the required concentration of glucose. All solutions were degassed with high purity nitrogen for at least 10 min prior to the electrochemical measurements in order to remove oxygen. Promising results were obtained from the GCEs fabricated with $3\mu\text{L}$ of the solution having the composition mixture, chitosan: Au-EDOT-FcNPs:GOx (1:1:1, mg/mL). In the absence of 1 mM glucose, the Fc^+ process was prominent in the cyclic voltammogram than the Fc process. Upon addition of glucose, electrocatalytic characteristics appeared as the oxidation current magnitude increased (Figure 7). However, the current output was less than predicted. This revealed the enzyme-dependent catalytic oxidation of glucose, originated from GOx and mediated by the Au-EDOT-FcNPs. This result implies, that the Fc moieties on the nanoparticle can effectively shuttle electrons from the electrode through the hydrogel to the redox center of GOx.

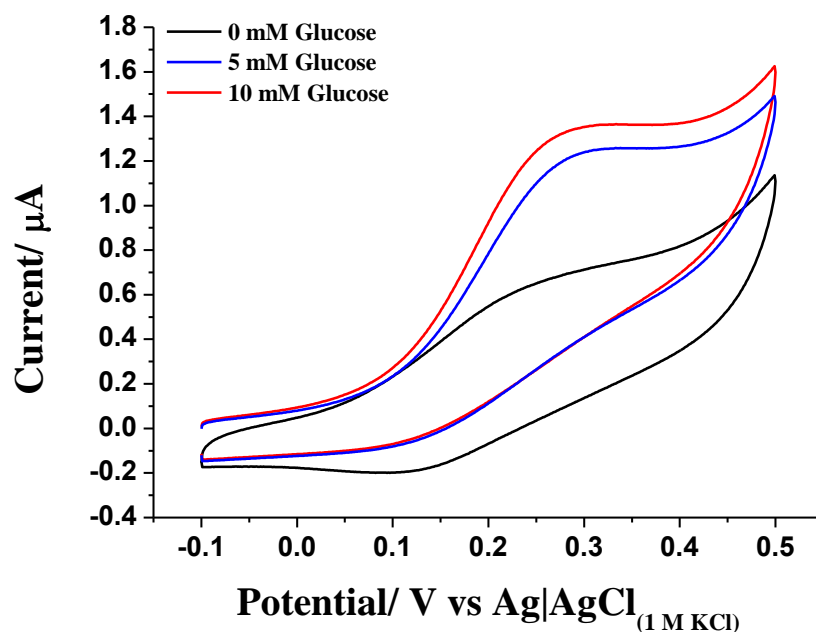


Figure 7: Cyclic voltammograms obtained in 0.04 M BRB at a scan rate of 0.02 V s^{-1} for chitosan: Au-EDOT-FcNPs:GOx (1:1:1, mg/mL) modified electrode in the absence (—) and presence (—) of 5 mM glucose (—) of 10 mM glucose.

6.1.4. Conclusion

A novel thiophene derivative monomer was successfully synthesised and characterised. This monomer was polymerised electrochemically and chemically to give poly(EDOT-EG-Fc-co-EDOT-OH). The enzyme electrode modified with the electropolymerisation method did not facilitate the mediated electron transfer process due to its rigidity and unsuccessful enzyme immobilisation. In contrast, electrodes modified with a mixture of chitosan, Au-EDOT-FcNPs and GOx allowed electrocatalytic oxidation of glucose. However, these preliminary results have not led to a composite material with competitive performance to other electrodes. To achieve the goal redesigning of the monomer by cooperating hydrophilic moieties is required to increase the hydrogel property of the CP. Thus, could increase the mobility of the mediator to achieve good electron transfer between the electrode and the enzyme.

6.2. Future perspectives

6.2.1. Advanced materials for enzymatic electrodes using conducting polymer nanocomposites

With the use of a single monomer, it is difficult to achieve a variety of properties needed in a conducting polymer. Therefore, it would be fascinating to incorporate a selection of monomers which provide a combination of properties needed for the synthesis of an ideal conducting copolymer. As PEDOT chemistry becomes more advanced, it may be possible to combine this with an EDOT monomer in the fabrication of a CP. The EDOT monomer would contribute to the polymer backbone and facilitate electron transfer. Due to relatively harsh conditions often required for in the synthesis of conducting polymers, enzymes are commonly loaded into the conducting polymer matrix after synthesis of the conducting polymers [35]. However, there are some disadvantages to this approach, such as leakage of enzymes. These problems may be overcome if enzymes are encapsulated with a conducting polymer like PEDOT, which has excellent biocompatibility. Enzymes can potentially be loaded onto the electrode via an encapsulation mechanism if they are firstly mixed uniformly with the polymer gel. As an example, a polymer gel prepared from a monomer which contains a base moiety at pH ~ 4.5 used to opens up the polymer matrix due to electrostatic interactions. However, good electrical communication and hence facile electron transfer between the polymer gel and the enzymes should be possible at pH~ 7, when the gel closes. The compact structure of the gel under this pH condition will also prevent the leakage of enzymes into the solution. In cases where PEDOT polymers are pH insensitive or encapsulation mechanisms are insufficient to prevent enzyme leakage, the monomers or polymers could be functionalised with a primary amine or carboxyl groups, which allow further bioconjugation with enzymes [36]. In this situation, enzymes could be immobilised on the electrode using covalent bonding. A ferrocene derivative wired EDOT monomer could act as the electron mediator to enhance electron transfer between the enzyme

and the electrode. Figure 8 illustrates a plausible CP, which could be employed for future studies of enzymatic electrode fabrication.

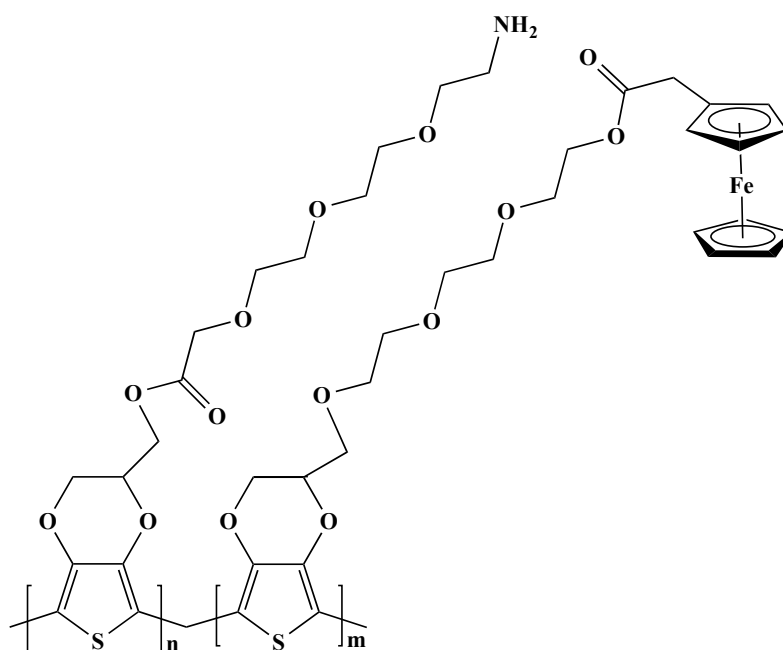


Figure 8: Copolymer of EDOT-EG-NH₂ and EDOT-EG-Fc monomers

6.2.2. Development of improved electron transfer to obtain higher current densities

Different electron transfer pathways are engaged by different electrocatalytic electrodes. In enzymatic electrodes, the electron transfer efficiency plays a critical role in the electrocatalytic current output. The hydrophilicity and the ease of mobility in redox polymer hydrogels enable the enzyme active sites to communicate efficiently with the electrode via mediators by giving a superior electrical contact between enzyme active site and the mediator [37-40]. Mano *et al.* [41] have introduced deglycosylation of glucose oxidase to improve the electrical communication between the enzyme and the electrode in enzyme electrodes [42]. Achieving high current density in a modified electrocatalytic electrode is essential in fuel cells.

6.2.3. Requirements of reliable sensors with high quality analytical performance

Glucose sensors are clinically important electronic devices for diabetic patients. It is crucial for Type 1 diabetes patients to continuously monitor their glucose level so that other health issues such as neuropathy, nephropathy, and cardiac disease [43] can be controlled. A review by Witkowska-Nery *et al.* [44] discussed the present need for more accurate and reliable commercialised glucose sensors since commercialised sensors and test strips do not maintain ISO 2003 standards after initially gaining approval. A glucose sensor should have high sensitivity, selectivity, a wide linear glucose detection range and a fast response [45]. Therefore, the design and development of new materials for the fabrication of high performance sensors are still in need. Literature reports are available that introduce high performance materials that could be employed in disposable test strips. However, studies have not usually moved from the laboratory level to actual used in biological samples [44].

6.2.4. Overcoming interferences on electrocatalytic electrodes

The enzymatic and non-enzymatic electrodes for electrocatalytic oxidation of glucose have the potential drawback, which is interference of other species in electrocatalytic glucose oxidation. This mainly affects in the sensor applications as biological samples contain a range of other oxidisable species. To overcome the interferences molecular selective membranes [43, 46] or selective polymers [47] in nanocomposites can be used. Enzymes are highly selective to their substrates. However, interferences sometimes arise upon incorporation of metal nanoparticles. Therefore, better materials to avoid interferences occurring from readily oxidised species present in biological fluids such as ascorbic acid, uric acid and drug metabolites [48] are still needed.

Reference

- [1] H. Shirakawa, Nobel lecture: The discovery of polyacetylene film—The dawning of an era of conducting polymers, *Rev. Mod. Phys.*, 73 (2001) 713.
- [2] J. Heinze, B.A. Frontana-Uribe, S. Ludwigs, *Electrochemistry of Conducting Polymers* □ Persistent Models and New Concepts†, *Chem. Rev.*, 110 (2010) 4724-4771.
- [3] C. Tang, N. Chen, X. Hu, *Conducting Polymer Nanocomposites: Recent Developments and Future Prospects*, *Conducting Polymer Hybrids*, Springer 2017, pp. 1-44.
- [4] T. Sen, S. Mishra, N.G. Shimpi, Synthesis and sensing applications of polyaniline nanocomposites: a review, *RSC Adv.*, 6 (2016) 42196-42222.
- [5] M.A. Olatunji, M.U. Khandaker, Y.M. Amin, H.N.M.E. Mahmud, Cadmium-109 Radioisotope Adsorption onto Polypyrrole Coated Sawdust of Dryobalanops aromatic: Kinetics and Adsorption Isotherms Modelling, *PloS one*, 11 (2016) e0164119.
- [6] L. Groenendaal, F. Jonas, D. Freitag, H. Pielartzik, J.R. Reynolds, Poly (3, 4-ethylenedioxythiophene) and its derivatives: past, present, and future, *Adv. Mater.*, 12 (2000) 481-494.
- [7] N. Zaquen, L. Lutsen, D. Vanderzande, T. Junkers, Controlled/living polymerization towards functional poly (p-phenylene vinylene) materials, *Polym. Chem.*, 7 (2016) 1355-1367.
- [8] P.C. Nien, T.S. Tung, K.C. Ho, Amperometric glucose biosensor based on entrapment of glucose oxidase in a poly (3, 4-ethylenedioxythiophene) film, *Electroanalysis*, 18 (2006) 1408-1415.
- [9] P. Santhosh, K. Manesh, S. Uthayakumar, S. Komathi, A. Gopalan, K.-P. Lee, Fabrication of enzymatic glucose biosensor based on palladium nanoparticles dispersed onto poly (3, 4-ethylenedioxythiophene) nanofibers, *Bioelectrochemistry*, 75 (2009) 61-66.
- [10] A. Kros, S.W. van Hövell, N.A. Sommerdijk, R.J. Nolte, Poly (3, 4-ethylenedioxythiophene)-Based Glucose Biosensors, *Adv. Mater.*, 13 (2001) 1555-1557.

- [11] M.F. Abasıyanık, M. Şenel, Immobilization of glucose oxidase on reagentless ferrocene-containing polythiophene derivative and its glucose sensing application, *J. Electroanal. Chem.*, 639 (2010) 21-26.
- [12] C. Janaky, C. Visy, Conducting polymer-based hybrid assemblies for electrochemical sensing: a material science perspective, *Anal. Bioanal. Chem.*, 405 (2013) 3489-3511.
- [13] V. Mazeiko, A. Kausaite-Minkstimiene, A. Ramanaviciene, Z. Balevicius, A. Ramanavicius, Gold nanoparticle and conducting polymer-polyaniline-based nanocomposites for glucose biosensor design, *Sens. Actuators, B*, 189 (2013) 187-193.
- [14] Q. Xu, S.-X. Gu, L. Jin, Y.-e. Zhou, Z. Yang, W. Wang, X. Hu, Graphene/polyaniline/gold nanoparticles nanocomposite for the direct electron transfer of glucose oxidase and glucose biosensing, *Sens. Actuators, B*, 190 (2014) 562-569.
- [15] D. Zhai, B. Liu, Y. Shi, L. Pan, Y. Wang, W. Li, R. Zhang, G. Yu, Highly Sensitive Glucose Sensor Based on Pt Nanoparticle/Polyaniline Hydrogel Heterostructures, *ACS Nano*, 7 (2013) 3540-3546.
- [16] A. Mirescu, U. Pruesse, Selective glucose oxidation on gold colloids, *Catal. Commun.*, 7 (2006) 11-17.
- [17] M. Kesik, H. Akbulut, S. Söylemez, Ş.C. Cevher, G. Hızalan, Y.A. Udum, T. Endo, S. Yamada, A. Çırpan, Y. Yağcı, Synthesis and characterization of conducting polymers containing polypeptide and ferrocene side chains as ethanol biosensors, *Polym. Chem.*, 5 (2014) 6295-6306.
- [18] E. Métay, M.C. Duclos, S. Pellet-Rostaing, M. Lemaire, J. Schulz, R. Kannappan, C. Bucher, E. Saint-Aman, C. Chaix, Conformational analysis and anion-binding properties of ferrocenyl-calixarene receptors, *Supramol. Chem.*, 21 (2009) 68-80.
- [19] A. Patel, T.K. Lindhorst, Multivalent glycomimetics: synthesis of nonavalent mannoside clusters with variation of spacer properties, *Carbohydr. Res.*, 341 (2006) 1657-1668.

- [20] M. Sassi, M.M. Salamone, R. Ruffo, C.M. Mari, G.A. Pagani, L. Beverina, Gray to Colorless Switching, Crosslinked Electrochromic Polymers with Outstanding Stability and Transmissivity From Naphthalenediimide-Functionalized EDOT, *Adv. Mater. (Weinheim, Ger.)*, 24 (2012) 2004-2008.
- [21] J. Roncali, Conjugated poly (thiophenes): synthesis, functionalization, and applications, *Chem. Rev.*, 92 (1992) 711-738.
- [22] Y. Degani, A. Heller, Direct electrical communication between chemically modified enzymes and metal electrodes. I. Electron transfer from glucose oxidase to metal electrodes via electron relays, bound covalently to the enzyme, *J. Phys. Chem.*, 91 (1987) 1285-1289.
- [23] W. Schuhmann, T.J. Ohara, H.L. Schmidt, A. Heller, Electron transfer between glucose oxidase and electrodes via redox mediators bound with flexible chains to the enzyme surface, *J. Am. Chem. Soc.*, 113 (1991) 1394-1397.
- [24] P. Hale, H. Lan, L. Boguslavsky, H. Karan, Y. Okamoto, T. Skotheim, Amperometric glucose sensors based on ferrocene-modified poly (ethylene oxide) and glucose oxidase, *Anal. Chim. Acta*, 251 (1991) 121-128.
- [25] S. Takahashi, J.-i. Anzai, Recent progress in ferrocene-modified thin films and nanoparticles for biosensors, *Materials*, 6 (2013) 5742-5762.
- [26] M. Kesik, H. Akbulut, S. Soylemez, S.C. Cevher, G. Hızalan, Y. Arslan Udum, T. Endo, S. Yamada, A. Crpan, Y. Yagc, L. Toppare, Synthesis and characterization of conducting polymers containing polypeptide and ferrocene side chains as ethanol biosensors, *Polym. Chem.*, 5 (2014) 6295-6306.
- [27] V. Vasantha, S.-M. Chen, Electrochemical preparation and electrocatalytic properties of PEDOT/ferricyanide film-modified electrodes, *Electrochim. Acta*, 51 (2005) 347-355.
- [28] W. Zhao, J.J. Xu, H.Y. Chen, Electrochemical Biosensors Based on Layer-by-Layer Assemblies, *Electroanalysis*, 18 (2006) 1737-1748.

- [29] J.G. Voet, J. Coe, J. Epstein, V. Matossian, T. Shipley, Electrostatic control of enzyme reactions: effect of ionic strength on the pKa of an essential acidic group on glucose oxidase, *Biochemistry*, 20 (1981) 7182-7185.
- [30] A. Heller, M.V. Pishko, Subcutaneous glucose electrode, Google Patents, 2001.
- [31] Y. Nakabayashi, H. Yoshikawa, Amperometric Biosensors for Sensing of Hydrogen Peroxide Based on Electron Transfer between Horseradish Peroxidase and Ferrocene as a Mediator, *Anal. Sci.*, 16 (2000) 609-613.
- [32] G.-C. Zhao, M.-Q. Xu, Q. Zhang, A novel hydrogen peroxide sensor based on the redox of ferrocene on room temperature ionic liquid film, *Electrochem. Commun.*, 10 (2008) 1924-1926.
- [33] J. Wang, X. Zhu, Q. Tu, Q. Guo, C.S. Zarui, J. Momand, X.Z. Sun, F. Zhou, Capture of p53 by electrodes modified with consensus DNA duplexes and amplified voltammetric detection using ferrocene-capped gold nanoparticle/streptavidin conjugates, *Anal. Chem.*, 80 (2008) 769-774.
- [34] C. MONGAY, VI/A BRITTON-ROBINSON BUFFER OF KNOWN IONIC STRENGTH, *Annali di Chimica*, 64 (1974) 409.
- [35] S. Krishnan, C.J. Weinman, C.K. Ober, Advances in polymers for anti-biofouling surfaces, *J. Mater. Chem.*, 18 (2008) 3405-3413.
- [36] H.G. T., *Bioconjugate Techniques*, 2nd ed., Academic Press: Amsterdam 2008.
- [37] P. Åsberg, O. Inganäs, Hydrogels of a conducting conjugated polymer as 3-D enzyme electrode, *Biosens. Bioelectron.*, 19 (2003) 199-207.
- [38] R.A. Etchenique, E.J. Calvo, Electrochemical Quartz Crystal Impedance Study of Redox Hydrogel Mediators for Amperometric Enzyme Electrodes, *Anal. Chem.*, 69 (1997) 4833-4841.
- [39] W.E. Hennink, C.F. van Nostrum, Novel crosslinking methods to design hydrogels, *Adv. Drug Delivery Rev.*, 54 (2002) 13-36.

- [40] S.E. Moulton, G.G. Wallace, 3-dimensional (3D) fabricated polymer based drug delivery systems, *J. Control. Release*, 193 (2014) 27-34.
- [41] A. PrévotEAU, O. Courjean, N. Mano, Deglycosylation of glucose oxidase to improve biosensors and biofuel cells, *Electrochem. Commun.*, 12 (2010) 213-215.
- [42] K. Murata, W. Akatsuka, T. Sadakane, A. Matsunaga, S. Tsujimura, Glucose oxidation catalyzed by FAD-dependent glucose dehydrogenase within Os complex-tethered redox polymer hydrogel, *Electrochimica Acta*, 136 (2014) 537-541.
- [43] X. Du, C.J. Durgan, D.J. Matthews, J.R. Motley, X. Tan, K. Pholsena, L. Árnadóttir, J.R. Castle, P.G. Jacobs, R.S. Cargill, Fabrication of a flexible amperometric glucose sensor using additive processes, *ECS J. Solid State Sci. Technol.*, 4 (2015) P3069-P3074.
- [44] E. Witkowska Nery, M. Kundys, P.S. Jelen, M. Jonsson-Niedziolka, Electrochemical Glucose Sensing: Is There Still Room for Improvement?, *Anal. Chem.* , 88 (2016) 11271-11282.
- [45] J. Wang, Electrochemical Glucose Biosensors, *Chem. Rev.* , 108 (2008) 814-825.
- [46] K.J. Babu, D.J. Yoo, A.R. Kim, Binder free and free-standing electrospun membrane architecture for sensitive and selective non-enzymatic glucose sensors, *RSC Adv.*, 5 (2015) 41457-41467.
- [47] H. Deng, A.K.L. Teo, Z. Gao, An interference-free glucose biosensor based on a novel low potential redox polymer mediator, *Sens. Actuators B Chem.*, 191 (2014) 522-528.
- [48] M.C.D. Cooray, Y. Liu, S.J. Langford, A.M. Bond, J. Zhang, One pot synthesis of poly(5-hydroxyl-1,4-naphthoquinone) stabilized gold nanoparticles using the monomer as the reducing agent for nonenzymatic electrochemical detection of glucose, *Anal. Chim. Acta*, 856 (2015) 27-34.

Chapter 7

Conclusion

Four nanocomposite materials that have potential for glucose electrocatalytic applications have been presented. Chapters 2 and 3 are based on enzymatic nanocomposites and chapters 4 and 5 are based on nonenzymatic materials. Synthesis of these nanocomposites and their analytical performance have been discussed in detail. The nanocomposites that have the capacity to be integrated into the design of glucose sensors and anodes for use in fuel cells. The development of glucose sensors that are accurate and reliable in monitoring glucose levels in human body fluids has had a major impact in managing the health of the drastically rising diabetes population. Glucose fuel cells have also attracted attention as a method for powering medical implants in human body.

Enzymatic electrodes require complex fabrication procedures while nonenzymatic electrode fabrication is simple. To obtain high performance, it is necessary to achieve a three dimensional electrode design for enzymatic electrodes as the active site of the enzyme glucose oxidase is occluded by a thick protein layer hindering the electron transfer process. Thus, remodelling the structure of the enzyme and exposing its active site to achieve more efficient glucose oxidation, can enhanced its activity in the sensing context.

To conclude, it is noted that all of the synthesised nanocomposites have been characterised by using a range of electrochemical, spectroscopic and microscopic techniques. All differ in their capacity to electrocatalytically oxidise glucose, but score equally for their employment in future development of advanced sensors or anodes for fuel cells.